Volcanic Rocks from Central Italy:
An Oxygen Isotopic Microanalytical and Geochemical Study

Dissertation
zur Erlangung des Doktorgrades
der Mathematisch-Naturwissenschaftlichen Fakultäten
der Georg-August-Universität zu Göttingen

vorgelegt von

Peter Barnekow
aus Bremen

Göttingen 2000

D 7

Referent:	Prof. Dr. J. Hoefs
Korreferent:	Prof. Dr. S.F. Foley
Tag der mündlichen Prüfung:	30. Oktober 2000

Table of Contents

1 Introduction

1.1 General Characteristics of the Tertiary to Quarternary Italian Magmatic Rocks

The Italian volcanism is a classical area to study magmatic petrology and geochemistry (e.g. Washington 1906). However the petrogenesis of the Italian rocks is not fully understood, yet. A common feature of the Italian magmatic rocks is their high enrichment of K, which classify them as potassic and ultrapotassic rocks. Potassic and ultrapotassic rocks within continental plates are distributed throughout the world but are not very abundant (e.g. Foley et al. 1992, Peccerillo 1992, Wilson 1995). According to Foley et al. (1987) the ultrapotassic rocks can be subdivided into three subgroups: lamproites, kamafugites, and Roman Province Type rocks. Lamproites have high K_2O and low Al_2O_3, Na_2O and CaO contents. They are slightly SiO_2 oversaturated to undersaturated and mineralogically characterized by the absence of plagioclase. Kamafugites are strongly SiO_2 undersaturated and typically contain kalsilite and melilite as sialic phases. The Roman type ultrapotassic rocks are also SiO_2 undersaturated but contain high Al_2O_3 and CaO contents. Plagioclase is in these rocks a common phase. Additionally Foley et al. (1987) distinguish a fourth group, which consists of transitional rocks between lamproites and Roman Province Type rocks. Within Italy rocks of all groups can be found (e.g. Peccerillo & Panza 1999). Additionally crustal anatectic rocks are common in central Italy (e.g. Innocenti et al. 1992). Consequently the Tertiary to Quarternary magmatism of Italy shows a great variability of different rock types.

The potassic and ultrapotassic rocks from Italy are highly enriched in LILE and LREE as well as in ^{87}Sr and ^{18}O and depleted in ^{143}Nd and ^{206}Pb. As summarized by Innocenti et al. (1992) and Peccerillo & Panza (1999) a northward increase in ^{87}Sr and ^{18}O and a depletion of ^{143}Nd and ^{206}Pb can be found. The overall geochemical composition of the igneous rocks is characterized by a crustal signature even for the least evolved rocks. The place of the interaction of mantle melts with crustal material is a matter of debate (Beccaluva et al. 1991, Ferrara et al. 1986b, Foley et al. 1992, Holm & Munksgaard 1982, Peccerillo & Panza 1999, Rogers et al. 1985, Scott Smith 1996, Shaw 1996, Taylor & Turi 1976, Turi & Taylor 1976): On the one hand the mantle source itself can be contaminated and on the other hand assimilation of crustal material during the uprise of mantle melts through the crust may be the reason for the uncommon signature of these rocks. These two possibilities have to be tested for every volcano or magmatic region. Additionally the influence of a hotspot in the genesis of the Italian rocks has been assumed (e.g. Vollmer 1989). Nevertheless a subduction related genesis of the Italian rocks is now commonly accepted (e.g. Peccerillo 1985, Wilson 1995).

1.2 Magmatic Provinces in Italy

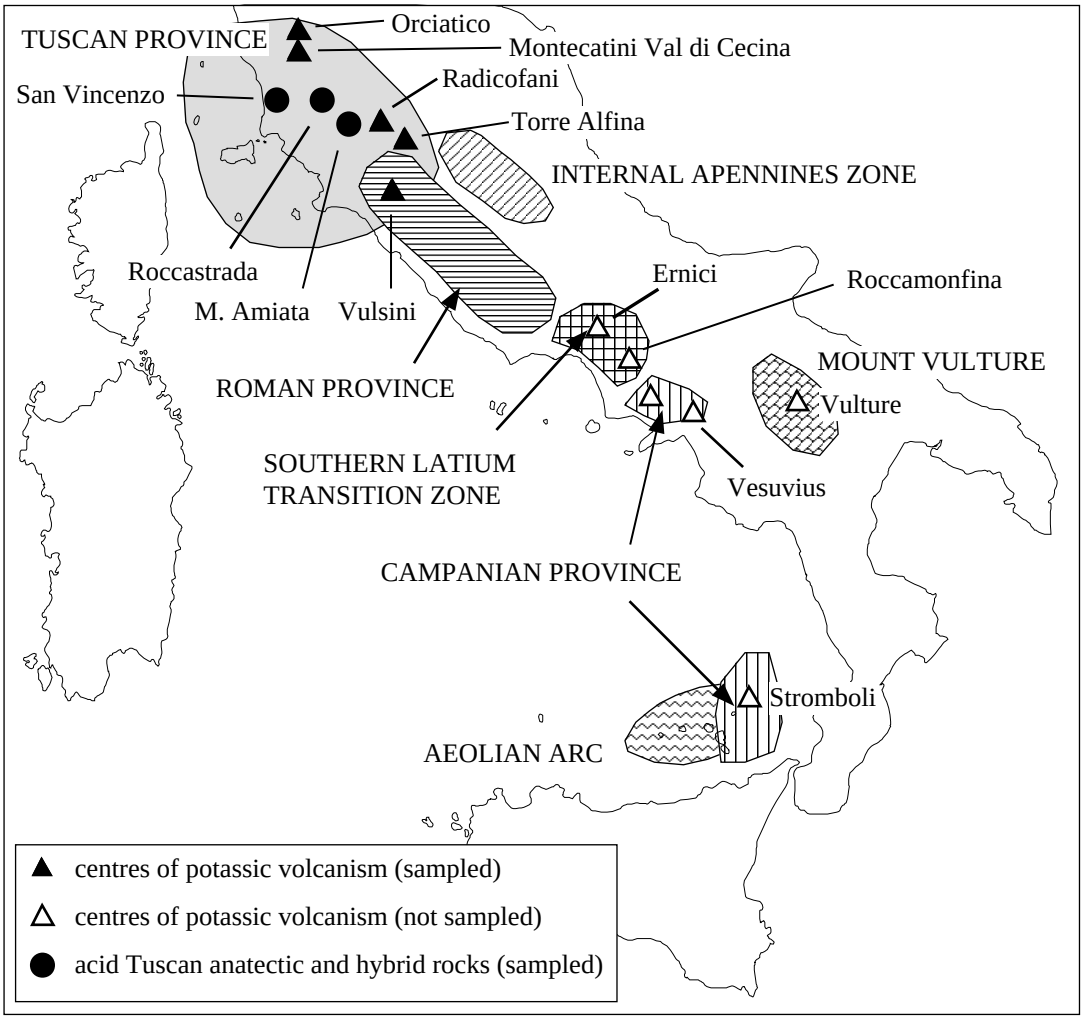

Fig. 1-1: Schematic map of the distribution of the major magmatic zones in central and southern Italy according to Peccerillo & Panza (1999). Additionally some localities, which are mentioned in this paper, are shown.

The magmatic rocks of the Italian peninsular have been subdivided into three magmatic provinces on the basis of their composition and geographical distribution. These provinces are the Tuscan, the Roman and the Campanian Magmatic Province. The Tuscan Province is characterized by frequently occuring crustal anatectic melts and by some lamproites. In contrast the Roman Province, stretching from southern Tuscany to northern Campania, and the Campanian Province are mainly built up by Roman Province type rocks. Additionally some kamafugites occur at the eastern part of the Roman Province. But this subdivision is somewhat arbitrary, because it does not consider the chemical differences within the Roman and Campanian Province. Therefore Peccerillo & Panza (1999) suggested a new subdivision into seven major zones according to the chemical and mineralogical composition of the rocks as well as on the basis of geophysical investigations. These major zones are the Tuscan Province, the Roman Province, the Campanian Province, the Southern Latium Transition

Zone, which is a transition zone between the Roman and the Campanian Province, the Internal Apennines Zone characterized by the occurence of kamafugites, the Aeolian arc being north of the island of Sicily, and the Mount Vulture in southern Italy (fig. 1-1).

1.3 Overview of the Different Genetic Models

The most debated topic in the genesis of the investigated rocks is the composition of the mantle beneath the Roman and the Tuscan Magmatic Province and the degree of interaction between mantle derived melts with the crust.

Since the mid seventies it was broadly accepted, that the high enrichment of LILE, especially K, and the high ^{87}Sr / ^{86}Sr ratios of the Roman Province type rocks indicate an enriched mantle source (e.g. Turi & Taylor 1976, Vollmer 1989). The process of enrichment appears to be a metasomatic mixing (Hawkesworth & Vollmer 1979) of a crustal component with mantle material. But the kind of metasomatism, the composition of the mantle source and the evolution of the mantle derived melts during the uprise through the crust is still a matter of debate.

Holm & Munksgaard (1982) postulated metasomatism of the primary mantle with a fluid enriched in LILE, ^{87}Sr and ^{18}O. During this metasomatism the mantle source got a heterogeneous composition. This heterogeneously composed mantle produced a large range of different primary melts with a range of $\delta^{18}O$ values from 7.8 - 9.4 ‰ at 15.5 wt.% CaO of the bulk rock. During fractional crystallization the oxygen isotope ratios increase to 9.0 - 10.6 ‰ (at 3 wt.% CaO). Generally not more than 10 wt.% of crustal material were assimilated. This model was also supported by Rogers et al. (1985), who believed that the compositional range of the Vulsinian rocks can be produced by fractional crystallization of mantle melts and only minor crustal assimilation. They distinguished three different mantle melts, HKS (high potassic series) and KS (potassic series) rocks as well as leucite basanites. The mantle source is a metasomatized enriched MORB source with an oxygen isotopic composition of about 8 ‰.

In contrast to Holm & Munksgaard (1982), Ferrara et al. (1986b) and Turi et al. (1986) assumed, that mantle derived melts unaffected by crustal assimilation are only rarely found at the Vulsinian mountains or that these mantle melts do not occur. On the basis of a $\delta^{18}O$ vs. ^{87}Sr / ^{86}Sr diagram they showed, that the Vulsinian rocks lie on a mixing line between Alban hill rocks and Tuscan anatectic rocks or the Tuscan basement. The Alban hills, lieing in the middle part of the Roman Province, represent the primary mantle melts, whereas the Vulsinian rocks are mixtures between primitive melts and crustal melts and suffered extensive crustal assimilation. Thus primitive melts from the Roman Province shall contain $\delta^{18}O$ values

of 5.5 - 7.5 ‰ (Ferrara et al. 1986b) or 6.5 - 7.0 ‰ (Turi et al. 1986). Consequently the mantle source is not so highly enriched in ^{18}O than Holm & Munksgaard (1982) presumed.

This two endmember model - Alban hill melts and Tuscan anatectic melts - of Ferrara et al. (1986b) and Turi et al. (1986) was modified by Varekamp & Kalamarides (1989). They suggested a four endmember model of the Vulsinian rocks. These endmembers are HKS leucitic melts, low K trachytic melts and assimilated crust, pelitic rocks and limestones. With these four endmembers the whole range of Sr isotope and bulk rock composition can be produced. In addition the large variability of the $\delta^{18}O$ values is generated by the influence of hydrothermal water.

Conticelli et al. (1991) and Conticelli & Peccerillo (1992) demonstrated on the basis of mass balances including major and trace elements, that the less evolved rocks from the Vulsinian mountains represent primitve melts and are not influenced by crustal assimilation. Like Rogers et al. (1985), Conticelli et al. (1991) found three different mantle derived melts in the Vulsinian mountains. Typical HKS and KS rocks, which are generated in a fertile metasomatized mantle at different depths, and a HKS like melt, the latter one being produced from an upper slightly depleted mantle part with a rough similarity to the Tuscan mantle. These results were supported by Kamenetsky et al. (1995), who showed on melt inclusions within olivines, that the less evolved rocks from the Vulsinian mountains are indeed unaffected by crustal assimilation.

Generally the metasomatism of the mantle source is believed to be related to a subduction zone (e.g. Wilson 1995). However Vollmer (1989, 1990) favoured the influence of a hotspot beneath the Italian peninsular now lieing below Pietre Nere, a small volcanic body in southern Italy. He believed that the Pietre Nere rocks are the mantle endmember and crustal material similar to the Tuscan basement is the other one. The mixing of these two endmembers can produce the variability of the mantle derived melts in central and sourthern Italy. This model was rejected by several authors like Kamenetsky et al. (1995), Conticelli & Peccerillo (1992), and Peccerillo (1990).

For the Tuscan mantle melts - lamproites from Orciatico and Montecatini Val di Cecina - only few papers are published. The Torre Alfina rocks can also be assigned to the lamproitic rocks. Originally the lamproites from Orciatico and Montecatini Val di Cecina were believed to belong to the Tuscan Anatectic Province and were produced from a granitic melt by filtration and gaseous transfer (Barberi & Innocenti 1967, Marinelli 1961). For the Torre Alfina rocks Ferrara et al. (1986b), Taylor & Sheppard (1986) and Turi et al. (1986) assumed on the basis of Sr and O isotopes and Sr and CaO contents of the bulk rock a genesis by mixing of Roman Province melts with crustal anatectic melts or basement rocks of the Tuscan Province. But Peccerillo (1994) and Peccerillo et al. (1988) presented strong evidence, that the lamproites

and the Torre Alfina rocks could not be produced by mixing of Roman type melts and crustal melts, because the concentrations of transitional metals are similar to a MORB source and the lamproites have high Mg values. A mixing of crustal and mantle melts should produce low Mg values and low contents of the transitional metals. Conticelli et al. (1992) and Conticelli (1998) additionally could show, that the lamproitic rocks contain Sr and Nd isotope ratios, which could not be generated by such a mixing. The Nd isotope ratios are lower than the ratios of the Roman Province rocks and the Tuscan anatectic melts or basement rocks. Therefore they explained the genesis of the lamproites by melting of a metasomatized harzburgitic mantle having different Sr and Nd isotopic composition compared to the Roman Province mantle. This was supported by the occurence of residual phlogopite bearing peridotitic xenoliths in the Torre Alfina lavas (Conticelli & Peccerillo 1990) indicating a residual metasomatized mantle beneath Tuscany.

Transitional rocks from Tuscany like the rocks from Radicofani display an intermediate composition between Roman Province rocks and lamproites (Peccerillo et al. 1987). Originally they were believed to be a mixture between mantle melts from a metasomatically enriched mantle and a crustal melt (Poli et al. 1984). Ferrara et al. (1986b) suggested for the Radicofani rocks a Roman Province type melt as a mantle melt. The genesis of the Radicofani rocks could be modelled by mixing of Vulsinian melts and basement rocks of Tuscany on the basis of Sr isotopes and Sr contents (Ferrara et al. 1986b). But Peccerillo (1994) demonstrated, that the trace elements of the less evolved rocks could only be produced by a mixing of lamproitic and Roman Province melts.

Compared to the mantle melts of the Italian peninsular the crustal anatectic melts of the Tuscan Province have not been discussed controversially. The acidic igneous rocks are explained by partial melting of the basement (Taylor & Turi 1976). For the Roccastrada and San Vincenzo rhyolites Taylor & Turi (1976) assumed anatectic melting of pelitic metamorphic rocks. Giraud et al. (1986) support the genesis by partial melting of metapelitic rocks but they also showed, that the enrichment of LILE, like K, in the crustal melts could not be produced by partial melting. Thus a fluid overprinting of the crustal source must be involved (Giraud et al. 1986). Giraud et al. (1986) suggested a relation of this fluid with the enriched mantle part beneath Tuscany.

For the San Vincenzo rhyolites Ferrara et al. (1986a, 1989) distinguished two rock suites. The first rock suite represents pure crustal anatectic melts whereas the second suite is a mixture of mantle and crustal melts because of a large Sr isotope heterogeneity among the minerals (Ferrara et al. 1989). A melt mixing was also assumed by Innocenti et al. (1992) and Serri et al. (1993). Feldstein et al. (1994) developed a model of a layered magma chamber, where a mantle melt underlies a crustal anatectic melt producing a range from pure crustal melts to

mixtures between both melts. In addition Masuda & O'Neil (1994) found in a rhyolite from San Vincenzo a heterogeneity in the oxygen isotope composition of the phenocrystals also indicating a magma mixing.

Hybrid rocks of the Tuscan Province are mixtures between mantle and crustal melts (Peccerillo et al. 1987). For Monte Amiata it is commonly accepted, that the rocks represent a mixture between crustal anatectic and Roman Province mantle melts (e.g. Giraud et al. 1986, Poli et al. 1984, Peccerillo et al. 1987, Ferrari et al. 1996). Whether they belong to the K series (Peccerillo et al. 1987) or to the HK series (Poli et al. 1984, van Bergen 1985) is a matter of debate. Because of the Sr and Nd isotopic similarity between HKS and KS rocks the isotope ratios do not allow to distinguish between both mantle endmembers for the Monte Amiata rocks (Innocenti et al. 1992).

1.4 Investigated Area and Petrogenetic Subdivision

In southern Tuscany the Tuscan and the Roman Province overlaps. Therefore within a narrow area a large variability of different igneous rocks can be observed. An important aim of the understanding of the petrological situation of the Tertiary to Quarternary rocks is not only the genesis of the different genetic types but also the reason why the different genetic types occur in a narrow area.

Most of the different igenous rocks of the Italian peninsular are present in Tuscany and northern Latium (fig. 2-1). Ultrapotassic and potassic Roman Province type rocks with different degrees of SiO_2 saturation as well as lamproites and crustal anatectic melts can be observed. Furthermore the petrogenetic situation is complicated by the occurence of mixtures between these rocks. Because of this large variability this investigation has been focussed on central Italy.

According to Peccerillo et al. (1987) five different genetic types can be distinguished in Tuscany and northern Latium:

1. Roman Province type rocks only occur in the Roman Province and are not typical rocks of the Tuscan Province. The Roman Province type rocks itself are subdivided into two groups (Civetta et al. 1981). The two groups differ in their K enrichment. The high potassic series (HKS) rocks are SiO_2 undersaturated and highly enriched in K. In contrast the rocks of the potassic series (KS) are SiO_2 saturated and contain less K at the same SiO_2 content compared to the HKS rocks.
2. Mantle melts are rarely found in Tuscany and only occur at Orciatico and Montecatini Val di Cecina. These rocks are lamproites.

3. Contrary to the mantle melts crustal anatectic melts frequently occur in the Tuscan Province both as plutonic and as volcanic rocks.

These three genetic types represent endmembers in the investigated region. Between these endmembers mixtures can be observed.

4. Between both mantle derived melts from the Tuscan Province and the Roman Province mixtures occur in the southern Tuscan Province. This kind of rocks are named as transitional rocks.

5. Additionally mixtures between mantle derived and crustal anatectic melts can also be found in the Tuscan and the northern Roman Province. These rocks display a high variability of composition and are classified as hybrid rocks.

The petrogenesis of these five genetic rock types is the subject of this paper, especially in the light of UV laser ablation mineral $\delta^{18}O$ data.

1.5 Oxygen Isotopes

In nature three oxygen isotopes occur: ^{16}O, ^{17}O and ^{18}O, which can be fractionated from each other by e.g. mineral reactions, crystallization of minerals from a liquid or isotope exchange reactions between minerals and fluids. The degree of fractionation mainly depends on the oxygen isotope composition of the involved phases and on the temperature. Because of the higher fractionation between ^{18}O and ^{16}O and the low abundance of ^{17}O, the ^{18}O / ^{16}O ratio is commonly used for investigations. The high abundance of oxygen in nature facilitates the use of oxygen isotopes as a tool to investigate geological and petrological processes.

Generally ^{18}O / ^{16}O ratios are measured, which are referred to a standard. For igneous systems this standard is Standard Mean Ocean Water (SMOW). Thus the notation for oxygen isotopes is:

$$\delta^{18}O = \left[\frac{\left(\frac{^{18}O}{^{16}O}\right)_{sample} - \left(\frac{^{18}O}{^{16}O}\right)_{standard}}{\left(\frac{^{18}O}{^{16}O}\right)_{standard}} \right] \bullet 1000 \quad [‰]$$

Large areas of the upper mantle are homogeneous with respect to the oxygen isotope composition. For example mid ocean ridge basalts show a narrow range of $\delta^{18}O$ values of about 5.7 ± 0.2 ‰ (Harmon & Hoefs 1995, Hoefs 1997). For the upper mantle a composition

of about 5.4 ± 0.2 ‰ for olivines, 5.9 ± 0.1 ‰ for orthopyroxenes, and 5.7 ± 0.2 ‰ for clinopyroxenes is assumed (Hoefs 1997).

The primary isotopic composition of mantle melts can be modified by contamination processes either of the source itself or during the uprise of the magma through the crust. Contamination within the crust is caused by assimilation of crustal material or by alteration with fluids. Fractional crystallization changes the isotopic composition only minor resulting in a shift to higher values with a maximum shift of about + 1.2 ‰ for a rock suite from mafic to acidic rocks (Holm & Munksgaard 1982).

In order to deduce the primary oxygen isotope composition of mantle melts, the rocks should not be influenced by secondary processes like weathering or hydrothermal reactions. These secondary processes cause a H_2O enrichment of the rocks combined with a change of the $\delta^{18}O$ values. Taylor et al. (1984) and Ferrara et al. (1985, 1986b) proposed, that the $\delta^{18}O$ values of the alterated rocks can be calculated back to primary values using the present H_2O content of the rock and the primary H_2O content of the magma. The primary H_2O content is believed to be lower than 0.5 wt.% for mantle derived melts (Ferrara et al. 1985, 1986, Taylor et al. 1984). However, if the mantle source itself is modified fluids or melts, the magmas can contain higher H_2O contents. Therefore a change of the $\delta^{18}O$ values by processes within the continental crust can not be computed back to original values. Furthermore the groundmass or late crystallizing phases like plagioclase or sanidine are often secondarily influenced and are therefore in disequilibrium to the first crystallizing clinopyroxenes or olivines (see also chapter 4). But this change of the $\delta^{18}O$ values of the feldspars is not significantly correlated to the H_2O content of the bulk rock. Thus bulk rock analysis must not reflect the original oxygen isotopic composition of the bulk rock, even if the H_2O content of the bulk rock is taken into account.

A method to circumvent this problem is to measure the oxygen isotope composition of phenocrystals in the rock. The first crystallizing minerals may give the best estimate of the original $\delta^{18}O$ composition of the melt. Furthermore possible isotopic heterogeneities can be shown. Therefore the study of phenocrystals may give better results with respect to the primary composition and the evolution history of the melt. For example some rocks contain phenocrystals being in isotopic disequilibrium with each other. This may indicate a mixing of different melts.

A laser ablation system for oxygen isotope analysis has the advantage that single minerals can be measured. Additionally using a high energy UV laser facilitates the in situ measurement, so that possible heterogeneities within a mineral or rock section can be shown. The new UV laser ablation method developed in Göttingen (Fiebig et al. 1999, Wiechert & Hoefs 1995) has thus been applied to the volcanic rocks of the various magmatic provinces in central Italy.

2 Sample Description

2.1 Sampling

In order to analyze oxygen isotopes of phenocrystals only porphyric rocks were sampled. From every genetic type rocks have been investigated (Tab. 2-1).

Roman Province rocks are represented by rocks from the Vulsinian mountains. Both HKS and KS rocks were sampled. Mantle derived rocks from the Tuscan Province occuring as lamproites have been taken from Orciatico and Montecatini Val di Cecina. As representatives of the crustal anatectic rocks rhyolites from Roccastrada and San Vincenzo have been analyzed. Transitional rocks between the Tuscan and the Roman Province mantle melts have been sampled at Torre Alfina and Radicofani. Samples from the Monte Amiata represent mixtures between mantle and crustal melts.

Tab. 2-1: Localities, sampled rocks and assignment to the genetic types according to Peccerillo et al. (1987). (1): Rhyolites from San Vincenzo have a prevailing crustal anatectic origin. (2): For the classification of the Torre Alfina rocks also see chapter 2.3. (3): The sample Montefiascone has kindly been put at disposal by Prof. Peccerillo (University of Perugia). Montefiascone is a volcano of the Vulsinian mountains.

Locality (Abbreviation)	Rocks	Type of Genesis
Monti Vulsini (VUL, Montefiascone (3))	potassic trachybasalts to phonolites shoshonites	Roman Province Type high potassic series (HKS) potassic series
Orciatico (ORC)	lamproites	Tuscan Province mantle melts
Montecatini Val di Cecina (MVC)	lamproites	Tuscan Province mantle melts
Roccastrada (ROC)	rhyolites	Tuscan Province anatectic melts
San Vincenzo (SVC)	rhyolites	Tuscan Province anatectic melts (1)
Torre Alfina (TA)	transitional rocks (2)	transitional rocks between Tuscan and Roman melts
Radicofani (RAD)	basaltic andesites	Transitional rocks between Tuscan and Roman melts
Monte Amiata (AMT)	shoshonites to trachytes	Hybrid rocks between mantle and crustal melts

2.2 Geological and Petrographical Description of the Samples

The geographic position and the petrological classification of the rocks are listed in tabular form in the appendix. The spatial distribution of the different genetic rock types is shown in fig. 2-1.

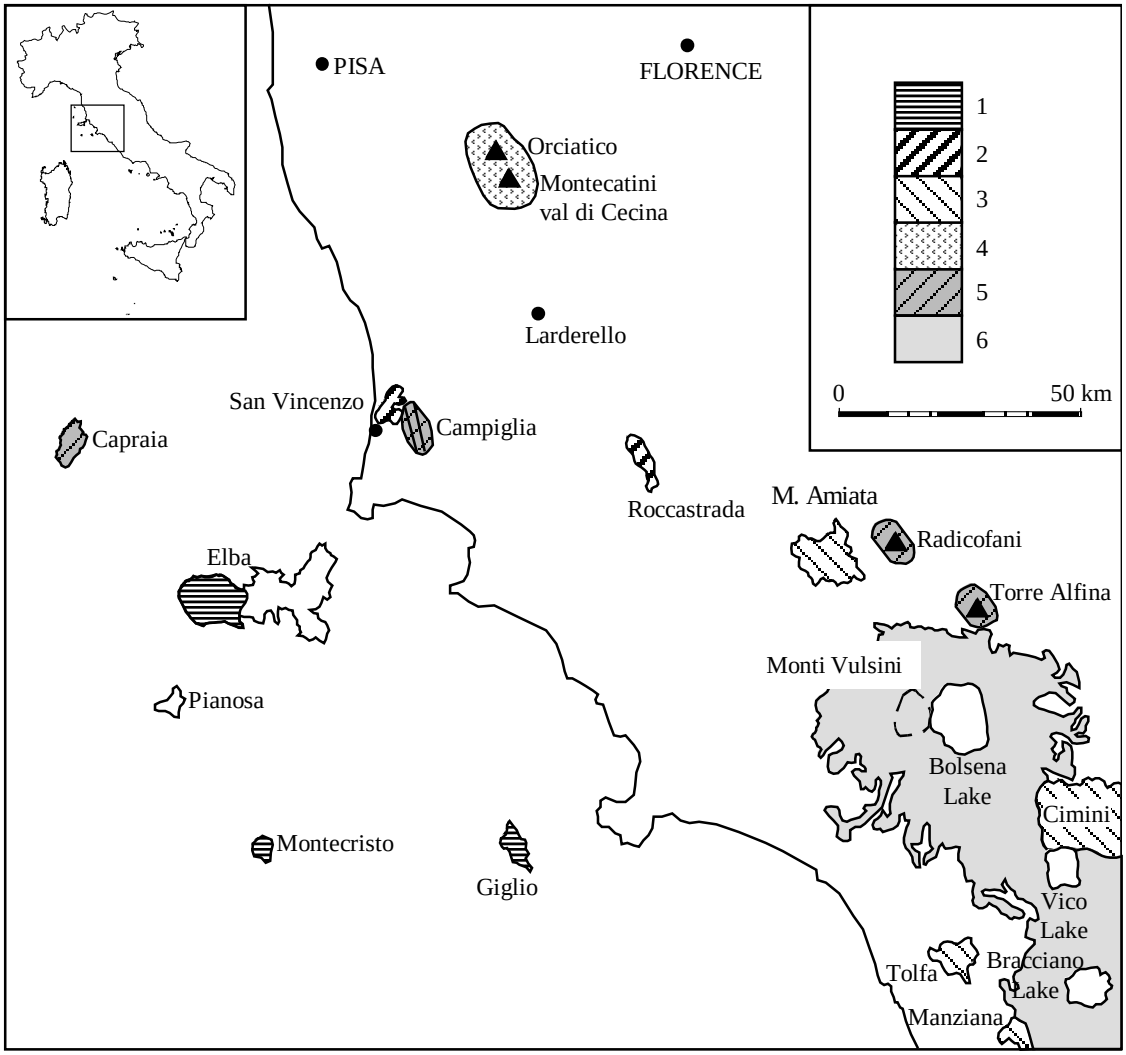

Fig. 2-1: Schematic map of the Tertiary to Quarternary volcanism in southern Tuscany and northern Latium (modified after Peccerillo et al. 1987). Genetic types: 1) Acidic plutonic rocks of prevailing anatectic origin; 2) acidic volcanic rocks of prevailing crustal anatectic origin; 3) Hybrid rocks between crustal and mantle melts; 4) Lamproites; 5) Transitional rocks between lamproites and Roman Province type rocks; 6) Roman Province type rocks.

2.2.1 Monti Vulsini - Roman Province Type Rocks

The Vulsinian Volcanic District is the northern part of the Roman Magmatic Province. It lies on the western slope of the central Apennines around the lake Bolsena and spreads over an area of about 2280 km^2, so that it is the largest volcanic system of the Roman Magmatic

Province. The district is built up by over 100 volcanoes and can be subdivided into four domains: the Latera Volcanic Complex in the western part, the Bolsena-Orvieto Volcanic Complex in the eastern part, the Montefiascone Volcanic Complex in the southeastern part and the Southern Vulsini Zone (Vezzoli et al. 1987). The region is characterized by calderas, cinder cones, pyroclastic layers, ignimbrites, and lava flows. The geology and petrology of the Vulsinian mountains is extensively described by Innocenti & Trigila (1987) and Varekamp (1979).

Both high potassic rocks as well as potassic rocks occur at the Vulsinian mountains. Major phases of the HKS rocks are olivine, clinopyroxene, and plagioclase and, additionally leucite in the more evolved rocks. The KS rocks consist of olivines, clinopyroxenes, and plagioclases. From the HK series less evolved rocks, potassic trachybasalts, to highly evolved phonolites have been sampled as well as tephriphonolites and phonotephrites. Also less evolved rocks, shoshonites, from the K series could be sampled from one lava flow.

2.2.2 Orciatico and Montecatini Val di Cecina - Lamproites

Mantle melts of the Tuscan Magmatic Province crop out near Orciatico and Montecatini Val di Cecina both lieing in the northern part of Tuscany. The magmas from both localities intruded as subvolcanic bodies in shallow level Pliocene argillaceous sediments (Peccerillo et al. 1988) and are located on the western edge of the Val d´Era graben (Conticelli et al. 1992). The outcrops are small with an area of less than 0.6 km^2 for each locality. Their emplacement was influenced by NNW-SSE trending faults, which are related to a post-tectonic extensional regime (Conticelli et al. 1992).

Rocks from both localities are petrographically classified as diopside sanidine phlogopite lamproites according to the classification scheme of Woolley et al. (1996) and Foley et al. (1987); following the older scheme of Sahama (1974) these rocks are orendites. Major phases are phenocrystals of olivines, diopsides, and phlogopites in a groundmass consisting of additional sanidines. Generally the phenocrystals are small.

The magmatic body of Orciatico displays a rough chemical homogeneity. A late-stage hydrothermal metamorphism has been recognized, which affected the Sr-isotopes of the country rock but without an influence of the Sr-isotopes of the magmatic body (Ferrara et al. 1988). In contrast to the rocks from Orciatico three different petrographic facies can be distinguished in the Montecatini magmatic body; a marginal facies in contact to the thermally metamorphosed country rock, a massive crystalline facies and a massive crystalline facies in contact to unmetamorphosed country rock (Conticelli et al. 1992). The groundmass of the Montecatini lamproites are fine grained and disintegrate easily.

The localities are described in detail by Barberi & Innocenti (1967), Conticelli et al. (1992) and Rodolcio (1934).

2.2.3 Roccastrada - Rhyolites

The Roccastrada volcanic centre represents crustal melts of the Tuscan Province and is composed of lava flows, ignimbrites, and one lava dome. It is placed in the Grosseto province, where acidic volcanic rocks form isolated outcrops stretching over 30 km^2 (Giraud et al. 1986, Taylor & Turi 1976). The magmas were erupted from fractures trending in an Apennine direction (Peccerillo et al. 1987).

The rocks from Roccastrada are rhyolites with plagioclase, sanidine, quartz, and biotite as major phenocrystalline phases and have a vitreous or microcrystalline groundmass.

2.2.4 San Vincenzo - Rhyolites

San Vincenzo is the second locality, where crustal anatectic rocks have been sampled. The volcanic centre covers an area of about 10 km^2 and is built up by lava flows and a highly altered volcanic unit (Feldstein et al. 1994). Petrologically these rocks are rhyolites with relatively low SiO_2 contents, so that they were sometimes classified as rhyodacites (Peccerillo et al. 1987).

After Ferrara et al. (1989) the San Vincenzo rhyolites can be subdivided into two groups according to their MgO content. Group A contains less than 0.61 wt.% MgO and group B more than 0.75 wt.%. Both groups also have different Sr concentrations with less than 140 ppm for group A and more than 200 ppm for group B. Group A rhyolites are characterized by plagioclase, sanidine, quartz, biotite, and cordierite assamblages. In contrast group B rhyolites additionally contain sometimes clinopyroxenes, orthopyroxenes, and mafic magmatic inclusions (Ferrara et al. 1989).

2.2.5 Torre Alfina - Transitional Rocks Between Tuscan and Roman Mantle Melts

The Torre Alfina volcano consists of a few lava flows erupted from a small volcanic centre and a small neck cropping out north of the village of Torre Alfina (Conticelli 1998) with a close spatial relation to the Vulsinian mountains. The eruptions were coeval with the nearby Radicofani volcano (Conticelli 1998). The volcano is placed on the sedimentary basement consisting of carbonaceous and argillaceous rocks (Conticelli 1998).

Petrographically the Torre Alfina rocks can be subdivided into two groups (Conticelli & Peccerillo 1990). Type A lavas are aphyric to slightly prophyric with olivine as the only phenocrystalline phase and a groundmass consisting of microphenocrystals of olivine, phlogopite, clinopyroxene, and sanidine (Conticelli 1998, Conticelli & Peccerillo 1990).

Often ultramafic xenoliths can be found in the type A lavas (Conticelli & Peccerillo 1990). In contrast type B lavas are porphyric with olivine as single phenocrystalline phase and xenocrystals of plagioclase, biotite, cordierite, orthopyroxene, and quartz and large amounts of crustal xenoliths (Conticelli 1998, Conticelli & Peccerillo 1990). The groundmass is comparable to the type A lavas but the micas are strongly oxidized (Conticelli 1998, Conticelli & Peccerillo 1990).

The geology and petrology of the Torre Alfina volcano is described in detail by Conticelli (1998) and Conticelli & Peccerillo (1990).

2.2.6 Radicofani - Transitional Rocks Between Tuscan and Roman Mantle Melts

The Radicofani volcano consists of a few remnants of thin lava flows and a small (~ 100 m elevation) heavily weathered neck surrounded by Pliocene clay rich sediments (Innocenti 1967, Poli et al. 1984). It lies at the eastern edge of the Siena-Radicofani graben opposite to the Monte Amiata (Ferrari et al. 1996). Petrographically the rocks range from trachybasalts to latites and trachytes (Innocenti 1967). The rocks can be assigned to the shoshonitic association (Poli et al. 1984). Major phenocrystals are olivines, clinopyroxenes and plagioclases (Innocenti 1967, Poli et al. 1984). The petrography is described in detail by Innocenti (1967).

From this volcano less evolved rocks, basaltic andesites, have been sampled.

2.2.7 Monte Amiata - Hybrid Rocks Between Mantle and Crustal Melts

The Monte Amiata volcano is one of the largest volcanoes in southern Tuscany (van Bergen 1984). It covers an area of about 85 km^2 with up to 1000 m thick volcanic products and is built up by lava flows and domes (van Bergen 1984). The volcano is located at the western edge of the Siena-Radicofani graben (Ferrari et al. 1996). According to the geochemical composition and age these rocks can be subdivided into three groups: 1) an early basal trachydacitic complex, 2) trachdacitic to trachytic and latitic domes and lava flows and 3) final ultrapotassic latite lava flows (Ferrari et al. 1996). In the volcanic rocks mafic inclusions as well as crustal xenoliths are embedded (e.g.: van Bergen 1984, van Bergen & Barton 1984, Ferrari et al. 1996). The petrography of the rocks - trachytic and mafic rocks as well as xenoliths - indicate two source components. On the one side mafic subcrustal melts and on the other side crustal anatectic melts (e.g. van Bergen et al. 1983, Poli et al. 1984). Therefore the rocks are classified as hybrid rocks between crustal and mantle melts.

From this volcano acidic and mafic rocks were sampled: two trachytes from the basis and the top of the volcano and two latites from a final stage lava flow. Additionally two xenoliths from a trachyte could be analyzed, a latitic and a shoshonitic xenolith.

2.3 Classification of the Investigated Rocks

The investigated rocks have been classified using their chemical and normative composition. According to the subdivision of Le Bas et al. (1986) all rocks are potassic ones with a ratio of K_2O / Na_2O greater than 1. From the potassic rocks ultrapotassic rocks can be separated but the definition of ultrapotassic rocks is still a matter of debate (Carmichael et al. 1974, Foley et al. 1987, Peccerillo 1992). In this paper the term ultrapotassic is used for rocks with the chemical criteria given by Foley et al. (1987): K_2O / Na_2O > 2, K_2O > 3 wt.% as well as MgO > 3 wt.% in order to restrict to mafic rocks.

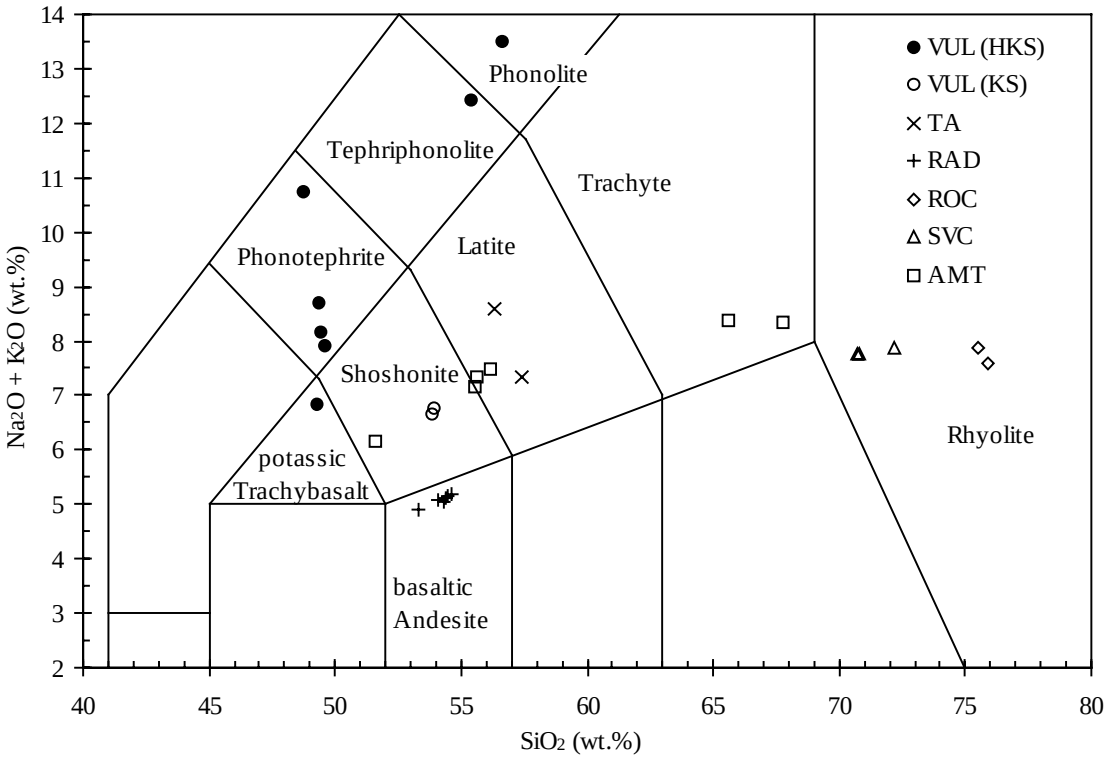

Fig. 2-2: Total alkali-silica diagram for the classification of the rocks according to Le Bas et al. (1986), VUL (HKS): Monti Vulsini, high potassic series, VUL (KS): Monti Vulsini, potassic series, TA: Torre Alfina, RAD: Radicofani, ROC: Roccastrada, SVC: San Vincenzo, AMT: Monte Amiata.

Ultrapotassic rocks occur at Monti Vulsini, Orciatico, Montecatini Val di Cecina, Monte Amiata, and Torre Alfina. These rocks belong to two different types of ultrapotassic rocks. According to Foley et al. (1987) the rocks from Monti Vulsini and Monte Amiata are members of the Roman Province Type. Woolley et al. (1996) suggest the classification of these rocks by either the QAPF diagram (Streckeisen 1979) or the total alkali-silica diagram (Le Bas et al. 1986). The rocks from Orciatico and Montecatini Val di Cecina are lamproites according to the classification schemes of Foley et al. (1987). Their mineralogical composition - major phases are sanidines, olivines, clinopyroxenes, and phlogopites combined

with the lack of plagioclases - is a typical mineral assemblage for lamproites (Mitchell & Bergman 1991, Woolley et al. 1996).

Figure 2-2 shows the classification scheme of Le Bas et al. (1986) for the rocks from Monti Vulsini, San Vincenzo, Roccastrada, Monte Amiata, Radicofani, and Torre Alfina. The rocks of HK series from the Vulsinian mountains are potassic trachybasalts, phonotephrites, tephriphonolites, and phonolites. The K series rocks have lower alkali contents at the same SiO_2 content and are shoshonites. From San Vincenzo and Roccastrada, rhyolites have been sampled. The rocks of Monte Amiata include a wide range of compositions from shoshonites to latites, and trachytes. The sampled rocks from Radicofani are very similar in their chemical composition and petrographically are basaltic andesites.

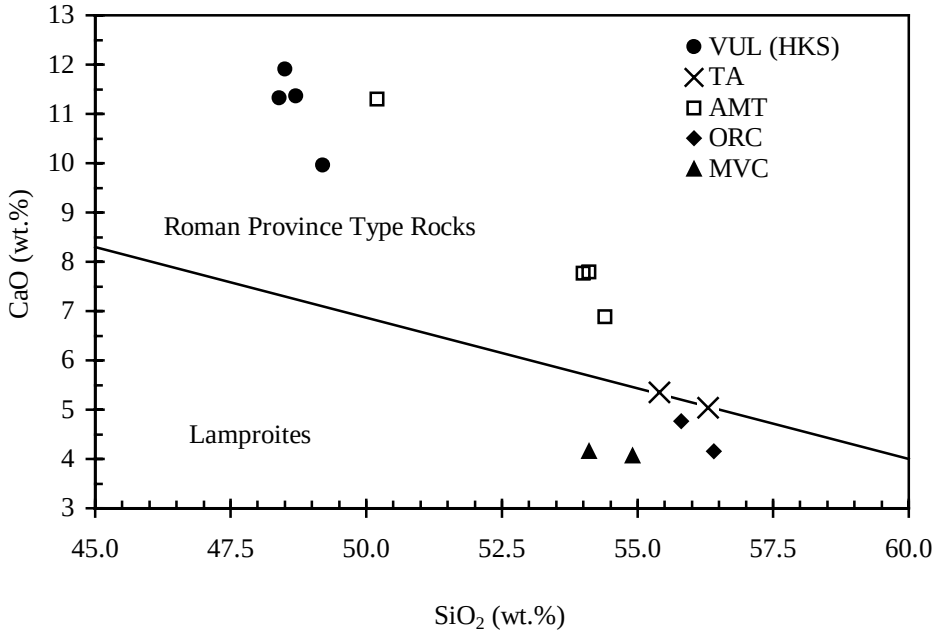

Fig. 2-3: Subdivision of ultrapotassic rocks in a CaO vs. SiO_2 diagram according to Foley et al. (1987). VUL (HKS): Monti Vulsini, high potassic series, TA: Torre Alfina, AMT: Monte Amiata, ORC: Orciatico, MVC: Montecatini Val di Cecina.

In fig. 2-3 one possible subdivision of the ultrapotassic rocks is shown on the basis of their CaO vs. SiO_2 contents (Foley et al. 1987). The rocks from Orciatico and Montecatini Val di Cecina are composed of diopside, sanidine, and phlogopite. Therefore they are classified as diopside sanidine phlogopite lamproites according to Mitchell & Bergman (1991); following the older scheme of Sahama (1974) these rocks are orendites. The rocks from Torre Alfina are a special case. They can be classified as latites according to Le Bas et al. (1986) and Woolley et al. (1996), but their chemical composition is intermediate between lamproites and Roman Province Type rocks (fig. 4-2). Thus Foley et al. (1987) suggest, that these rocks should be

classified as "transitional rocks" between both ultrapotassic types. The Torre Alfina rocks thus will be named transitional rocks in the following discussion.

3 Analytical Methods

3.1 Sample Preparation

One part of each sample was powdered for chemical bulk rock analysis. From the other part thin sections for microscopy and thick sections (about 0.6 - 1 mm) for chemical mineral investigations (electron microprobe and LA-ICP-MS) were prepared. Furthermore thick sections for oxygen isotope ratio analysis have been prepared. Additionally some samples were crushed and the phenocrystals were separated optically or separated by their densities for single grain analysis of oxygen isotope ratios.

3.2 Bulk Rocks Analysis

For bulk rock analysis international reference material (JA-2, JB-3, JR-2; Ando et al. 1989) were analyzed to control the quality of the analytical results.

3.2.1 X-ray Fluorescence Analysis (XFA)

Major elements (Si, Ti, Al, Fe, Mn, Mg, Ca, Na, K and P) and selected trace elements (Ba, Co, Cr, Ga, Nb, Ni, Pb, Rb, Sc, Sr, V, Y, Zn, Zr) were measured with a XFA (Philips PW 1480 automated sequential spectrometer). For analysis the sample powder was melted with Li-borate to glass disks. The detection limit for most trace elements is 5 ppm except for Ba, Ni, Pb, and Zr with 10 ppm. The relative error of the measurement is < 2 % for SiO_2, TiO_2, Al_2O_3, Fe_2O_3, MnO, MgO, CaO, and K_2O, < 7 % for Na_2O and P_2O_5, and < 10 % for the trace elements. The method with the analytical setup of the XFA is described by Hartmann (1994).

3.2.2 C and S Analysis by Infrared Absorption Spectroscopy

C and S were analyzed by infrared detection (ELTRA Metalyt CS 100 / 1000 RF). The rock powder is mixed with Fe and W and then inductively heated up to 1600 °C in an oxygen stream. The released oxidized C and S is finally measured by infrared absorption. Analytical precision (1s) is better than 14 % for S and better than 10 % for C.

3.2.3 H_2O Analysis by the Method of Karl Fischer

H_2O of the samples were measured with the method after Karl Fischer (Scholz 1984) with a Karl Fischer device from Metrohm Herisau Inc.. The relatively error (1s) is better than 10 %.

3.2.4 FeO Analysis

The FeO content of the bulk rock were titrimetrically measured by the method of Pratt (1894) with an analytical precision better than 4 %.

3.2.5 Inductively Coupled Plasma - Mass Spectrometry (ICP-MS)

Additional trace elements (^{7}Li, ^{45}Sc, ^{59}Co, ^{60}Ni, ^{63}Cu, ^{120}Sn, ^{121}Sb, ^{133}Cs, ^{139}La, ^{140}Ce, ^{141}Pr, ^{146}Nd, ^{147}Sm, ^{151}Eu, ^{157}Gd, ^{159}Tb, ^{163}Dy, ^{165}Ho, ^{166}Er, ^{169}Tm, ^{172}Yb, ^{175}Lu, ^{176}Hf, ^{181}Ta, ^{205}Tl, ^{208}Pb, ^{209}Bi, ^{232}Th, ^{238}U) were measured with an ICP-MS (Fisons VG PlasmaQuad PQ 2+). For this analysis the rock powder (ca. 100 mg) was dissolved in 3 ml $HClO_4$ and 6 ml HF at 180 °C (10 h) under pressure. The method of acid dissolution is described by Heinrichs & Hermann (1990). The relative errors (1s) of the analyses are ≤ 30 % for Sn, ≤ 20 % for Co, Ni, and Sb, ≤ 15 % for Hf and Pb and ≤ 10 % for the other trace elements. Internal reference elements were In and Re.

3.3 Analysis of the Mineral Chemistry

From every genetic rock type representative samples were prepared for the analysis of the chemical composition of the minerals.

3.3.1 Electron Microprobe Analysis (EMPA)

For EMPA analysis thick sections (0.5 - 1 mm) were used. On these thick sections the trace element chemistry were also analyzed by LA-ICP-MS.

The analyses were carried out on a JEOL JXA 8900 R electron microprobe using the correction methods of Armstrong (1991).

For major element composition of the minerals Si, Ti, Al, Fe, Mn, Mg, Ca, Ba, Na, and K were analyzed at 15 kV acceleration voltage, 12 nA probe current and a defocussed beam with a diameter of 5 µm. In addition some rock samples have been analyzed for major REE containing phases especially feldspars and phosphates. For this Si, Al, Fe, Ti, Mg, Ca, Na, K, P, La, Ce, Pr, and Nd were measured at 20 kV acceleration voltage, 12 nA probe current and a focussed electron beam. Fe is always expressed as total FeO.

The detection limit can be estimated by three times standard deviation of the background plus the background in counts per second (Reed 1996, Scott et al. 1995). It depends on the composition of the minerals but can generally estimated with 3000 ppm for SiO_2, 1200 ppm for TiO_2, 1800 ppm for Al_2O_3, 1600 ppm for FeO, 1400 ppm for MgO, 500 ppm for CaO, 300 ppm for MnO, 270 ppm for BaO, 1600 ppm for Cr_2O_3, 600 ppm for Na_2O and 450 ppm for K_2O for the major element analyses. For the REE investigation of the apatites the

detection limits are about: SiO_2 7600 ppm, TiO_2 1470 ppm, Al_2O_3 950 ppm, FeO 620 ppm, MgO 530 ppm, CaO 290 ppm, Na_2O 1450 ppm, K_2O 230 ppm, P_2O_5 2.44 wt.%, La_2O_3 580 ppm, Ce_2O_3 700 ppm, Pr_2O_3 1200 ppm, Nd_2O_3 780 ppm. Generally the reproducibility of the measurements is better than 4 %. But element concentrations near the detection limit can have higher errors.

3.3.2 Laser Ablation - Inductively Coupled Plasma - Mass Spectrometry (LA-ICP-MS)

The trace element composition of the phenocrystals were analyzed by a LA-ICP-MS (Fisons VG Plasmaquad PQ 2) with a 266 nm Nd:YAG laser (VG-UV-Microprobe). The trace elements ^{52}Cr, ^{60}Ni, ^{85}Rb, ^{88}Sr, ^{137}Ba, ^{139}La, ^{140}Ce, ^{141}Pr, ^{143}Nd, ^{147}Sm, ^{151}Eu, ^{157}Gd, ^{163}Dy, and ^{172}Yb were measured. ^{29}Si was used as internal reference element. The system was calibrated with NIST SRM 610 and NIST SRM 612 glass disks (Pearce et al. 1997); the glass references were regulary measured for a drift correction - every third to eigth analysis was an analysis of the glass reference material. The detection of the isotopes by the mass spectrometer was carried out in a time resolved modus, so that heterogeneities within a mineral like inclusions could be recognized. The acquisition time was 100 s with a laser repitition rate of 10 Hz and a pit size of 100 µm. Analytical precision (1s) is ≤ 30 % for Cr, Ni, Sm, Gd, Dy, and Yb and ≤ 25 % for Rb, Sr, La, Ce, Pr, Nd, and Eu. The method is described by Simon et al. (1997).

3.4 Oxygen Isotope Analyses by UV Laser Ablation System

3.4.1 Introduction

In the conventional method established by Baertschi & Silverman (1951) and later by Clayton & Mayeda (1963) oxygen is extracted by reaction of a heated sample with fluorine gas or halogene-fluoride gas. In 1990, Sharp (1990) first successfully used an infrared (IR) laser for heating the sample. In both methods a thermally induced chemical reaction between the sample and the F containing gas is used to liberate the oxygen. The advantage of the laser fluorination technique is, that small samples can be analyzed including refractory minerals like olivine, zircon, garnet or kyanite (Elsenheimer & Valley 1992, Mattey & Macpherson 1993, Valley et al. 1994). But because of the heating of the sample by the laser, partial melting occurs around the laser pits generating isotope fractionation (Conrad & Chamberlain 1992, Elsenheimer & Valley 1992, Kirschner et al. 1993, Sharp 1990, Sharp 1992, Young & Rumble 1993). In order to avoid these fractionation effects the sample must completely be vaporized. Therefore in situ analysis are not practicable.

Recently the problem of isotope fractionation was solved by evaporation of the sample with a high energy ultraviolet excimer laser facilitating the in situ analysis of silicate and oxide minerals (Fiebig et al. 1999, Rumble et al. 1997, Wiechert & Hoefs 1995). In contrast to the ablation behaviour of IR lasers, like CO_2 laser, UV lasers liberate oxygen by electronic excitation of the chemical bonds and thus breaking of these bonds (Fiebig et al. 1999). Nevertheless fluorine is necessary for the measurement in order to prohibit the recombination of the vaporized metal atoms with the oxygen. The metal atoms generate fluorides, which are precipitated or frozen out in cold traps like SiF_4.

3.4.2 Sample Pretreatment

In situ measurements have several advantages compared to the analysis of single grains because in situ measurements can show spatial distributions of possible oxygen isotope inhomogeneities within a mineral or rock section. Another reason to use in situ measurements is the grain size. Many samples contain only small grains, which cannot be separated for analysis. Because the minerals can not be fixed within the sample holder the minimun size of single grains is generally about 1 mm • 1 mm • 1 mm. Otherwise the grains are generally shot out of the holder by the laser pulses.

The main problem of in situ measurements of volcanic rocks is the groundmass. It reacts with the fluorine gas without using the laser resulting in the release of oxygen and other impurities like HF and CF_4, which can influence the measurement. Secondary minerals like hydroxides, zeolithes and carbonates are very reactive. Additionally vitreous groundmass and fine grained feldspar (Elsenheimer & Valley 1992) reacts easily with the fluorine. Therefore a pretreatment of the sample is necessary. The aim of any sample pretreatment is the removal of secondary minerals and a reduction of the reaction of vitreous and feldspar containing groundmass with the fluorine gas.

In principle three different methods can be used to reduce the blank. I) The sample can be coated to prohibit a contact between fluorine and sample. The coating material must be transparent to observe the phenocrystal during laser ablation, so that an evaporation of the surrounding groundmass or a sampling of underlaying material can be prohibited. Furthermore the coating material must be resistant against fluorine, should not cause any oxygen fractionation and must not consist of carbon, oxygen or sulphur because these elements influence the analysis. A material which fulfils these requirements has not been found. II) The sample can be passivated by the fluorine itself. The secondary minerals are removed through reaction with the fluorine and the groundmass is protected by the reaction products with the fluorine. Tests have shown, that this method works, but the duration of the sample pretreatment is a disadvantage. III) The third method is a pretreatment with acids. The

disadvantage of this method is, that the success of the etching can only be tested in the sample chamber of the laser ablation device.

A combination of acid pretreatment and passivation was used to prepare the samples for analysis. The etching was carried out in four steps:

1. The rock section is pretreated in acetone or ethanole to remove organic impurities.
2. The sample is etched with HF (10%) for 1 to 6 min in order to dissolve secondary minerals and to produce a coating on the sample surface. The coating is generated by the reaction of the silicates of the groundmass with the HF. Reaction products are fluorine salts and fluorosilicates (Meyer 1926, Meyer & Pietsch 1959, Wiberg 1995). The longer the duration of treatment with HF the better the blank is minimized but the stronger the structure of the rock section is weakened.
3. The third step is an etching with HCl (10 %) for 5 to 15 min. The remaining secondary minerals are solved and the fluorine salts are removed. This is necessary because the fluorine salts are partly hygroscopic and water produces a high blank in the laser ablation system.
4. The sample is cleaned with demineralized water for about 10 to 15 min.

Every cleaning step is done in an ultrasonic bath and between steps 1 to 3 the sample is additionally cleaned with demin. water. The duration of etching depends on the composition of the sample. Generally the higher the content of vitreous or feldspar containing groundmass the longer the sample is treated with acids. After etching the sample is dried within a drying box for at least 1 h and then heated up to 300 °C in a vacuum oven for at least 10 h to remove any adsorbed water.

Single grains were treated in the same way except the HF etching.

After pretreatment of the rock sections or single grains the sample is introduced in the sample chamber. Rock sections are placed on the bottom of the sample chamber without fixing. For individual mineral analyses single grains are put into a holder, a Ni disk with drilled holes. After loading of the sample chamber it is heated (approximately 80 °C) under vacuum for at least 8 h. In addition the sample is passivated to minimize the blank.

Figure 3-1 shows the development of $\delta^{18}O$ values depending on the kind of pretreatment and the duration of passivation. The sample chamber was filled with a rock section and olivine reference minerals ($\delta^{18}O$ = 5.1 ‰). The raised $\delta^{18}O$ values for the reference olivines are generated by the mixing of oxygen from the olivines and blank oxygen from the sample. The rock section, which was only cleaned by water, had to be treated with fluorine for 5 days in order to get a neglegible blank. The pretreatment with HCl reduced the passivation for 2 days.

An additional cleaning step with HF minimized the duration of passivation depending on the time of treatment of the sample with HF.

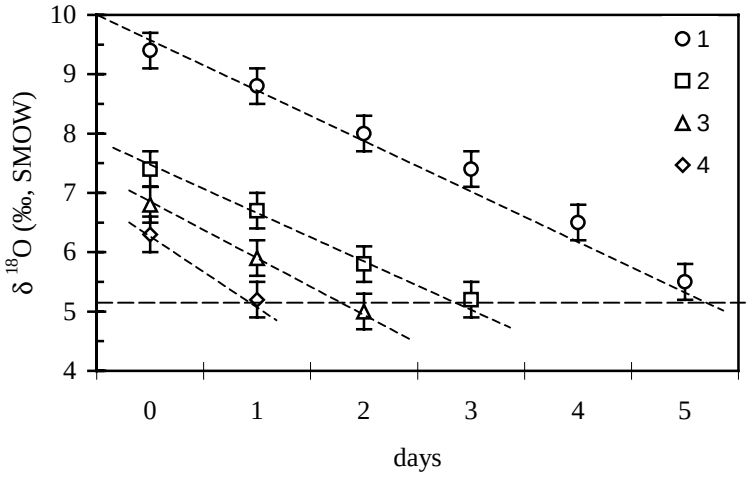

Fig. 3-1: $\delta^{18}O$ values of olivine reference minerals as a function of the time of passivation of a rock section from Torre Alfina. 1) untreated rock section; 2) rock section treated with HCl (10 %) for 4 min.; 3) rock section treated with HCl (10 %) for 4 min. and HF (10 %) for 1.5 min.; 4) rock section treated with HCl (10 %) for 4 min. and HF (10 %) for 3 min. Dashed horizontal line is the true value of the olivine reference minerals (5.1 ‰).

3.4.3 Instrumentation

Because the laser ablation method is still in a stage of development two different devices have been used for the analyses.

The device is built up by a laser, an optical bench to observe the sample and to focus the laser beam, a vacuum extraction line with a fluorine generator and a mass spectrometer. The sample chamber, made of stainless steel, has a volume of 20 cm^3 and an inner diameter of 2 cm.

Pure fluorine gas is neccessary for the ablation process in order to prohibit the recombination of evaporated metal atoms with the released oxygen gas. The fluorine gas is produced by heating a K_3NiF_7 salt within a nickel vessel to 400 °C. At 200 °C K_3NiF_7 reacts to K_2NiF_6 • KF and impurities are pumped away. At 400 °C K_3NiF_6 and F_2 is generated (Asprey 1976). The fluorine is then condensed in a cold finger at liquid nitrogen temperature. At the end of one measurement day the surplus fluorine is reacted back in the nickel vessel to K_3NiF_7.

Two different UV excimer lasers were used. A KrF laser (Lextra 200 excimer laser, Lambda Physik Inc.) radiating at 248 nm and an ArF laser (Compex 205 excimer laser, Lambda Physik Inc.) radiating at 193 nm. The used parameters of the lasers are 10 - 25 Hz and 220 - 400 mJ per puls for the ArF laser and 10 - 25 Hz and 300 - 580 mJ per puls for the KrF laser.

3.4.4 Conversion of Oxygen to CO_2

This technique has been described in detail by Wiechert & Hoefs (1995) with the modifications of Fiebig et al. (1999). An ArF laser was employed.

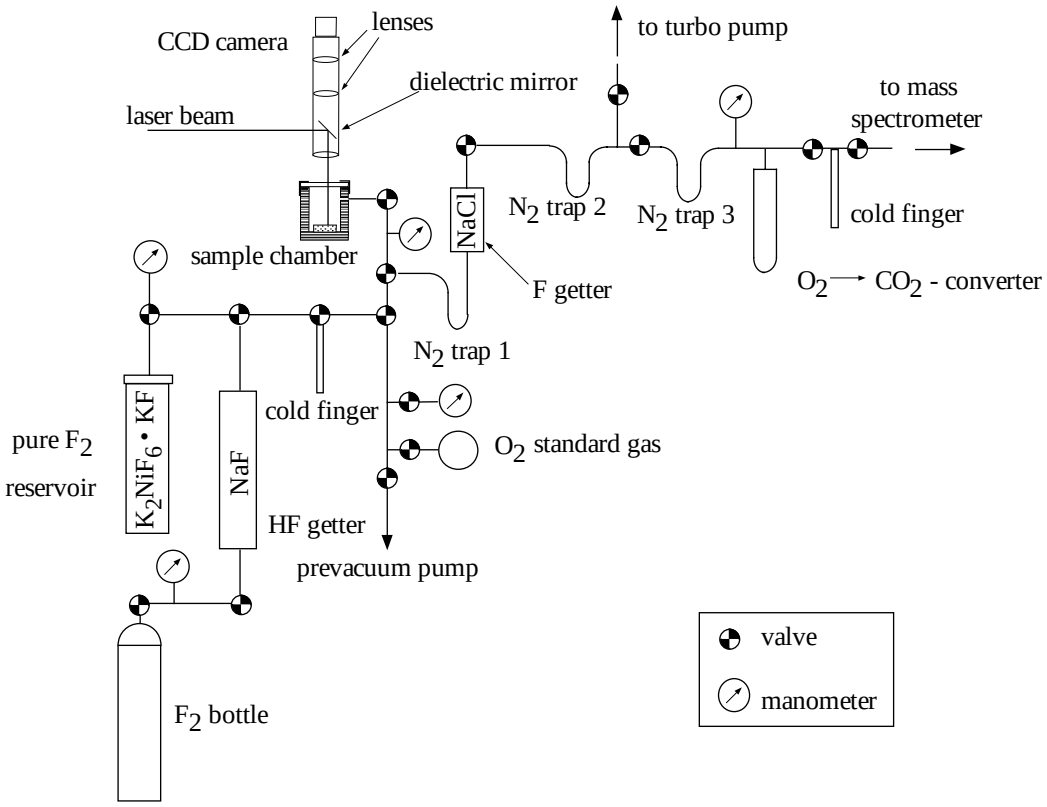

Fig. 3-2: Schematic outline of the gas extraction and fluorine delivery system modified after Wiechert & Hoefs (1995).

For the ablation process the sample chamber is filled with 30 to 50 mbar fluorine. The amount of vaporized oxygen is limited by the vacuum line and the mass spectrometer. In order to prohibit large fractionation effects within the gas lines 3 to 5.5 µmol O_2 were produced. After the ablation of the sample under a fluorine atmosphere, gaseous impurities like SiF_4 and HF are frozen out in a cold trap at liquid nitrogen temperature. Then the surplus fluorine is reacted to chlorine and solid NaF over heated NaCl. Afterwards the chlorine is frozen out in a nitrogen cold trap. The generated oxygen is converted to CO_2 with heated diamonds and then fixed in a cold trap. The O_2 have to be converted to CO_2 because the mass spectrometer (Finnigan MAT 251) cannot detect O_2 but CO_2. After fixing the CO_2 the sample gas is heated to room temperature and analyzed by the mass spectrometer.

During daily analysis the laser line showed sometimes a shift to smaller $\delta^{18}O$ values. This shift can be explained by fractionation effects within the vacuum line probably occuring by the conversion of O_2 to CO_2. The values were therefore corrected by a regular measurement of reference minerals.

3.4.5 Direct Measurement of Oxygen Without Conversion

The laser fluorination device without O_2 conversion is the next stage of development compared to the device described above. Because another mass spectrometer (Delta Plus, Finnigan) has been used O_2 can directly be measured without conversion to CO_2. This method has been applied with an ArF and a KrF laser.

This device is similar to the device described above. But behind the F getter an U-tube of a known volume is set. After laser ablation the released oxygen is expanded in this U-tube. An aliquot of the gas is then purged with He over a molesieve 5Å, GC and open split into the mass spectrometer (Fiebig et al. 2000). Compared to the system with CO_2 conversion this method needs less fluorine (5 - 15 mbar) and less amounts of the sample must be evaporated (down to 300 nmol O_2).

3.4.6 Accuracy of the Oxygen Isotope Measurements

Reference minerals have been used to guard against unexpected errors such as leaks and for data correction. As reference minerals olivines (FIN 9506-1, 5.1 ‰ - Wiechert, personal information), garnets (UWG-2, 5.8 ‰ - Valley et al. 1995), and quartz (Dörentrup, 12.1 ‰ - see Fiebig et al. 1999) have been analyzed.

The error (1s) of the isotope ratio measurements using the method with O_2 conversion is ± 0.2 - 0.3 ‰ and the standard deviation for the method without O_2 conversion is ± 0.3 ‰.

3.5 Oxygen Isotope Analyses by CO_2 Laser Ablation System

Selected mineral grains were also analyzed by a CO_2 laser ablation system.The analyses were carried out by B. Hagen at the University of Bonn. The CO_2 laser ablation system in Bonn also works with fluorine gas and oxygen is directly measured by a mass spectrometer (ANCA-SL 20-20 Stable Isotope Analyser, Europa Scientific Inc.). The device is described by Hagen (2000).

3.6 Comparison of the Different Methods for Oxygen Isotope Ratio Measurement

Selected rock samples were analyzed by the three different methods of oxygen isotope ratio measurement - UV laser ablation system with O_2 conversion to CO_2, the direct measurement of oxygen and the CO_2 laser ablation system - in order to control the correctness of the individual methods.

In tab. 3-1 the analytical results of the different methods are compared. They correspond well to each other.

Tab. 3-1: Comparison of the results of the different methods of oxygen isotope ratio measurement (n = number of analyses, n.a. = not analyzed).

sample	mineral	UV laser with O_2 conversion		UV laser without O_2 conversion		CO_2 laser without O_2 conversion	
		$\delta^{18}O$ (‰)	n	$\delta^{18}O$ (‰)	n	$\delta^{18}O$ (‰)	n
VUL 9701	cpx	8.7 ± 0.3	3	9.0 ± 0.3	5	9.1 ± 0.2	2
Montefiascone	plg	n.a.		11.8 ± 0.4	3	11.5 ± 0.1	2
Montefiascone	cpx	7.5 ± 0.3	4	7.7 ± 0.3	5	7.3 ± 0.3	3
Montefiascone	ol	6.7 ± 0.4	6	6.7 ± 0.4	7	7.1 ± 0.4	3
ORC 9701	ol	n.a.		7.2 ± 0.3	3	7.2 ± 0.1	2
ROC 9701	san	12.3 ± 0.2	3	12.4 ± 0.3	6	12.5 ± 0.2	2
AMT 9701	san	12.4 ± 0.2	6	12.6 ± 0.3	4	12.5 ± 0.1	2
AMT 9704 B	cpx	9.0 ± 0.3	5	9.1 ± 0.3	2	8.8 ± 0.2	2

4 Results

The volcanic rocks of central Italy are characerterized by a large diversity within a narrow area. As mentioned in chapter 1 the sampled rocks can be assigned to five different genetic types:

1. mantle derived melts of the Roman Magmatic Province occuring at the Vulsinian mountains,
2. lamproitic mantle melts of the Tuscan Magmatic Province,
3. crustal anatectic rocks of the Tuscan Province,
4. transitional rocks between Roman and Tuscan mantle melts, and
5. hybrid rocks representing mixtures between mantle and crustal melts.

For a better comparison of the results, rocks from the different localities have been embraced into three groups, I) mantle derived rocks, II) crustal derived rocks and III) hybrid rocks between crustal and mantle melts.

Major and trace element composition of the bulk rocks has been analyzed for all samples. Because the oxygen isotope analyses are the major aspect of this work nearly all samples have been investigated. Only some samples could not be analyzed because of the small grain size of the phenocrystals.

Additionally the mineral chemistry of some samples has been analyzed. Representative rock samples from each genetic type have been selelected as well as less and highly evolved rocks from the Vulsinian mountains. An overview of the applied analytical methods is shown in table 4-1.

Tab. 4-1: The different analytical methods used are summarized (+ applied on the sample). (LA-SIRMS: laser ablation – stable isotope ratio mass spectrometry, EMPA: electron beam microprobe analysis, LA-ICP-MS: laser ablation – inductively coupled plasma – mass spectrometry).

Locality	Sample	Bulk Rock	Mineral Analysis		
		Chemical Composition	O-Isotope Ratios	Chemical Analysis	
			LA-SIRMS	EMPA	LA-ICP-MS
Monti Vulsini	VUL 9701	+	+	+	+
	VUL 9702	+	+	+	+
	VUL 9703 A	+	+		
	VUL 9703 B	+	+	+	+
	VUL 9704	+	+		

Locality	Sample	Bulk Rock	Mineral Analysis		
		Chemical Composition	O-Isotope Ratios	Chemical Analysis	
			LA-SIRMS	EMPA	LA-ICP-MS
Monti Vulsini	VUL 9705	+	+	+	+
	VUL 9706	+			
	VUL 9707	+	+	+	+
	Montefiascone	+	+	+	
Orciatico	ORC 9701	+	+	+	+
	ORC 9702	+			
Montecatini Val di Cecina	MVC 9701	+			
	MVC 9702	+			
Torre Alfina	TA 9701 bulk rock	+	+	+	+
	TA 9701 peridot. xenolith		+	+	+
	TA 9701 crustal xenolith		+		
Radicofani	RAD 9701	+	+	+	+
	RAD 9702 A	+	+	+	+
	RAD 9702 B	+	+		
	RAD 9703	+	+		
	RAD 9705	+	+		
	RAD 9706	+	+		
Roccastrada	ROC 9701	+	+	+	+
	ROC 9702	+	+		
San Vincenzo	SVC 9701	+	+		
	SVC 9702	+	+	+	+
	SVC 9703	+	+	+	+
Monte Amiata	AMT 9701	+	+		
	AMT 9702	+	+	+	+
	AMT 9703 I	+	+		
	AMT 9703 II	+	+	+	+
	AMT 9704 A	+	+	+	+
	AMT 9704 B	+	+		

The analytical results are summarized in tabular form in the appendix.

4.1 Mantle Derived Rocks

4.1.1 Introduction

For a discussion of the mantle composition beneath central Italy the most primitive rocks are important. In general primitive rocks are charaterized by high Mg values, high Ni-, and Cr-contents and a narrow SiO_2 concentration in tectonic regimes, for example oceanic plates, where low pressure evolution and interaction with the crust is negligible (Sun & McDonough 1989). But in the case of potassic continental volcanics, where a metasomatized mantle is considered as a potential source, the identification of primitive magmas using the traditional geochemical parameters is at least problematically (Peccerillo 1994, Wilson 1995). In order to deduce the composition of the mantle the investigation should be focused on the less modified rocks. Rogers et al. (1985) suggested rocks with MgO > 6 wt.% and CaO > 8 wt.% as the least evolved rocks for the Roman Province.

Mantle derived melts are common in the Roman Province and thus are also common in the Vulsinian mountains. But they are often modified by processes like crystal fractionation and assimilation of crustal material. According to Civetta et al. (1981) two different rock suites can be distinguished in the Roman Province, a high potassic series (HKS) with SiO_2 undersaturated rocks and a potassic series (KS) with SiO_2 saturated rocks. Major phases of the rocks are olivine, clinopyroxene, and plagioclase and additionally leucite in the evolved rocks of the HK series.

Mantle melts in the Tuscan Province occur as lamproites at Orciatico and Montecatini Val di Cecina. They can be classified as sanidine clinopyroxene phlogopite lamproites according to the classification proposals of Woolley et al. (1996) and Foley et al. (1987).

These two kinds of mantle melts - the Roman Province Type rocks and the Tuscan Province lamproites - represent two endmembers. Between these endmembers mixtures occur, which are classified as transitional rocks on a petrogenetic basis. Rocks from Torre Alfina and Radicofani are assumed to belong to those transitional rocks (Peccerillo et al. 1987).

Rocks from Torre Alfina display a clear affinity to the lamproites because of their chemical and mineralogical composition: the assemblage of olivine, clinopyroxene, sanidine, and phlogopite (Conticelli 1998). However their chemical composition is not identical with the lamproitic compositon. Thus there is no common agreement on the petrographical classification of these rocks (e.g. Conticelli 1998, Peccerillo et al. 1987). According to Foley et al. (1987) the rocks are classified as transitional rocks between Roman Province Type rocks and lamproites on the basis of their chemical composition (short: transitional rocks).

The rocks from Radicofani show an intermediate composition between the Roman Province rocks and the Tuscan Province lamproites. They can be assigned to the shoshonitic association (Poli et al. 1984). Major phenocrystals are olivines, clinopyroxenes and plagioclases (Innocenti 1967, Poli et al. 1984).

4.1.2 Whole Rock Chemistry

Both rock series, HKS and KS, occur at the Vulsinian mountains. The subdivision of the series used differs slightly from the suggestions of Civetta et al. (1981). Rocks of the HKS are SiO_2 undersaturated with K_2O > 4.5 wt.% and K_2O / Na_2O > 2. Petrologically they range from potassic trachybasalts to phonotephrites, tephriphonolites and finally phonolites with olivines, clinopyroxenes, plagioclases, and leucites as major minerals depending on the degree of evolving stage. In contrast rocks of the KS are SiO_2 saturated and contain less K_2O (< 4.5 wt.%) with a lower K_2O / Na_2O ratio (< 2). From this series shoshonites were sampled. Major minerals are olivine, clinopyroxene and plagioclase.

The less evolved rocks from the Vulsinian mountains contain relatively high Al_2O_3 (13.7-15.5 wt.%) and CaO (10 - 11.3 wt.%) contents. The general trend of increasing SiO_2 with an increase in K_2O, Na_2O, and Al_2O_3 and a decrease of MgO, CaO, and $Fe_2O_{3(tot)}$ can be explained by fractional crystallization and crustal assimilation processes.

Compared to lamproites from elsewhere the central Italian lamproites are SiO_2 rich - between 54.1 and 56.4 wt.% and quartz normative - and have a low K_2O / Na_2O ratio of 3.5 - 4.4; generally lamproite ratios lie above 5 (Mitchell & Bergman 1991). They are neither peralkaline (molar (K_2O + Na_2O) / Al_2O_3 = 0.8 - 1.0) nor perpotassic (molar K_2O / Al_2O_3 = 0.87 - 0.8). But the chemical composition is similar to the composition of the Spanish lamproites (Venturelli et al. 1984a). Further geochemical features are the low Al_2O_3, CaO, and Na_2O contents compared to the less evolved rocks from the Roman Province.

Tab. 4-2: Chemical composition of some major and trace elements for selected, less evolved, mantle derived rock samples from the three different genetic types: Roman Province rocks from the Vulsinian mountains, Tuscan Province lamproites from Orciatico, transitional rocks from Torre Alfina and Radicofani. (*) For comparison the chemical composition of a MORB is shown (Schilling et al. 1983).

Oxides (wt.%)	Roman Prov. Type – HKS Montefiascone	Roman Prov. Type – KS VUL 9703 A	Tuscan Province ORC 9701	Transitional Rocks TA 9701	Transitional Rocks RAD 9706	MORB*
SiO_2	48.9	53.4	57.2	56.0	52.8	50.55
TiO_2	0.647	0.734	1.386	1.332	0.986	1.31
Al_2O_3	13.83	15.61	11.11	12.98	16.30	16.38
Fe_2O_3	3.01	2.00	1.84	0.89	3.86	1.27
FeO	3.73	3.87	3.16	4.90	3.08	7.76
MnO	0.135	0.126	0.085	0.094	0.119	0.16
MgO	10.47	7.02	8.74	8.76	8.39	7.80
CaO	11.44	9.55	4.21	5.41	8.30	11.62
Na_2O	1.92	2.35	1.48	0.97	1.66	2.79
K_2O	4.85	4.23	7.85	7.57	3.19	0.09
H_2O	0.84	0.36	2.18	0.45	1.03	0.29
Σ	100.0	100.1	100.0	100.0	100.0	100.0
Elements (ppm)						
Cr	850	312	506	560	496	278
Ni	239	158	362	370	193	132
Rb	299	306	521	443	182	0.96
Sr	1140	552	629	726	356	106.4
Ba	803	401	1163	1285	650	10.7
La	80	65	147	111	52	2.73
Sm	11	9.5	32	24	11	3.23
Eu	2.3	1.7	4.6	4.5	2.3	1.12
Yb	2.0	2.7	1.9	2.2	2.4	0.96

Two samples have been collected from the Torre Alfina volcano, one sample from the type A lavas (TA 9701) and one from the type B lavas (TA 9702). The major element chemistry is similar to the lamproites but with higher Al_2O_3 and CaO contents.

From Radicofani less evolved rocks have been sampled, which can be classified as basaltic andesites. The rocks are SiO_2 oversaturated (quartz normative) and have relatively low K_2O contents (2.99 - 3.29 wt.%). The K_2O / Na_2O ratios (1.5 - 1.9) are lower than those in the

lamproites or in less evolved rocks from the Vulsinian mountains. Major element concentrations of the Radicofani rocks lie between the values of the lamproites from Orciatico and Montecatini on the one hand and the less evolved rocks from the Vulsinian mountains on the other hand.

A common feature of all rocks is a high enrichment of LREE, high LREE / HREE ratios, a negative Eu anomaly and a flat curve of enrichment for the HREE (fig. 4-1 and 4-2). Vulsinian rocks however show a relatively steep gradient in the LREE (La, Ce, Pr) whereas the lamproites and the transitional rocks from Torre Alfina and Radicofani display a flat curve of enrichment.

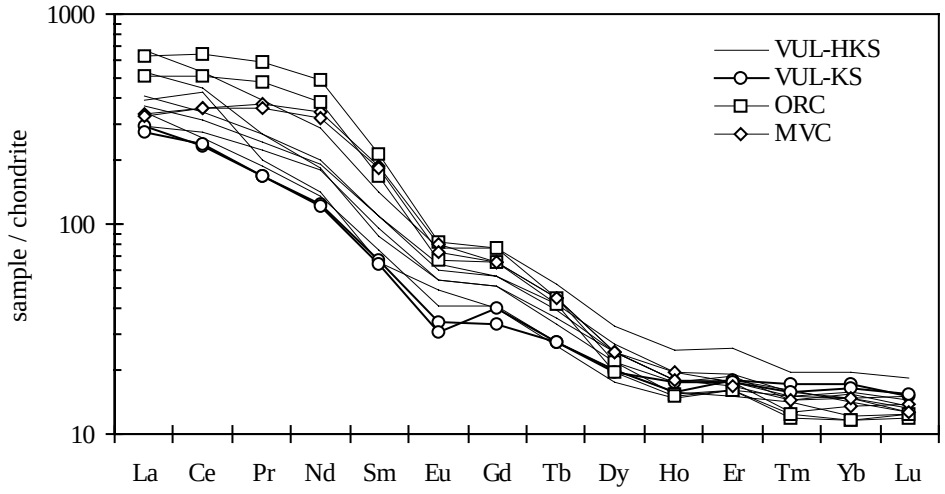

Fig. 4-1: Chondrite normalized REE patterns of the Vulsinian rocks (VUL) from the Roman Province and the lamproites from the Tuscan Province (ORC: Orciatico, MVC: Montecatini Val di Cecina). Normalizing values are taken from Anders & Grevesse (1989).

The lamproites are more enriched in HREE and middle REE than the less evolved rocks from the Vulsinian mountains. In addition HKS rocks from the Vulsinian mountains are more enriched in LREE and middle REE than the KS rocks. For the Torre Alfina rocks the degree of enrichment is the same as for the lamproites but the Radicofani rocks show an enrichment of REE similar to the KS rocks from the Vulsinian mountains.

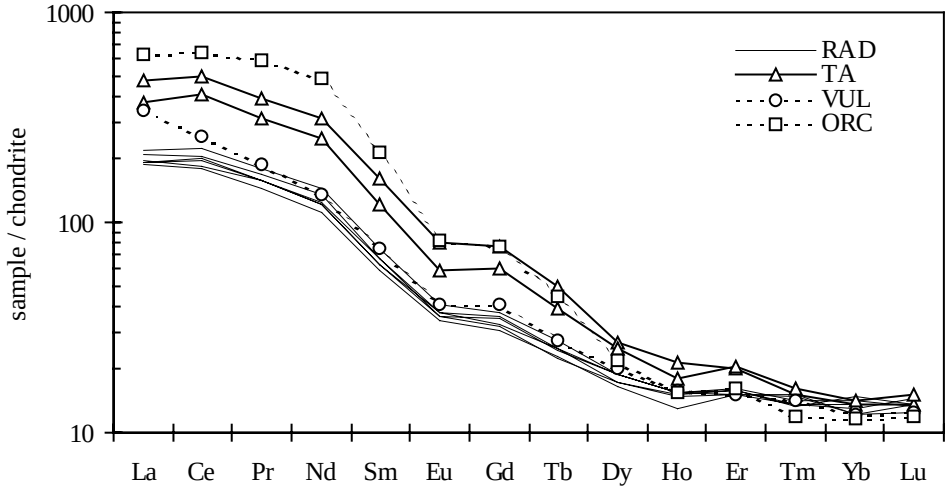

Fig. 4-2: Chondrite normalized REE patterns of the transitional rocks between Roman Province type rocks and Tuscan Province lamproites. RAD: basaltic andesites from Radicofani, TA: rocks from Torre Alfina; for comparison are also shown: VUL: less evolved rock sample from the Vulsinian mountains, ORC: lamproite sample from Orciatico (normalizing values are taken from Anders & Grevesse 1989)

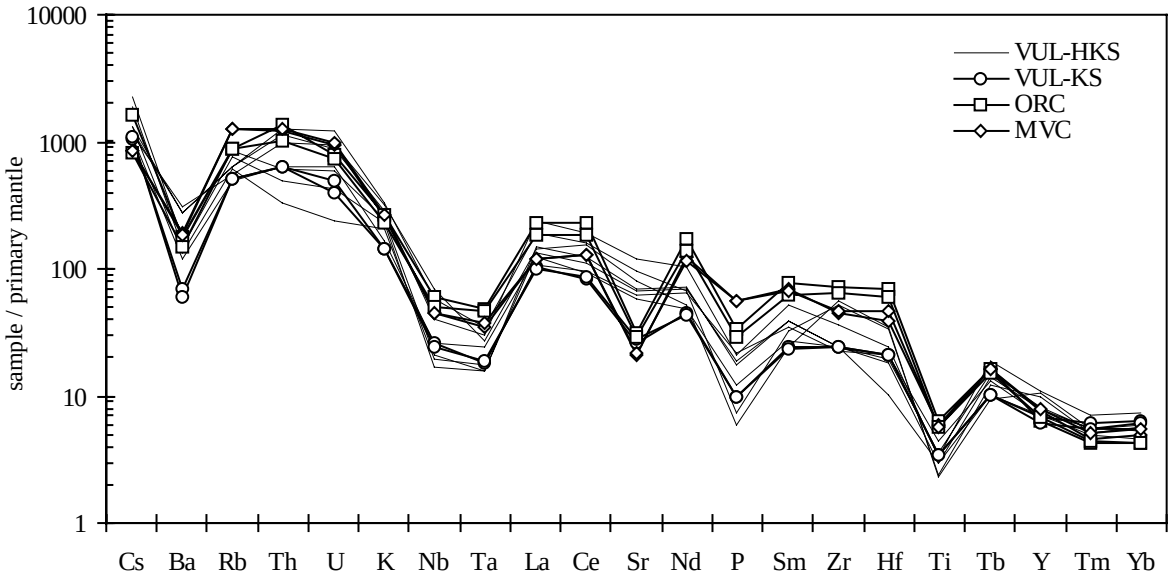

Fig. 4-3: Multi element diagram of the Vulsinian rocks and the lamproites, element concentrations are normalized to primary mantle (values of McDonough & Sun 1995). VUL: Vulsini, ORC: Orciatico, MVC: Montecatini Val di Cecina.

Other common features of the mantle derived rocks from central Italy are high enrichments of LILE and high LILE / HFSE ratios. Multi element diagrams (fig. 4-3 and 4-4) are typical for crustal or crustally influenced rocks (e.g. Wilson 1995). Rocks from different localities display a similar multi element pattern. Generally a decrease of enrichment is observed in the

order of lamproites > Torre Alfina rocks > less evolved rocks from the Vulsinian mountains > Radicofani rocks.

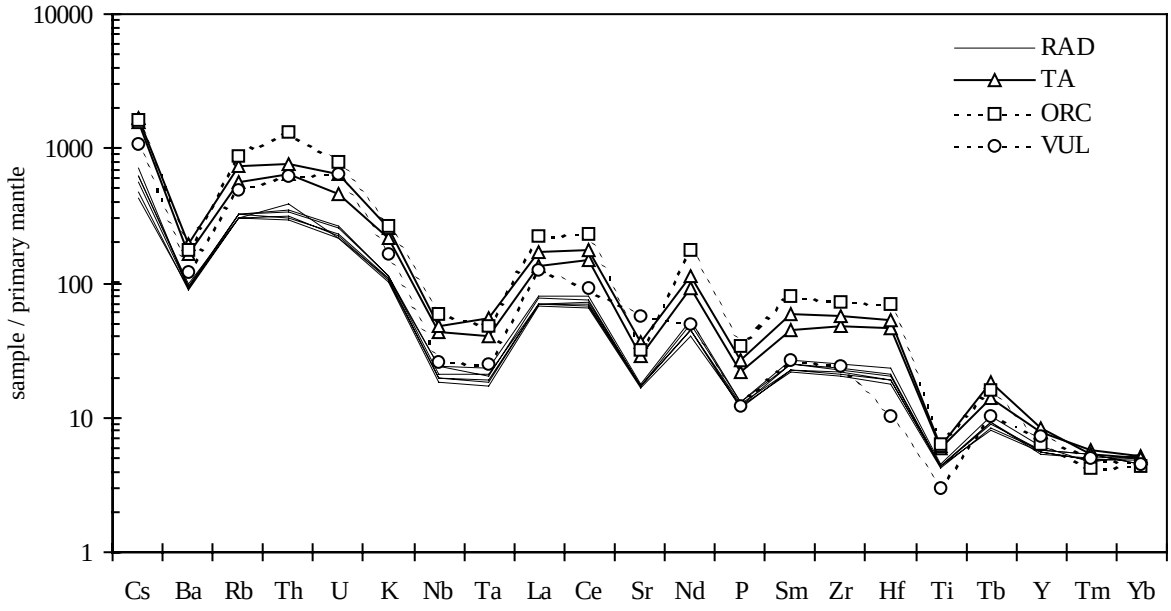

Fig. 4-4: Multi element diagram of transitional rocks, element concentrations are normalized to primary mantle (values of McDonough & Sun 1995). RAD: Radicofani, TA: Torre Alfina, for comparison are also shown a less evolved rock sample from the Vulsinian mountains (VUL) and a lamproitic sample from Orciatico (ORC).

4.1.3 Mineral Chemistry

Mineral chemistry has been investigated on selected samples from each genetic type. The selected samples are shown in table 4-1.

From the Vulsinian Mountains rock samples from the HK series and the K series have been analyzed. From the HK series less, intermediately and highly evolved rocks have been investigated. Major phenocrystalline phases in the less evolved rocks are olivine, clinopyroxene, and plagioclase and additionally leucite in the highly evolved rocks. As a representative of the lamproites the sample ORC 9701 has been analyzed. From Torre Alfina a rock sample from the type A lavas has been investigated. This sample contains an embedded ultramafic xenolith, so that both - the bulk rock and the xenolith - have been analyzed. From Radicofani two samples have been selected.

4.1.3.1 Olivines

In all mantle derived rocks olivines occur. Their chemical composition is shown in tab. 4-3 for representative samples.

Olivines only occur in the less evolved rocks of the HKS from the Vulsinian mountains. The cores are forsteritic (fo91-fo92) with increasing fayalite component to the mineral rim (fig. 4-5). FeO / MgO ratios of the olivines approximately are in equilibrium with the bulk rock using the experimentally determined partitioning coefficients of Roeder & Emslie (1970). CaO contents vary between 0.46 and 0.59 wt.% and MnO between 0.12 and 0.29 wt.%. CaO / MgO ratios do not fit with any of the trends for olivines of potassic igneous suites reported by Ferguson (1978). They have, however, similar compositions to olivines from other localities of the Roman Province (Federico et al. 1994).

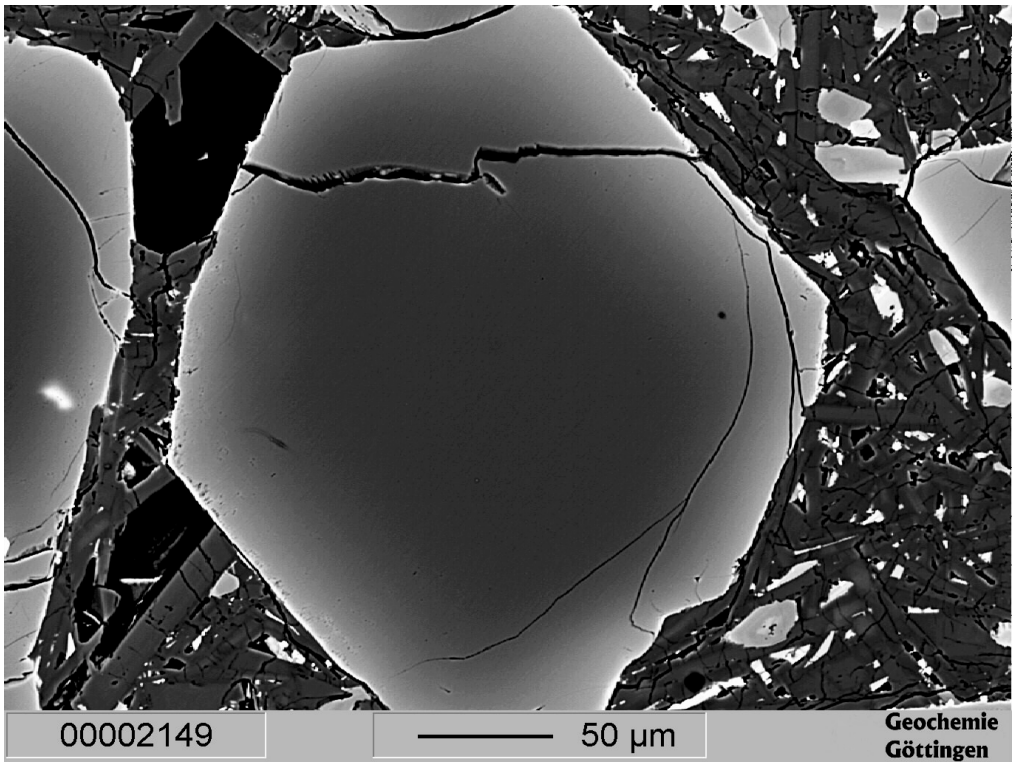

Fig. 4-5: EMPA picture (composition mode) of an olivine from the Vulsinian mountains, K series (VUL 9703 B)

Olivines from the KS are homogeneous with lower MgO contents (fo86 - fo90), CaO between 0.30 - 0.37 wt.% and a greater variability of MnO contents (≤ 0.50 wt.%). Like olivines of the high potassic series they show an increasing fayalitic component to the rim. The forsteritic component decreases to fo76 with increasing MnO and no significant change of the CaO content. The REE content is below the detection limit of the LA-ICP-MS.

Tab.4-3: Comparison of representative olivine analyses from different rock types. HKS: Vulsinian mountains, HK series; KS: Vulsinian mountains, K series; ORC: lamproite from Orciatico, RAD: Radicofani; TA-px: Torre Alfina, peridotitic xenolith (b.d.l.: below detection limit of the EMPA).

wt.%	HKS	KS	ORC	RAD	TA-px
SiO_2	40.4	40.7	39.5	37.8	40.9
FeO	10.53	10.13	16.90	25.20	9.42
MgO	48.3	49.4	44.4	37.7	49.1
CaO	0.377	0.349	0.116	0.242	b.d.l.
MnO	b.d.l.	b.d.l.	0.296	0.407	b.d.l.
fo component	89	90	82	72	90

Olivines from the lamproites show a larger compositional range (fo79 - fo90) than the Vulsinian olivines with a continuously increasing fayalitic component to the mineral rim. CaO and MnO increase sympathetically with decreasing MgO. Trace elements in olivines are homogeneously composed with high LREE / HREE ratios due to the high LREE / HREE ratio of the bulk rock. The HREE are often below the detection limit.

In the case of the Torre Alfina rocks the chemical similarity of the phenocrystals of the whole rock to the olivines of the ultramafic xenolith supports a xenocrystic origin of the phenocrystals by disintegration of ultramafic xenoliths. Olivines of the ultramafic xenolith contain a narrow range of forsterite composition of fo89 - fo90 with low CaO (< 0.121 wt.%) and MnO (below detection limit of the electron microprobe) contents. They display no chemical zonation but the olivines at the boundary to the host lava show a reaction rim with slightly higher CaO (~ 0.12 wt.%) and lower forsteritic contents (fo84 - fo86). The low CaO and MnO concentrations are typically for high pressure olivines (Simkin & Smith 1970). Olivines of the bulk rock have a similar composition with an additional reaction rim. The rim is also higher concentrated in FeO and CaO. The REE content of the olivines of the ultramafic xenolith is mostly below the detection limit of the LA-ICP-MS. For olivines of the host rock the LREE could be sometimes measured with 0.01 fold bulk rock concentration.

In the Radicofani rocks olivines are homogeneously composed with a forsteritic component of 66 - 74 mol%, which is lower than in mantle melts from other localities. Olivines of the sample RAD 9702 A show secondary alteration processes - iddingsite was produced at the outer parts of some small olivines in the groundmass (Innocenti 1967). Generally the REE contents were below the detection limit. Only in some olivines the REE concentrations could

be measured showing a higher depletion of the LREE than the HREE compared to the bulk rock concentration.

4.1.3.2 Clinopyroxenes

Pyroxenes are classified according to the scheme of Morimoto (1989). Some representative analyses are shown in tab. 4-4.

Tab. 4-4: Comparison of representative clinopyroxene analyses from different rock types. HKS: Vulsinian mountains, HK series; KS: Vulsinian mountains, K series; ORC: lamproite from Orciatico, RAD: Radicofani; TA-px: Torre Alfina, peridotitic xenolith (b.d.l.: below detection limit of the EMPA).

wt.%	HKS	KS	ORC	RAD	TA-px
SiO_2	52.0	52.4	54.0	51.1	53.3
TiO_2	0.419	0.496	0.585	0.759	0.657
Al_2O_3	3.14	3.37	0.56	3.77	1.22
FeO	3.96	4.08	3.58	4.66	4.19
MgO	16.0	16.4	18.0	16.7	16.9
CaO	23.7	23.6	22.4	21.5	22.5
MnO	b.d.l.	b.d.l.	b.d.l.	0.162	b.d.l.
Cr_2O_3	0.419	b.d.l.	0.776	1.042	0.473
Na_2O	0.199	0.207	0.162	0.161	0.106

From the Vulsinian mountains HKS clinopyroxenes are diopsides whereas KS clinopyroxenes range from a diopsidic to an augitic composition. Oszillatory zoning is a common feature of these minerals (fig. 4-7, fig. 4-8). Sometimes inherited, Fe-rich, and patchy zoned cores are observed within the clinopyroxenes (fig. 4-6, fig. 4-9). Resorption edges are also visible in some minerals. As typically found in clinopyroxenes from the Roman Magmatic Province, the tetrahedral site is filled only with Si and Al, with significant Al in the M1 site and a Ca deficiency in the M2 site (Bindi et al. 1999, Caggianelli et al. 1990, Cellai et al. 1994, Dal Negro et al. 1985, De Fino et al. 1986). The Ca content of the HKS clinopyroxenes increase with increasing Fe content up to 52 mol% wollastonite component. Na and Ti contents of the clinopyroxenes are variably with a negative correlation between Mg and Ti for the HKS clinopyroxenes. Clinopyroxenes with similar Mg / (Mg + Fe) ratios of both series have similar Ti and Al^{IV} contents indicating a similar pressure regime of crystallization (Thompson 1974, Tracy & Robinson 1979, Vieten 1980, Wass 1979).

A

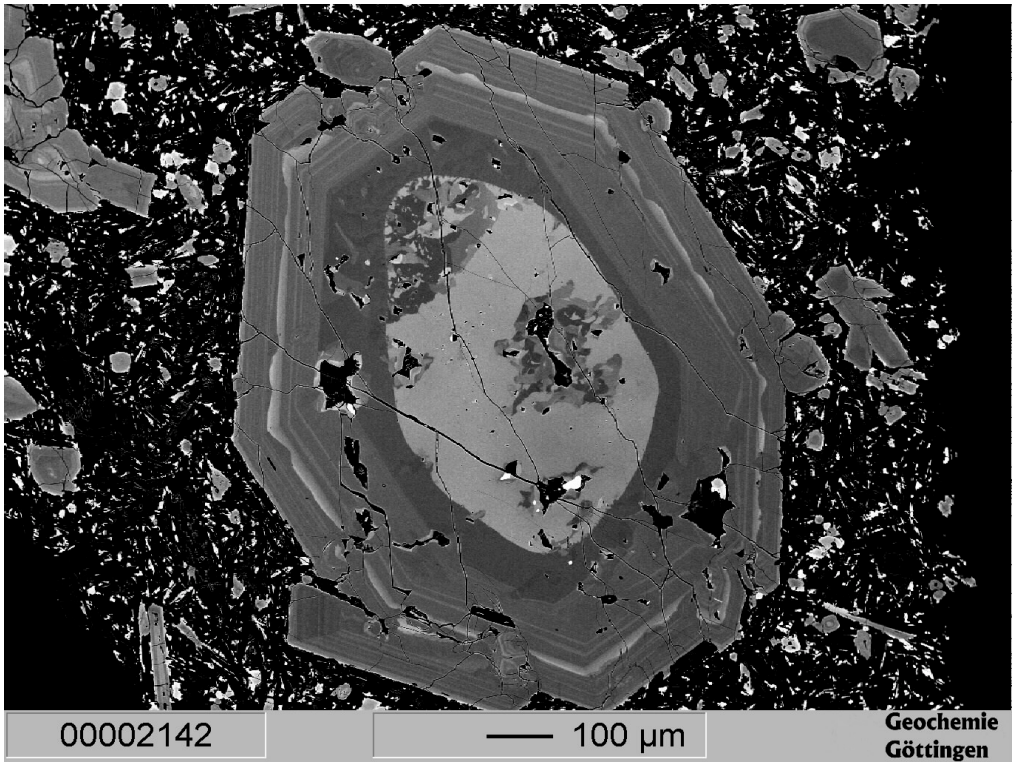

B

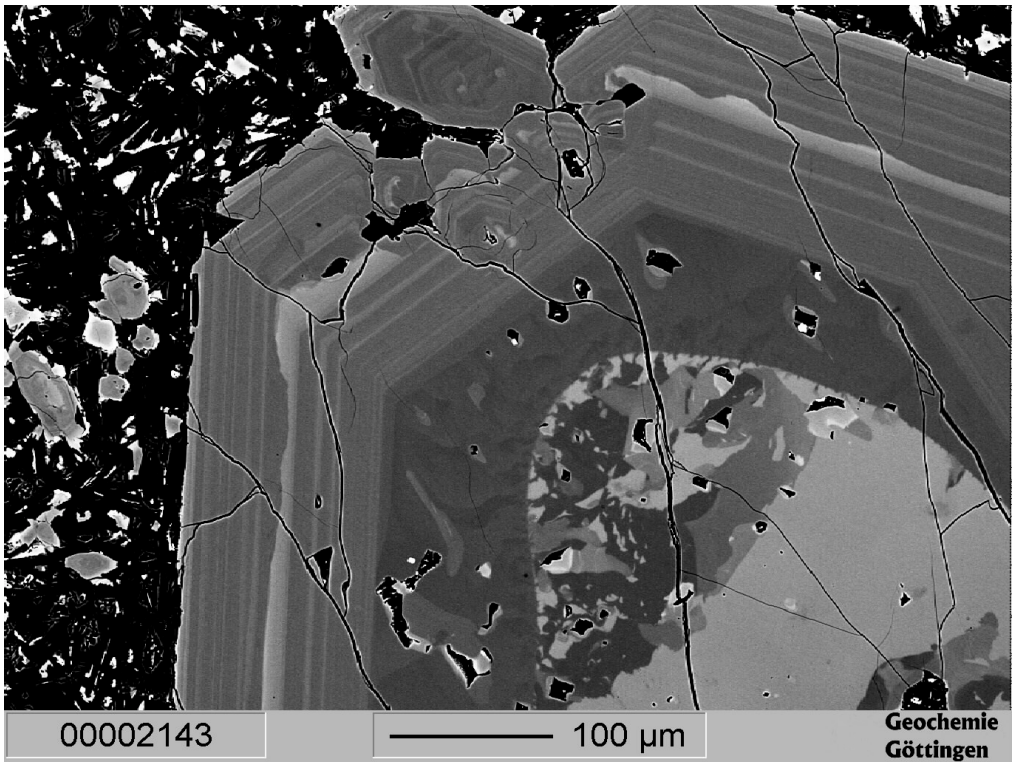

Fig. 4-6: EMPA images (composition mode) of clinopyroxenes from the Vulsinian mountains, K series (VUL 9703 B); A: overview, B: detail.

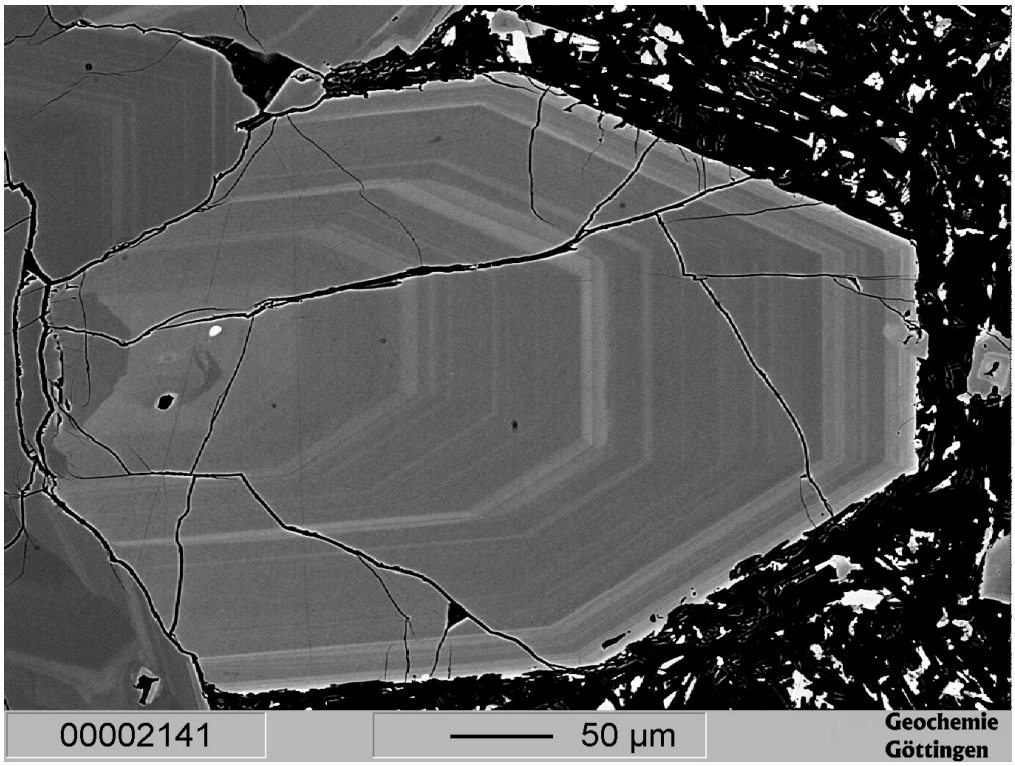

Fig. 4-7: EMPA image (composition mode) of a clinopyroxene from the Vulsinian mountains, K series (VUL 9703 B).

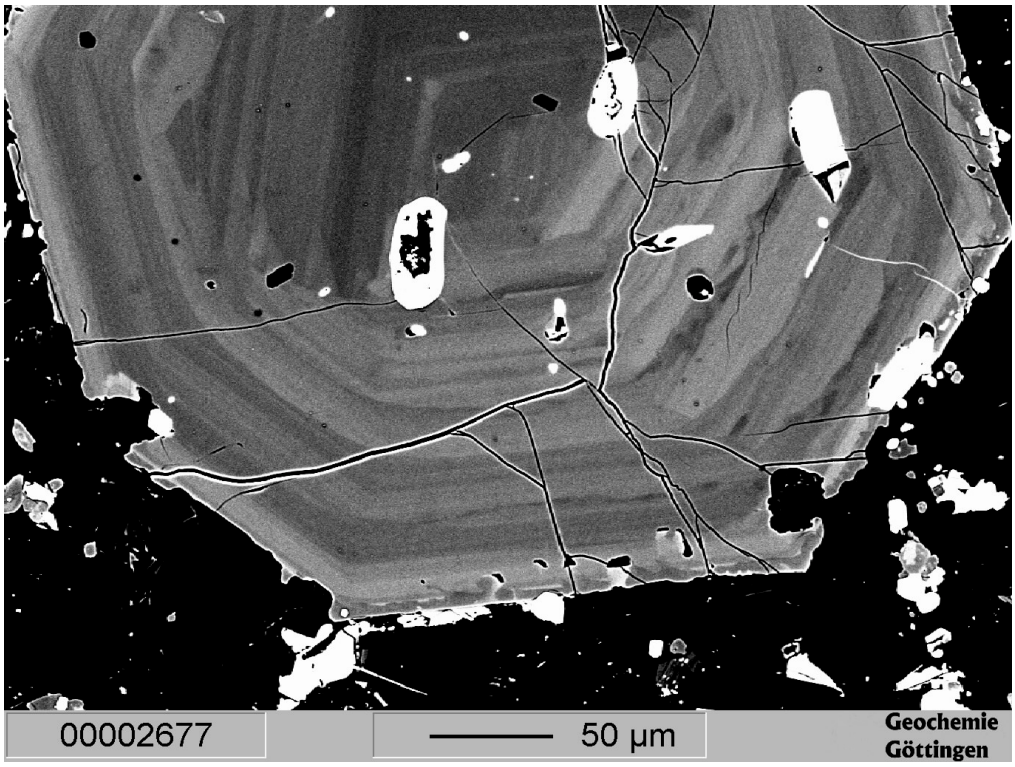

Fig. 4-8: EMPA image (composition mode) of a clinopyroxene from the Vulsinian mountains, HK series (VUL 9701).

A

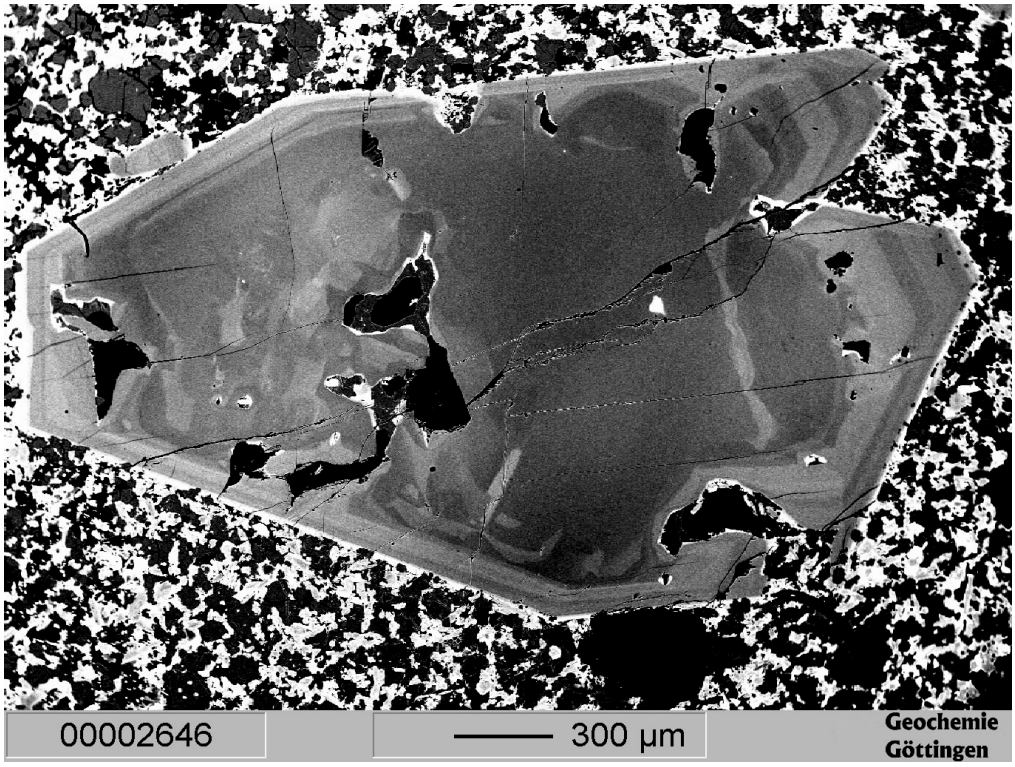

B

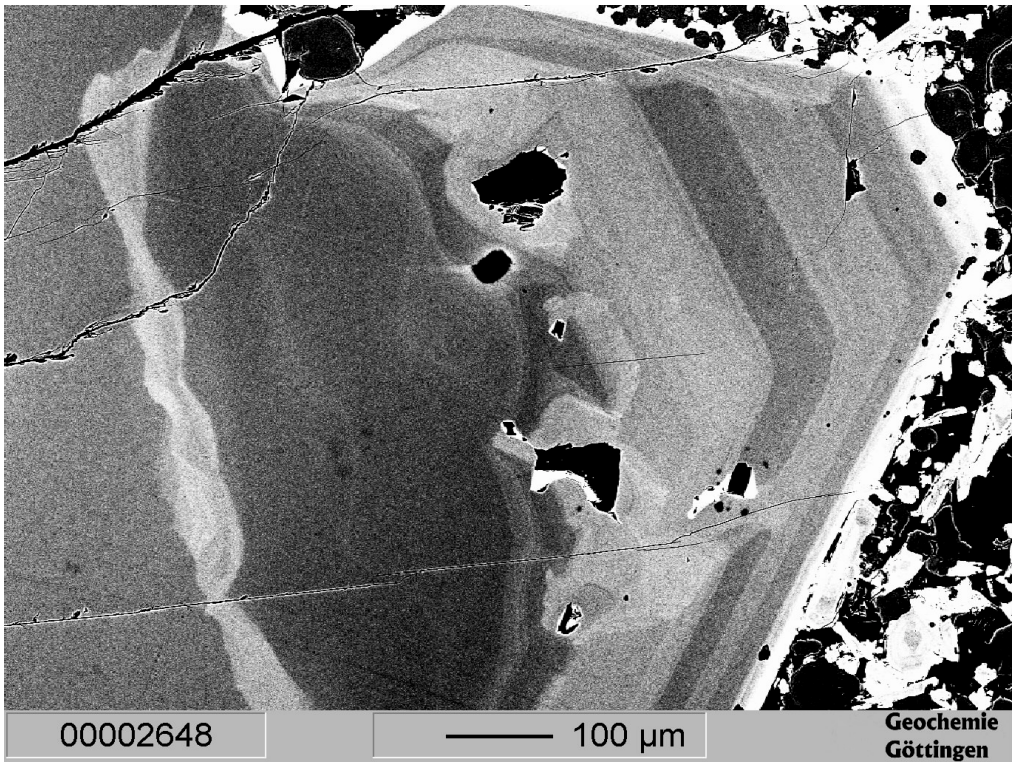

Fig. 4-9: EMPA images (composition mode) of clinopyroxenes from the Vulsinian mountains, HK series (VUL 9705); A: overview, B: detail.

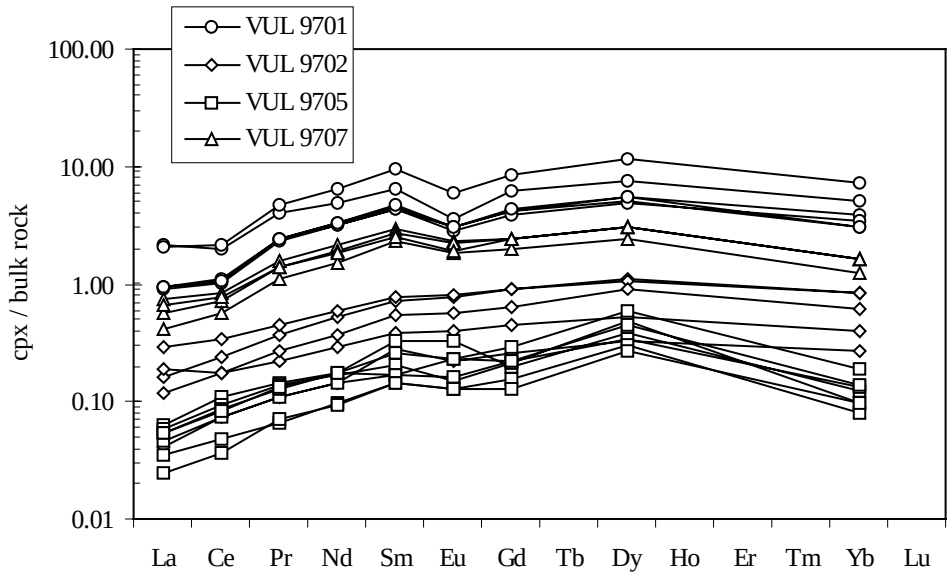

Fig. 4-10: REE patterns of clinopyroxenes from HKS rocks from Monti Vulsini normalized to bulk rock data. Mg values of the bulk rock: VUL 9701: 27, VUL 9702: 51, VUL 9705: 65, VUL 9707: 28.

Cr, Ni, Rb and Ba contents are low or beneath the detection limit of the electron microprobe or LA-ICP-MS whereas Sr concentrations between 50 and 860 ppm were found for HKS clinopyroxenes. Contrary KS pyroxenes have higher Cr contents. For all Vulsinian rocks clinopyroxenes are partly enriched or depleted in the REE normalized to bulk rock (fig. 4-10, fig.4-11). The REE_{cpx} / $REE_{bulk\ rock}$ ratios generally increase with increasing atomic number. The highest enrichment of REE is found in the more evolved rocks with lower Mg values. Additionally some clinopyroxenes show a minor negative Eu anomaly.

Clinopyroxenes from the lamproites are diopsides and are characterized by high Mg values of 84 - 92. They display a weak oscillatory zoning. Compared to Vulsininan clinopyroxenes they contain less Al contents (Al_2O_3 < 0.83 wt.%). Si and Al are not sufficient to fill the T site completely, which is a characteristic feature of clinopyroxenes from lamproitic magmas (Jaques et al. 1984, Mitchell & Bergman 1991, Mitchell et al. 1987). The tetrahedral site deficiency can be compensated by Ti^{4+} or Fe^{3+} (Cellai et al. 1994). Also the Ca deficiency in the M2 site is higher compared to Roman Province clinopyroxenes. In contrast to Roman Province clinopyroxenes they show a rough negative correlation between Ca and Fe.

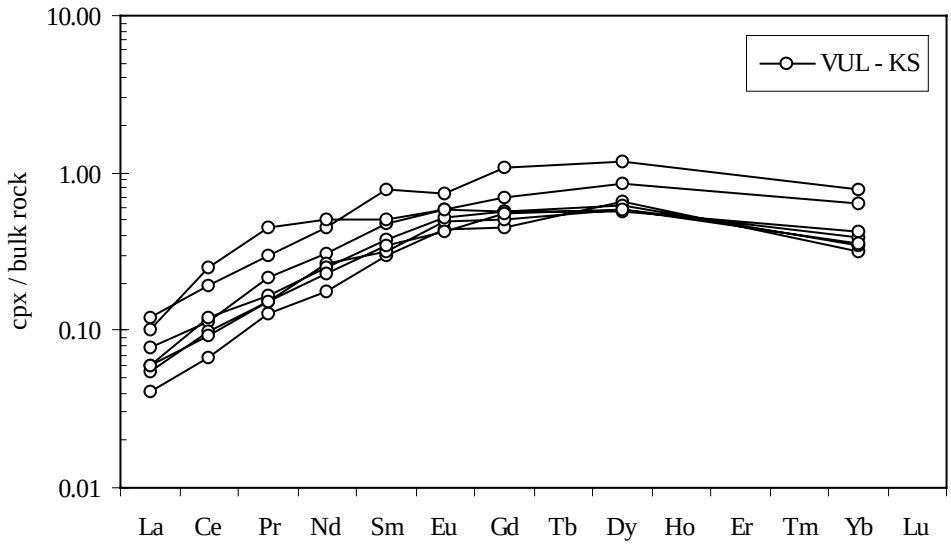

Fig. 4-11: REE patterns of clinopyroxenes from KS rocks from Monti Vulsini normalized to bulk rock data.

Cr_2O_3 contents are below 0.92 wt.% and Ni concentrations range between 60 - 150 ppm. The chondrite normalized REE patterns display a higher enrichment of LREE than HREE with a peak at Nd. These patterns are generated by the REE pattern of the bulk rock what can also explain the negative Eu anomaly. Remarkable is that the clinopyroxenes can be subdivided into two groups with different degrees of depletion of the REE compared to bulk rock data (fig. 4-12). But there is no other difference between these two groups, neither in the major element concentration nor in the shape of the trace element pattern. The major element chemistry clearly points to a melt origin of the clinopyroxenes (Conticelli et al. 1992), so that a xenocrystic origin can be excluded.

Clinopyroxenes of the ultramafic xenolith from Torre Alfina display an augitic to diopsidic composition (wo43 - wo46, en48 - en51). Their chemical composition - low Na_2O, TiO_2, and Al_2O_3 contents - is typically for ultramafic xenoliths from Torre Alfina (Conticelli & Peccerillo 1990). The LREE are more enriched than the HREE with about 100 times chondritic values for La and 20 times chondritic values for Yb. Additionally they display a negative Eu anomaly.

Clinopyroxenes of the bulk rock from Torre Alfina show a slightly oscillatory zoning. Their chemical composition is similar to the clinopyroxenes of the ultramafic xenolith. For the whole rock suite from Torre Alfina Conticelli (1998) found a range of clinopyroxene compositions from lamproitic to Roman Province type clinopyroxenes with the more lamproitic clinopyroxenes in the type A lavas. The analyzed rocks in this work display clinopyroxenes with an intermediate composition. Al and Si are sufficient to fill the

tetrahedral site completely, what is a characteristic feature of the Roman type clinopyroxenes. Contrary the Ca deficiency of the M2 site is higher than for Roman type clinopyroxenes and is in the range of lamproitic clinopyroxenes.

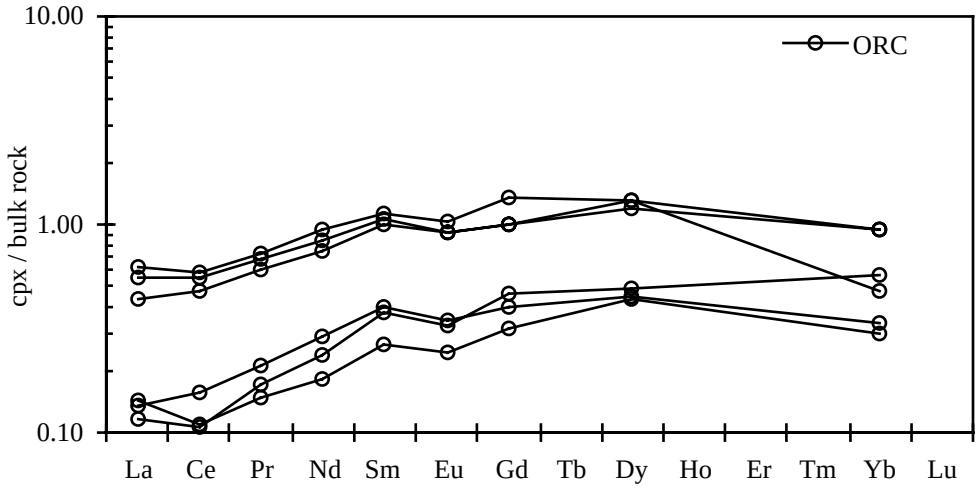

Fig. 4-12: REE patterns of clinopyroxenes from the Orciatico lamproite normalized to bulk rock data.

The Radicofani clinopyroxenes are homogeneously composed showing only weak oscillatory and sometimes patchy zoning. They are augites with an enstatite component of 43 - 53 mol% and wollastonite of 39 - 45 mol%. Si and Al are sufficient to fill the tetrahedral site completely with minor amount of Al in the M1 site as it is typically for Roman Province type rocks (Bindi et al. 1999, Caggianelli et al. 1990, Cellai et al. 1994, Dal Negro et al. 1985, De Fino et al. 1986). But the Ca deficiency in the M2 site for the Radicofani clinopyroxenes is higher and comparable to the Orciatico lamproites. A correlation for Mg and Ti as well as for Ca and Fe, as being typical for Roman Province clinopyroxenes, could not be found. The Cr_2O_3 content is high up to 1.4 wt.%. The homogeneous composition is also reflected by the REE concentrations. Normalized to the bulk rock composition the HREE are only slightly and the LREE are more depleted. The negative Eu anomaly of the augites can be caused by different oxidation stages of Eu.

4.1.3.3 Orthopyroxenes

Orthopyroxenes only occur in the ultramafic xenolith from the Torre Alfina lava. They are homogeneously composed and do not show any zonation. The orthopyroxenes are enstatites (en88 - en89, wo ~ 2) with Cr_2O_3 of 0.449 - 0.579 wt.% and Al_2O_3 of 3.56 - 3.77 wt.%.

4.1.3.4 Alkali Feldspars

K feldspar in the Vulsinian rocks only occur as phenocrystals in the phonolite. They are homogeneously composed with a slight increase of Si and Na and a decrease of Al, Ca, Ba, and, K from the core to the rim. Alkali feldspars of the phonolite range from sanidine to hyalophane with 49.2 - 59.6 mol% orthoclase and 4.9 - 9.3 mol% celsian component.

Sanidine is a groundmass phase of the lamproites and is homogeneously composed with or77 - or80 and FeO concentrations between 0.48 and 0.95 wt.%. Compared with the sanidines of the Roman Province the lamproitic feldspars contain less Na_2O and BaO and higher K_2O. The sanidine composition is typically for lamproites (Mitchell & Bergman 1991). The REE patterns of the sanidines show a great variability of enrichment, which is caused by enclosed apatites. The apatites are highly enriched in REE so that small amounts of apatite can overprint the REE patterns of the sanidines. Using distribution coefficients of Francalanci et al. (1987) and Wörner et al. (1983) a maximum content of apatite of about 1.5 wt.% in the sanidines can be calculated.

Sanidines are also common phases of the groundmass of the Torre Alfina lavas. They are comparable to the lamproitic sanidines with high orthoclase contents (or80 - or83), low Na_2O (~ 1.4 wt.%) and CaO (0.8 - 1.4 wt.%) concentrations as well as low BaO concentrations (below the detection limit of the electron microprobe). The REE content of the sanidines is heterogeneous what may be caused by inclusions of apatites as it is observed for the Oricatico lamproites.

In the Radicofani rocks sanidines are absent.

4.1.3.5 Plagioclases

In the Vulsinian rocks plagioclase is a common phase of the groundmass and occurs sometimes as larger crystals (mm-scale). The anorthite content of the plagioclases from the different Vulsinian rocks range between 76 - 95 mol% for the HKS and 45 - 84 mol% for the KS, respectively. Besides the lower anorthite content KS plagioclases differ from HKS plagioclases by lower Fe contents. Minerals of both series are charaterized by high Sr (0.18 - 1.1 wt.%) and relatively high Ba contents (170 - 4000 ppm). The plagioclases show the feature that LREE are more enriched than HREE resulting in a continuously decreasing curve. The HREE are sometimes below the detection limit. All plagioclases show a positive Eu anomaly. Sometimes the plagioclases display an uncommen REE pattern, which is caused by embedded apatites with high REE concentrations. The amount of apatite, which is neceassary to produce the uncommon REE patterns of the plagioclases, can be calculated. For this calculation the REE concentrations of the plagioclases is computed using the bulk rock

concentrations of REE and the distribution coefficients of Wörner et al. (1983). A maximum amount of 2 wt.% apatite enclosed in the plagioclases may be responsible for the REE patterns.

Plagioclases from the Radicofani rocks occur as small laths and display a weak oscillatory zoning. The anorthite component ranges between 69 - 87 mol%. Ba concentrations are between 70 - 190 ppm and Sr between 450 - 1000 ppm. Therefore they are depleted in Ba and Sr compared to Roman Province plagioclases. Normalized to the bulk rock the REE with the exception of Eu are depleted in the plagioclases. The HREE are often below the detection limit. Sometimes analysis of plagioclases were distorted by enclosed apatites containing high REE concentrations.

Lamproites as well as the Torre Alfina rocks do not contain plagioclases.

4.1.3.6 Leucites

Leucites only occur as phenocrystals in the evolved rocks of the HK series from the Vulsinian mountains. In the less evolved rocks they are only present as a groundmass constituent. The minerals are rather homogeneous in composition. Low FeO and high Na_2O contents are a characteristic feature of Roman Province leucites (Conticelli et al. 1997). The leucites contain low REE concentrations with an enrichment of LREE and a depletion of HREE relative to chondritic values. The HREE are often below the detection limit. But the analyses are often influenced by enclosed apatites. Another feature is the varying Rb, Sr, and, Ba content of the leucites from different localities of the Vulsinian mountains.

4.1.3.7 Micas

According to Deer et al. (1996) the distinction between biotites and phlogopites has been carried out on the basis of Mg / Fe ratios. Phlogopites contain Mg / Fe > 2 and biotites < 2.

Phlogopites are common minerals of lamproites but are rarely found in the Roman Province type rocks. Only sample VUL 9702, a phonotephrite, contains phlogopite in the groundmass. Phlogopites display dissolution processes at their crystal rim pointing to a xenocrystic origin. Compared to lamproitic micas Vulsinian phlogopites contain lower TiO_2, BaO, and SiO_2 and higher Al_2O_3 contents. Low Ti contents and low K / Al ratios indicate a high pressure (Foley 1990), although differentiation may also affect the mica composition. Si and Al are sufficient to fill the tetrahedra site and K + Na are also sufficient to fill the interlayer site, completely. In summary the phlogopites have preserved their characteristic features of a higher pressure origin compared to lamproitic micas but probably are of xenocrystic origin.

Phlogopites from the Orciatico lamproite are fairly homogeneous in their composition with minor core - rim variations and a BaO decrease to the mineral rim (fig. 4-13). They have high

concentrations of TiO_2, BaO, and MgO and low contents of SiO_2, Al_2O_3, and Cr_2O_3. The content of K + Na is not sufficient to fill the interlayer sites completely. Low K and Na contents are typical for lamproitic phlogopites but the Si and Al contents are high enough to fill the tetrahedral site completely - what is uncommon for lamproitic phlogopites (Conticelli et al. 1992, Wagner & Velde 1986). Mitchell et al. (1987) believed, that a negative correlation of Al and Ti is a specific characteristic feature of the evolution of micas in lamproites. In contrast the Orciatico phlogopites show a weak positive correlation between both elements, what is also observed in Spanish lamproites (Venturelli et al. 1988). Venturelli et al. (1988) and Conticelli et al. (1992) suggested the bulk rock composition to be the important factor controlling the behaviour of Al, Fe, Mg and Ti in the micas. With regard to the physico-chemical conditions of crystallization Ti solubility in phlogopite is considered to depend on pressure (Trönnes et al. 1985, Foley 1990), whereas K / Al ratios reflect variations in oxygen fugacity (Foley 1989). Therefore the phlogopites from Orciatico crystallized in a narrow p-T range at relatively low pressure and high temperature (Conticelli et al. 1992).

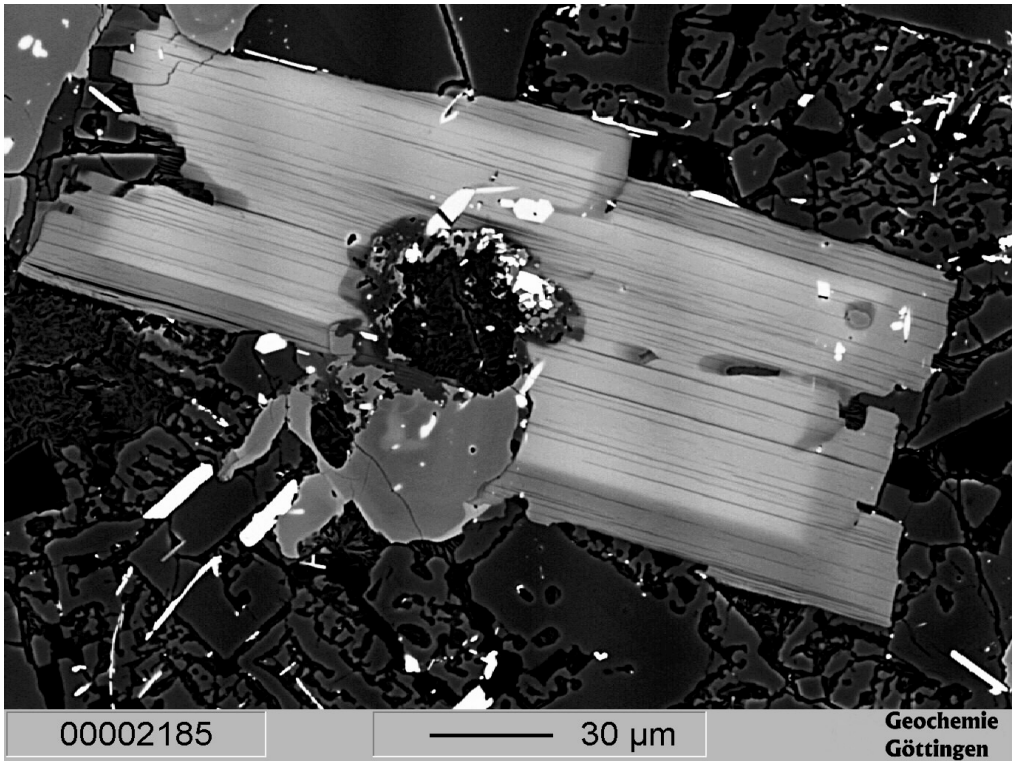

Fig. 4-13: EMPA image (composition mode) of a phlogopite from Orciatico lamproite (ORC 9701).

Micas of the ultramafic xenolith from Torre Alfina are phlogopites with only a minor chemical variation. Compared to phlogopites in lamproites from Oricatico the micas from the ultramafic xenolith contain similar contents of SiO_2, lower concentrations of TiO_2 and FeO and higher concentrations of Al_2O_3 and Cr_2O_3. But their chemical composition still falls in the range of mantle phlogopites (Conticelli & Peccerillo 1990). Normalized to chondritic

values REE are enriched with a higher enrichment of the LREE than the HREE. But compared to the REE contents of the host rock the phlogopites of the ultramafic xenolith contain the same abundance of REE. In contrast to micas from the ultramafic xenolith micas from the bulk rock can be subdivided into two groups. The first group are phlogopites with same or similar composition of the ultramafic xenolith phlogopites. The phlogopites show resorption edges and reaction rims with the surrounding melt. These features indicate a xenocrystic origin of the micas resulting from the disintegration of ultramafic xenoliths. The second group of micas are more variable in composition and have a biotitic composition. For these micas a crystallization within the magma can be assumed. The TiO_2 content is similar to the lamproitic phlogopites whereas the SiO_2 and Al_2O_3 contents and K / Al ratios correspond to phlogopites from Roman Province type rocks. Biotites are higher enriched in REE than phlogopites of the ultramafic xenolith. Additionally LREE / HREE ratios of the biotites are higher.

4.1.3.8 Oxides

Oxides of the HKS are Ti-magnetite with variable ulvöspinel and magnesioferrite content. Some samples display spinels with a narrow range in composition whereas other rocks have oxides with a wider range. Oxides of the KS are spinels with a lower magnetite content or magnesioferrite and spinel sensu stricto.

In the Orciatico lamproites oxides are represented by ilmenite and spinel. Ilmenites contain relatively high MgO contents whereas spinels are characterized by high FeO and high Cr_2O_3 concentrations and are believed to represent a liquidus phase (Conticelli et al. 1992).

Spinel is a common oxide in the ultramafic xenolith from Torre Alfina. It is Cr_2O_3 (54.7 - 58.3 wt.%) and FeO (17.6 - 22.0 wt.%) rich. Spinels of the bulk rock are Cr_2O_3 (63.8 - 65.7 wt.%) and FeO (10.1 - 14.2 wt.%) rich, too. Additionally ilmenites occur in the lavas.

In the Radicofani rocks ilmenite and spinel occur in the groundmass.

4.1.3.9 Apatites

Apatite is a common component in the Tuscan and Roman rocks. REE analysis of feldspars from the Vulsinian mountains and the Orciatico lamproites were distorted by enclosed apatites. In order to calculate the influence of apatites on the REE analysis of the feldspars the concentration of La, Ce, Pr, and Nd of the apatites were measured. Apatites from both rock types - lamproites and Roman Province type rocks - contain high REE concentrations, e.g. up to 1.24 wt.% Ce_2O_3 for the Vulsinian rocks and up to 1.76 wt.% Ce_2O_3 for the lamproites.

4.1.4 Oxygen Isotopes

From the Vulsinian mountains clinopyroxenes were analyzed in all samples and, when possible, plagioclase and olivine, too. Olivines only occur in the KS samples and in the less evolved sample from the HKS (sample Montefiascone). HKS clinopyroxenes display a positive trend of increasing $\delta^{18}O$ values with increasing SiO_2 content of the bulk rock from 7.6 ‰ up to 8.9 ‰. The observed range of $\delta^{18}O$ values nearly coincides with the range of 7.8 - 9.4 ‰ for primary $\delta^{18}O$ values of the Vulsinian rocks suggested by Holm & Munksgaard (1982). With 7.4 - 7.6 ‰ KS clinopyroxenes display the same values as the less evolved sample of the HKS indicating the same $\delta^{18}O$ values of the source. But KS clinpyroxenes show a large variation in oxygen isotope ratios ranging from 6.9 to 8.3 ‰. This inhomogeneity may be a result of some enclosed old inherited clinopyroxene cores, which may differ in their $\delta^{18}O$ composition from the other clinopyroxenes. But these cores were too small to be analyzed.

$\delta^{18}O$ values of olivines of the less evolved HKS rock are 6.7 ‰ and for the KS rocks 7.0 ‰ and 7.1 ‰, respectively. These and the clinopyroxene values are too high for a melt derived from a primary unmodified mantle (Harmon & Hoefs 1995, Hoefs 1997, Mattey et al. 1994). Normal mantle values for olivines are about 5.2 ‰ (Hoefs 1997, Mattey et al. 1994). Oxygen isotope fractionations between olivines and clinopyroxenes agree with the high temperatures of the melts (Chiba et al. 1989, Zheng 1993).

Plagioclases from Vulsinian rocks display $\delta^{18}O$ values from 9.5 to 12.1 ‰. Only the plagioclases of the sample VUL 9701 with 9.6 ‰ are in isotopic equilibrium with the clinopyroxenes (8.9 ‰). The fractionation of $\delta^{18}O$ values between clinopyroxenes and plagioclases of the two samples VUL 9705 and Montefiascone are too large for magmatic processes indicating a disequilibrium (Chiba et al. 1989, Matthews et al. 1983, Zheng 1993). Therefore the isotopic composition of the plagioclases may have changed during secondary low temperature processes.

The case of plagioclase clearly shows that it is necessary to analyze phenocrystals for estimating the oxygen isotopic composition of the less evolved rocks and the source. Bulk rock data may be affected by such secondary processes and result in too high values. For example Turi & Taylor (1976) measured a range of 8.1 - 11.7 ‰ for the Vulsinian rocks using bulk rock data, which are higher than the values of Holm & Munksgaard (1982) or of this work. However Turi & Taylor (1976) also found an augite with 7.08 ‰.

The lamproites are relatively fine grained, so that only few oxygen isotope analyses could be carried out for the sample ORC 9701. Olivines display $\delta^{18}O$ values of 7.2 ‰ and sanidines in the groundmass of 11.1 ‰. The olivine values are too high for a melt generated in an

unmodified mantle. Additionally the oxygen isotope fractionation of 3.9 ‰ between sanidines and olivines is too high for magmatic processes (Zheng 1993). Therefore it seems plausible, that the oxygen isotope ratios of the groundmass sanidines are modified by low temperature alteration processes such as an oxygen isotope exchange with a fluid. Olivines itself display no characteristic feature of a low temperature reaction with a fluid. Compared to the less evolved Vulsinian rocks olivines of the lamproites approximately show the same $\delta^{18}O$ values indicating a similar $\delta^{18}O$ composition of the source.

For the Torre Alfina rocks oxygen isotope investigations have been done on an ultramafic xenolith, a crustal xenolith and on olivines from the samples TA 9701 and TA 9702.

The ultramafic xenolith displays heterogeneous $\delta^{18}O$ compositions of the olivines with increasing values from the core of the xenolith to its rim (fig. 4-14). The total range lies between 5.9 ‰ and 10.9 ‰. In the centre, olivines are also variable with $\delta^{18}O$ values of 5.9 - 7.4 ‰. Additionally an orthopyroxene could be analyzed with 8.8 ‰. Unmodified mantle minerals have lower $\delta^{18}O$ values with 5.2 - 5.4 ‰ for olivines and about 5.9 ‰ for orthopyroxenes (Hoefs 1997, Mattey et al. 1994).

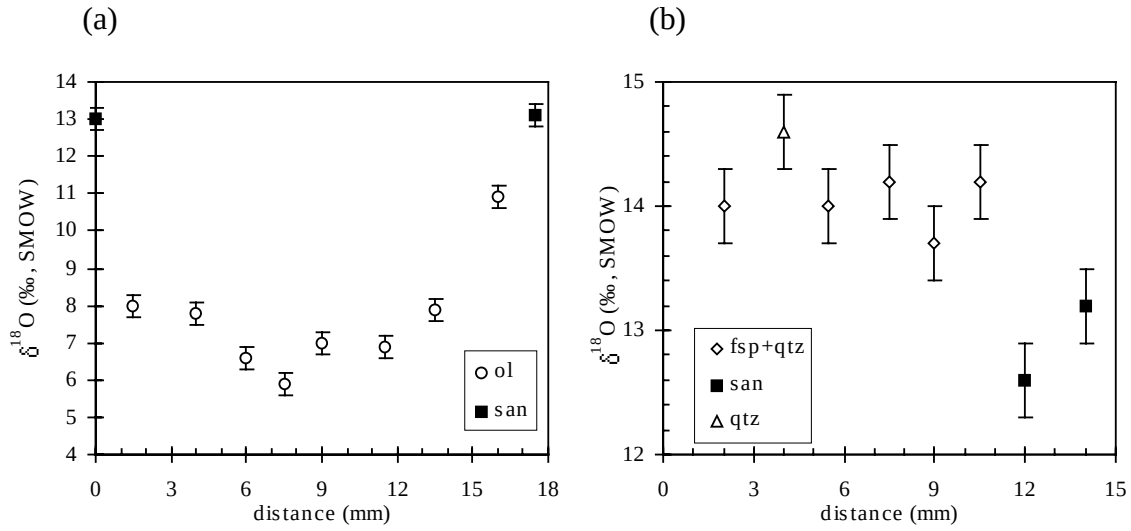

Fig. 4-14: Traverse of oxygen isotope ratios in a peridotitic xenolith (a) and a crustal xenolith (b) from the Torre Alfina group A lavas (Barnekow et al. 1998). Sanidines are from the groundmass of the host rock. Fsp+qtz means a fine grained feldspar quartz intergrowth of the crustal xenolith. For diagram 4-8 a the analytical error is in the range of the symbol size.

A crustal xenolith consisting of a larger quartz crystal embedded in a fine grained intergrowth of feldspar and quartz does not show any inhomogeneity (fig. 4-14). The quartz has an $\delta^{18}O$ value of 14.6 ‰ and the fine grained groundmass of 13.7 - 14.2 ‰.

From the sample TA 9701 larger olivines could be analyzed. They also show a wide range of composition from 5.3 ‰ to 9.1 ‰. Therefore minerals are not in equilibrium with the bulk

rock. The chemical composition indicate a xenocrystalline origin from the disintegration of ultramafic xenoliths, which is supported by the $\delta^{18}O$ values. The sanidine groundmass has a $\delta^{18}O$ value of 13.1 ‰. This value agree well with two bulk rock data by Ferrara et al. (1986b), who calculated the oxygen isotope ratios with 13.26 and 13.80 ‰, respectively.

The sample TA 9702 is fine grained, so that only two separated olivines could be analyzed with the CO_2 laser at the University of Bonn. These two olivines show typical mantle values of 5.3 ‰ and 5.5 ‰, respectively.

From Radicofani only few minerals could be analyzed from each sample, because of the small size of the phenocrystals. Mostly olivines have been analyzed and in the case of the sample RAD 9702 A also clinopyroxenes have been investigated. In the other samples the clinopyroxenes were always to small.

All samples from Radicofani display a very homogeneous composition of the oxygen isotope ratios. The range of $\delta^{18}O$ values of olivines lie between 7.1 - 7.4 ‰. This difference is within the reproducibility of the LA-SIRMS. In the sample RAD 9702 A clinopyroxenes contain slightly higher $\delta^{18}O$ values of 7.4 ‰ compared to the olivines with 7.1 ‰. Even this difference is within the error of the measurement. Despite the inaccuracy of the Δ value between clinopyroxenes and olivines the temperature of the melt can roughly estimated as being around or above 1000 °C but a large error must be taken into account (fractionating equations of Chiba et al. 1989, Zheng 1993). Generally for a mantle derived melt these $\delta^{18}O$ values are also too high and indicate an ^{18}O enriched mantle source.

Comparing the different genetic mantle types $\delta^{18}O$ values of olivines are similar within the reproducibility (± 0.3‰) of the LA-SIRMS: Orciatico lamproite 7.2 ‰, Roman Province HK series 6.7 ‰, Roman Province K series 7.0 - 7.1 ‰ and Radicofani 7.1 - 7.4 ‰. Compared to olivines from an unaffected mantle these values are considerably higher.

4.2 Crustal Derived Rocks

4.2.1 Introduction

Crustal anatectic melts are widely distributed in the Tuscan Province and occur as volcanic and plutonic rocks (e.g. Innocenti et al. 1992, Peccerillo et al. 1987). Two rhyolite localities have been sampled. The first locality is Roccastrada, where two samples from a lava flow have been sampled (ROC 9701 and ROC 9702) and San Vincenzo is the second. San Vincenzo rhyolites have relatively low SiO_2 contents, so that they were sometimes classified as rhyodacites (Peccerillo et al. 1987). After Ferrara et al. (1989) San Vincenzo rhyolites can be subdivided into two groups according to their MgO content. Group A contains less than 0.61 wt.% MgO and group B more than 0.75 wt.%. Both groups also have different Sr concentrations with less than 140 ppm for group A and more than 200 ppm for group B. Group A rhyolites are characterized by plagioclase, sanidine, quartz, biotite, and cordierite assamblages. In contrast group B rhyolites additionally contain sometimes clinopyroxenes, orthopyroxenes, and magmatic inclusions (Ferrara et al. 1989).

4.2.2 Whole Rock Chemistry

Roccastrada rhyolites are the most SiO_2 enriched volcanic rocks of the Tuscan Province (Taylor & Turi 1976) with up to 74.5 wt.% SiO_2. They are peraluminous with corundum as an norm-mineral. Compared to the Roccastrada rocks rhyolites from San Vincenzo contain less SiO_2 (68.5 - 69.6 wt.%). Rhyolites of both groups have been sampled, sample SVC 9703 (MgO = 0.52 wt.%, Sr = 105 ppm) belongs to group A and samples SVC 9701 (MgO = 0.78 wt.%, Sr = 190 ppm) as well as SVC 9702 (MgO = 0.72 wt.%, Sr = 260 ppm) can be assigned to group B.

Compared to mantle derived rocks trace element concentrations are low. REE are enriched less than 100 fold chondritic with a higher enrichment of the LREE than the HREE (fig. 4-15). Also a negative Eu anomaly is visible indicating the influence of plagioclase in the source or crystal fractionation of plagioclase. REE patterns of San Vincenzo rhyolites (fig. 4-15) are similar to REE patterns of Roccastrada rhyolites but group A rhyolite (SVC 9703) is less enriched in HREE. Rhyolites of group B (SVC 9701, SVC 9702) are higher enriched compared to group A rhyolite and are also higher enriched in LREE compared to Roccastrada samples. The multi element diagram of the rhyolites is typical for crustal derived rocks with a similar pattern for both Roccastrada and San Vincenzo rocks (fig. 4-16).

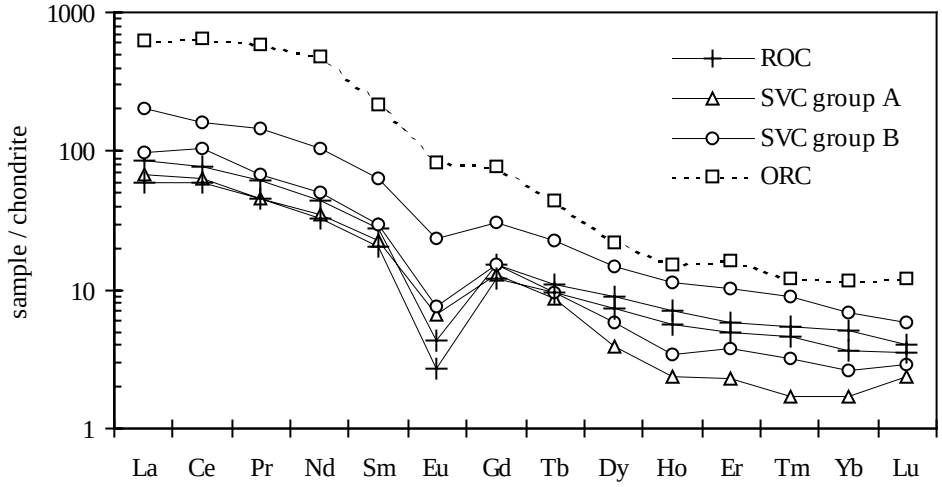

Fig. 4-15: Chondrite normalized (values from Anders & Grevesse 1989) REE patterns of the rhyolites (ROC: Roccastrada, SVC: San Vincenzo). For comparison a lamproite from Orciatico is shown (ORC).

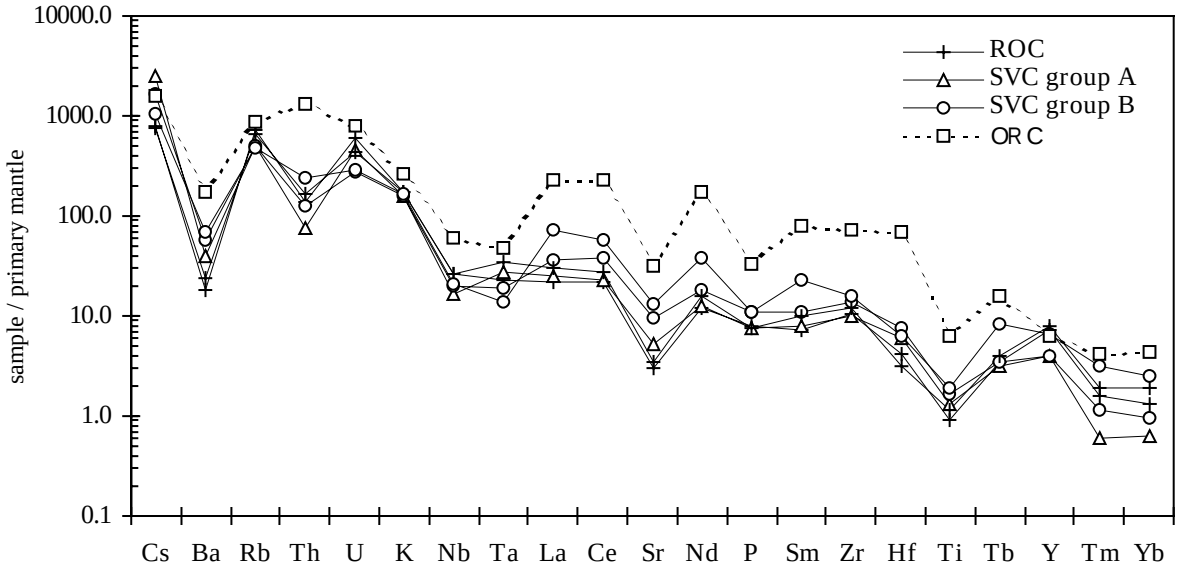

Fig. 4-16: Multi element diagram of the rhyolites (ROC: Roccastrada, SVC: San Vincenzo). Elements are normalized to primary mantle (values of McDonough & Sun 1995). For comparison the normalized concentrations of one Orciatico lamproite are shown.

4.2.3 Mineral Chemistry

The investigation has focussed on one sample (ROC 9701) from Roccastrada and on one sample of each group from San Vincenzo (SVC 9702, SVC 9703).

Groundmasses of the rhyolites are vitreous or microcrystalline. Phenocrystals in the Roccastrada rhyolites are plagioclase, sanidine, quartz, and biotite. Accessory phases and important trace element carriers of the bulk rock are zircon, apatite, and monazite. San Vincenzo rhyolites also contain plagioclase, sanidine, quartz, and biotite as phenocrystals and sample SVC 9703 additionally contain cordierite.

4.2.3.1 Plagioclases

Plagioclases from Roccastrada show a slightly oscillatory zoning. The anorthite content varies between an57 and an72. Sr contents are between 280 and 550 ppm and Ba between 10 and 120 ppm. Contrary REE concentrations are relatively constant with a decreasing enrichment of 190 fold chondritic for La and 1 fold for Yb (fig. 4-17). A positive Eu anomaly is well shaped.

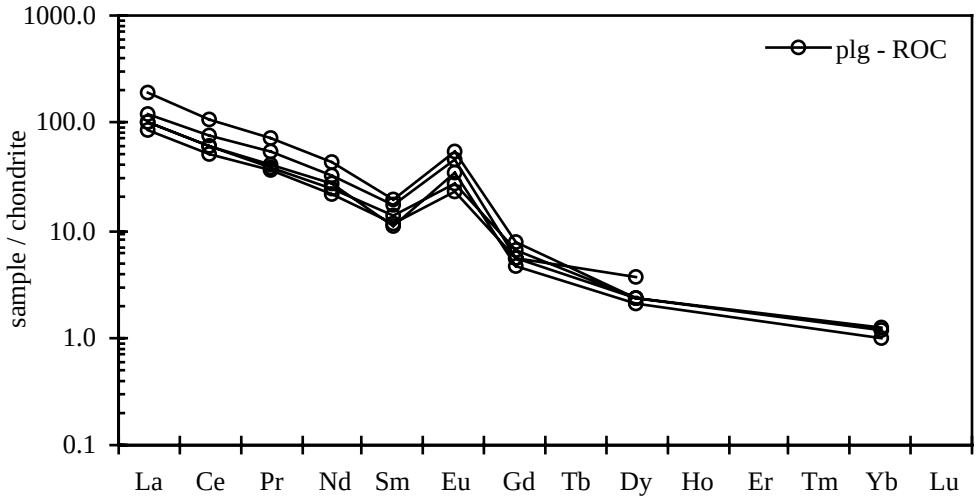

Fig. 4-17: Chondrite normalized REE patterns of plagioclases from Roccastrada (normalizing values from Anders & Grevesse 1989).

San Vincenzo plagioclases also display an oscillatory zoning with a Ca rich core and a decreasing anorthite component to the mineral rim. Plagioclases from group A are less calcic with a narrow range of composition from an48 in the core to an37 at the mineral rim. Group B plagioclases show a wider range of composition between an59 in the core and an32 at the rim. Feldstein et al. (1994) observed a larger range of plagioclase compositions. When normalizing REE concentrations of the plagioclases to the bulk rock concentration the patterns are chaotic

with different degrees of enrichment or depletion and positive or negative Eu anomalies. Sample SVC 9702 shows LREE / HREE ratios of more and less than 1, whereas sample SVC 9703 only contains ratios lower than 1. These uncommon REE patterns are caused by enclosed apatites with high REE contents - LREE / HREE ratios of below 1 indicate this, too. Using the partitioning coefficients of Arth (1976) and Nash & Crecraft (1985) REE concentrations of the plagioclases can roughly be calculated and therefore the amount of apatite, which is necessary to produce the observed REE patterns. The Ce contents has been used for this calculation. For SVC 9702 a maximum value of 5 wt.% and for SVC 9703 of 1 wt.% of enclosed apatites within the plagioclases is necessary to produce the resulting REE patterns.

4.2.3.2 Sanidines

Sanidines from Roccastrada are homogeneous with a composition of about or70 - ab29 - an01. Ba concentrations up to 2100 ppm are higher than in plagioclases and Sr is in the range of 130 - 320 ppm. The REE are less enriched showing a positive Eu anomaly. HREE concentrations are often below the detection limit.

Sanidines from San Vincenzo also show minor chemical variations. The orthoclase component of sample SVC 9702 is similar to the Roccastrada sample with or72 - or 77, whereas sanidines from sample SVC 9703 display a lower orthoclase component (or55 - or61). Feldstein et al. (1994) found inclusions of biotite and plagioclase oriented parallel to the crystal faces. These textures point to a magmatic origin of sanidines in the San Vincenzo rhyolites (Wall et al. 1987). But in the rhyolites investigated for this study these textures could not be observed. Normalizing REE concentrations to bulk rock composition the REE patterns are flat with a small decrease to the HREE and a positive Eu anomaly. Sample SVC 9702 is less enriched in REE with 0.3 - 1.1 times the value of the bulk rock for La. The composition seems to be heterogeneous but concentrations are near the detection limit of the LA-ICP-MS, so that a larger standard deviation has to be taken into account. The REE patterns of sample SVC 9703 are similar with a higher enrichment, e.g. La 2.3 - 3.4 fold the bulk rock. These values are uncommonly high, because the partition coeffcient of the $REE_{sanidine}$ / $REE_{bulk\ rock}$ is normally below 1 with the exception of Eu (Arth 1976, Nash & Crecraft 1985, Mahood & Hildreth 1983). Although apatites with high REE contents are sometimes enclosed in sanidines, the relatively high REE concentrations of sanidines can not solely be influenced by apatites, because the REE patterns of the sanidines show a positive Eu anomaly and apatites do not display positive Eu anomalies (Arth 1976, Fujimaki 1986).

4.2.3.3 Biotites

Biotites are common phenocrystals in the rhyolites from both localities. But their chemical composition differs, Roccastrada biotites are MnO rich and MgO poor whereas biotites from San Vincenzo are MnO poor and MgO rich. REE concentrations are highly variable and may result from inclusions (Giraud et al. 1986).

4.2.3.4 Cordierites

Cordierites were found in sample SVC 9702 from San Vincenzo. They display zonation with Mg values from 43 - 73, which is a wider range than observed by Feldstein et al. (1994). In a detailed study of cordierites Feldstein et al. (1994) showed, that some cordierites have textures of a restitic or xenocrystalline origin whereas other cordierites have textures pointing to a magmatic origin (Clemens & Wall 1984, Wall et al. 1987). Clemens & Wall (1981, 1984) showed that cordierite can crystallize as a solidus phase in peraluminous magmas.

4.2.3.5 Ilmenites

Ilmenite is a common oxide mineral in the rhyolites.

4.2.3.6 Apatites

Apatites are important REE containing minerals with high REE concentrations, e.g. Ce_2O_3 between 0.157 - 0.244 wt.% for San Vincenzo rhyolites. Because some apatites are embedded in feldspars they can influence the REE signatures of the feldspars.

4.2.4 Oxygen Isotopes

Phenocrystals of quartz, sanidine, and plagioclase from all rhyolitic samples has been analyzed. Additionally orthopyroxenes from sample SVC 9701 could be analyzed. The values are shown in fig. 4-18 and fig. 4-19.

The two samples from Roccastrada rhyolites have similar $\delta^{18}O$ values within the reproducibility of the LA-SIRMS (± 0.3 ‰). Differences of $\delta^{18}O$ values between quartz, sanidine, and plagioclase are in a typical range for volcanic rocks. Therefore the minerals are in isotopic equilibrium with respect to oxygen. Also minerals of the San Vincenzo group A rhyolite (SVC 9703) are homogeneously composed and are in equilibrium. In contrast two samples from group B rhyolites from San Vincenzo display a large range of $\delta^{18}O$ values indicating a disequilibrium. For example δ values of the sample SVC 9701 vary between 13.3 - 15.7 ‰ for quartz and 10.8 - 14.6 ‰ for plagioclase so that some plagioclases have higher $\delta^{18}O$ values than quartz. This heterogeneity of oxygen isotope ratios cannot be produced by fractional crystallization of a melt.

However the high $\delta^{18}O$ values of > 10 ‰ for feldspars and > 11 ‰ for quartzes from all rhyolites are typical for melts of crustal anatectic origin. Differentiation products of mantle melts cannot reach such high values (Hoefs 1997, Sheppard & Harris 1985).

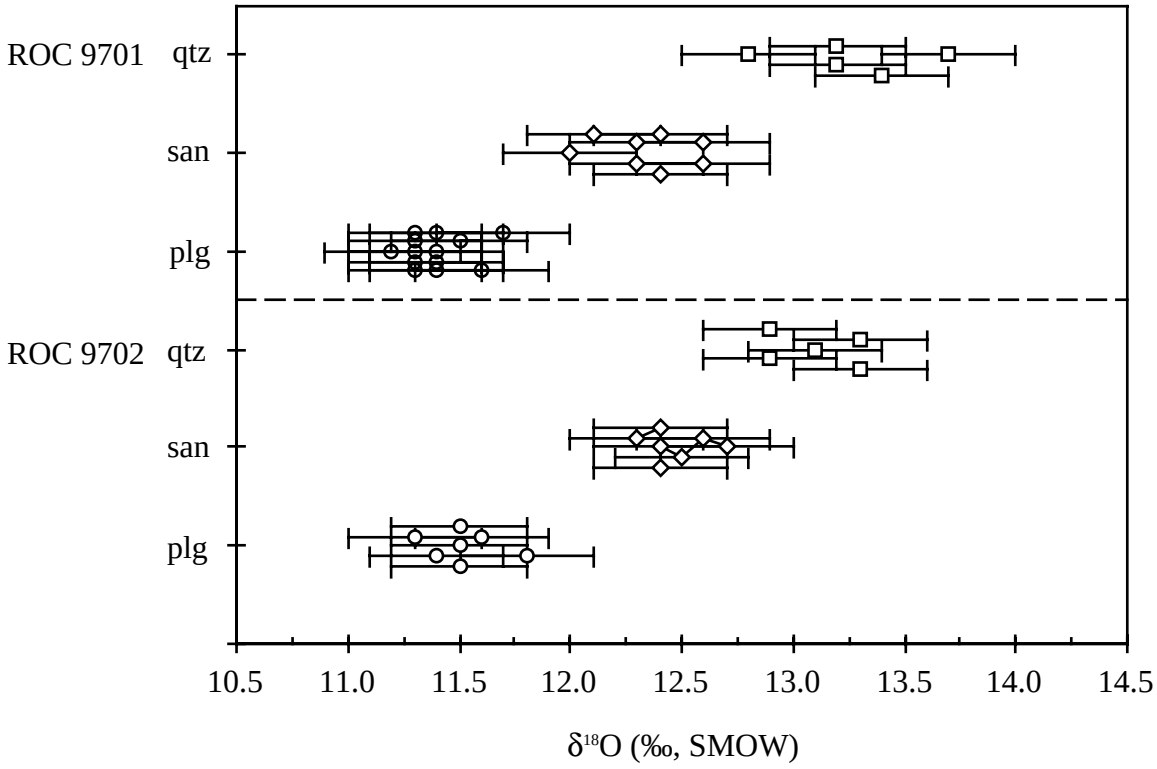

Fig. 4-18: Oxygen isotope ratios of phenocrystals of the rhyolites from Roccastrada.

Analyzed $\delta^{18}O$ values correspond well with data from the literature. Taylor & Turi (1976) analyzed one quartz with 13.09 ± 0.08 ‰ and one K-feldspar with 12.03 ± 0.05 ‰ from Roccastrada rhyolites. In this study values of 13.3 / 13.1 ‰ for quartz and 12.3 / 12.5 ‰ for sanidines were measured for samples ROC 9701 / ROC 9702. By comparison Taylor & Turi (1976) investigated one quartz (13.90 ‰) and one K-feldspar (13.05 ‰) from a San Vincenzo rhyolite but their sample could not be assigned to one of the two groups. Masuda & O'Neil (1994) carried out a CO_2 laser microprobe investigation on one rhyolite, presumably belonging to group B. They found $\delta^{18}O$ values of 13.9 - 14.3 ‰ for quartz, 12.1 - 14.6 ‰ for alkali feldspar and 11.9 - 13.8 ‰ for plagioclase within a small rock section. This range of δ values for alkali feldspars and plagioclases indicates an oxygen isotopic disequilibrium.

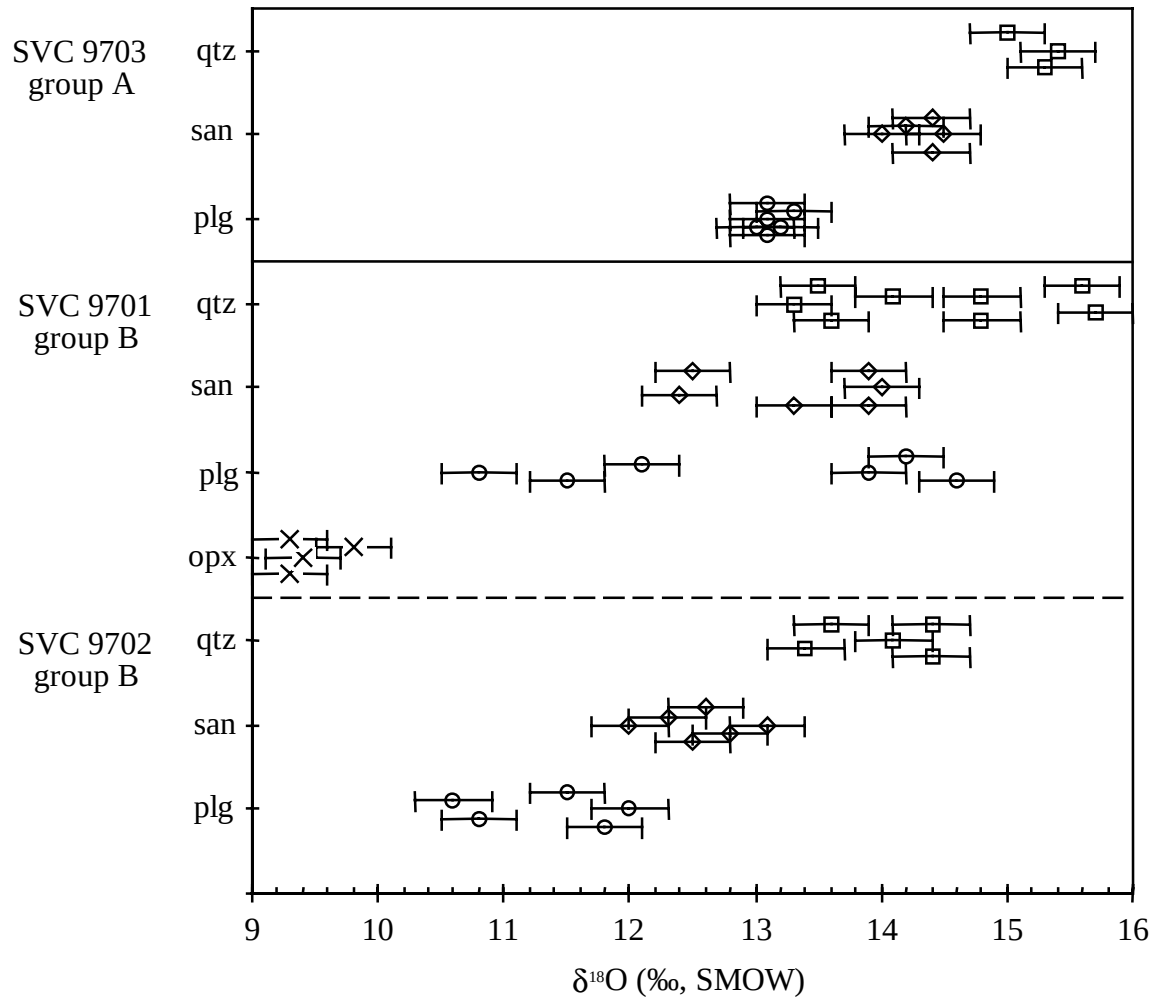

Fig. 4-19: Oxygen isotope ratios of phenocrystals of group A and B rhyolites from San Vincenzo.

4.3 Hybrid Rocks Between Mantle and Crustal Melts

4.3.1 Introduction

In the Tuscan Province rocks derived from mixtures between mantle and crustal melts can be observed. These mixtures are classified as hybrid rocks (Peccerillo et al. 1987). At Monte Amiata trachytic and mafic rocks as well as mafic xenoliths occur indicating magma mixing between a crustal and a mantle melt (e.g. van Bergen et al. 1983, Poli et al. 1984). Therefore Monte Amiata rocks have been sampled as representatives of hybrid rocks.

4.3.2 Whole Rock Chemistry

To cover the whole chemical range of Monte Amiata rocks two trachytes and two latites (AMT 9704 A, B) from the late stage Ermeata lava flow (on top of Monte Amiata) have been sampled. Also two xenoliths from trachyte AMT 9702 have been investigated. These xenoliths have a shoshonitic (AMT 9703 I) and latitic (AMT 9703 II) composition.

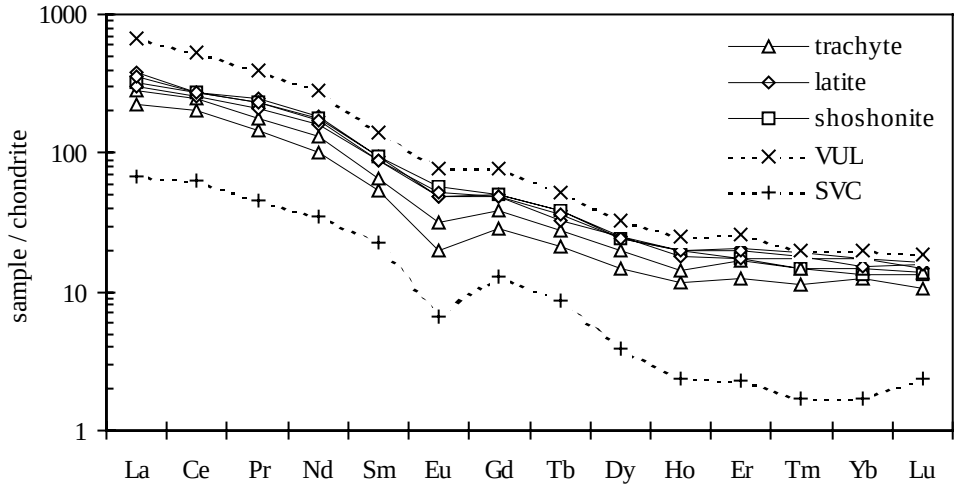

Fig. 4-20: Chondrite normalized REE patterns of Monte Amiata rocks (normalizing values from Anders & Grevesse 1989). For comparison a less evolved rock from the Vulsinian mountains (VUL) and a rhyolite from San Vincenzo (SVC) is shown.

Rocks from Monte Amiata thus range from shoshonites to trachytes (fig. 2-2). Trachytes and latites are SiO_2 oversaturated with quartz in the norm whereas the shoshonitic xenolith lies at the boundary between SiO_2 saturated to undersaturated rocks. The major element chemistry of trachytes is similar to San Vincenzo rhyolites with slightly higher MgO, CaO, K_2O and TiO_2 and lower Na_2O contents. Contrary the shoshonite is similar to less evolved rocks from the Vulsinian mountains but with slightly lower Al_2O_3 contents. Latites have an intermediate composition between shoshonite and trachytes. Both the shoshonite and the latites are ultrapotassic rocks.

REE concentrations and patterns (fig. 4-20) are similar to the Vulsinian rocks. For SiO_2 rich rocks like trachytes REE patterns can be produced by a mixture of Vulsinian and rhyolitic melts like the San Vincenzo rhyolites. Trace element patterns (fig. 4-21) reflect this mixing. Latites and the shoshonite contain trace element concentrations similar to the Vulsinian rocks.

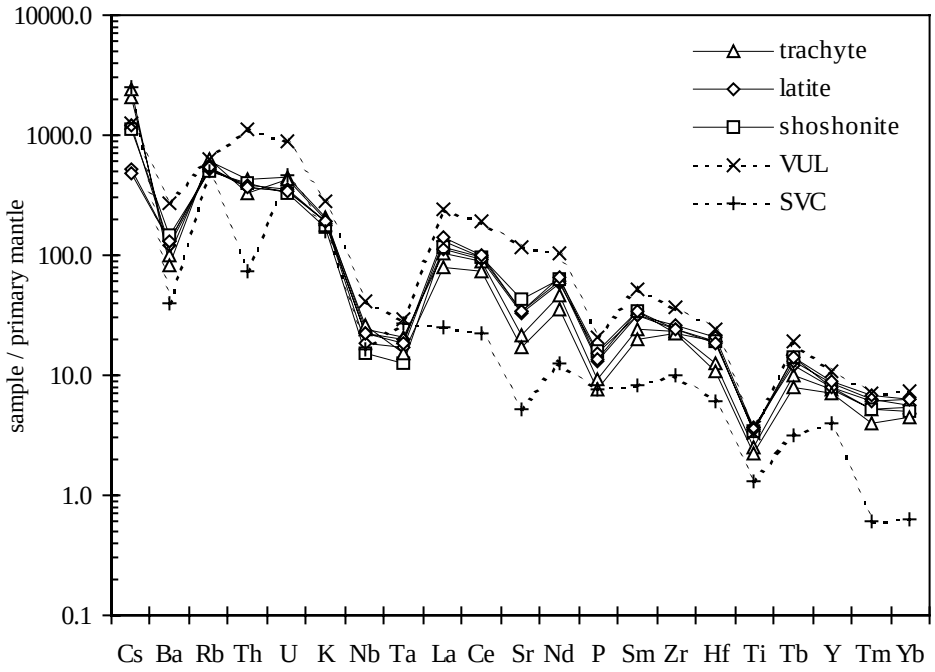

Fig. 4-21: Primary mantle normalized multi element diagram for Monte Amiata rocks (normalizing values are taken from McDonough & Sun 1995). For comparison a less evolved rock from the Vulsinian mountains (VUL) and a rhyolite from San Vincenzo (SVC) is plotted.

4.3.3 Mineral Chemistry

Mineral compositions have been analyzed in three samples: trachyte - AMT 9702, latite AMT 9704 A, shoshonite - AMT 9703 II. The trachyte consists of sanidine and quartz as major phenocrystals and minor amounts of plagioclases, biotites, orthopyroxenes, and oxides. The latite and shoshonite samples display a fine grained groundmass. Major phenocrystals are clinopyroxenes and sanidines in the shoshonite and clinopyroxenes and plagioclases in the latites. Less abundant minerals are micas and oxides in both rocks as well as sanidines in the latite.

4.3.3.1 Clinopyroxenes

Clinopyroxenes occur as phenocrystals in the latite and the shoshonitic xenolith. They display an oscillatory zoning. According to the classification of Morimoto (1989) clinopyroxenes in the latite are diopsides, except the outer part of the mineral rim, which have an augitic composition with a wollastonite component slightly lower than 45 mol% (fig. 4-22). Cores are Mg rich with Mg values of 92 (AMT 9704 A) and 88 (AMT 9703 II), respectively. Towards the mineral rim the Mg content decreases to Mg values of 56 (AMT 9704 A) and 52 (AMT 9703 II). Si and Al are sufficient to fill the tetrahedral site with Al in the M1 site as it is typically for Roman Province type rocks. Also the Ca deficiency is similar to the Vulsinian rocks. In contrast Ca and Fe do not correlate positively but Mg and Ti correlate negatively. Compared with Vulsinian clinopyroxenes Monte Amiata clinopyroxenes contain similar Ti and Al^{IV} for rocks with the same Mg / (Mg + Fe) ratios. Major and minor element characteristics of the Monte Amiata clinopyroxenes are thus similar to the Vulsinian clinopyroxenes (fig. 4-23).

Tab.4-5: Comparison of representative clinopyroxene analyses from Monte Amiata shoshonite (less evolved rock) with clinopyroxenes from Vulsinian mountains and Tuscan lamproites. HKS: Vulsinian mountains, KS series; KS: Vulsinian mountains, K series; ORC: lamproite from Orciatico, RAD: Radicofani; TA-px: Torre Alfina, peridotitic xenolith (b.d.l.: below detection limit of the EMPA).

wt.%	HKS	KS	ORC	AMT
SiO_2	52.0	52.4	54.0	51.7
TiO_2	0.419	0.496	0.585	0.518
Al_2O_3	3.14	3.37	0.56	3.09
FeO	3.96	4.08	3.58	4.40
MgO	16.0	16.4	18.0	16.5
CaO	23.7	23.6	22.4	2.9
MnO	b.d.l.	b.d.l.	b.d.l.	0.149
Cr_2O_3	0.419	b.d.l.	0.776	b.d.l.
Na_2O	0.199	0.207	0.162	0.119

Normalized to the bulk rock the REE of the clinopyroxenes are depleted with LREE / HREE ratios lower than 1 (fig. 4-16). Generally REE patterns are similar to Vulsinian

clinopyroxenes. Concentrations of Cr and Ni are also similar to the contents in KS clinopyroxenes.

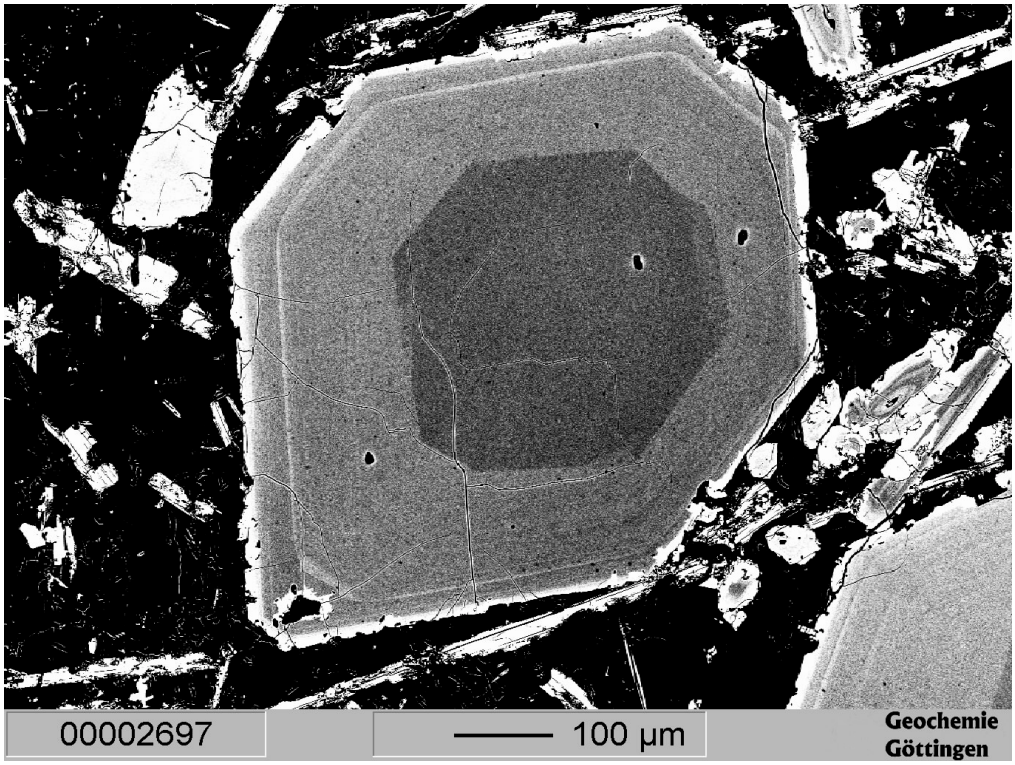

Fig. 4-22: EMPA image (composition mode) of a clinopyroxene of a latite from the Monte Amiata (AMT 9704 A).

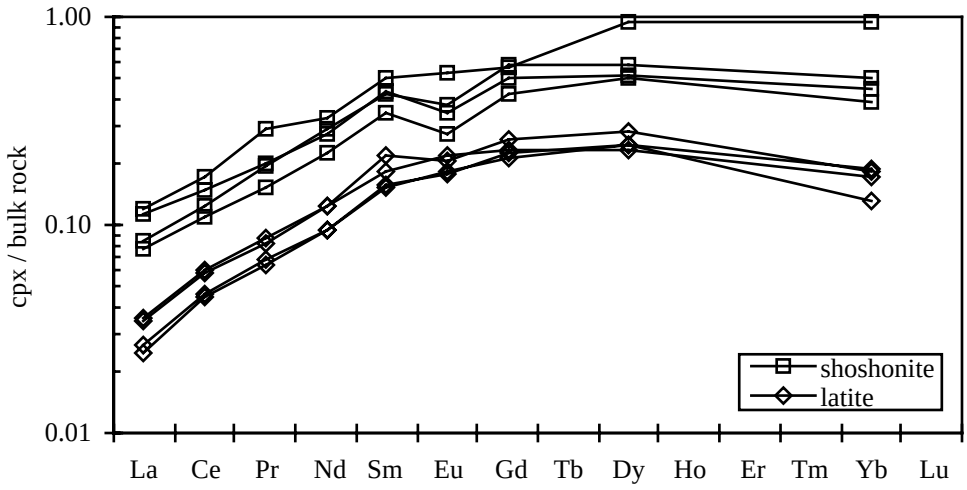

Fig. 4-23: REE patterns of clinopyroxenes from a shoshonite and a latite, values are normalized to chondritic values (Anders & Grevesse 1989).

4.3.3.2 Orthopyroxenes

Orthopyroxenes are present in the trachyte sample only. They have a homogeneous composition and display no zonation. Orthopyroxenes are ferrosilites with 51 - 55 mol% ferrosilite component and 2 - 3 mol% wollastonite component (classification according to Morimoto 1989). The chemical compositon is typical for orthopyroxenes from Monte Amiata (van Bergen 1984).

4.3.3.3 Plagioclases

Plagioclases occur as small crystals in the groundmass of the trachyte and are a major constituent of the latite. In the trachyte plagioclase shows a minor oscillatory zoning with anorthite components between 51 - 69 mol% whereas plagioclases in the latite are oscillatory zoned and contain a wide range of composition with an anorthite component of 47 - 82 mol%. This variability is in the range of KS plagioclases from the Vulsinian mountains.

Plagioclases of both samples have high Sr concentrations (400 - 1200 ppm) whereas Ba concentrations of plagioclases in the latite (130 - 480 ppm) are higher than in the trachyte (30 - 50 ppm). Normalized to the bulk rock the REE content is depleted with a higher depletion in the trachyte than in the latite. The HREE of trachyte plagioclases are below the detection limit of the LA-ICP-MS. Plagioclases of both rocks, trachytes and latites, display a positive Eu anomaly. REE patterns of the plagioclases from the latite are sometimes overprinted by enclosed apatites. Using REE concentrations of the plagioclases without embedded apatites the maximum amount of apatites in the plagioclases with the disturbed REE pattern can be calculated with less than 2 wt.%.

4.3.3.4 Sanidines

Sanidines as phenocrystals display a weak or no chemically zoning whereas sanidines from the groundmass show a variability with lower orthoclase contents compared to the phenocrystals. The phenocrystals generally contain higher orthoclase components with 79 - 81 mol% for the trachyte, 70 - 81 mol% for the latite and 79 - 84 mol% for the shoshonite than sanidines of the rhyolites from San Vincenzo and Roccastrada.

Trace element investigations by LA-ICP-MS have been carried out for trachyte AMT 9702 and shoshonite AMT 9703 II. Sanidines from the trachyte are depleted in REE compared to the bulk rock chemistry. They show a positive Eu anomaly; the HREE are sometimes below the detection limit. Contrary the REE patterns of the shoshonitic plagioclases are heterogeneously composed with different degrees of enrichment or depletion compared to the bulk rock and with positive or negative Eu anomalies. This can be caused by enclosed

apatites. REE and P containing phases have been found in the sanidines but they were too small to be quantitatively analyzed.

4.3.3.5 Micas

According to Deer et al. (1996) the Mg / Fe atomic ratio can be used as a dividing criterion between biotite and phlogopite. When the ratio is higher than 2 the mineral is named phlogopite otherwise it is classified as biotite.

Micas occur as phenocrystals in the trachytes, whereas in the latite micas are a constituent of the groundmass. In the shoshonitic xenolith micas are rarely found. When they occur they show resorption edges. In trachyte the micas are biotites with a similar composition to biotites from San Vincenzo rhyolites with Mg values between 53 - 56, K_2O 9.12 - 9.50 wt.% and TiO_2 5.74 - 6.48 wt.%. They display no large chemical variation. In contrast micas of the shoshonite have a biotitic to phlogopitic composition and show a larger variability with Mg values ranging between 47 - 82. The chemical characteristics are similar to phlogopites of the Vulsinian mountains, e.g. the K / Al ratio and the concentration of Na and K. Groundmass micas of the latite are biotites with a composition between the micas of the trachyte and the shoshonite.

Only biotites of the trachyte were large enough for LA-ICP-MS analysis but their REE patterns are extremely heterogeneous as it is observed for biotites from San Vincenzo or Roccastrada. This may also be a result of inclusions of oxides and apatites within the biotites.

4.3.3.6 Oxides

The shoshonite contains magnetites with high contents of Ti and Al. Contrary the trachyte and the latite have as major oxides Mg and Mn containing ilmenites.

4.3.3.7 Apatites

Apatites are common minerals in Monte Amiata rocks. They are important REE bearing minerals. In sample AMT 9704 A (latite) apatites were large enough to be analyzed with the electron microprobe. High REE concentrations could be found, e.g. Ce_2O_3 0.398 - 0.464 wt.%.

4.3.4 Oxygen Isotopes

Oxygen isotope compositions of the phenocrystals have been measured for all samples (fig. 4-24) except the latitic xenolith (AMT 9703 I) where minerals were too small.

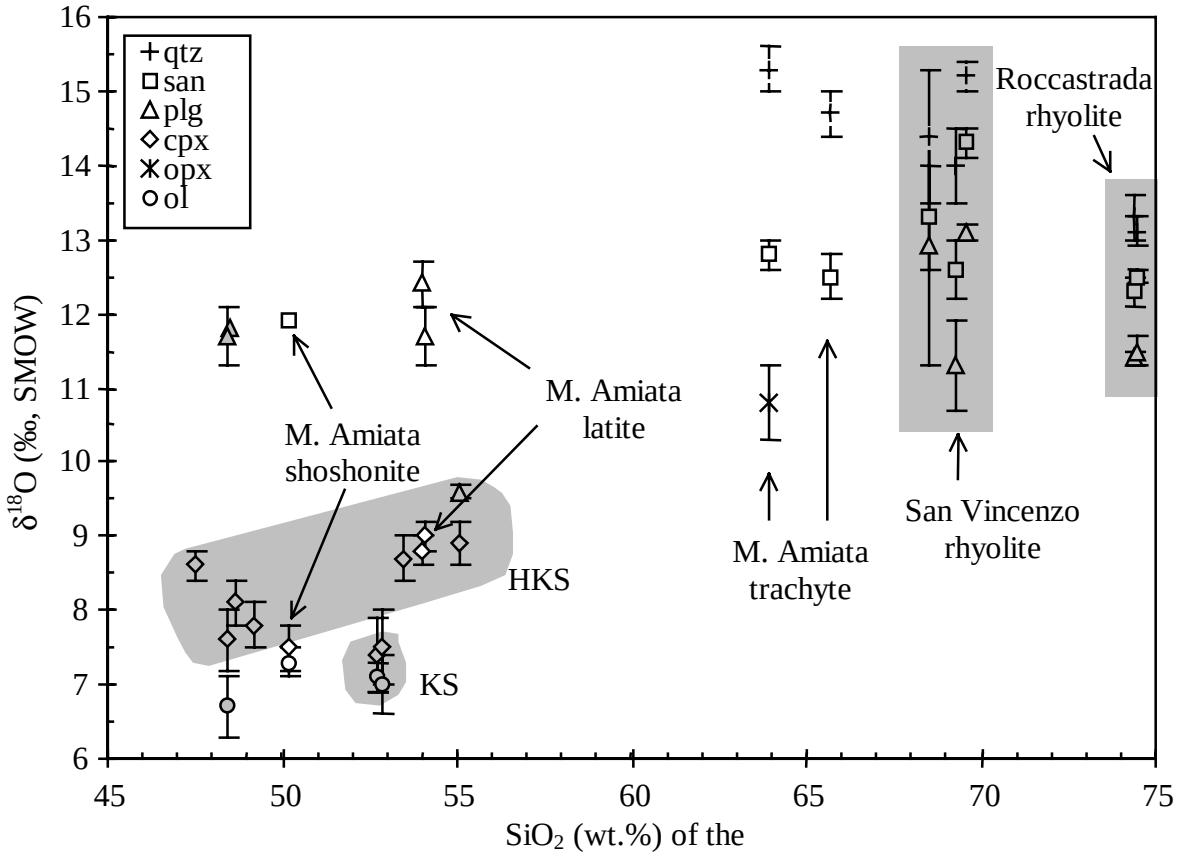

Fig. 4-24: $\delta^{18}O$ values of phenocrystals vs. SiO_2 content of the bulk rock. Monte Amiata phenocrystals are open symbols. Mineral data from the Vulsinian mountains (HKS and KS), San Vincenzo and Roccastrada are filled with gray. Gray fields represent the composition of the rhyolites from Roccastrada and San Vincenzo as well as the composition of clinopyroxenes from the HK series and the K series rocks from the Vulsininan mountains.

The trachytes display similar $\delta^{18}O$ values for sanidines with 12.5 ‰ (AMT 9701) and 12.8 ‰ (AMT 9702), respectively. These values correspond to oxygen isotope ratios of Roccastrada sanidines (12.3 - 12.5 ‰) and to one rhyolite sample from San Vincenzo (SVC 9702: 12.6 ‰). Quartz phenocrystals have high $\delta^{18}O$ values of 14.7 and 15.3 ‰. Fractionations between quartz and sanidine are too large for magmatic temperatures (Zheng 1993). Therefore a xenocrystic origin of the quartz must be assumed, as has been found by Balducci & Leoni (1981) in some SiO_2 rich volcanic rocks from Monte Amiata. On the other hand the biotite of sample AMT 9701 is in isotopic equilibrium with the sanidines. The temperature can be calculated to 850 °C using the equations of Zheng (1993). In contrast orthopyroxenes of the sample AMT 9702 display a different behaviour. They show an oxygen isotope range of 10.1 -

11.2 ‰, which indicate an isotopic disequilibrium between the individual orthopyroxenes. Thus orthopyroxenes are also xenocrystals. In general high $\delta^{18}O$ values of the phenocrystals from the trachytes indicate a crustal anatectic origin of these rocks.

From two latites (AMT 9704 A, B) and the shoshonitic xenolith clinopyroxenes could be analyzed. The shoshonite contains the lowest $\delta^{18}O$ value with 7.4 ‰, whereas the latites display higher values with 8.8 ‰ and 9.0 ‰, respectively. $\delta^{18}O$ values of clinopyroxenes from the shoshonite agree well with the oxygen isotopic compositon of the less evolved rocks from the Vulsinian mountains: KS 7.4 - 7.5 ‰, HKS 7.6 ‰. Even clinopyroxenes of the latites are in the range of the Vulsinian mountains. Fractionations between clinopyroxene and feldspar for the latites and the shoshonite are too large for igneous processes (Chiba et al. 1989, Zheng 1993). Therefore a secondary process, at lower temperatures than the crystallization temperature, has obviously affected the oxygen isotope ratios of the feldspars. This explanation is supported by the wide range of the plagioclase compositon of the sample AMT 9704 B with 11.1 - 12.0 ‰.

The present data agree with one analysis of Taylor & Turi (1976), who analyzed a quartz latite with 12.36 ‰ for the bulk rock and 12.67 ‰ for a K-feldspar.

5 Discussion

In this chapter constraints on the petrogenesis of the central Italian rocks are discussed on the basis of the results of this study. First the tectonic setting of the mantle derived rocks is described. In the following parts of this chapter the petrogenesis is discussed on the basis of bulk rock chemistry, mineral chemistry, and oxygen isotope composition. Additionally radiogenic isotope data, which kindly have been carried out for selected samples by Prof. Peccerillo, University of Perugia (personal information), are also taken into account. In the last part of this chapter a model of the petrogenesis of the central Italian rocks is set in a broader geodynamic context of the central Mediterranean region developed by Peccerillo & Panza (1999).

5.1 Tectonic Setting

Geochemical fingerprints of igneous rocks can be used to discriminate between different tectonic settings. These geochemical characteristics will briefly be described in the following section especially for the mantle melts.

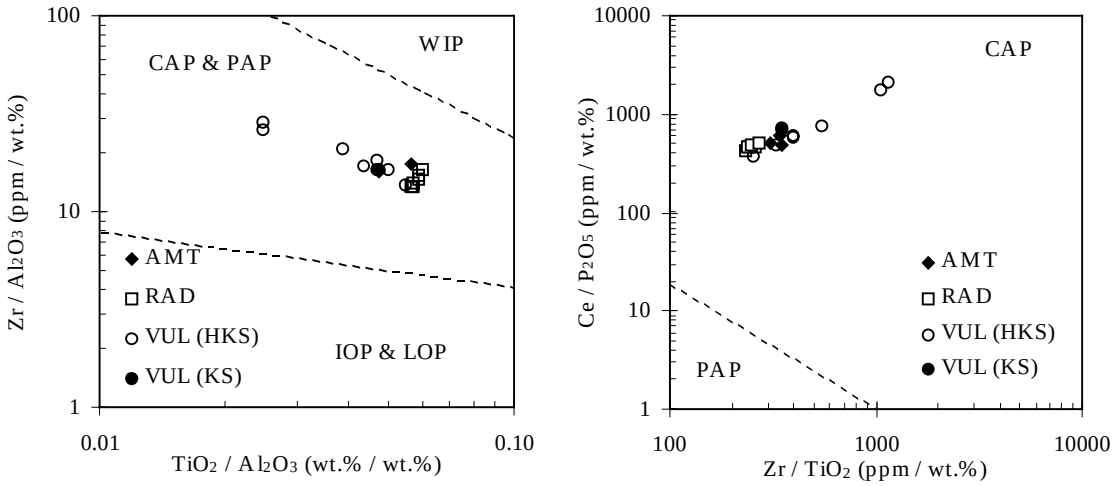

Fig. 5-1: Discrimination diagrams for potassic volcanic rocks from different tectonic settings according to Müller et al. (1992). Circles are HKS rocks and squares are KS rocks. Abbreviations: CAP = continental arc potassic rocks, IOP = initial oceanic arc potassic rocks, LOP = late oceanic arc potassic rocks, PAP = postcollosional arc potassic rocks, WIP = within-plate potassic rocks.

The mantle derived rocks display geochemical characteristics reinforcing the association of these rocks with a subduction zone. One characteristic feature is the trace element distribution shown in chapter 4.1.2, which is typical for subduction related rocks (Pearce 1983, White 1997/1998, Wilson 1995). However the multi element diagram is not sufficient to define the tectonic setting for potassic rocks exactly (Müller et al. 1992). Other chemical features are low

Zr concentrations combined with high Nb contents pointing to either a subduction or a post-collision tectonic regime of petrogenesis (Thompson & Fowler 1986).

Müller et al. (1992) developed a flow-diagram to discriminate different tectonic settings of potassic rocks using their geochemical composition. Intermediate Zr / Al_2O_3 and TiO_2 /Al_2O_3 ratios combined with high Ce / P_2O_5 and Zr / TiO_2 ratios point to a continental arc setting of the Vulsinian rocks (fig. 5-1). For lamproites or lamproitic rocks the situation is more complicated (Mitchell & Bergman 1991). But the multi element pattern also indicate a subduction related genesis.

5.2 Evidence from Bulk Rock Major and Tace Element Chemistry

In the Roman Province, of which the northern part is formed by the Vulsinian mountains, two different mantle derived rock types generally can be distinguished, the HK and the K series. The less evolved rocks of both series display high Mg values and transitional metal concentrations similar to a MORB source indicating a genesis by partial melting of a mantle source without assimilation of crustal material. In addition high Al_2O_3 and CaO contents point to a fertile mantle. The high enrichment of LILE and LREE points to an involvement of crustal material. It cannot be produced, however, by assimilation of crustal material during uprise of a mantle melt through the crust. Such an assimilation would dilute the transitional metal concentration and would decrease the Mg values of the less evolved rocks. In addition mantle derived rocks from the Roman Province display a higher enrichment of LILE and LREE than crustal anatectic rocks like the rhyolites from Roccastrada. Thus an assimilation of crustal material would also result in a dilution of LILE and LREE. The only explanation of the uncommon crustal signature of the Roman Province volcanic rocks is a contamination of the mantle source. The possible mechanism for this contamination process is the penetration of the mantle by fluids or melts with a crustal signature generated in a subducted slab. The source of the LILE and LREE could be the sediments of the subducted crust. The exact composition of the sediments is not known but marly sediments have been suggested by several authors (Beccaluva et al. 1991, Conticelli & Peccerillo 1992, Peccerillo 1985 and 1999, Peccerillo & Panza 1999, Rogers et al. 1985). A contamination of the mantle is also supported by trace element signatures like the Ta / Yb and Th / Yb ratios of the Vulsinian rocks. During magmatic processes Th and Ta behave similar but both elements are decoupled during dehydration and melting processes in a subducted slab. Th together with the other LILE is enriched in the generated fluid or melt. These fluids or melts can penetrate the mantle wedge above the subducted slab. They react with the mantle and consequently the mantle is enriched in LILE like Th and LREE. Therefore the melts generated by this modified mantle contain a higher Th / Yb ratio at the same Ta / Yb ratio of MORB than an unmodified mantle.

A contamination of the mantle with a fluid or melt would result in a reaction producing a chemically and mineralogically modified mantle. A possible reaction is the formation of a veined mantle (Foley 1992a, b) with phlogopite as an important new phase because phlogopite is a carrier of K and other LILE as well as H_2O (Wendlandt & Eggler 1980a, b, Wyllie & Sekine 1982). Melting of such a modified mantle could produce the uncommon potassic to ultrapotassic mantle melts of the Roman Province. The combined melting of veins and wall rocks in varying proportions can produce a relatively wide span of different potassic and ultrapotassic rocks. The exact composition of the mantle, whether it is composed of peridotites (Peccerillo & Manetti 1985, Kamenetsky et al. 1995) or pyroxenites (Rogers et al. 1985), is still a matter of debate.

The major difference between the rocks of the HK and the K series is their content of K and Si. HK rocks are more enriched in K and more depleted in Si than K series rocks. This difference is caused by changes of the melting parameters. Either the HKS source contains more phlogopite than the source of the KS (Rogers et al. 1985) or HKS melts were produced under higher pressure and X_{CO_2} of a fluid phase (Peccerillo 1994). Additionally the ratio of melted vein to melted wall rock is important for the melt composition (Foley 1992b) as well as the composition as possibly involved fluids (Foley et al. 1986).

In order to explain the range of volcanic rocks from the Vulsinian mountains from potassic trachybasalts to phonolites, magmatic processes modifying the melt composition as well as differences in the mantle composition has to be taken into account. Kamenetsky et al. (1995) suggested the existence of a continuous spectrum of different primary melts for the Vulsinian mountains. Even the mantle composition for only one volcano seems to be very complex (Conticelli et al. 1991). For example Conticelli et al. (1991) found three different source regions for the late stage eruptions of the Latera Volcano. One mantle source is identical with the source for KS rocks but the HKS source may be divided into a high Ba and a low Ba portion. Generally besides different source compositions for single volcanoes mantle melts are changed by processes within the crust. Processes like assimilation and fractional crystallization, as observed for individual volcanoes (Conticelli et al. 1991, Holm et al. 1982, Turbeville 1993), are not sufficient to generate the whole spectrum of evolved rocks (Conticelli et al. 1991, Kamenetsky et al. 1995). More complex processes like refilling + tapping + crystal fractionating + assimilation (Conticelli et al. 1997) are necessary to produce the whole range of volcanic rocks.

The second important group of mantle derived melts are the lamproites from the Tuscan Province. The igneous rocks from Orciatico and Montecatini Val di Cecina belong to this rock group. The Torre Alfina rocks differ slightly from the lamproites but they can also be assigned to this group. Thus the petrogenesis of the lamproites and the Torre Alfina rocks is discussed

together. Compared to the less evolved rocks from the Vulsinian mountains the lamproites also contain high Mg values, ferromagnesian and compatible elements supporting a mantle origin. The pattern of transitional elements is similar to MORB, which also points to a melt generation in the mantle. In contrast to the Roman Type rocks the Al_2O_3, CaO and Na_2O contents are low and V as well as Sc are moderately concentrated. Thus the source of the lamproites must be a residual mantle, which suffered a basaltic melt extraction. But the lamproites show the highest enrichment of LILE and LREE of all mantle derived rocks in central Italy. The trace element pattern – the high LILE / HFSE and LREE / HREE ratios – suggest the involvement of crustal material. Any assimilation of crustal material within the crust would dilute the concentrations of compatible and ferromagnesian elements and would lower the Mg values so that crustal assimilation could not produce the composition of the lamproites. The crustal signature of the lamproites thus must be a feature of the mantle source. Like the mantle beneath the Roman Province, the mantle beneath Tuscany could be contaminated by crustal material, which was incorporated into the mantle by a subducted slab. The reaction of the crustal material with the mantle could also produce a phlogopite containing veined mantle (Foley 1992b).

Summarizing the mantle source of the lamproites is a residual, metasomatized mantle. High SiO_2, high MgO lamproites can be generated by partial melting of such a mantle under special physico-chemical conditions (Arima & Edgar 1983). High SiO_2 contents point to a partial melting at low pressure and under high H_2O acitvity (Wendlandt & Eggler 1980a, b, Arima & Edgar 1983). The pressure can be estimated to a maximum of about 10 – 15 kbar (Foley 1992b) or about 12 kbar (Edgar & Vukadinovic 1992), which is in accordance with an upper mantle origin.

The small variations in the composition of the Orciatico lamproites can be generated by crystal fractionation in a shallow level environment (Conticelli et al. 1992), whereas the Montecatini Val di Cecina lamproites suffered a more complex history of crustal assimilation, low pressure crystallization and squeezing processes during the late stage crystallization (Conticelli et al. 1992). The Torre Alfina rocks of type A represent mantle melts, which are relatively unaffected by crustal assimilation or fractional crystallization (Conticelli 1998). On the other hand the differences of type B lavas to type A rocks can be explained by assimilation of crustal material (Conticelli 1998, Peccerillo 1994). This explanation is supported by the high abundance of crustal xenoliths in type B lavas.

The last group of mantle derived melts in central Italy are the transitional rocks, which were sampled at Radicofani. Their high Mg values and high MgO, Cr, and Ni concentrations of the less evolved rocks clearly point to a mantle origin. Extensive fractional crystallization and crustal assimilation for the less evolved rocks can be excluded (Poli et al. 1984). Chemically

they are mixtures between Roman Province type and lamproitic melts. Mixing the two endmembers with different proportions can thus produce the observed range of volcanic rocks from Radicofani (Peccerillo 1994). On the basis of trace elements Peccerillo (1994) suggested a Roman type melt similar to the KS rocks from Ernici – a volcanic region lieing in the transition zone between the Roman and the Campanian Province – as the Roman type endmember. On the basis of this study it can not be decided, whether the Roman type endmember belongs to the K or the HK series.

Rocks from the Vulsinian mountains, from Radicofani, and the lamproitic rocks from the Tuscan Province represent mantle derived melts. On the other hand the situation in central Italy is complicated by the occurrence of crustal anatectic rocks, which frequently occur in the Tuscan Magmatic Province. Representatives for crustal anatectic rocks are the rhyolites from Roccastrada. Their chemical composition is typical for melts generated by partial melting of metapelitic rocks (Green 1976). Metapelitic rocks form large parts of the Paleozoic basement of central Italy (Giraud et al. 1986, Taylor & Turi 1976). The residue may be characterized by biotite, quartz, cordierite, and feldspar (Giraud et al. 1986). But the relatively high enrichment of K, Rb, Pb, U, and Th cannot result from partial melting of this metapelitic material (Giraud et al. 1986). Because of the homogeneity of these rhyolites an addtional process of enrichment like hydrothermal systems can be excluded. Giraud et al. (1986) suggested that the metapelitic source has been contaminated by fluids generated in the deeper crust, which are possibly related to a subducted slab, and which might also have contaminated the mantle beneath central Italy.

Another occurrence of crustal anatectic rocks are the rhyolites from San Vincenzo. Using the major and trace element composition of the bulk rocks these rocks could also be produced by partial melting of metapelitic basement rocks, which had been contaminated by fluids like the Roccastrada rhyolites (Feldstein et al. 1994, Ferrara et al. 1989, Giraud et al. 1986, Taylor & Turi 1976). As shown in chapter 5.4 the petrogenesis of the San Vincenzo rhyolites is, however, more complicated than the genesis of the Roccastrada rhyolites.

Hybrid rocks have been sampled at the Monte Amiata and represent mixtures between crustal anatectic rocks and mantle derived mafic rocks. The petrographic composition ranges from latites to trachytes with mafic shoshonitic inclusions in trachytes. These inclusions already point to a mixing between mafic and acidic melts. The most mafic rocks are the shoshonitic inclusions mentioned above. The trace element signature of these shoshonites is similar to the less evolved rocks from the Vulsinian mountains. But a matter of debate is whether the mafic melts belong either to the HK series or to the K series. Peccerillo et al. (1987) favoured the KS melts, whereas Poli et al. (1984) and van Bergen (1985) preferred the HKS melts. The

chemical composition of the bulk rock rather indicates KS melts as mafic melts of the Monte Amiata volcano.

For the acidic rocks, the trachytes, a petrogenesis of partial melting of metapelitic material is assumed (Giraud et al. 1986, Innocenti et al. 1992, Pinarelli 1991). However the high concentrations of K, Rb, Pb, Li and REE requires a further source of these elements (Giraud et al. 1986). Giraud et al. (1986) explained this with a mixing of a pure crustal anatectic melt similar in composition to San Vincenzo and Roccastrada rhyolites with a mantle derived melt of a K series composition. A contribution of about 15 - 30 % of mantle melt is neccessary to produce the trace element signatures of the acidic rocks from Monte Amiata (Giraud et al 1986, Innocenti et al. 1992). The crustal melt endmember is believed to be similar to the Roccastrada or San Vincenzo rhyolites (Giraud et al. 1986). But the trace element signature of the trachytes rather indicate a composition corresponding to the San Vincenzo rhyolites. However the metapelitic basement of central Italy displays a large variability so that crustal anatectic rocks from Tuscany shows a large variability. Thus the exact composition of the crustal anatectic endmember of the Monte Amiata volcano is not known.

Summarizing, the Monte Amiata rocks can be generated by mixing of a mantle and a crustal anatectic melt. Mantle melts correspond to the mantle melts of the Vulsinian mountains, probably the K series melts. Crustal anatectic melts are generated by partial melting of metapelitic rocks. Neither pure mantle melts nor pure crustal melts occur at the Monte Amiata.

A major aspect to understand the variability of different rocks in central Italy is the composition of the mantle source beneath central Italy and the different metasomatic agents for the mantle source. Summarizing two different mantle derived rocks can be distinguished, the Roman Type melts from the Vulsinian mountains and the mantle derived melts from the Tuscan Province occuring as lamproites. Using trace element ratios it can be tested whether the mantle beneath the Tuscan and the Roman Province were metasomatized by the same agent or not. Rb and Sr as well as La and Ta behave similar during partial melting of a mantle source and fractional crystallization of a melt. Thus different Rb / Sr and La / Ta ratios indicate a different source composition and consequently differently composed metasomatic agents. In fig. 5-3 these element ratios are shown. The lamproite composition can be explained by mixtures of a mantle derived with crustal derived material similar to the Dora Maira metagranites (Peccerillo 1999). The Roman Province rocks display another enrichment trend with higher La / Ta ratios and lower Rb / Sr ratios. Marly sediments are suggested as a possible contaminant (e.g. Beccaluva et al. 1991, Peccerillo 1999). The mafic endmembers of the Monte Amiata volcano lie in the enrichment trend of the Roman Province rocks thus supporting a Roman type melt as a mafic endmember. Rocks from Radicofani show

intermediate trace element ratios between Roman Province type and lamproitic melts indicating a petrogenesis by mixing of both melt types. Because of the relatively low Rb / Sr ratios Torre Alfina rocks can represent either pure lamproitic melts or lamproitic melts

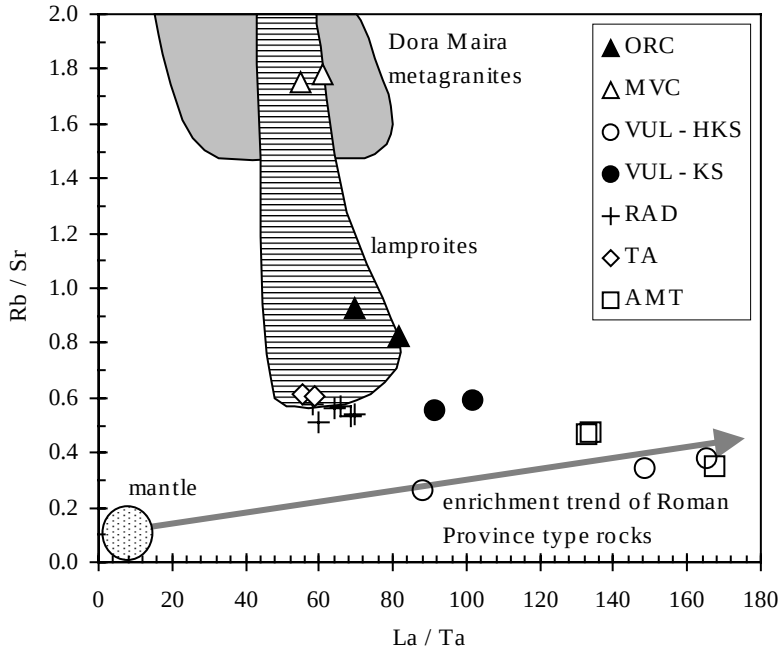

slightly influenced by Roman Province type melts.

Fig.5-3: Rb / Sr vs. La / Ta diagram for mafic rocks of central Italy (Mg values > 60) after Peccerillo (1999). The arrow displays the enrichment trend of the Roman type rocks. Mafic rocks from Monte Amiata are identical with the Roman type rocks. The lamproite - field can be generated by a mixing of material similar to Dora Maira metagranites and mantle material. Rocks from Torre Alfina and Radicofani lie in the lamproite field and between the lamproite field and the Roman Province enrichment trend, respectively. Primary mantle values are taken from McDonough & Sun (1995).

5.3 Evidence from the Chemical Composition of Minerals

Mineral chemistry of selected rock samples has been analyzed using representative samples for every petrogenetic rock type.

The compositions of olivines and clinopyroxenes from the less evolved rocks of the Vulsinian mountains support a mantle derived origin of the rocks. Their composition is in accordance with their bulk rock composition and typical for Roman Province K rich rocks. As mentioned in chapter 5.2 the compositional range of the Vulsinian rocks can only be explained by complex processes like refilling + tapping + crystal fractionating + assimilation (Conticelli et al. 1997). These processes are reflected in the structure of the minerals. Some clinopyroxenes show oscillatory zoning, which indicate a complex history of the melts with changing pressure

and temperature conditions or melt compositions. Magma mixing is indicated by chemically different inherited cores within the clinopyroxenes. In addition melt inclusions in clinopyroxenes point to a rapid growth of the minerals, which is sometimes interrupted by processes of resorption.

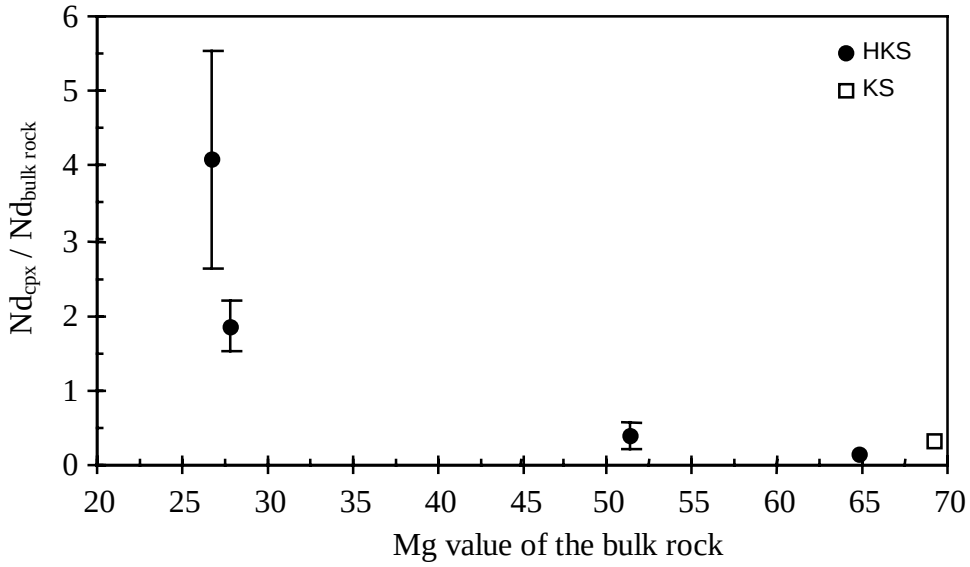

Fig. 5-4: Enrichment of Nd in clinopyroxenes - Nd concentrations are normalized to the bulk rock concentration - vs. the Mg values of the bulk rock. Filled circles are clinopyroxenes from HKS open squares from KS. For symbols without an error bar, the error is within the symbol size.

Another remarkable feature is the increasing REE content of clinopyroxenes with decreasing Mg values or increasing evolving stage of the rocks. The change of REE concentrations is not only caused by higher REE concentrations of the bulk rock. Figure 5-4 shows the Nd concentrations of the clinopyroxenes normalized to the bulk rock versus the Mg values of the bulk rock. The less evolved rocks have lower REE_{cpx} / $REE_{bulk\ rock}$ ratios than the more evolved rocks. During a magmatic evolution of a melt, especially fractional crystallization, the partition coefficient $D_{cpx/melt}$ of the REE increases because the physicochemical conditions and the chemical composition of the melt change (Dobosi & Jenner 1999, Francalanci et al. 1987). The Al concentration of the melt and the clinopyroxenes have a major influence on the partition coefficient. Increasing Al contents in the melt and the clinopyroxenes induce an increase of the partition coefficient. But the partition coefficient does not depend on the Al content linearily (Lundstrom et al. 1998, Schosnig & Hoffer 1998). A positive trend of an increase of Al in the bulk rock and in the clinopyroxenes can also be observed in the Vulsinian samples.

In some rocks from the Vulsinian mountains phlogopites can be observed displaying dissolution processes at their mineral rim. This points to a xenocrystalline origin. The

chemical composition of the phlogopites like low Ti contents and high K / Al ratios indicate a high pressure origin (Foley 1990). Thus phlogopites may be of mantle origin and also indicate a metasomatized mantle beneath central Italy.

The forsteritic rich olivines of the lamproites also indicate a mantle origin for this rock type. Their chemical composition, especially the enrichment of LREE compared to HREE, reflect the chemical composition of the bulk rock. Clinopyroxenes of the Orciatico lamproites display only a minor zoning pointing to a small interaction of the melts with the crust. Changes of the chemical composition of the primary melt by assimilation of crustal material should also affect the composition of the clinopyroxenes. Compared to the Vulsinian micas the chemical composition of lamproitic phlogopites suggest a formation under relatively low pressures and high temperatures (Conticelli et al. 1992, Foley 1990, Trönnes et al. 1985). However phlogopites from the lamproites reflect the conditions of crystallization of the melts whereas the phlogopites from the Vulsinian rocks probably are xenocrystals from the mantle source. Thus the phlogopites from the lamproites give only an indirect indication of the mantle and the primary melt composition of the Tuscan Province. In order to produce a phlogopite-sanidine-clinopyroxene containing lamproite the mantle source had to be melted at low pressures.

In summary mineral compositions of the Vulsinian and lamproitic rocks support the petrogenetic model based on bulk rock chemistry.

Another important piece of evidence for a petrogenetic model are peridotitic xenoliths embedded in the Torre Alfina lavas. Their olivines have a chemical composition, e.g. low CaO and high MnO contents, which is typically for a high pressure origin. Additionally the peridotitic xenolith contains spinels as the Al bearing phase indicating a mantle origin. Clinopyroxenes from the xenoliths contain relatively high REE concentrations pointing to a metasomatically enriched mantle. An important mineral of the peridotitic xenoliths are phlogopites with a typical mantle composition (Conticelli & Peccerillo 1990) indicating a metasomatically enriched mantle. Therefore the peridotitic xenolith strongly indicates an metasomatically enriched mantle beneath the Tuscan Province, which is in accordance with the bulk rock chemistry of the lamproites. Phlogopites are the K, LILE and REE carrier in the metasomatically enriched mantle beneath central Italy.

Clinopyroxenes of the host rocks from Torre Alfina have a chemically intermediate composition between Tuscan lamproites and Vulsinian rocks emphasizing the transitional character of these rocks. The mineralogical composition and mineral chemistry supports a transitional character of the Torre Alfina lavas. The bulk rock chemistry and the mineral chemistry, especially the absence of plagioclases and the composition of sanidines, display a lamproitic affinity of these rocks.

In contrast to the Torre Alfina rocks the Radicofani lavas show a different affinity. They also belong to the transitional rock type but their mineralogy – olivines, clinopyroxenes, and plagioclases as major phases as well as the lack of phlogopites and sanidines - is more close to the Vulsinian rocks. The mineral composition is intermediate between lamproites and Roman Province type rocks, too. This can be shown especially for the clinopyroxenes. Si and Al contents are similar to the Vulsinian rocks but Ca deficiency is similar to the clinopyroxenes from the lamproites. Generally the mineral chemistry of the Radicofani rocks support the transitional character and the closeness to the Roman Province type rocks, as it is reflected by the bulk rock chemistry.

Besides the mantle derived melts, crustal anatectic rocks are the second important rock type in central Italy. The rhyolites of Roccastrada and San Vincenzo are dominantly generated by partial melting of metapelitic rocks. This conclusion has been drawn using bulk rock composition. The mineral chemistry reflects this genesis. For a crustal anatectic melt the minerals have a common composition. Especially cordierite xenocrystals from San Vincenzo supports the petrogenesis by partial melting of a metapelitic source. Comparing the chemical composition of the phenocrystals, differences between the Roccastrada and San Vincenzo rhyolites can be observed, e.g. biotites from Roccastrada are MnO rich and MgO poor whereas biotites from San Vincenzo show the opposite behaviour, which may result from heterogeneities of the crustal composition of central Italy. Summarizing mineral chemistry is in accordance with the petrogenetic model based on the bulk rock chemistry.

Finally the hybrid rocks from Monte Amiata have to be discussed. From the bulk rock composition mixing of a mantle melt with a crustal melt has been concluded. The crustal melt has a composition similar to the San Vincenzo rhyolites whereas the mantle melt is similar to the Roman Province type rocks, especially the K series rocks. Minerals from a shoshonitic xenolith reflect the mafic endmember, minerals from a trachyte the SiO_2 rich endmember and minerals from a latite an intermediate representative. The chemical composition of clinopyroxenes and phlogopites from the shoshonite is similar to the Vulsinian rocks. Therefore the mineral chemistry supports a genetic model of a Roman type melt as a mafic endmember for the Monte Amiata hybrid rocks. On the other hand minerals of the trachytes are similar in composition as the minerals from the San Vincenzo rhyolites. A crustal source similar to the San Vincenzo rocks is thus likely. The intermediate latites can be produced by mixing of the two endmembers. In general the mineral chemistry supports the conclusions drawn on the basis of the bulk rock chemistry.

Summarizing the mineral chemistry of all rock samples investigated, the results support the petrogenetic models deduced from whole rock data presented. Additionally a better knowledge of the processes during crystallization can be obtained such as a changing

distribution coefficient of REE in clinopyroxenes depending on the composition of clinopyroxenes and melt.

5.4 Evidence from the Oxygen Isotope Ratios

Oxygen isotope ratios of the phenocrystals have been analyzed to characterize the original isotopic composition of the melts. Using bulk rock analyses oxygen isotope ratios may have been changed by secondary processes like hydrothermal alteration. A secondary alteration of the isotopic ratios has been observed in some rock samples; e.g. plagioclases of the groundmass are not in isotopic equilibrium with clinopyroxenes or olivines as the liquidus phases. Thus the analyses of the first crystallizing minerals will give a better estimate of the original composition of the rocks.

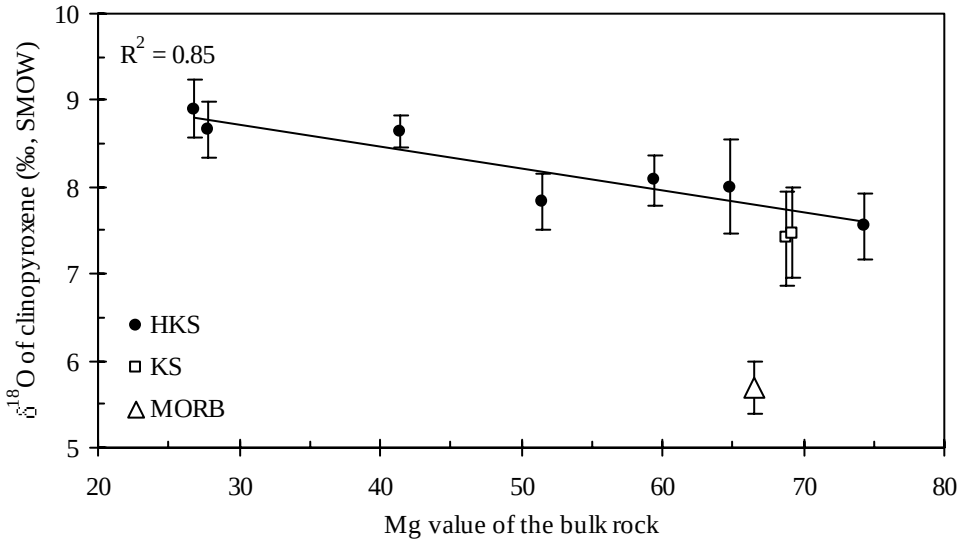

Fig. 5-5: $\delta^{18}O$ values of clinopyroxenes vs. Mg values of the bulk rock. For comparison a MORB value (Hoefs 1997, Schilling et al. 1983, White 1997/1998) is shown.

Oxygen isotope ratios of clinopyroxenes from the Vulsinian rocks range from 7.4 - 8.9 ‰. An increase of the $\delta^{18}O$ values with decreasing Mg values of the bulk rock can be explained by fractional crystallization and assimilation of crustal material (fig. 5-5). However an increase of 1.3 ‰ of the oxygen isotope ratios with an increase of 6.7 wt.% SiO_2 of the bulk rock is too high for a fractional crystallization process alone (Hoefs 1997). Because of that assimilation of crustal material during the uprise of the melt has to occur.

In order to increase the oxygen isotope ratios, assimilation of carbonatitic material has been suggested (Varekamp & Kalamarides 1989) as it is observed at other localities in central Italy (Peccerillo 1998). If the oxygen isotope ratios are affected by assimilation of carbonates the $\delta^{18}O$ values should be positively correlated with the CaO content of the bulk rock. But the

contrary is observed (fig. 5-6). Therefore the assimilation of large amounts of carbonatitic material can be excluded. An explanation of the observed negative correlation may be a combination of fractional crystallization of clinopyroxenes or anorthite rich plagioclases and assimilation of SiO_2 rich crustal material.

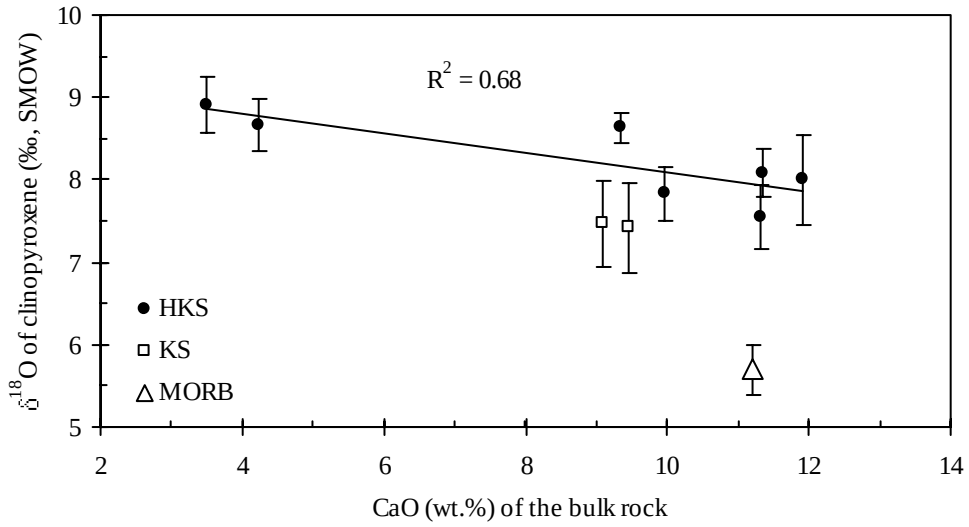

Fig. 5-6: $\delta^{18}O$ values of clinopyroxenes vs. CaO content of the bulk rock. For comparison a MORB value (Hoefs 1997, Schilling et al. 1983 and White 1997/1998) is shown.

The composition of the primitive mantle melts from the Vulsinian mountains can be estimated from the data of the less evolved rocks. These rocks show $\delta^{18}O$ values of 7.4 - 7.6 ‰ for clinopyroxenes and 6.7 ‰ for olivines. Thus the mantle source or the mantle melts should have $\delta^{18}O$ values of about 6.7 ‰. This is in agreement with Turi et al. (1986) and Ferrara et al. (1986b), who stated that the mantle source is similar in composition with the Alban hills mantle source of about 6.5 - 7.0 ‰. The estimated primary range of mantle melts from the Vulsinian mountains of 7.8 - 9.4 ‰ from Holm & Munksgaard (1982) seems to be too high. Summarizing the mantle source must be enriched in ^{18}O but to a lesser degree than Holm & Munksgaard (1982) or Rogers et al. (1985) suggested.

Only one lamproite sample displays no secondary alteration of the olivines, so that only few oxygen isotope data are available. These few olivines have high $\delta^{18}O$ values of 7.2 ‰. The $\delta^{18}O$ differences between olivines and sanidines of the groundmass can be explained by secondary alteration of the groundmass. Because of low oxygen diffusion coefficients in olivine the $\delta^{18}O$ values should represent the original values of the melt. Thus the source of the lamproites must be enriched in ^{18}O.

The oxygen isotopic composition of the peridotitic xenolith from Torre Alfina gives strong evidence for an ^{18}O enriched mantle. As shown in chapter 4.1.4 olivines of the peridotitic xenolith contain the lowest values in the core and the highest at the boundary to the host rock.

Oxygen isotope ratios of the olivines in the core are up to 7 ‰ whereas typical mantle olivines have an oxygen isotopic composition of about 5.2 – 5.4 ‰ (Hoefs 1997, Mattey et al. 1994). Oxygen diffusion in olivines is low, so that the enrichment of the olivines could not occur during uprise of the melt. Conticelli (1998) has calculated the uprise of the Torre Alfina melts from the mantle source to the surface to be about several hours. A minimum time of 350 ka to 1.6 Ma is required for diffusion of oxygen from the outer part of the xenolith into the core using the diffusion coefficients of Cherniak & Lanford (1989), Jaoul et al. (1980), Ryerson et al. (1989), and Yurimoto et al. (1992).

Phenocrystals from Radicofani rocks are characterized by a homogeneous composition. Their values are in accordance with a mixing model of lamproites and Roman type melts.

Comparing the different genetic types the $\delta^{18}O$ values of olivines are identical within the reproducibility (± 0.3‰) of the LA-SIRMS: Orciatico lamproite 7.2 ‰, Roman Province HK series 6.7 ‰, Roman Province K series 7.0 - 7.1 ‰ and Radicofani 7.1 - 7.4 ‰. Compared to olivines from an unaffected mantle these values are too high and clearly indicate an ^{18}O enriched mantle beneath central Italy.

On the basis of the bulk rock and mineral chemistry data the rhyolites from Roccastrada and San Vincenzo have been explained as crustal anatectic melts. The crustal source had to be enriched by fluids in order to produce the high K, Rb, Pb, U, and Th contents. For the Roccastrada ryholites oxygen isotope data of the phenocrystals support a crustal anatectic origin. Oxygen isotope ratios are typically for crustal derived rocks (Hoefs 1997) and minerals like the quartzes, sanidines, and plagioclases are in isotopic equilibrium to each other. This is also true for the San Vincenzo type A rhyolites. But type B rhyolites indicate oxygen isotopic disequilibrium among the phenocrystals.

Oxygen isotopic characteristics of the San Vincenzo rhyolites are supported by Sr isotopes (Ferrara et al. 1989). Phenocrystals of type A rocks are in Sr isotopic equilibrium to each other whereas group B rocks also show a Sr isotopic disequilibrium among the minerals. Therefore a genetic model for the San Vincenzo rhyolites has to explain the inhomogeneous composition of the group B rocks. Feldstein et al. (1994) have calculated that the inhomogeneity can not be produced by large assimilation of crustal material. Thus the heterogeneity has to be due to magma mixing. Magma mixing has also be suggested by Ferrara et al. (1989), Peccerillo et al. (1987) and Serri et al. (1993), which is supported by mafic inclusions and andesitic xenoliths in the rhyolites (Ferrara et al. 1986a, b; 1989). A possible model for this process is a layered or stratified magma chamber, where a more mafic magma underlies the rhyolitic magma (Feldstein et al. 1994). The mafic magma has to be differentiated to a latitic melt, so that mixing between a latitic and a rhyolitic melt can produce the variability of Sr isotope ratios without changing the major elements of the

rhyolites (Feldstein et al. 1994). Consequently the rhyolites of group A originated from parts of the magma chamber, where no mixing between mantle and crustal melts occured. In contrast sources of the phenocrystals within group B rhyolites are (I) small amounts of assimilated crystals from the wall rock, (II) minerals crystallized from the pure anatectic rhyolitic melt, (III) minerals crystallized from a mixture of the rhyolitic and the latitic melt and (IV) phenocrystals of the mantle melt itself, e.g. clinopyroxenes and orthopyroxenes (Feldstein et al. 1994). In order to prohibit a reequilibration of Sr isotopes the residence time for the phenocrystals probably has to be less than 10 ka in the mixed melt. Using diffusion coefficients of Eiler et al. (1992, 1993) and Fortier & Giletti (1989) the inhomogeneity in oxygen isotope ratios would also be preserved. Therefore the model can explain both the Sr isotope and the oxygen isotope heterogeneity. On the other hand the nature and source of the mantle melt has not been clarified yet. Peccerillo et al. (1987) suggested a calc alkaline subcrustal melt akin to the mantle melts of the Roman Province. Contrary Feldstein et al. (1994) argued for a basaltic melt. But the mafic inclusions are characterized by relatively low Sr isotope ratios and high Nd isotope ratios (Innocenti et al. 1992, Ferrara et al. 1989), which do not agree with the values of the Roman Province rocks (Ferrara et al. 1986a, b) nor to the values of the lamproites from Orciatico or Montecatini (Conticelli et al. 1992).

Besides bulk rock and mineral chemistry data oxygen isotope ratios of phenocrystals from the Monte Amiata rocks support a model of mixing of a crustal anatectic and a mantle derived melt. Using the SiO_2 content of the bulk rock and oxygen isotope ratios (fig. 4-17, chapter 4.3.4) the mafic endmember has a similar composition as the Vulsinian melts and the crustal endmember is similar to the San Vincenzo rhyolites.

5.5 Combined Oxygen and Strontium Isotopic Data

In fig. 5-7 a schematic diagram of $\delta^{18}O$ vs. $^{87}Sr / ^{86}Sr$ for the central Italian rocks is shown. The data are compiled from Ferrara et al. (1985, 1986b), Giraud et al. (1986), Holm & Munksgaard (1982), Innocenti et al. (1992), Poli et al. (1984), Taylor & Turi (1976), Vollmer (1976) and this work. Oxygen isotopic compositions are shown for rocks prior to a secondary alteration of the groundmass.

Two different mantle compositions can be observed. The first one is the mantle beneath the Vulsinian mountains with a $\delta^{18}O$ value of about 6.7 ‰ and a $^{87}Sr / ^{86}Sr$ ratio of less than 0.712. In contrast the lamproites have higher $^{87}Sr / ^{86}Sr$ ratios (> 0.714) but similar $\delta^{18}O$ values of about 7.2 ‰.

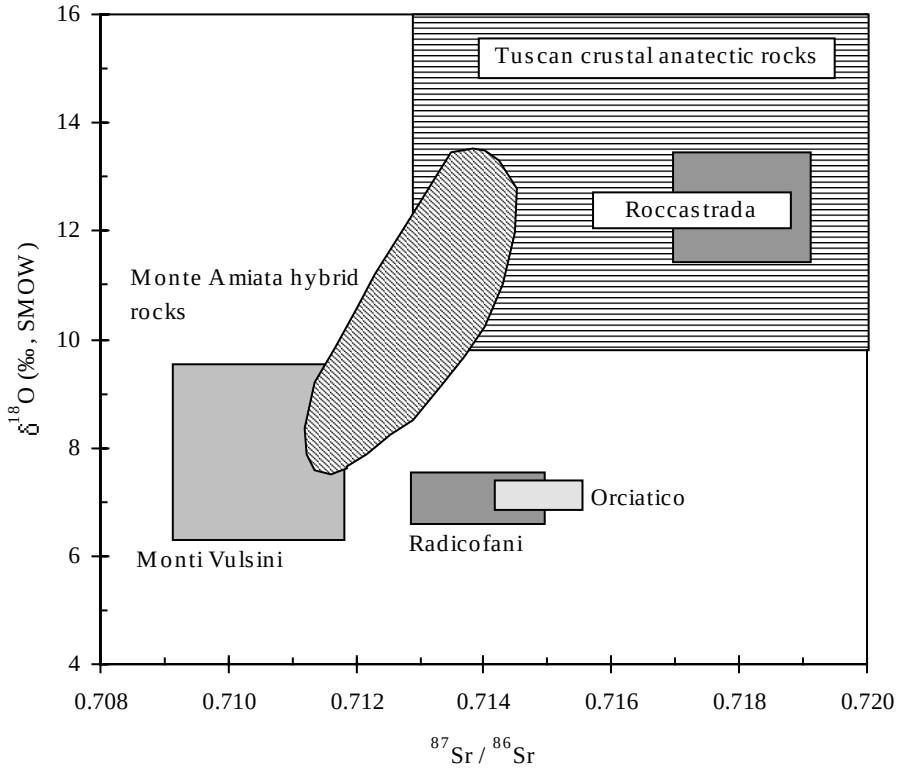

Fig. 5-7: $\delta^{18}O$ values vs. $^{87}Sr / ^{86}Sr$ (i) of central Italian magmatic rocks. $\delta^{18}O$ values are estimated for melts prior to a possible secondary low temperature alteration. Orciatico lamproites show the $\delta^{18}O$ values, which are estimated for the rocks prior to a secondary alteration of the groundmass. Data are compiled from Ferrara et al. (1985, 1986b), Giraud et al. (1986), Holm & Munksgaard (1982), Innocenti et al. (1992), Poli et al. (1984), Taylor & Turi (1976), and this work.

From the Torre Alfina rocks only olivine phenocrystals could be analyzed. These phenocrystals show a large range of $\delta^{18}O$ values. For the high oxygen isotope ratios of the groundmass (13.1 ‰) a secondary alteration must be taken into account. Therefore the Torre Alfina rocks have not been plotted in the diagram. If similar $\delta^{18}O$ compositions of the Torre Alfina rocks and the lamproites is assumed then they lie in the lamproite field because Sr isotope ratios agree with the Sr isotope ratios of the lamproites.

The rocks from Radicofani display a relatively large variability of Sr isotopic ratios but a low variability of oxygen isotopes. This relationship is not a sign of source contamination (James 1981) but a result of mixing between two mantle melts with different Sr isotopic and similar O isotopic compositions. A mixing of a mantle and a crustal melt as it is proposed by Ferrara et al. (1986b) can not explain the composition of the Radicofani rocks.

$\delta^{18}O$ values and $^{87}Sr / ^{86}Sr$ ratios of the rhyolites from Roccastrada are typical for crustal anatectic rocks in Tuscany. The San Vincenzo rhyolites display a more complex pattern.

Generally their $^{87}Sr / ^{86}Sr$ ratios are higher than 0.720 with $\delta^{18}O$ values higher than 11 ‰. But some ryholites with low $^{87}Sr / ^{86}Sr$ occur (Innocenti et al. 1992).

The Sr and O isotopic data from Monte Amiata confirm a petrogenetic model of a mixing between crustal anatectic and Vulsinian melts.

5.6 Radiogenic Isotopic Data

In this subchapter radiogenic isotopes from the literature are compiled and discussed with regard to a few new data from the rocks investigated. The analyses of the radiogenic isotope ratios have kindly been carried out by A. Peccerillo (personal communication). In fig. 5-8 and 5-9 ratios of $^{143}Nd / ^{144}Nd$ vs. $^{87}Sr / ^{86}Sr$ and $^{206}Pb / ^{204}Pb$ vs. $^{87}Sr / ^{86}Sr$ are shown.

In general a continuous change in the isotopic composition of the mantle melts from the Roman Province, the Southern Latium Transition Zone (Ernici - Roccamonfina), the Campanian Province (Stromboli - Vesuvius) and the Monte Vulture can be observed with a northward decrease of $^{143}Nd / ^{144}Nd$ and $^{206}Pb / ^{204}Pb$ ratios and an increase in $^{87}Sr / ^{86}Sr$ ratios (data summarized by Innocenti et al. 1992, Peccerillo 1999, Peccerillo & Panza 1999, Vollmer 1976, see fig. 5-8, 5-9). This regional distribution may be caused by a change of the amount of fluids or melts, metasomatizing the mantle, or by a change of the composition of the fluids or melts.

As in the $\delta^{18}O$ vs. $^{87}Sr / ^{86}Sr$ diagram (fig. 5-7) three different groups can be distinguished in central Italy. The first group are the Roman Province melts, the second group are the Tuscan anatectic rocks and the third group are the lamproites.

The radiogenetic isotope ratios diagrams also show, that mantle sources between the Tuscan Province and the Roman Province are different and that the lamproites can not be generated by mixing of Roman Province melts or mantle domains with crustal material from Tuscany.

The similarity of the radiogenic isotope ratios between the Torre Alfina rocks and the lamproites confirm the genetic model, that the Torre Alfina rocks are lamproites. Even the Radicofani rocks, which from mineral and bulk rock chemistry are a mixture of lamproitic melts and Roman Province melts, lie in or near the lamproite field.

For Monte Amiata only few Nd and Pb isotopic data are available (Innocenti et al. 1992) but these data support a model of mixing between Roman Province and crustal melts.

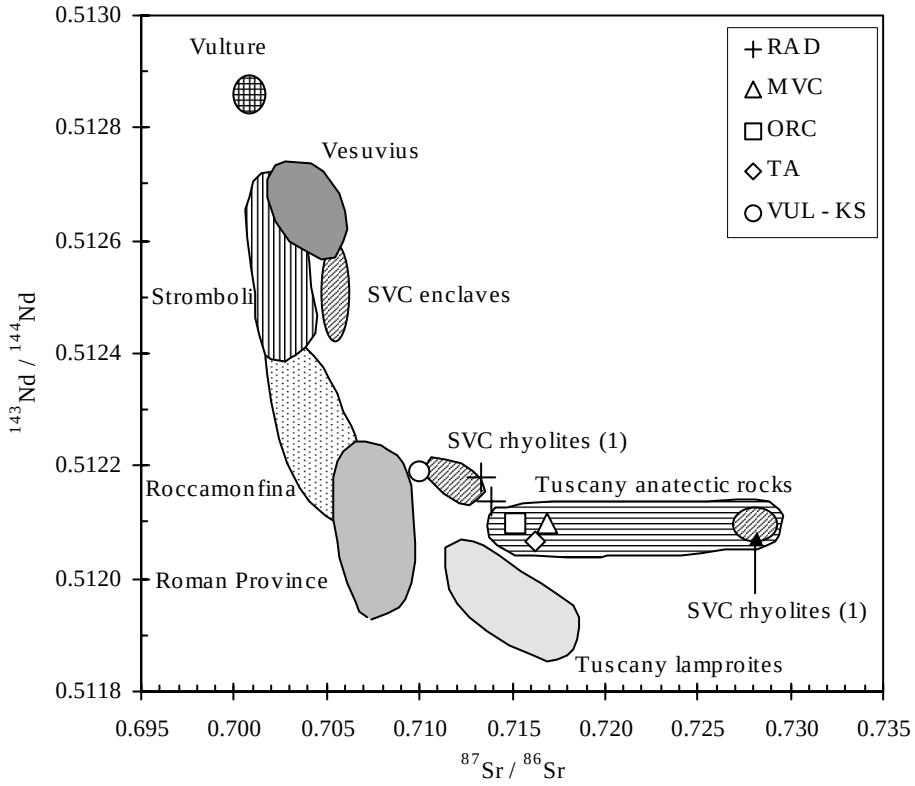

Fig. 5-8: $^{143}Nd / ^{144}Nd$ vs. $^{87}Sr / ^{86}Sr$ ratios for igneous rocks from Italy (RAD: Radicofani, MVC: Montecatini Val di Cecina, ORC: Orciatico, TA: Torre Alfina, VUL-KS: Monti Vulsini K series, SVC: San Vincenzo, SVC rhyolites (1): rhyolites with a low $^{87}Sr / ^{86}Sr$ ratio, SVC rhyolites (2): rhyolites with a high $^{87}Sr / ^{86}Sr$ ratio, SVC enclaves: mafic enclaves in the rhyolites). Data are summarized from Innocenti et al. (1992) and Peccerillo & Panza (1999).The new data are represented by symbols (Peccerillo, personal information, see tab. A-22).

Rhyolites from Roccastrada agree with the Tuscan anatectic rocks, but San Vincenzo rhyolites display a different behaviour. They are not plotted in the diagram because Pb isotope ratios are not available. Mafic inclusions have very high $^{143}Nd / ^{144}Nd$ ratios. Thus the mafic melt, which influenced the group B rhyolites, must be different from the Roman and the Tuscan mantle melts. This may indicate a heterogenic composition of the mantle beneath the Tuscan Province.

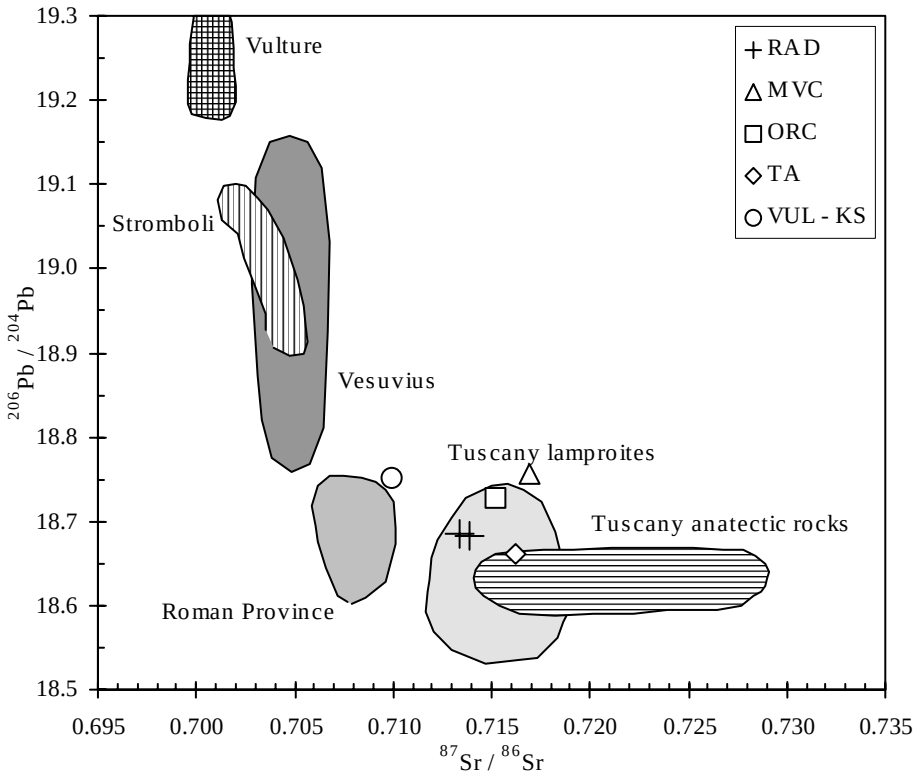

Fig. 5-9: ^{206}Pb / ^{204}Pb vs. ^{87}Sr / ^{86}Sr ratios for the igneous rocks from Italy (RAD: Radicofani, MVC: Montecatini Val di Cecina, ORC: Orciatico, TA: Torre Alfina, VUL-KS: Monti Vulsini K series). Data are summarized by Peccerillo & Panza (1999) and Vollmer (1976). Additional isotopic analyses (symbols) were carried out at the University of Perugia (Peccerillo, personal information, see tab. A-22).

5.7 Petrogenesis and Geodynamic Model

In this section the petrogenesis of the central Italian igenous rocks is set in a broader geodynamic model. The complex petrological and geochemical situation of the Tertiary and Quarternary magmatism in central Italy and on the Italian peninsular has often been described but without a consideration of the geodynamic situation of the Mediterranean region. On the other hand the magmatic evolution in Italy in relation to the geodynamic situation has been investigated but without an explanation of the geochemical and petrological composition of the single magmatic zones or provinces in Italy. Recently Peccerillo (1999) and Peccerillo & Panza (1999) have developed a combined petrological and geodynamic model of the Italian magmatism. The petrogenetic results of this study are tested whether they confirm this model or not.

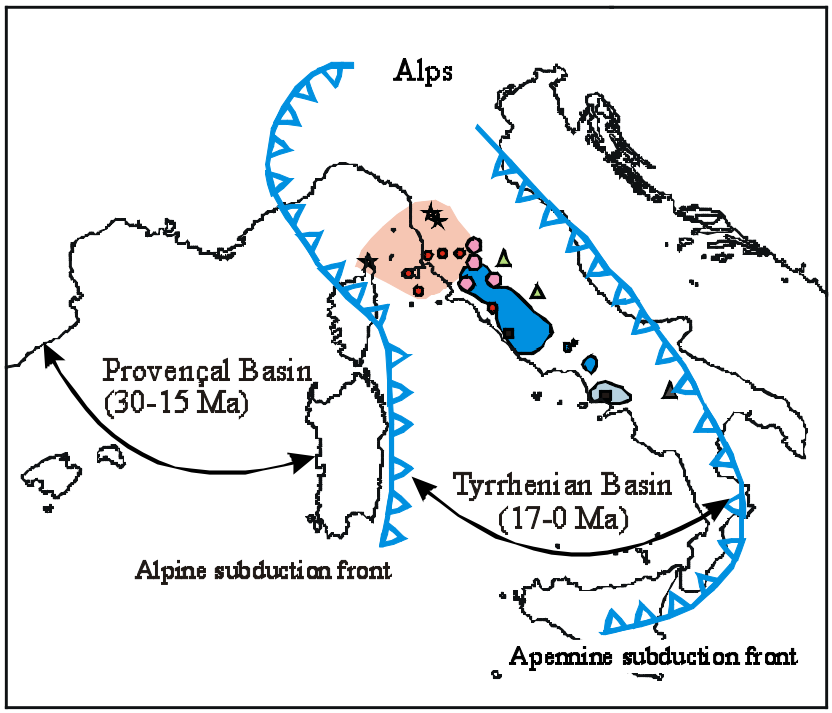

Fig. 5-10: Schematic distribution of magmatism on the Italian peninsular (modified after Peccerillo 1999): Three provinces are shown: I) in the northern part the Tuscan Province (bright red) with lamproites (stars) and crustal anatectic rocks (red circles); II) in the central part the Roman Province (dark blue field), transitional rocks (big, bright red circles) and kamafugitic rocks (green triangles); III) in the southern part the Campanian Province (bright blue field) and the Mount Vulture (black triangle). Subduction fronts are plotted as lines, the Alpine subduction front in the western part and the present Apennine front in the eastern part (Gueguen et al. 1997). The arrows indicate backarc extension.

In central Italy two general trends of eruption ages can be observed. Rock ages decrease from west to east and from north to south (e.g. Peccerillo et al. 1987, Innocenti et al. 1992, Serri et al. 1993). The oldest rocks are the crustal anatectic rocks and lamproites with an age of older than 6 and about 4 Ma, respectively (e.g. Peccerillo et al. 1987, Innocenti et al. 1992). The igneous rocks from the islands lieing west of cental Italy display a higher age, e.g. the lamproites from Corsica are 14 - 15 Ma old (e.g. Peccerillo et al. 1987). Generally the Roman Province rocks are younger than 0.6 Ma (e.g. Peccerillo et al. 1987). A geodynamic model has to explain the different compositions of the rocks including the differences between the mantle compositions beneath the Tuscan and Roman Province as well as the sequence of ages.

Villemant & Fledoc (1989) dated on the basis of Th-U disequibrium investigations an age of about 300 ka for the metasomatism of the Vico volcano mantle source, Roman Province. Therefore the metasomatism of the Roman Province type rocks on the Italian peninsular is temporally related to the eruption age of the rocks without a large time gap. But on the other hand such implications are not given for the metasomatism of the lamproitic mantle source. In

this case the metasomatic event must not neccessarily be related to the eruption age but may be older (Peccerillo 1999, Peccerillo & Panza 1999).

The Tuscan lamproites display an almost identical composition to lamproitic rocks from the western Alps and from Corsica (Mitchell & Bergman 1991, Peccerillo 1999). Therefore the source of these lamproites must be similar in composition. Furthermore all lamproites are sited east of the Alpine collision front (Gueguen et al. 1997, Peccerillo 1999). The geochemical and geological data indicate a similar source with a corresponding evolutionary history of these lamproites (Peccerillo 1999). Furthermore a possible mantle contaminant may be rocks with a similar composition like the Dora Maira metapelitic rocks (Peccerillo 1999). For these rocks Tilton et al. (1989) have shown a deep subduction to a depth of about 100 km and suggested that rocks with a similar composition had been the contaminant of the mantle source of the Spanish lamproites. The Spanish lamproites from the Murcia-Almeria region complete the tectonic view of a similar genesis of lamproites from the western Mediterranean region including Tuscany. The Spanish lamproites are situated on the south - the African site - of the Alpine front (e.g. Mitchell & Bergman 1991).

As mentioned before the lamproitic rocks in the central Mediterranean region - Corsica and Tuscany - and in the western Alps are located east of the Alpine front and thus on the overriding plate during the collision of the Apulia-Africa and European plates (Rehault et al. 1989). During upper Cretaceous the oceanic crust of the European plates were subducted under the overriding Apulia-Africa plate (Rehault et al. 1989). As a consequence pelitic sediments could possibly be subducted beneath the Apulia plate and contaminate the mantle beneath the Apulian plate. After collision of the Apulia with the European plate subduction of the European plate ceased and parts of the Apulia-Africa plate overthrusted the European plate. Then the Apulia plate started to be subducted beneath Europe (Rehault et al. 1989). During subduction of the Apulian plate induced by a higher density of the Apulian lithosphere compared to the underlieing astenosphere (Malinverno & Ryan 1986) the subducted slab rolled back into a southern direction in the western Mediterranean area and into an eastern direction in the middle Mediterranean region (Malinverno & Ryan 1986). Today subduction occurs beneath the Italian peninsular (e.g. Gueguen et al 1997, Marson et al. 1995). Because the roll back of the subducted slab is faster than the movement of the African plate in the European direction, extension occurs in the central Mediterranean region resulting in the opening of the Provençal and Tyrrhenian basin (Malinverno & Ryan 1986). During the anticlockwise rotation of the arc, the Corsica-Sardinia microplate were detached from the European continent and were translated to its recent position (Keller et al. 1994). This tectonic movement can explain the sequence of the emplacement of lamproitic rocks in the middle Mediterranean region. 42 Ma ago lamproitic rocks in the western Alps were formed in an

extensional regime. A subduction related genesis of the Alpine lamproitic rocks was suggested by Venturelli et al. (1984b). Then 14 - 15 Ma ago the lamproites from Corsica were produced and finally 4 Ma ago the Tuscan lamproites (Civetta et al. 1978, Peccerillo et al 1987). Source of the lamproites are preserved parts of the metasomatized Apulian lithospheric mantle. Partial melting of this mantle part was triggered by two factors. The vacant space by rolling back of the lithospheric part of the Apulia plate was replaced by the upwelling hot asthenospheric mantle (Keller et al. 1994). Thus a high heat flow beneath the Provençal and Thyrrenian basin as well as beneath central Italy was produced (Della Vedova et al. 1991). The second factor is the extensional stress regime in parts of the central Mediterranean region and of the Italian peninsular (e.g. Carmignani et al. 1994, Montone et al. 1995, Keller et al. 1994). Increasing temperature and decreasing pressure resulted in a partial melting of the lamproitic mantle source.

In contrast the Roman Province magmatism is related to the subduction of the Apulian plate itself. The sinking Apulian plate beneath Italy may be the source of the metasomatic agents - fluids or melts - generated by marly metasediments. This metasomatic agent raised upwards in the upwelling mantle material and contaminated it. Metasomatism and partial melting can not have occured with a long time gap (Villemant & Fledoc 1989). Therefore the magmatism of the Roman Province is directly related to the metasomatic event.

Partial melting of the Tuscan basement resulting in the crustal anatectic rocks like the Roccastrada and San Vincenzo rhyolites was related to the same extensional tectonic situation like the generation of the lamproites. Reasons for crustal melting are the high heat flow and the extension in Tuscany (Carmignani et al. 1994, Montone et al. 1995, Keller et al. 1994). Furthermore fluids mobilized in the mantle support the melting (Civetta et al. 1978). These fluids can be the contaminant of the crustal rocks like the Roccastrada rhyolites resulting in an enrichment in LILE like K, Rb, Li, and Th. Additionally for the crustal derived melts with a contribution of mantle melts, like the rocks from Monte Amiata and the San Vincenzo group B rhyolites, the mantle melt itself can also heat up the surrounding crustal rocks.

The sequence of the eruptions in central Italy - southeast decreasing ages - can be explained by a continuous southeast movement of the extensional regime (Montone et al. 1995 , Keller et al. 1994). In contrast the southwards decrease of the eruption ages within the Roman and Campanian Province should be related to the ages of metasomatism of the mantle sources (Peccerillo & Panza 1999).

The present mantle reconstruction beneath the Italian peninsular has been described by Peccerillo & Panza (1999). Beneath the Tuscan Province the upper part of the mantle consists of an old metasomatically veined restitic soft lid approximately metasomatized during the Alpine subduction. This lithospheric mantle part is the source of the lamproitic melts like the

rocks from Orciatico, Montecatini Val di Cecina and Torre Alfina. Lithospheric roots of the Apulia plate underlie this region. In the Roman Province this soft lid of a metasomatically veined restitic mantle also occurs. But this part is underlain by a fertile mantle of asthenospheric origin. It is probably contaminated by Ca rich marly sediments. This fertile metasomatized mantle is the source region of the Roman Province type rocks. The differences between the undersaturated HK series and the K series can result from a lower pressure regime of melting for the K series. The volcano of Radicofani is thus located above a mantle region where both mantle types melted, the metasomatically veined restitic part and the fertile mantle part. This produced the transitional rocks from Radicofani. However the variability of the composition within the HK and the K series (Conticelli et al. 1991) points to a heterogeneous mantle composition beneath the Roman Province. Therefore the mantle beneath the Roman Province is not homogeneously metasomatized but probably display lateral and vertical heterogeneities.

6 Conclusions

Tertiary to Quarternary mantle derived igneous rocks of Italy are characterized by a crustal signature of the trace elements and isotope ratios as well as a potassic to ultrapotassic composition. The reason for the crustal signature is a matter of debate, whether crustal assimilation or source contamination occured and to which degrees these two processes influenced the mantle derived rocks.

This investigation has focussed on central Italy because this region is of special interest. Within a narrow area a large diversity of different igeneous rocks can be observed. In this area two different magmatic provinces overlap - the Roman Magmatic Province in southern central Italy with the Vulsinian mountains and the Tuscan Magmatic Province. The Tuscan Magmatic Province is characterized by lamproites, crustal anatectic rocks as well as hybrid rocks from crustal and mantle derived melts and transitional rocks between Roman type rocks and Tuscan lamproites.

In central Italy three different types of mantle derived rocks can be distinguished. These are the Roman Province type rocks from the Vulsinian mountains, the lamproites and the transitional rocks. For the whole mantle beneath central Italy a metasomatic enrichment of LILE like K, LREE, ^{18}O, ^{87}Sr, and ^{206}Pb is assumed.

Lamproites from the Tuscan Province are mantle derived melts. They are produced by partial melting of a metasomatically overprinted depleted mantle source. Characteristics of the mantle source are high contents of LILE, LREE, and high $\delta^{18}O$ values and high $^{87}Sr/^{86}Sr$ values. Metasomatic agents had a composition similar to the Dora Maira metagranites. An alpine age of the metasomatism has been suggested by Venturelli et al. (1984b) and thus the metasomatism could be a consequence of the subduction of the African plate beneath the European plate.

Roman Province type rocks occuring at the Vulsinian mountains are also mantle derived melt type. The mantle source of these rocks is a fertile mantle, which was metasomatized by fluids or melts rich in LILE, LREE, ^{18}O, and ^{87}Sr. The oxygen isotope compositon of the mantle source is about 6.7 – 7.6 ‰ and thus lower than Holm & Munksgaard (1982) proposed. Therefore the oxygen isotopic composition of the Vulsinian mountains mantle source is similar to volcanic regions of the Roman Province lieing south (Ferrara et al. 1985, Turi et al. 1986). The oxygen isotope composition of the Roman Province mantle seems to be homogeneous. The metasomatic agents were produced recently during the subduction of the Apulian plate beneath central Italy. The source of the metasomatizing melts or fluids are marly sediments. These melts penetrated the mantle beneath the Roman Province producing a veined mantle. The major carrier of the LILE, especially K, and LREE is probably phlogopite.

The differences of K and HK series rocks are the chemical composition of the bulk rock. The isotopic composition, especially the oxygen isotopes, are similar. Thus the K and HK series rocks were probably produced in a roughly homogeneously composed mantle but under different pressure conditions with a lower pressure for the KS and a higher pressure for the HKS rocks. The range from less to highly evolved rocks from the Vulsinian mountains can be produced by fractional crystallization and crustal assimilation processes or more complex processes like refilling + tapping + crystal fractionating + assimilation (Conticelli et al. 1997). However large assimilation of carbonatic material in order to produce the high oxygen isotope ratios can be excluded. Although the general composition of the mantle beneath the Roman Province is homogeneous, variations in the composition could be observed by (Conticelli et al. 1991) leading to the conclusion that for every volcano the source composition had to be determined and that the source compositions for the single volcanoes of the Vulsinian mountains differ slightly.

Comparing both mantle sources from the Tuscan and Roman Province the following differences and common grounds can be observed. Prior to metasomatism the mantle of the Tuscan Province was depleted whereas the Roman Province mantle was fertile. The metasomatic agents were differently composed producing different radiogenic isotope characteristics for the two mantle sources. But their oxygen isotopic compositions are probably similar ranging between 6.5 – 7.5 ‰. The metasomatism of the Tuscan mantle is an old one of an Alpine age, whereas the metasomatism of the Roman mantle is relatively young. Lamproitic melts were generated in the mantle at low depth (lithospheric mantle) whereas the KS rocks from the Roman Province were generated at an intermediate depth and the HKS rocks at greater depths.

The third group of mantle derived melts are transitional rocks between Tuscan and Roman Type melts. Two different volcanoes have been sampled. The Torre Alfina volcano has a great geochemical affinity to the lamproites. But particularly clinopyroxenes display an influence of Roman type melts in the genesis of the Torre Alfina lavas. The peridotitic xenolith clearly indicates an metasomatically overprinted and ^{18}O enriched mantle beneath central Italy.

The other transitional rocks are the volcanic rocks from Radicofani. They are also a mixture of lamproitic and Roman type melts but with a stronger affinity to the Roman type melts. These rocks display a large variability in Sr isotope ratios and a homogeneous composition of oxygen isotope ratios. A combination of these two isotopic systems is often used to distinguish between crustal assimilation and source contamination (James 1981) – a large range of Sr and a small range of oxygen isotope ratios is interpreted as source contamination. But in this case the two endmembers of the Radicofani rocks have different Sr isotope ratios and similar oxygen isotope ratios, so that the previous interpretation cannot be used for these

rocks. The generation of the transitional rocks can be explained by a transition zone between the Roman and the Tuscan mantle. The Roman Province mantle underlies the Tuscan Province mantle in this zone. Generated melt in the Roman Province mantle raised up and mixed with melts in the Tuscan mantle with different degrees producing the rocks from Torre Alfina and Radicofani.

In the Tuscan Province acidic crustal anatectic rocks also occur like the rhyolites from Roccastrada and San Vincenzo. Their chemical compositions point to an enriched crustal source. The enriching agents for the Roccastrada and parts of the San Vincenzo rhyolites (group A) were probably fluids derived from the mantle. The oxygen isotope ratios are common for crustal anatectic rocks. However the San Vincenzo group B rhyolites are assumed to be influenced by a mantle derived melt. The mixing of mantle and crustal melts is preserved by the oxygen isotope and Sr isotope (Ferrara et al. 1989) heterogeneities of the phenocrystals.

Hybrid rocks between crustal and mantle melts occur at Monte Amiata. The crustal melts are similar to the San Vincenzo rhyolites whereas the mantle endmember is similar to the K series rocks from the Vulsinian mountains.

7 References

Anders E & Grevesse N (1989): Abundances of the elements: Meteorictic and solar.- Geochimica et Cosmochimica Acta, 53: 197-214.

Ando A, Kamioka H & Terashima S (1989): 1988 values for GSJ rock reference samples, "Igneous rock series".- Geochemical Journal, 23: 143-148.

Arima M & Edgar A D (1983): A high pressure experimental study on a magnesian rich leucite-lamproite from a West Kimberley area, Australia: petrogenetic implication.- Contributions to Mineralogy and Petrology, 84: 228-234.

Armstrong J T (1991): Quantitative elemental analysis of individual microparticles with electron beam instruments.- 261-315 in: Heinrich K F J & Newbury D E [eds]: Electron probe quantitation.- 1st ed: 400 pp, New York, U.S.A. (Plenum Press).

Arth J G (1976): Behaviour of trace elements during magmatic processes - a summary of theoretical models and their applications.- Journal of Research of the U.S. Geological Survey, 4: 41-47.

Asprey L B (1976): The preparation of very pure fluorine.- Journal of Fluorine Chemistry, 7: 359-361.

Baertschi P & Silverman S R (1951): The determination of relative abundances of the oxygen isotopes in silicate rocks.- Geochimica et Cosmochimica Acta, 1: 317-328.

Balducci S & Leoni L (1981): Sanidine megacrysts from M. Amiata trachytes and Roccastrada rhyolites.- Neues Jahrbuch Mineralogische Abhandlungen, 143: 15-36.

Barberi F & Innocenti F (1967): Le rocce selagitiche di Orciatico e Montecatini in Val di Cecina.- Atti della Società Toscana di Scienze Naturali, Memorie Serie A, 74: 103-190.

Barnekow P, Hoefs J & Peccerillo A (1998): In situ measurement of oxygen isotope ratios by laser ablation mass spectrometry - an example from the Torre Alfina volcano, central Italy.- Mineralogical Magazine, 62A: 120-121.

Beccaluva L, Di Girolamo P & Serri G (1991): Petrogenesis and tectonic setting of the Roman Volcanic Province, Italy.- Lithos, 26: 191-221.

Bindi L, Cellai D, Melluso L, Conticelli S, Morra V & Menchetti S (1999): Crystal chemistry of clinopyroxene from alkaline undersaturated rocks of the Monte Vulture, Italy.- Lithos, 46: 259-274.

Caggianelli A, De Fino M, La Volpe L & Picarreta G (1990): Mineral chemistry of Monte Vulture volcanics: Petrological implications.- Mineralogy and Petrology, 41: 215-227.

Carmichael I S E, Turner F J & Verhoogen J (1974): Igneous Petrology.- 1st ed: 739 pp, New York, U.S.A. (McGraw-Hill Book Company).

Carmignani L, Decandia F A, Fantozzi P L, Lazzarotto A, Liotta D & Meccheri M (1994): Tertiary extensional tectonics in Tuscany (northern Apennines, Italy).- Tectonophysics, 238: 295-315.

Cellai D, Conticelli S & Menchetti S (1994): Crystal-chemistry of clinopyroxenes from potassic and ultrapotassic rocks in central Italy: Implications on their genesis.- Contributions to Mineralogy and Petrology, 116: 301-315.

Cherniak D J & Lanford W A (1989): Oxygen diffusion in olivine: effect of oxygen fugacity and implications for creep.- Journal of Geophysical Research, 94, B4: 4105-4118.

Chiba H, Chacko T, Clayton R N & Goldsmith J R (1989): Oxygen isotope fractionations involving diopside, forsterite, magnetite, and calcite. Application to geothermometry.- Geochimica et Cosmochimica Acta, 53: 2985-2995.

Civetta L, Innocenti F, Manetti P, Peccerillo A & Poli G (1981): Geochemical characteristics of potassic volcanism from Mts. Ernici (southern Latium, Italy).- Contributions to Mineralogy and Petrology, 78: 37-47.

Civetta L, Orsi G & Scandone P (1978): Eastward migration of the Tuscan anatectic magmatism due to anticlockwise rotation of the Apennines.- Nature, 276: 604-605.

Clayton R N & Mayeda T K (1963): The use of bromine pentafluoride in the extraction of oxygen from oxides and silicates for isotoic analysis.- Geochimica et Cosmochimica Acta, 27: 43-52.

Clemens J D & Wall V J (1981): Origin and crystallization of some peraluminous (S-type) granitic magmas.- Canadian Mineralogist, 19: 111-131.

Clemens J D & Wall V J (1984): Origin and evolution of a peraluminous silicic ignimbrite suite: the Violet Town volcanics.- Contributions to Mineralogy and Petrology, 88: 354-371.

Conrad M E & Chamberlain C P (1992): Laser-based, in situ measurements of fine-scale variations in the $\delta^{18}O$ values of hydrothermal quartz.- Geology, 20: 812-816.

Conticelli S (1998): The effect of crustal contamination on ultrapotassic magmas with lamproitic affinity: mineralogical, geochemical and isotope data from the Torre Alfina lavas and xenoliths, Central Italy.- Chemical Geology, 149: 51-81.

Conticelli S, Francalanci L, Manetti P, Cioni R & Sbrana A (1997): Petrology and geochemistry of the ultrapotassic rocks from the Sabatini Volcanic District, central Italy: the role of evolutionary processes in the genesis of variably enriched alkaline magmas.- Journal of Volcanology and Geothermal Research, 75: 107-136.

Conticelli S, Francalanci L & Santo A P (1991): Petrology of final-stage Latera Lavas (Vulsini Mts.): mineralogical, geochemical and Sr-isotopic data and their bearing on the genesis of some potassic magmas in central Italy.- Journal of Volcanology and Geothermal Research, 46: 187-212.

Conticelli S, Manetti P & Menichetti S (1992): Mineralogy, geochemistry and Sr-isotopes in orendites from South Tuscany, Italy: constraints on their genesis and evolution.- European Journal of Mineralogy, 4: 1359-1375.

Conticelli S & Peccerillo A (1990): Petrological significance of high-pressure ultramafic xenoliths from ultrapotassic rocks of Central Italy.- Lithos, 24: 305-322.

Conticelli S & Peccerillo A (1992): Petrology and geochemistry of potassic and ultrapotassic volcanism in central Italy: Petrogenensis and inferences on the evolution of the mantle sources.- Lithos, 28: 221-240.

Dal Negro A, Carbonin S, Salviulo G, Piccirillo E M & Cundari A (1985): Crystal chemistry and site configuration of the clinopyroxene from leucite-bearing rocks and related genetic significance: the Sabatini lavas, Roman Region, Italy.- Journal of Petrology, 26: 1027-1040.

Deer W A, Howie R A & Zussman J (1996): An introduction to the rock-forming minerals.- 2nd ed: 696 pp, Harlow, UK (Longman).

De Fino M, La Volpe L, Peccerillo A, Piccarreta G & Poli G (1986): Petrogenesis of Monte Vulture volcano (Italy): inferences from mineral chemistry, major and trace element data.- Contributions to Mineralogy and Petrology, 92: 135-145.

Della Vedova B, Marson I, Panza G F & Suhadolc P (1991): Upper mantle properties of the Tuscan-Tyrrhenian area: A framework for its recent tectonic evolution.- Tectonophysics, 195: 311-318.

Dobosi G & Jenner G A (1999): Petrologic implications of trace element variation in clinopyroxene megacrysts from the Nograd volcanic province, north Hungary; a study by laser ablation microprobe-inductively coupled plasma-mass spectrometry.- Lithos, 46: 731-749.

Edgar A D & Vukadinovic D (1992): Implications of experimental petrology to the evolution of ultrapotassic rocks.- Lithos, 28: 205-220.

Eiler J M, Baumgartner L P & Valley J W (1992): Intercrystalline stable isotope diffusion: a fast grain boundary model.- Contributions to Mineralogy and Petrology, 112: 543-557.

Eiler J M, Valley J W & Baumgartner L P (1993): A new look at stable isotope thermometry.- Geochimica et Cosmochimica Acta, 57: 2571-2583.

Elsenheimer D & Valley J W (1992): In situ oxygen isotope analysis of feldspar and quartz by Nd:YAG laser microprobe.- Chemical Geology, 101: 21-42.

Federico M, Peccerillo A, Barbieri M & Wu T W (1994): Mineralogical and geochemical study of granular xenoliths from the Alban Hills volcano, Central Italy: bearing on evolutionary processes in potassic magma chambers.- Contributions to Mineralogy and Petrology, 115: 384-401.

Feldstein S N, Halliday A N, Davies G R & Hall C M (1994): Isotope and chemical microsampling: Constraints on the history of an S-type rhyolite, San Vincenzo, Tuscany, Italy.- Geochimica et Cosmochimica Acta, 58: 943-958.

Ferguson A K (1978): Ca-enrichment in olivine from volcanic rocks.- Lithos, 11: 189-194.

Ferrara G, Laurenzi M A, Taylor H P jr, Tonarini S & Turi B (1985): Oxygen and strontium isotope studies of K-rich volcanic rocks from the Alban Hills, Italy.- Earth and Planetary Science Letters, 75: 13-28.

Ferrara G, Leoni L, Sartori F & Tonarini S (1988): Sr-content and Sr isotopic compositions in contact metamorphosed argillaceous sediments (Orciatico, Tuscany, central Italy): relation to fluid circulation.-Rendiconti della Società Italiana di Mineralogia e Petrologia, 43: 121-128.

Ferrara G, Petrini R, Serri G & Tonarini S (1989): Petrology and isotope-geochemistry of San Vincenzo rhyolites (Tuscany, Italy).- Bulletin of Volcanology, 51: 379-388.

Ferrara G, Petrini R & Tonarini S (1986a): S. Vincenzo volcanites (italy): A Sr-Nd isotopic study.- Terra Cognita, 6: 200.

Ferrara G, Preite-Martinez M, Taylor H P jr, Tonarini S & Turi B (1986b) Evidence for crustal assimilation, mixing of magmas and a ^{87}Sr-rich upper mantle.- Contributions to Mineralogy and Petrology, 92: 269-280.

Ferrari L, Conticelli S, Burlamacchi L & Manetti P (1996): Volcanological evolution of the Monte Amiata, southern Tuscany: New geological and petrochemical data.- Acta Vulcanologica, 8: 41-56.

Fiebig J, Simon K & Hoefs J (2000): Exchange mechanisms, fluid flow and fluid evolution during hydrothermal alteration of granites: A case study from the southeastern Schwarzwald, Germany.- Geochimica et Cosmochimica Acta, submitted.

Fiebig J, Wiechert U, Rumble III D, Hoefs J (1999): High-precision in situ oxygen isotope analysis of quartz using an ArF laser.- Geochimica et Cosmochimica Acta, 63: 687-702.

Foley S F (1989): Experimental constraints on phlogopite chemistry in lampoites: 1. The effect of water activitiy and oxygen fugacity.- European Journal of Mineralogy, 1: 411-426.

Foley S F (1990): Experimental constraints on phlogopite chemistry in lampoites: 2. Effect of pressure-temperature variations.- European Journal of Mineralogy, 2: 327-341.

Foley S F (1992a): Petrological characterization of the source componenets of potassic magmas: geochemical and experimental constraints.- Lithos, 28: 187-204.

Foley S F (1992b): Vein-plus-wall-rock melting mechanism in the lithosphere and the origin of potassic alkaline magmas.- Lithos, 28: 435-453.

Foley S F & Peccerillo A (1992): Potassic and ultrapotassic magmas and their origin.- Lithos, 28: 181-185.

Foley S F, Taylor W R & Green D H (1986): The effect of fluorine on phase relationships in the system $KAlSiO_4$-Mg_2SiO_4-SiO_2 and the solution mechanism of fluorine in silicate melts.- Contributions to Mineralogy and Petrology, 93: 46-55.

Foley S F, Venturelli G, Green D H & Toscani L (1987): The ultrapotassic rocks: Characteristics, classification, and constraints for petrogenetic models.- Earth-Science Reviews, 24: 81-134.

Fortier S M & Giletti J (1989): An empirical model for predicting diffusion coefficients in silicate minerals.- Science, 245: 1481-1484.

Francalanci L, Peccerillo A & Poli G (1987): Partition coefficients for minerals in potassium-alkaline rocks; data from Roman Province (central Italy).- Geochemical Journal, 21: 1-10.

Fujimaki H (1986): Partition coefficients of Hf, Zr and REE between Zircon, apatite and liquid.- Contributions to Mineralogy and Petrology, 94: 42-45.

Giraud A, Dupuy C & Dostal J (1986): Behaviour of trace elements during magmatic processes in the crust: Application to acidic volcanic rocks of Tuscany (Italy).- Chemical Geology, 57: 269-288.

Green T H (1976): Experimental generation of cordierite or garnet-bearing granitic liquids from a pelitic composition.- Geology, 4: 85-88.

Gueguen E, Doglioni C & Fernandez M (1997): Lithospheric boudinage in the Western Mediterranean back-arc basin.- Terra Nova, 9: 184-187.

Hagen B (2000): Thesis in preparation, University of Bonn, Germany.

Harmon R S & Hoefs J (1995): Oxygen isotope heterogeneity of the mantle deduced from global ^{18}O systematics of basalts from different geotectonic settings.- Contributions to Mineralogy and Petrology, 120: 95-114.

Hartmann G (1994): Late-medievial glass manufacture in the Eichsfeld region (Thuringia, Germany).- Chemie der Erde, 54: 103-128.

Hawkesworth C J & Vollmer R (1979): Crustal contamination versus enriched mantle: ^{143}Nd / ^{144}Nd and ^{87}Sr / ^{86}Sr evidence from the Italian volcanics.- Contributions to Mineralogy and Petrology, 69: 151-165.

Heinrichs H & Hermann A G (1990): Praktikum der analytischen Geochemie.- 1st ed: 669 pp, Berlin, Heidelberg, New York (Springer Verlag).

Hoefs J (1997): Stable isotope geochemistry.- 4th enlarged ed: 201 pp, Berlin, Heidelberg, New York (Springer).

Holm P M, Lou S & Nielsen A (1982): The geochemistry and petrogenesis of the lavas of the Vulsinian district, Roman Province, Central Italy.- Contributions to Mineralogy and Petrology, 80: 367-388.

Holm P M & Munksgaard N C (1982): Evidence for mantle metasomatism: an oxygen and strontium isotope study of the Vusinian District, Central Italy.- Earth and Planetary Science Letters, 60: 376-388.

Innocenti F (1967): Studio chimico-petrografico delle vulcaniti di Radicofani.- Rendiconti della Società Italiana di Mineralogia e Petrologia, 23: 99-128.

Innocenti F, Serri G, Ferrara G, Manetti P & Tonarini S (1992): Genesis and classification of the rocks of the Tuscan Magmatic Province: thirty years after Marinelli's model.- Acta Vulcanologica, 2: 247-265.

Innocenti F & Trigila R [eds] (1987): Vulsini Volcanoes.- Periodico di Mineralogia, 56: 89-318.

James D E (1981): The combined use of oxygen and radiogenic isotopes as indicators of crustal contamination.- Annual Review of Earth and Planetary Sciences, 9: 311-344.

Jaoul O, Froidevaux C, Durham W B & Michaut M (1980): Oxygen self-diffusion in forsterite: Implications for the high-temperature creep mechanism.- Earth and Planetary Science Letters, 47: 391-397.

Jaques A L, Lewis G D, Smith C B, Gregory C P , Ferguson J, Chappell B W & McCulloch M T (1984): The diamond-bearing ultrapotassic (lamproitic) rocks of the West-Kimberley region, Western Australia.- in: Kornprobst J. [ed.]: Proceedings of the third International Kimberlite conference, Volume I, Kimberlites and related rocks, 11a: 223-254.

Kamenetsky V, Métrich N & Cioni R (1995): Potassic primary melts of Vulsini (Roman Province): evidence from mineralogy and melt inclusions.- Contributions to Mineralogy and Petrology, 120: 186-196.

Keller J V A, Minelli G & Pialli G (1994): Anatomy of late orogenic extension: the northern Apennines case.- Tectonophysics, 238: 275-294.

Kirschner D L, Sharp Z D & Teyssier C (1993): Vein growth mechanisms and fluid sources revealed by oxygen isotope laser microprobe.- Chemical Geology, 21: 85-88.

Le Bas M J, Le Maitre R W, Streckeisen A & Zanettin B (1986): A Chemical Classification of Volcanic Rocks Based on the Total Alkali-Silica Diagram.- Journal of Petrology, 27: 745-750.

Lundstrom C C, Shaw H F, Ryerson F J, Williams Q & Gill J (1998): Crystal chemical control of clinopyroxene-melt partitioning in the Di-Ab-An system; implications for elemental fractionations in the depleted mantle.- Geochimica et Cosmochimica Acta, 62: 2849-2862.

Mahood G & Hildreth W (1983): Large partition coefficients for trace elements in high-silica rhyolites.- Geochimica et Cosmochimica Acta, 47: 11-30.

Malinverno A & Ryan W B F (1986): Extension in the Tyrrhenian sea and shortening in the Apennines as result of arc migration driven by sinking of the lithosphere.- Tectonics, 5: 227-245.

Marinelli G (1961): Genesi e classificazione delle vulcaniti recenti toscane.- Atti della Società Toscana di Scienze Naturali, Memorie Serie A, 68: 74-116.

Marson I, Panza G F & Suhadolc P (1995): Crust and upper mantle models along the active Tyrrhenian rim.- Terra Nova, 7: 348-357.

Masuda H & O'Neil J R (1994): Oxygen isotope heterogeneity of phenocysts in rhyolite from San Vincenzo, Italy, by laser microprobe analysis.- Geochemical Journal, 28: 377-385.

Mattey D P, Lowry D & Macpherson C (1994): Oxygen isotope composition of mantle peridotites.- Earth and Planetary Science Letters, 70: 196-206.

Mattey D, Macpherson C (1993): High precision oxygen isotope microanalysis of ferromagnesian minerals by laser fluorination.- Chemical Geology, 105: 305-318.

Matthews A, Goldsmith, J R & Clayton R N (1983): Oxygen isotope fractionation involving pyroxenes: The calibration of mineral-pair geothermometers.- Geochimica et Cosmochimica Acta, 47: 645-654.

McDonough W F & Sun S S (1995): The composition of the Earth.- Chemical Geology, 120: 223-253.

Meyer R J (1926): Gmelins Handbuch der anorganischen Chemie, Fluor.- Vol. 5, 8th completey revised ed: 86 pp, Leipzig, Berlin (Verlag Chemie G.m.b.H.).

Meyer R J & Pietsch E H E (1959): Gmelins Handbuch der anorganischen Chemie, Fluor Ergänzungsband.- Vol. 5, 8th completey revised ed: 258 pp, Weinheim (Verlag Chemie G.m.b.H.).

Mitchell R H & Bergman S C (1991): Petrology of lamproites.- 1st ed: 447 pp, New York, London (Plenum Press).

Mitchell R H, Platt R G & Downey M (1987): Petrology of lamproites from Smoky Butte, Montana.- Journal of Petrology, 28: 645-677.

Montone P, Amato A, Chiarabba C, Buonasorte G & Fiordelisi A (1995): Evidence of active extension in Quarternary volcanoes of central Italy from breakout analysis and seismicity.- Geophysical Research Letters, 22: 1909-1912.

Morimoto N (1989): Nomenclature of pyroxenes.- Canadian Mineralogist, 27: 143-156.

Müller D, Rock N M S & Groves D I (1992): Geochemical discrimination between shoshonitic and potassic volcanic rocks in different tectonic settings: a pilot study.- Mineralogy and Petrology, 46: 259-289.

Nash W P & Crecraft H R (1985): Partition coefficients for trace elements in silicic magmas.- Geochimica et Cosmochimica Acta, 49: 2309-2322.

Pearce N J G (1983): Role of sub-continental lithosphere in magma genesis at active continental margins.- 203-249 in: Hawkesworth C J & Norry M J [eds]: Continental basalts and mantle xenoliths.- Shiva Geology Series, 1st ed: 272 pp, Nantwich, UK (Shiva Publishing Ltd.).

Pearce N J G, Perkins W T, Westgate J A, Gorton M P, Jackson S E, Neal C R & Chenery S P (1997): A compilation of new and published major and trace element data for NIST SRM 610 and NIST SRM 612 glass reference materials.- Geostandards Newsletters, The Journal of Geostandards and Geoanalysis: 21: 115-144.

Peccerillo A (1985): Roman comagmatic province: Evidence for subduction-related magma genesis.- Geology, 13: 103-106.

Peccerillo A (1990): On the origin of the Italian potassic magmas - comments.- Chemical Geology, 85: 183-191.

Peccerillo A (1992): Potassic and ultrapotassic rocks: Compositional characteristics, petrogenesis, and geologic significance.- Episodes, 15: 243-251.

Peccerillo A (1994): Mafic ultrapotassic magmas in central Italy: geochemical and petrological evidence against primary compositions.- Mineralogica et Petrographica Acta, 27: 229-245.

Peccerillo A (1998): Relationships between ultrapotassic and carbonate-rich volcanic rocks in central Italy: Petrogenetic and geodynamic implications.- Lithos, 43: 267-279.

Peccerillo A (1999): Multiple mantle metasomatism in central-southern Italy: Geochemical effects, timing and geodynamic implications.- Geology, 27: 315-318.

Peccerillo A, Conticelli S & Manetti P (1987): Petrological characteristics and the genesis of the recent magmatism of southern Tuscany and northern Latium.- Periodico di Mineralogia, 56: 157-172.

Peccerillo A & Manetti P (1985): The potassium alkaline volcanism of central Southern Italy: a review of the data relevant to the petrogenesis and geodynamic significanc.- Transactions of the Geological Society of South Africa, 88: 379-394.

Peccerillo A & Panza G F (1999): Upper mantle domains beneath central-southern Italy: Petrological, geochemical and geophysical constraints.- Pure and Applied Geophysics, 156: 421-443.

Peccerillo A, Poli G & Serri G (1988): Petrogenesis of orenditic and kamafugitic rocks from central Italy.- Canadian Mineralogist, 26; 45-65.

Pinarelli L (1991): Geochemical and isotopic (Sr, Pb) evidence of crust-mantle interaction in acidic melts. The Tolfa Cerveteri Manziana volcanic complex (Central Italy): a case history.- Chemical Geology, 92: 177-195.

Poli G, Frederick A F & Ferrara G (1984): Geochemical characteristics of the south Tuscany (Italy) volcanic province: constraints on lava petrogenesis.- Chemical Geology, 43: 203-221.

Pratt J H (1894): On the determination of ferrous iron in silicates.- American Journal of Sciences, 3rd series, 48: 149-151.

Reed S J B (1996): Electron microprobe analysis and scanning electron microscopy in geology.- 1st edition: 201 pp, Cambridge, UK (Cambridge University Press).

Rehault J-P, Boillot G & Mauffret A (1989): The western Mediterranean basin.- 101-130 in: Stanley DJ & Wezel F-C [eds]: Geological evolution of the Mediterranean basin.- 1st ed: 589 pp, New York, Berlin, Heidelberg, Tokyo (Springer Verlag)

Rodolico F (1934): Ricerche sulle rocce eruttive recenti della Toscana; II, Le rocce di Orciatico e di Montecatini in val di Cecina.- Atti della Società Toscana di Scienze Naturali, Memorie Serie A, 44: 177-202.

Roeder P L & Emslie R F (1970): Olivine-liquid equilibrium.- Contributions to Mineralogy and Petrology, 29: 275-289.

Rogers N W, Hawkesworth C J, Parker R J & Marsh J S (1985): The geochemistry of potassic lavas from Vulsini, central Italy and implications for mantle enrichment processes beneath the Roman region.- Contributions to Mineralogy and Petrology, 90: 244-257.

Rumble III D R, Farquhar J, Young E D & Christensen C P (1997): In situ oxygen isotope analysis with an excimer laser using F_2 and BrF_5 reagents and O_2 gas as analyte.- Geochimica et Cosmochimica Acta, 61: 4229-4234.

Ryerson F J, Durham W B, Cherniak D J & Lanford D A (1989): Oxygen diffusion in olivine: Effect of oxygen fugacity and implications for creep.-Journal of Geophysical Research, B94: 4105-4118.

Sahama Th G (1974): Potassium-rich alkaline rocks.- 96-109 in: Sörensen H [ed]: The Alkaline Rocks.- 1st ed: 622 pp, London, New York, Sydney, Toronto (John Wiley & Sons).

Schilling J-G, Zajac M, Evans R, Johnston T, White W, Devine J D & Kingsley R (1983): Petrologic and geochemical variations along the Mid-Atlantic Ridge from 27°N to 73°N.- American Journal of Science, 283: 510-586.

Scholz E (1984): Karl Fischer Titration. Methoden zur Wasserbestimmung.- 1st ed: 136 pp, Berlin, Heidelberg, New York, Tokyo (Springer Verlag).

Schosnig M & Hoffer E (1998): Compositional dependence of REE partitioning between diopside and melt at 1 atmosphere.- Contributions to Mineralogy and Petrology, 133: 205-216.

Scott Smith B H (1996): Lamproites.- 259-270 in: Mitchell R H [ed]: Undersaturated alkaline rocks: mineralogy, petrogenesis, and economic potential.- Mineralogical Association of Canada Short Courses Series, 24: 312 pp.

Scott V D, Love G & Reed S J B (1995): Quantitative electron-probe microanalysis.- 2nd ed: 311 pp, New York, London, Toronto, Sydney, Tokyo, Singapore (Ellis Horwood).

Serri G, Innocenti F & Manetti P (1993): Geochemical and petrological evidence of the subduction of delaminated Adriatic continental lithosphere in the genesis of the Neogene-Quaternary magmatism of central Italy.- Tectonophysics, 223: 117-147.

Simon K, Wiechert U, Hoefs J & Grote B (1997): Microanalysis of minerals by laser ablation ICPMS and SIRMS.- Fresenius' Journal of Analytical Chemistry, 359: 458-461.

Sharp Z D (1990): A laser-based microanalytical method for the in-situ determination of oxygen isotope ratios of silicates and oxides.- Geochimica et Cosmochimica Acta, 54: 1353-1357.

Sharp Z D (1992): In situ laser microprobe techniques for stable isotope analysis.- Chemical Geology, 101: 195-203.

Shaw C S J (1996): The petrology and petrogenesis of Roman Province-Type lavas and ultrapotassic leucitites.- 175-192 in: Mitchell R H [ed]: Undersaturated alkaline rocks: mineralogy, petrogenesis, and economic potential.- Mineralogical Association of Canada Short Courses Series, 24: 312 pp.

Sheppard S M F & Harris C (1985): Hydrogen and oxygen isotope geochemistry of Ascension Island lavas and granites: variation with crystal fractionation and interaction with sea water.- Contributions to Mineralogy and Petrology, 91: 74-81.

Simkin T & Smith J V (1970): Minor element distribution in olivine.- Journal of Geology, 78: 133-147.

Streckeisen A (1979): Classification and nomenclature of volcanic rocks, lamprophyres, carbonatites, and melilitic rocks: Recommendations and suggestions of the IUGS Subcommission on the Systematics of Igenous Rocks.- Geology, 7: 331-335.

Sun S S & McDonough W F (1989): Chemical and isotopic systematics of oceanic basalts.- 313-346 in: Saunders A D & Norry M J [eds]: Magmatism in the ocean basins.- Geological Society Special Publication, 42: 398 pp, Oxford (Blackwell).

Taylor H P jr & Sheppard S M F (1986): Igneous Rocks: I. Processes of isotopic fractionation and isotope systematics.- 227-271 in: Valley J W, Taylor H P jr & O'Neil J R [eds]: Stable isotopes in high temperature geological processes.- Reviews in Mineralogy, 16: 570 pp.

Taylor H P jr & Turi B (1976): High-^{18}O igneous rocks from the Tuscan Magmatic Province, Italy.- Contributions to Mineralogy and Petrology, 55: 33-54.

Taylor H P jr, Turi B & Cundari A (1984): Oxygen isotope studies of potassic volcanic rocks of the Roman Province, Central Italy.- Contributions to Mineralogy and Petrology, 55: 1-31.

Thompson R N (1974): Some high-pressure pyroxenes.- Mineralogical Magazine, 39: 768-787.

Thompson R N & Fowler M B (1986): Subduction-related shoshonitic and ultrapotassic magmatism: a study of Siluro-Ordovician syenites from the Scottish Caledonides.- Contributions to Mineralogy and Petrology, 94: 507-522.

Tilton G R, Schreyer W & Schertl H P (1989): Pb-Sr-Nd isotopic behavior of deeply subducted crustal rocks from the Dora Maira massif, western Alps, Italy.- Geochimica et Cosmochimica Acta, 53: 1391-1400.

Tracy R J & Robinson P (1979): Zoned titanian augite in alkali olivine basalt from Tahiti and the nature of titanium substitution in augite.- American Mineralogist, 62: 634-645.

Trönnes R G, Edgar A D & Arima M (1985): A high pressure - high temperature study of TiO_2 solubility in the Mg-rich phlogopites: implications to phlogopite chemistry.- Geochimica et Cosmochimica Acta, 49: 2323-2329.

Turbeville B N (1993): Sidewall differentiation in an alkalic magma chamber, evidence from syenite xenoliths in tuffs of the Latera Caldera, Italy.- Geological Magazine, 130:453-470.

Turi B & Taylor J R jr (1976): Oxygen isotope studies of potassic volcanic rocks of the Roman Province, Central Italy.- Contributions to Mineralogy and Petrology, 55: 1-31.

Turi B, Taylor H P jr & Ferrara G (1986): A criticism of the Holm-Munksgaard oxygen and strontium isotope study of the Vulsinian District, Central Italy.- Earth and Planetary Science Letters, 78: 447-453.

Valley J W, Chiarenzelli J R & McLelland J M (1994): Oxygen isotope geochemistry of zircon.- Earth and Planetary Science Letters, 126:187-206.

Valley J, Kitchen N, Kohn M J, Niendorf C R & Spicuzza M (1995): UWG-2, a garnet standard for oxygen isotope ratios: Strategies for high precision and accuracy with laser heating.- Geochimica et Cosmochimica Acta, 59: 5223-5231.

van Bergen M J (1984): Magmas and inclusions of Monte Amiata volcano, Tuscany, Italy.- Geologica Ultraiectina, 37: 175 pp.

van Bergen M J (1985): Common trace-element characteristics of crustal- and mantle-derived K-rich magmas at Mt. Amiata (central Italy).- Chemical Geology, 48: 125-135.

van Bergen M J & Barton M (1984): Complex interaction of aluminous metasedimentary xenoltihs and silicous magma; an example from Mt. Amiata (Central Italy).- Contributions to Mineralogy and Petrology, 86: 374-385.

van Bergen M J , Ghezzo C & Ricci C A (1983): Minette inclusions in the rhyodacitic lavas of Mt. Amiata (central Italy): Mineralogical and chemical evidence of mixing between Tuscan and Roman type magmas.- Journal of Volcanology and Geothermal Research, 19: 1-35.

Varekamp J C (1979): Geology and Petrology of the Vulsinian Volcanic Area (Latium, Italy).- Geologica Ultraiectina, 22: 384 pp.

Varekamp J C & Kalamarides R I (1989): Hybridization processes in leucite tephrites from Vulsini, Italy, and the evolution of the Italian potassic suite.- Journal of Geophysical Research, 94, B4: 4603-4618.

Venturelli G, Capedri S, Di Battistini G, Crawford A, Kogarko L N & Celestini S (1984a): The ultrapotassic rocks from southeastern Spain.- Lithos, 17: 37-54.

Venturelli G, Salvioli-Mariani E, Foley S F, Capedri S & Crawford A J (1988): Petrogenesis and conditions of crystallization of Spanish lamproitic rocks.- Canadian Mineralogist, 26: 67-80.

Venturelli G, Thorpe R S, Dal Piaz G V, Del Moro A & Potts P J (1984b): Petrogenesis of calc-alkaline, shoshonitic and associated Oligocene volcanic rocks from the northwestern Alps, Italy.- Contributions to Mineralogy and Petrology, 86: 209-220.

Vezzoli L, Conticelli S, Innocenti F, Landi P, Manetti P, Palladino D M & Trigila R (1987): Stratigraphy of the Latera Volcanic Complex: proposals for a new nomenclature.- Periodico di Mineralogia, 56: 89-110.

Vieten K (1980): The minerals of the volcanic rock associations of the Siebengebirge. 1. Clinopyroxenes 2. Variation of chemical composition of Ca-rich clinopyroxenes (salites) in the course of crystallisation.- Neues Jahrbuch Mineralogische Abhandlungen, 140: 54-88.

Villemant B & Fledoc C (1989): Th-U fractionation in the Vico Vulcano.- Earth and Planetary Science Letters, 91: 312-326.

Vollmer R (1976): Rb-SR and U-Th-Pb systematics of alkaline rocks: the alkaline rocks from Italy.- Geochimica et Cosmochimica Acta, 40: 109-118.

Vollmer R (1989): On the origin of the Italian potassic magmas. 1. A discussion contribution.- Chemical Geology, 74: 229-239.

Vollmer R (1990): On the origin of the Italian potassic magmas - reply.- Chemical Geology, 85: 191-196.

Wagner C & Velde D (1986): The mineralogy of K-richterite-bearing lamproites.- American Mineralogist, 71: 17-37.

Wall V J, Clemens J D & Clarke J D (1987): Models for granitoid evolution and source compositions.- Journal of Geology, 95: 731-749.

Washington H S (1906): The Roman Comagmatic Region.- Carnegie Institute of Washington Publication, 57: 199 pp.

Wass S Y (1979): Multiple origins of clinopyroxenes in alkali basaltic rocks.- Lithos, 12: 115-132.

Wendlandt R F & Eggler D H (1980a): The origins of potassic magmas: 1. Melting relations in the system $KAlSiO_4$-Mg_2SiO_4-SiO_2 and $KAlSiO_4$-MgO-SiO_2-CO_2 to 30 kb.- American Journal of Science, 280: 385-420.

Wendlandt R F & Eggler D H (1980b): The origins of potassic magmas: 2. Stability of phlogopite in natural spinel lherzolite and in the system $KAlSiO_4$-MgO-SiO_2-H_2O-CO_2 at high pressures and temperatures.- American Journal of Science, 280: 421-458.

White W M (1997, 1998): Geochemistry.- 701 pp. online in Internet, URL: http://www.geo.cornell.edu/geology/classes/Chapters/ [date of retrieval: 25th of June 2000].

Wiberg N (1995): Holleman-Wiberg, Lehrbuch der Anorganischen Chemie.- 101st enlarged ed: 2033 pp, Berlin, New York (Walter de Gruyter).

Wiechert U & Hoefs J (1995): An excimer laser-based micro analytical preparation technique for in-situ oxygen isotope analysis of silicate and oxide minerals.- Geochimica et Cosmochimica Acta, 59: 4093-4101.

Wilson M (1995): Igneous Petrogenesis, A Globa Tectonic Approach.- reprint of the 1st ed: 466 pp, London, Glasgow, New York, Tokyo, Melbourne, Madras (Chapman & Hall).

Woolley A R, Bergman S C, Edgar A D, Le Bas A J, Mitchell R H, Rock N M S & Scott Smith B H (1996): Classification of, lamproites, kimberlites, and the kalsilitic, melilitic, and leucitic rocks.- The Canadian Mineralogist, 34: 175-186.

Wörner G, Beusen J-M, Duchateau N, Gijbels R & Schmincke H-U (1983): Trace element abundances and mineral/melt distribution coefficients in phonolites from the Laacher See volcano (Germany).- Contributions to Mineralogy and Petrology, 84: 152-173.

Wyllie P J & Sekine T (1982): The formation of mantle phlogopite in subduction zone hybridization.- Contributions to Mineralogy and Petrology, 79: 375-380.

Young E D & Rumble D (1993): The origin of correlated variations in in-situ $^{18}O/^{16}O$ and elemental concentrations in metamorphic garnet from southeastern Vermont, USA.- Geochimica et Cosmochimica Acta, 59: 2859-2864.

Yurimoto H, Morioka M & Nagasawa H (1992): Oxygen self-diffusion along high diffusivity paths in forsterite.- Geochemical Journal, 26: 181-188.

Zheng Y F (1993): Calculation of oxygen isotope fractionation in anhydrous silicate minerals.- Geochimica et Cosmochimica Acta, 57: 1079-1091.

8 Appendix

Abbreviations

ab	albite
ac	acmite
an	anorthite
av.	Average
b.d.l.	below detection limit
bio	biotite
cel	celsian
cpx	clinopyroxene
EMPA	electron beam microprobe analysis
en	enstatite
excimer	excited dimer
fa	fayalite
FeO_{tot}	total iron content expressed as FeO
fo	forsterite
fs	ferrosilite
HFSE	high field strengh elements
HKS	high potassic series (rocks from Vulsinian mountains, Roman Province)
HREE	heavy rare earth elements
ICP-MS	inductively coupled plasma - mass spectrometry
IR	infra-red
KS	potassic series (rocks fom Vulsinian mountains, Roman Province)
LA	laser ablation
LA-ICP-MS	laser ablation - inductively coupled plasma - mass spectrometry
LILE	large ion lithophile elements
LREE	light rare earth elements
n.a.	not analyzed
Mg#	Magnesium-number; defined as molar Mg / (Mg + Fe_{tot})
MORB	mid ocean ridge basalt
Nd-YAG	Neodymium-Yttrium-Aluminium-Garnet
ol	olivine
opx	orthopyroxene
or	orthoclase
phl	phlogopite
plg	plagioclase
ppm	parts per million, equal to mg / kg
qtz	quartz
REE	rare earth elements (La to Lu)
s	standard deviation
san	sanidine
SIRMS	stable isotope ratio mass spectrometry
SMOW	standard mean ocean water
tsch	Tschermak's molecule
UV	ultra-violet
wo	wollastonite
XFA	X-ray fluorescence analysis

Tab. A-1: Samples, localities and petrological classification.

Sample	Locality	Rock Type
VUL 9701	Monti Vulsini, Acquapendente	phonolite
VUL 9702	Monti Vulsini, Valento	phonotephrite
VUL 9703 A	Monti Vulsini, Selva del Lamone	shoshonite
VUL 9703 B	Monti Vulsini, Selva del Lamone	shoshonite
VUL 9704	Monti Vulsini, 2.5 km E' Viterbo	phonotephrite
VUL 9705	Monti Vulsini, 1.5 km E' Viterbo	phonotephrite
VUL 9706	Monti Vulsini, 1 km S' Bolsena	phonotephrite
VUL 9707	Monti Vulsini, 3 km E' Bolsena	tephriphonolite
Montefiascone	Monti Vulsini, Montefiascone	potassic trachybasalt
ORC 9701	200 m E' Orciatico	lamproite
ORC 9702	100 m E' Orciatico	lamproite
MVC 9701	50 m E' Montecatini Val di Cecina	lamproite
MVC 9702	250 m E' Montecatini Val di Cecina	lamproite
RAD 9701	Radicofani, 700 m N' top	basaltic andesite
RAD 9702 A	Radicofani, 50 m SW' top	basaltic andesite
RAD 9702 B	Radicofani, 50 m SW' top	basaltic andesite
RAD 9703	Radicofani, on the top	basaltic andesite
RAD 9705	2 km SW' Radicofani	basaltic andesite
RAD 9706	2 km SW' Radicofani	basaltic andesite
TA 9701	Torre Alfina, 300 m SSW' village	transitional rock between lamproites and Roman Province type rocks
TA 9702	Torre Alfina, 200 NNW' village	transitional rock between lamproites and Roman Province type rocks
ROC 9701	Roccastrada, Piloni	rhyolite
ROC 9702	5 km N' Roccastrada	rhyolite
SVC 9701	1.2 km ESE' San Vincenzo	rhyolite
SVC 9702	1.2 km E' San Vincenzo	rhyolite
SVC 9703	500 m NNE' San Vincenzo	rhyolite
AMT 9701	Monte Amiata, 400 m E' Castel del Piano	trachyte

Sample	Locality	Rock Type
AMT 9702	Monte Amiata, Prato Contessa	trachyte
AMT 9703 I	Monte Amiata, Prato Contessa	latite, xenolith
AMT 9703 II	Monte Amiata, Prato Contessa	shoshonite, xenolith
AMT 9704 A	Monte Amiata, Ermeata	latite
AMT 9704 B	Monte Amiata, Ermeata	latite

Tab. A-2: Chemical composition of the bulk rock.

wt.%	VUL 9701	VUL 9702	VUL 9703 A	VUL 9703 B	VUL 9704	VUL 9705	VUL 9706	VUL 9707	Montefiascone
SiO_2	56.3	49.4	53.4	53.3	49.2	49.0	48.3	54.5	48.9
TiO_2	0.512	0.961	0.734	0.730	0.769	0.642	0.724	0.520	0.647
Al_2O_3	20.55	17.55	15.61	15.57	15.40	14.83	18.68	20.94	13.83
Fe_2O_3	2.48	5.97	2.00	1.94	2.81	4.33	3.83	3.63	3.01
FeO	1.49	2.56	3.87	3.92	5.02	2.62	3.85	1.07	3.73
MnO	0.157	0.146	0.126	0.123	0.145	0.136	0.186	0.152	0.135
MgO	0.77	4.71	7.02	7.14	6.22	6.74	2.90	0.94	10.47
CaO	3.57	10.02	9.55	9.17	11.39	12.04	9.50	4.31	11.44
Na_2O	4.02	1.83	2.35	2.47	1.48	1.32	2.29	2.46	1.92
K_2O	9.40	6.06	4.23	4.22	6.65	7.34	8.35	9.78	4.85
P_2O_5	0.126	0.448	0.205	0.202	0.392	0.365	0.440	0.157	0.257
H_2O	0.60	0.21	0.36	0.58	0.43	0.58	0.70	1.29	0.84
CO_2	0.033	0.028	0.092	0.25	< 0.026	0.035	0.21	0.040	< 0.019
SO_3	< 0.015	0.020	0.57	0.37	< 0.015	< 0.015	0.021	0.018	< 0.017
Σ	100.0	99.9	100.1	100.0	99.9	100.0	100.0	99.8	100.0

ppm	VUL 9701	VUL 9702	VUL 9703 A	VUL 9703 B	VUL 9704	VUL 9705	VUL 9706	VUL 9707	Montefiascone
Li	113	28	71	73	41	40	44	79	41
Sc	2.8	18	29	22	24	23	6	3.4	29
V	106	250	156	157	221	203	256	156	199
Cr	< 5	20	312	317	102	285	10	< 5	850
Co	4.8	30	28	28	33	25	22	8.9	37
Ni	1.2	32	158	176	87	94	18	2.6	239
Cu	2.5	49	56	41	54	88	48	10	61
Zn	118	92	71	73	95	80	137	106	71
Ga	21	17	15	17	15	13	19	19	15
Rb	335	370	306	309	460	516	375	377	299
Sr	1625	1236	552	522	1338	1368	2350	1909	1140
Y	46	31	26	29	35	34	47	42	31
Zr	578	241	254	252	251	251	385	537	252
Nb	46	13	16	17	11	14	27	38	17
Sn	4.9	5.4	3.7	3.9	4.3	4.3	4.0	4.4	3.1
Sb	3.3	0.41	0.42	0.50	0.64	0.69	1.5	2.3	n.a.
Cs	24	28	23	22	39	47	26	28	23
Ba	2011	894	401	467	969	1122	1802	1843	803
La	92	69	65	68	86	96	157	123	80
Ce	255	164	145	142	190	205	322	270	154
Pr	18	20	15	15	22	24	35	24	17
Nd	64	82	55	56	88	91	130	84	61
Sm	9.8	14	9.5	10	16	16	21	13	11
Eu	2.7	3.0	1.7	1.9	3.6	3.4	4.3	3.0	2.3
Gd	7.9	10	7.8	6.6	11	11	15	9.9	8.0
Tb	0.95	1.3	1.0	1.0	1.5	1.4	1.9	1.2	1.0
Dy	4.3	6.0	4.8	4.9	6.5	5.9	7.9	5.3	4.9
Ho	0.82	1.0	0.98	0.89	1.1	1.0	1.4	0.98	0.89
Er	2.6	2.9	2.8	2.9	3.1	2.8	4.1	3.0	2.4
Tm	0.37	0.39	0.38	0.42	0.38	0.37	0.48	0.35	0.34
Yb	2.6	2.3	2.7	2.8	2.4	2.4	3.2	2.5	2.0
Lu	0.35	0.31	0.38	0.37	0.37	0.32	0.45	0.33	0.3
Hf	10	6.0	6.0	6.0	5.6	5.2	6.8	9.4	2.9
Ta	1.0	0.65	0.71	0.67	0.58	0.58	1.1	1.3	0.91
Tl	3.3	1.2	1.4	1.5	1.8	2.0	5.3	2.5	n.a.
Pb	161	32	51	45	62	65	115	175	65
Bi	0.68	0.052	0.41	0.34	0.14	0.16	0.61	0.34	n.a.
Th	77	26	51	51	39	48	89	100	50
U	19	4.9	9.9	8.1	8.6	12	18	25	13

Tab. A-2: continued

wt.%	ORC 9701	ORC 9702	MVC 9701	MVC 9702	TA 9701	TA 9702	RAD 9701	RAD 9702 A	RAD 9702B	RAD 9703
SiO_2	57.2	56.4	55.6	54.7	56.0	57.0	53.8	54.2	54.0	54.1
TiO_2	1.386	1.248	1.243	1.283	1.332	1.284	0.927	0.941	0.926	0.955
Al_2O_3	11.11	10.75	12.33	12.17	12.98	14.68	16.28	16.10	16.44	16.13
Fe_2O_3	1.84	2.61	3.19	3.40	0.89	0.34	1.22	3.89	3.48	0.81
FeO	3.16	2.12	2.59	2.64	4.90	5.72	5.21	2.92	3.29	5.53
MnO	0.085	0.077	0.083	0.079	0.094	0.100	0.115	0.121	0.120	0.117
MgO	8.74	8.60	7.32	7.66	8.76	7.55	7.79	7.22	7.56	7.91
CaO	4.21	4.80	4.13	4.20	5.41	5.11	8.48	8.63	8.65	8.35
Na_2O	1.48	1.16	1.22	1.13	0.97	1.01	1.98	1.90	2.00	1.81
K_2O	7.85	6.80	7.74	7.53	7.57	6.26	3.02	3.21	3.07	3.32
P_2O_5	0.703	0.616	1.170	1.187	0.559	0.452	0.254	0.258	0.248	0.273
H_2O	2.18	4.55	3.15	3.66	0.45	0.60	0.83	0.31	0.21	0.69
CO_2	0.051	0.40	0.12	0.037	0.044	0.036	0.035	0.051	0.044	0.031
SO_3	< 0.015	0.035	0.027	< 0.015	< 0.015	0.017	0.020	< 0.015	< 0.015	< 0.015
Σ	100.0	100.2	100.0	99.7	100.0	100.2	100.0	99.7	100.0	100.0

ppm	ORC 9701	ORC 9702	MVC 9701	MVC 9702	TA 9701	TA 9702	RAD 9701	RAD 9702 A	RAD 9702 B	RAD 9703
Li	33	53	52	67	43	44	33	37	40	35
Sc	18	11	15	18	13	13	27	27	25	20
V	105	95	122	124	123	134	178	182	184	174
Cr	506	536	372	395	560	459	393	446	423	437
Co	28	28	27	33	34	35	30	35	26	31
Ni	362	381	168	165	370	303	140	164	157	150
Cu	48	38	62	35	41	41	37	35	27	36
Zn	81	82	87	86	117	102	80	81	87	82
Ga	17	17	19	20	19	19	17	17	17	17
Rb	521	535	765	752	443	342	180	196	184	197
Sr	629	577	437	422	726	567	335	347	344	344
Y	27	29	34	33	36	33	25	24	24	23
Zr	747	678	482	468	601	509	213	229	219	247
Nb	39	33	30	30	32	28	12	13	13	16
Sn	10	9.4	8.2	7.8	9.2	8.0	4.1	4.7	3.8	4.5
Sb	< 0.16	< 0.16	< 0.16	< 0.16	0.24	0.15	0.17	0.26	0.34	0.28
Cs	34	17	18	18	35	33	9.9	13	12	15
Ba	1163	991	1209	1248	1285	1067	592	620	613	606
La	147	118	77	79	111	88	44	45	46	50
Ce	391	308	216	217	296	245	108	118	112	125
Pr	53	42	32	33	35	28	13	14	14	15
Nd	219	171	144	155	143	114	50	55	55	61
Sm	32	25	27	28	24	18	8.7	9.2	9.2	10
Eu	4.6	3.8	4.1	4.5	4.5	3.3	1.9	2.0	2.1	2.1
Gd	15	13	13	13	15	12	6.0	6.3	6.4	7.0
Tb	1.6	1.5	1.6	1.6	1.8	1.4	0.83	0.81	0.92	0.91
Dy	5.3	4.8	6.0	6.0	6.5	6.1	4.0	4.2	4.2	4.6
Ho	0.86	0.84	1.0	1.1	1.2	1.0	0.73	0.83	0.84	0.86
Er	2.6	2.6	2.7	2.8	3.2	3.3	2.4	2.4	2.5	2.6
Tm	0.29	0.3	0.35	0.31	0.37	0.39	0.36	0.33	0.33	0.34
Yb	1.9	1.9	2.4	2.2	2.2	2.3	2.0	2.1	2.2	2.3
Lu	0.29	0.30	0.31	0.34	0.33	0.37	0.3	0.35	0.33	0.32
Hf	20	17	13	11	15	13	5.0	5.4	5.4	5.9
Ta	1.8	1.7	1.4	1.3	2.0	1.5	0.63	0.70	0.67	0.76
Tl	2.8	3.0	4.7	4.5	2.4	2.3	0.96	1.4	1.2	1.1
Pb	47	49	54	39	66	60	32	27	44	34
Bi	0.14	0.12	0.13	0.13	0.16	0.045	0.073	0.10	0.22	0.10
Th	107	80	101	96	61	52	23	24	25	28
U	16	15	20	19	13	9.3	4.4	4.7	4.6	5.3

Tab. A-2: continued

wt.%	RAD 9705	RAD 9706	ROC 9701	ROC 9702	SVC 9701	SVC 9702	SVC 9703
SiO_2	54.2	52.8	74.8	74.8	68.9	69.8	70.0
TiO_2	0.950	0.986	0.200	0.243	0.363	0.408	0.286
Al_2O_3	16.20	16.30	13.44	13.48	15.53	15.34	15.20
Fe_2O_3	0.98	3.86	0.46	0.60	0.60	1.76	0.37
FeO	5.46	3.08	0.80	0.67	1.53	0.77	1.35
MnO	0.116	0.119	0.015	0.013	0.042	0.026	0.030
MgO	7.61	8.39	0.36	0.28	0.78	0.73	0.52
CaO	8.35	8.30	0.83	0.96	1.89	2.15	1.42
Na_2O	1.90	1.66	2.61	2.69	2.87	2.87	3.05
K_2O	3.26	3.19	4.97	5.11	4.71	4.79	4.60
P_2O_5	0.257	0.267	0.163	0.158	0.229	0.227	0.156
H_2O	0.39	1.03	1.32	0.99	2.51	1.26	3.02
CO_2	< 0.026	0.035	0.066	< 0.026	< 0.026	0.026	< 0.026
SO_3	< 0.015	< 0.015	0.023	< 0.015	< 0.015	< 0.015	< 0.015
Σ	99.7	100.0	100.1	100.0	100.0	100.2	100.0

ppm	RAD 9705	RAD 9706	ROC 9701	ROC 9702	SVC 9701	SVC 9702	SVC 9703
Li	34	32	272	241	201	215	202
Sc	21	23	10	2.5	7.0	7.0	6.0
V	173	176	11	21	29	35	28
Cr	439	496	< 5	5.0	17	29	14
Co	31	36	7.0	1.5	4.3	5.0	3.4
Ni	151	193	4.5	7.8	7.1	16	5.7
Cu	39	30	5.0	5.9	6.8	11	5.3
Zn	80	94	66	62	84	76	74
Ga	17	20	22	20	26	23	25
Rb	194	182	429	396	306	291	298
Sr	338	356	61	68	190	260	105
Y	25	26	31	34	17	28	17
Zr	236	263	110	129	145	170	104
Nb	14	16	17	17	13	14	11
Sn	4.5	4.9	17	14	18	15	23
Sb	0.29	0.26	0.47	0.33	< 0.16	< 0.16	0.54
Cs	9.1	13	17	16	35	22	52
Ba	603	650	122	160	378	458	261
La	45	52	14	20	23	48	16
Ce	122	135	36	47	64	98	38
Pr	14	16	4.1	5.4	6.0	13	4.0
Nd	56	66	15	20	23	47	16
Sm	10	11	3.0	4.1	4.4	9.2	3.3
Eu	2.0	2.3	0.15	0.24	0.43	1.3	0.37
Gd	6.9	7.4	2.4	3.0	3.0	6.1	2.5
Tb	0.90	1.0	0.35	0.40	0.35	0.83	0.31
Dy	4.6	4.6	1.8	2.2	1.4	3.6	0.94
Ho	0.87	0.87	0.31	0.39	0.19	0.62	0.13
Er	2.4	2.5	0.78	0.93	0.59	1.6	0.37
Tm	0.37	0.32	0.11	0.13	0.078	0.22	0.041
Yb	2.0	2.4	0.59	0.84	0.43	1.1	0.28
Lu	0.33	0.33	0.085	0.098	0.07	0.14	0.057
Hf	5.7	6.7	1.2	0.91	2.1	1.8	1.7
Ta	0.77	0.87	0.84	1.3	0.70	0.52	1.0
Tl	1.1	1.1	2.6	2.3	1.7	1.5	1.4
Pb	27	28	54	38	47	43	45
Bi	0.097	0.15	0.056	0.06	0.74	0.092	1.1
Th	27	31	11	13	10	19	5.9
U	5.2	4.4	12	8.9	5.6	5.9	9.3

Tab. A-2: continued

wt.%	AMT 9701	AMT 9702	AMT 9703 I	AMT 9703 II	AMT 9704 A	AMT 9704 B
SiO_2	66.2	64.3	55.1	50.9	54.6	54.7
TiO_2	0.493	0.542	0.804	0.756	0.756	0.748
Al_2O_3	15.68	16.39	17.04	13.40	16.01	15.87
Fe_2O_3	0.43	0.40	1.92	4.67	2.31	2.32
FeO	2.64	3.13	4.37	2.88	3.95	3.89
MnO	0.052	0.063	0.112	0.127	0.113	0.111
MgO	1.16	1.59	4.13	8.13	5.36	5.32
CaO	2.52	3.19	6.96	11.45	7.86	7.78
Na_2O	2.23	2.21	1.69	1.04	1.42	1.53
K_2O	5.91	5.89	5.63	5.04	5.64	5.71
P_2O_5	0.156	0.190	0.322	0.330	0.279	0.273
H_2O	2.26	1.91	1.77	1.25	1.60	1.54
CO_2	0.073	0.070	0.11	0.099	0.036	0.033
SO_3	< 0.015	< 0.015	0.042	0.047	0.023	0.022
Σ	99.8	99.9	100.0	100.1	100.0	99.9

ppm	AMT 9701	AMT 9702	AMT 9703 I	AMT 9703 II	AMT 9704 A	AMT 9704 B
Li	214	189	59	37	70	82
Sc	9.0	9.0	19	31	26	22
V	43	61	144	218	154	149
Cr	15	23	70	156	277	268
Co	6.9	9.9	20	31	22	22
Ni	8.7	16	31	138	46	47
Cu	6.2	20	18	49	32	29
Zn	69	71	92	76	84	86
Ga	19	21	19	14	18	20
Rb	377	363	314	299	320	318
Sr	337	421	655	853	673	681
Y	31	33	34	34	38	37
Zr	239	245	277	232	258	252
Nb	17	16	15	10	15	12
Sn	12	12	6.7	4.6	5.9	5.9
Sb	0.92	0.99	0.50	0.23	0.32	0.23
Cs	51	44	25	24	10	11
Ba	551	652	806	963	850	876
La	52	67	72	77	91	85
Ce	122	149	157	164	166	164
Pr	13	16	19	21	22	21
Nd	45	59	72	80	82	77
Sm	8.0	9.7	13	14	14	13
Eu	1.1	1.8	2.7	3.2	2.7	2.9
Gd	5.6	7.5	9.7	10	10	9.7
Tb	0.78	1.0	1.2	1.4	1.4	1.3
Dy	3.6	4.8	6.0	5.9	6.1	5.8
Ho	0.65	0.8	1.0	1.1	1.1	1.1
Er	2.0	2.7	2.8	2.8	3.3	3.2
Tm	0.27	0.36	0.42	0.36	0.46	0.43
Yb	2.0	2.4	2.8	2.2	2.8	2.5
Lu	0.26	0.34	0.40	0.32	0.36	0.38
Hf	3.1	3.5	5.8	5.4	5.3	5.4
Ta	0.57	0.78	0.74	0.46	0.68	0.64
Tl	2.4	2.3	1.8	1.3	1.9	2.0
Pb	63	67	50	67	50	50
Bi	0.41	4.8	0.09	0.32	0.069	0.10
Th	26	34	31	32	29	29
U	8.8	9.0	7.2	6.6	6.9	6.9

Tab. A-3: Chemical composition of olivines by EMPA.

No	SiO_2	FeO	MgO	CaO	MnO	Σ		fo	fa	tephroite
Montefiascone										
1	40.9	8.57	50.2	0.381	b.d.l.	100.3		91.26	8.74	0.00
6	40.3	11.47	48.3	0.383	b.d.l.	100.8		88.23	11.77	0.00
12	40.2	12.19	47.3	0.427	b.d.l.	100.4		87.37	12.63	0.00
13	40.2	12.65	46.9	0.438	b.d.l.	100.6		86.86	13.14	0.00
14	41.1	8.20	50.5	0.455	b.d.l.	100.5		91.64	8.36	0.00
16	40.3	8.63	50.1	0.435	b.d.l.	99.8		91.18	8.82	0.00
25	40.1	11.99	47.2	0.530	b.d.l.	100.2		87.53	12.47	0.00
28	40.3	12.43	47.2	0.324	b.d.l.	100.6		87.12	12.88	0.00
33	40.3	12.02	47.5	0.450	b.d.l.	100.6		87.57	12.43	0.00
43	40.4	12.11	47.5	0.392	b.d.l.	100.8		87.49	12.51	0.00
106	40.5	10.65	48.6	0.400	b.d.l.	100.5		89.04	10.96	0.00
107	40.4	10.53	48.4	0.377	b.d.l.	100.1		89.12	10.88	0.00
108	40.4	10.48	48.3	0.387	b.d.l.	99.9		89.14	10.86	0.00
109	40.4	10.69	48.0	0.391	b.d.l.	99.9		88.89	11.11	0.00
110	40.4	10.68	48.3	0.393	b.d.l.	100.1		88.97	11.03	0.00
111	40.8	10.88	48.5	0.389	b.d.l.	100.8		88.81	11.19	0.00
112	40.6	10.89	48.6	0.430	b.d.l.	100.8		88.82	11.18	0.00
113	40.3	11.08	48.2	0.386	b.d.l.	100.3		88.57	11.43	0.00
114	40.4	11.04	48.5	0.383	b.d.l.	100.6		88.67	11.33	0.00
115	40.4	11.24	48.1	0.459	b.d.l.	100.5		88.40	11.60	0.00
116	40.5	11.23	48.0	0.431	b.d.l.	100.4		88.39	11.61	0.00
117	40.3	11.18	48.1	0.444	b.d.l.	100.4		88.46	11.54	0.00
118	40.4	11.19	48.0	0.458	b.d.l.	100.3		88.43	11.57	0.00
119	40.1	11.18	48.0	0.428	b.d.l.	100.1		88.44	11.56	0.00
120	40.6	11.50	48.0	0.445	b.d.l.	100.9		88.15	11.85	0.00
121	40.1	12.32	47.1	0.433	b.d.l.	100.4		87.20	12.80	0.00
122	39.0	17.77	42.6	0.374	0.516	100.3		80.57	18.88	0.55
123	36.3	34.20	29.3	0.426	1.280	101.6		59.49	39.03	1.48
124	40.2	11.33	47.9	0.434	b.d.l.	100.1		88.27	11.73	0.00
125	40.2	11.36	47.9	0.378	b.d.l.	100.2		88.27	11.73	0.00
126	40.4	11.53	47.6	0.407	b.d.l.	100.4		88.04	11.96	0.00
127	40.0	11.47	48.1	0.444	b.d.l.	100.3		88.20	11.80	0.00
128	40.3	11.40	47.6	0.442	b.d.l.	100.0		88.15	11.85	0.00
129	40.1	11.46	47.8	0.391	b.d.l.	100.1		88.15	11.85	0.00
130	40.5	11.38	48.0	0.437	b.d.l.	100.6		88.27	11.73	0.00
131	40.5	11.28	47.7	0.415	b.d.l.	100.2		88.29	11.71	0.00
132	40.4	11.43	48.0	0.446	b.d.l.	100.5		88.20	11.80	0.00
133	40.3	11.36	47.8	0.416	b.d.l.	100.3		88.25	11.75	0.00
134	40.3	11.46	47.3	0.444	b.d.l.	99.8		88.03	11.97	0.00
135	40.1	11.50	47.9	0.429	b.d.l.	100.4		88.14	11.86	0.00
136	40.3	11.45	47.5	0.489	b.d.l.	100.1		88.08	11.92	0.00
137	40.2	11.86	47.3	0.474	b.d.l.	100.2		87.67	12.33	0.00
138	40.2	12.19	47.0	0.415	b.d.l.	100.2		87.30	12.70	0.00
139	40.2	13.63	45.4	0.464	b.d.l.	100.0		85.58	14.42	0.00
140	39.4	17.54	42.8	0.425	0.434	100.6		80.92	18.61	0.47
141	37.7	26.24	35.8	0.442	0.831	101.1		70.19	28.89	0.93
142	36.8	31.91	30.6	0.428	1.276	101.1		62.13	36.40	1.47

Tab. A-3: continued

No	SiO_2	FeO	MgO	CaO	MnO	Σ		fo	fa	tephroite
VUL 9703 B										
4	40.4	10.31	49.1	0.341	0.204	100.4		89.28	10.51	0.21
8	40.7	10.36	48.6	0.346	b.d.l.	100.4		89.32	10.68	0.00
12	38.6	22.66	39.4	0.359	0.503	101.4		75.18	24.28	0.55
23	39.8	13.60	47.2	0.330	0.227	101.1		85.87	13.89	0.24
26	40.8	10.34	49.5	0.324	0.214	101.1		89.32	10.47	0.22
142	40.7	10.17	49.5	0.355	b.d.l.	100.7		89.65	10.35	0.00
143	40.7	10.13	49.4	0.349	0.187	100.7		89.50	10.30	0.19
144	40.8	10.20	49.4	0.344	0.195	100.9		89.44	10.36	0.20
145	41.0	10.81	48.8	0.313	b.d.l.	100.9		88.94	11.06	0.00
146	40.1	12.53	47.1	0.312	0.220	100.3		86.82	12.95	0.23
147	39.8	16.46	44.2	0.348	0.330	101.1		82.43	17.22	0.35
148	40.9	10.68	49.1	0.321	b.d.l.	100.9		89.11	10.89	0.00
149	39.1	20.09	41.7	0.316	0.416	101.7		78.38	21.18	0.44
245	39.5	18.98	42.0	0.330	0.388	101.2		79.45	20.13	0.42
246	40.3	14.23	46.6	0.356	0.255	101.7		85.14	14.59	0.26
247	40.4	12.45	47.7	0.311	0.225	101.1		87.03	12.74	0.23
248	40.7	11.60	48.2	0.326	0.198	101.0		87.92	11.87	0.21
249	40.8	11.08	48.5	0.299	0.187	100.9		88.47	11.33	0.19
250	40.9	10.52	48.9	0.320	0.208	100.9		89.04	10.74	0.22
251	41.0	10.59	49.4	0.353	b.d.l.	101.3		89.27	10.73	0.00
252	41.0	11.00	48.5	0.321	0.191	101.0		88.54	11.26	0.20
253	40.7	12.14	48.0	0.354	0.178	101.3		87.41	12.40	0.19
254	40.4	12.94	47.4	0.332	0.190	101.2		86.53	13.27	0.20
255	40.5	11.92	48.1	0.350	0.232	101.1		87.58	12.18	0.24
256	40.4	10.70	48.9	0.318	0.254	100.6		88.84	10.90	0.26
257	40.7	10.43	49.3	0.340	0.203	101.0		89.21	10.58	0.21
258	41.0	10.58	49.0	0.365	b.d.l.	101.0		89.20	10.80	0.00
259	40.3	13.48	46.7	0.327	0.258	101.1		85.81	13.92	0.27
260	39.5	18.38	42.5	0.303	0.433	101.1		80.10	19.44	0.46
261	39.4	18.38	42.6	0.303	0.427	101.1		80.14	19.40	0.46
VUL 9705										
184	40.9	7.98	50.1	0.460	0.183	99.7		91.63	8.18	0.19
185	41.1	8.25	50.4	0.491	0.166	100.4		91.42	8.41	0.17
186	40.6	8.04	50.3	0.513	0.124	99.6		91.65	8.22	0.13
187	40.9	8.30	50.7	0.525	0.173	100.6		91.43	8.39	0.18
188	40.8	8.08	50.6	0.550	0.152	100.1		91.63	8.22	0.16
189	40.8	8.07	50.4	0.532	0.172	100.0		91.60	8.22	0.18
190	40.9	8.27	50.2	0.514	0.173	100.0		91.38	8.44	0.18
191	40.8	8.77	49.7	0.536	0.170	100.0		90.84	8.99	0.18
192	40.9	9.97	49.0	0.561	0.273	100.7		89.49	10.22	0.28
193	40.3	11.44	47.4	0.591	0.291	100.0		87.80	11.89	0.31

Tab. A-3: continued

No	SiO_2	FeO	MgO	CaO	MnO	Σ		fo	fa	tephroite
ORC 9701										
9	39.1	19.49	42.4	0.170	0.307	101.4		79.23	20.45	0.33
22	38.9	20.66	41.1	0.165	0.365	101.2		77.67	21.93	0.39
41	39.6	16.46	44.5	0.130	0.260	100.9		82.57	17.15	0.27
118	39.5	17.10	44.4	0.091	0.354	101.4		81.92	17.71	0.37
119	39.5	16.90	44.4	0.116	0.296	101.2		82.14	17.55	0.31
120	39.7	17.33	44.5	0.120	0.287	101.9		81.81	17.89	0.30
121	39.4	17.43	44.1	0.097	0.360	101.3		81.53	18.09	0.38
122	39.4	17.48	44.0	0.132	0.312	101.3		81.50	18.17	0.33
123	39.3	18.04	43.7	0.134	0.348	101.5		80.90	18.73	0.37
124	39.7	18.23	43.2	0.164	0.289	101.6		80.62	19.08	0.31
125	39.1	18.99	43.1	0.143	0.305	101.6		79.93	19.74	0.32
126	39.5	19.37	42.0	0.167	0.319	101.3		79.19	20.47	0.34
127	39.1	19.89	41.8	0.140	0.322	101.3		78.66	20.99	0.34
128	41.2	9.98	49.7	b.d.l.	0.163	101.1		89.73	10.10	0.17
129	40.9	10.09	49.6	0.069	b.d.l.	100.6		89.75	10.25	0.00
130	41.0	10.26	49.8	0.091	0.177	101.3		89.47	10.35	0.18
131	40.7	10.23	49.6	0.070	0.211	100.9		89.44	10.34	0.22
132	40.6	10.30	49.6	0.081	b.d.l.	100.6		89.57	10.43	0.00
133	40.7	10.59	49.6	0.067	b.d.l.	101.0		89.30	10.70	0.00
134	40.7	10.72	49.4	0.059	b.d.l.	100.8		89.14	10.86	0.00
135	40.9	10.75	49.4	0.074	b.d.l.	101.1		89.11	10.89	0.00
136	40.5	11.12	49.3	0.062	b.d.l.	100.9		88.76	11.24	0.00
137	40.8	11.09	48.7	b.d.l.	b.d.l.	100.5		88.66	11.34	0.00
138	40.6	11.30	48.9	0.069	b.d.l.	100.9		88.51	11.49	0.00
139	40.7	11.40	48.6	0.060	b.d.l.	100.7		88.36	11.64	0.00
140	40.8	11.60	48.4	b.d.l.	b.d.l.	100.8		88.15	11.85	0.00
141	40.6	12.02	48.4	b.d.l.	0.169	101.2		87.63	12.20	0.17
142	40.8	12.03	48.4	0.070	b.d.l.	101.2		87.76	12.24	0.00
143	40.4	12.12	48.3	0.078	0.217	101.1		87.46	12.32	0.22
144	40.6	12.61	47.9	b.d.l.	b.d.l.	101.1		87.13	12.87	0.00
145	40.6	12.77	48.0	0.059	0.187	101.6		86.85	12.96	0.19
146	40.4	12.83	47.4	0.079	0.207	100.9		86.63	13.16	0.21
147	40.5	13.27	47.3	0.078	0.237	101.4		86.19	13.56	0.25
148	40.8	13.74	47.0	0.077	0.231	101.9		85.71	14.05	0.24
149	40.4	13.91	46.7	0.083	0.200	101.3		85.49	14.30	0.21
150	40.0	14.58	45.9	0.110	0.212	100.8		84.68	15.09	0.22
151	40.0	15.38	45.7	0.107	0.265	101.4		83.88	15.84	0.28
152	39.8	15.67	45.2	0.134	0.254	101.1		83.50	16.24	0.27
153	39.6	16.55	44.5	0.172	0.310	101.1		82.46	17.21	0.33

Tab. A-3: continued

No	SiO_2	FeO	MgO	CaO	MnO	Σ		fo	fa	tephroite
RAD 9701										
76	37.8	26.74	36.6	0.177	0.460	101.8		70.55	28.95	0.50
79	37.3	28.68	34.8	0.149	0.431	101.3		68.02	31.50	0.48
80	37.6	26.63	37.0	0.203	0.413	101.8		70.90	28.65	0.45
81	37.3	27.57	36.1	0.165	0.451	101.6		69.66	29.85	0.49
82	38.0	24.10	38.8	0.230	0.366	101.4		73.85	25.75	0.40
94	38.0	24.75	38.4	0.210	0.397	101.7		73.11	26.46	0.43
96	38.2	24.85	38.7	0.208	0.451	102.4		73.14	26.37	0.49
212	38.1	25.15	37.9	0.240	0.468	101.8		72.48	27.01	0.51
213	38.1	25.25	37.6	0.261	0.401	101.5		72.29	27.27	0.44
214	37.8	25.20	37.7	0.242	0.407	101.3		72.40	27.16	0.44
215	38.2	24.96	37.8	0.218	0.449	101.6		72.60	26.90	0.49
216	38.0	25.32	37.9	0.210	0.446	101.9		72.39	27.13	0.48
217	38.4	25.39	37.9	0.229	0.403	102.4		72.37	27.19	0.44
218	38.3	25.28	38.0	0.216	0.457	102.2		72.43	27.07	0.50
219	38.4	25.31	37.8	0.223	0.427	102.2		72.36	27.18	0.46
220	38.3	25.76	37.9	0.223	0.408	102.6		72.06	27.50	0.44
221	38.3	25.51	37.8	0.194	0.421	102.2		72.19	27.35	0.46
222	38.2	25.68	37.5	0.207	0.390	102.0		71.94	27.64	0.42
223	38.1	25.44	37.9	0.182	0.388	102.0		72.32	27.26	0.42
224	38.0	25.31	37.7	0.199	0.442	101.6		72.28	27.24	0.48
225	38.1	25.44	37.9	0.210	0.401	102.0		72.31	27.25	0.44
226	38.0	25.68	37.6	0.196	0.427	101.9		71.98	27.56	0.46
292	37.7	26.88	36.5	0.211	0.440	101.7		70.42	29.10	0.48
RAD 9702 A										
60	37.9	23.64	38.5	0.241	b.d.l.	100.3		74.39	25.61	0.00
62	37.9	25.64	37.3	0.461	b.d.l.	101.3		72.16	27.84	0.00
65	37.8	27.38	35.7	0.122	b.d.l.	101.0		69.90	30.10	0.00
69	37.8	25.15	37.8	0.275	b.d.l.	101.0		72.82	27.18	0.00
79	37.2	29.54	34.0	0.187	b.d.l.	100.9		67.23	32.77	0.00
81	37.5	25.21	36.0	0.355	b.d.l.	99.1		71.80	28.20	0.00
85	36.6	27.66	33.8	0.280	b.d.l.	98.3		68.54	31.46	0.00
234	38.1	24.20	38.2	0.249	b.d.l.	100.7		73.76	26.24	0.00
235	36.8	27.08	32.7	0.435	b.d.l.	97.0		68.27	31.73	0.00
236	37.2	27.80	30.9	0.446	b.d.l.	96.3		66.44	33.56	0.00
237	36.0	27.86	31.2	0.496	b.d.l.	95.8		66.63	33.37	0.00
238	36.7	27.83	31.5	0.458	0.549	97.0		66.44	32.90	0.66
239	36.3	28.78	29.9	0.461	0.485	96.2		64.53	34.88	0.60
240	36.3	29.37	29.5	0.501	0.518	96.1		63.74	35.62	0.64
241	36.6	29.12	29.2	0.464	0.494	95.9		63.74	35.64	0.61
242	36.6	29.80	28.7	0.459	0.587	96.1		62.74	36.54	0.73
243	36.5	29.44	30.2	0.406	0.580	97.1		64.20	35.09	0.70
244	36.1	29.89	29.0	0.483	0.548	96.0		62.91	36.42	0.68
245	36.6	27.45	30.3	0.426	0.615	95.6		65.80	33.44	0.76
246	37.2	25.61	32.5	0.446	0.575	96.6		68.85	30.46	0.69

Tab. A-3: continued

No	SiO_2	FeO	MgO	CaO	MnO	Σ		fo	fa	tephroite
TA 9701 whole rock										
26	40.7	10.91	48.0	b.d.l.	b.d.l.	99.6		88.69	11.31	0.00
33	40.7	9.51	48.9	0.169	b.d.l.	99.3		90.17	9.83	0.00
34	41.1	9.63	49.0	0.145	b.d.l.	99.9		90.08	9.92	0.00
36	41.4	6.85	51.2	0.159	b.d.l.	99.6		93.02	6.98	0.00
41	41.5	5.86	51.9	0.133	b.d.l.	99.4		94.03	5.97	0.00
196	40.9	9.79	49.0	0.182	b.d.l.	99.9		89.91	10.09	0.00
197	40.8	9.70	49.0	0.154	b.d.l.	99.6		89.99	10.01	0.00
198	34.2	9.79	47.8	0.160	b.d.l.	91.9		89.69	10.31	0.00
199	40.7	10.37	48.3	0.134	b.d.l.	99.5		89.25	10.75	0.00
200	40.8	12.65	46.9	0.214	b.d.l.	100.5		86.86	13.14	0.00
201	40.2	15.49	44.3	0.216	b.d.l.	100.2		83.60	16.40	0.00
202	39.3	24.73	34.4	0.371	b.d.l.	98.8		71.23	28.77	0.00
TA 9701 peridotitic xenolith										
4	41.0	9.83	49.1	b.d.l.	b.d.l.	100.0		89.90	10.10	0.00
5	40.9	9.42	49.1	b.d.l.	b.d.l.	99.4		90.28	9.72	0.00
7	40.9	10.37	48.5	0.121	b.d.l.	99.9		89.29	10.71	0.00
14	40.7	9.84	49.1	b.d.l.	b.d.l.	99.7		89.90	10.10	0.00
15	40.8	9.79	49.2	0.092	b.d.l.	99.9		89.95	10.05	0.00
20	41.1	9.58	49.1	b.d.l.	b.d.l.	99.8		90.14	9.86	0.00
194	40.1	14.90	45.1	0.190	b.d.l.	100.3		84.37	15.63	0.00
195	39.7	13.17	45.8	0.201	b.d.l.	98.9		86.11	13.89	0.00

Tab. A-4: Chemical composition of clinopyroxenes by EMPA.

No	SiO_2	TiO_2	Al_2O_3	FeO	MgO	CaO	MnO	Cr_2O_3	Na_2O	Σ		en	fs	wo	ac	tsch
Montefiascone																
11	51.9	0.411	3.10	4.21	15.8	23.9	b.d.l.	0.346	0.257	99.9		44.64	5.90	48.52	0.95	0.04
22	50.7	0.604	4.37	4.76	15.2	23.8	b.d.l.	b.d.l.	0.188	99.9		43.35	7.00	48.95	0.70	0.06
23	46.2	1.311	8.13	8.15	12.4	23.2	b.d.l.	b.d.l.	0.362	99.9		37.20	11.20	50.18	1.42	0.10
26	52.0	0.419	3.14	3.96	16.0	23.7	b.d.l.	0.419	0.199	100.0		45.22	5.78	48.27	0.73	0.04
30	50.4	0.637	4.77	4.56	15.2	23.7	b.d.l.	0.381	0.168	99.9		43.88	6.44	49.06	0.63	0.07
61	52.2	0.358	2.60	2.87	16.5	24.9	b.d.l.	0.435	0.084	99.9		46.15	3.60	49.95	0.31	0.02
62	53.0	0.303	2.09	2.69	16.6	24.5	b.d.l.	0.784	0.120	100.2		46.45	3.95	49.17	0.44	0.02
63	52.9	0.266	2.05	2.74	16.4	24.7	b.d.l.	0.706	0.141	100.0		45.97	3.92	49.59	0.51	0.02
64	53.0	0.245	1.70	2.51	16.7	24.7	b.d.l.	0.569	0.158	99.7		46.59	3.48	49.36	0.57	0.01
65	53.5	b.d.l.	1.61	2.58	17.0	24.6	b.d.l.	0.538	0.104	100.1		46.83	3.99	48.80	0.37	0.02
66	53.0	b.d.l.	1.66	2.45	17.2	24.9	b.d.l.	0.560	0.088	100.2		47.33	3.21	49.15	0.31	0.01
67	53.2	0.261	1.76	2.65	17.1	24.8	b.d.l.	0.401	0.129	100.4		47.03	3.46	49.05	0.46	0.01
68	52.7	0.346	2.43	3.14	16.3	24.4	b.d.l.	0.366	0.106	99.9		45.79	4.60	49.22	0.39	0.03
69	50.0	0.506	5.06	4.33	14.8	25.1	b.d.l.	b.d.l.	0.122	100.2		42.30	5.63	51.61	0.45	0.06
70	49.2	0.703	5.43	5.37	14.2	24.1	b.d.l.	b.d.l.	0.142	99.3		41.39	7.49	50.58	0.54	0.07
71	51.2	0.492	3.42	4.26	15.6	24.2	b.d.l.	b.d.l.	0.095	99.6		44.28	6.11	49.27	0.35	0.04
72	50.3	0.605	4.27	4.70	15.1	24.1	b.d.l.	b.d.l.	0.148	99.5		43.17	6.66	49.63	0.55	0.05
73	49.4	0.662	4.69	6.05	14.2	23.6	b.d.l.	b.d.l.	0.254	99.0		41.33	8.37	49.34	0.96	0.06
74	49.1	0.697	4.94	6.14	14.4	23.6	b.d.l.	b.d.l.	0.239	99.4		41.83	8.15	49.13	0.90	0.06
75	49.3	0.622	4.74	5.96	14.3	23.5	b.d.l.	b.d.l.	0.300	98.9		41.61	8.10	49.14	1.14	0.06
76	52.1	0.374	2.90	4.08	15.9	24.0	b.d.l.	b.d.l.	0.197	100.0		44.72	6.12	48.44	0.72	0.04
77	51.6	0.399	3.12	4.39	15.8	24.0	b.d.l.	b.d.l.	0.186	99.8		44.62	6.16	48.54	0.68	0.04
78	51.3	0.376	3.21	4.22	15.7	24.2	b.d.l.	b.d.l.	0.155	99.3		44.54	5.66	49.23	0.57	0.04
79	51.6	0.401	3.11	4.08	15.8	24.2	b.d.l.	0.321	0.188	99.7		44.62	5.54	49.15	0.69	0.04
80	51.5	0.393	3.03	4.11	15.7	23.8	b.d.l.	0.315	0.187	99.1		44.76	5.80	48.75	0.69	0.04
81	52.2	0.345	2.93	3.98	16.0	23.9	b.d.l.	0.433	0.173	100.0		45.25	5.72	48.40	0.63	0.04
82	51.6	0.391	3.18	4.20	15.9	23.9	b.d.l.	0.313	0.222	99.7		44.96	5.68	48.55	0.82	0.04
83	51.6	0.405	3.18	4.08	15.7	23.8	b.d.l.	0.302	0.159	99.3		44.82	5.88	48.71	0.59	0.04
84	50.5	0.589	3.94	5.24	15.2	23.8	b.d.l.	b.d.l.	0.185	99.8		43.42	7.08	48.81	0.69	0.05
85	51.5	0.442	3.18	3.98	15.7	24.0	b.d.l.	b.d.l.	0.184	99.4		44.51	5.93	48.88	0.68	0.04
86	51.5	0.369	2.88	3.98	16.0	23.6	b.d.l.	0.443	0.199	99.0		45.50	5.54	48.23	0.74	0.03
87	51.6	0.380	3.22	4.28	15.9	23.6	b.d.l.	b.d.l.	0.223	99.5		44.97	6.22	47.98	0.82	0.05
88	51.0	0.536	3.82	4.98	15.6	23.4	b.d.l.	b.d.l.	0.257	99.8		44.25	6.93	47.86	0.95	0.05
89	48.0	0.872	5.97	6.49	14.3	23.2	b.d.l.	b.d.l.	0.366	99.5		41.75	8.25	48.61	1.39	0.06
90	51.7	0.426	3.04	4.00	16.2	23.9	b.d.l.	0.302	0.159	99.8		45.63	5.36	48.43	0.58	0.03
91	48.9	1.045	5.17	7.90	13.0	22.7	b.d.l.	b.d.l.	0.482	99.5		38.39	11.76	48.00	1.85	0.07
92	52.6	0.330	2.08	3.19	16.9	24.0	b.d.l.	0.418	0.141	99.8		47.13	4.25	48.11	0.51	0.02
93	52.8	0.261	1.87	3.11	17.1	24.3	b.d.l.	0.275	0.111	99.9		47.31	3.98	48.31	0.40	0.01
94	51.8	0.465	3.14	4.21	16.0	23.9	b.d.l.	b.d.l.	0.164	100.0		44.94	6.18	48.28	0.60	0.04
95	51.4	0.429	3.14	3.99	15.9	23.8	b.d.l.	0.346	0.178	99.3		45.19	5.56	48.59	0.66	0.04
96	51.3	0.460	3.31	4.40	15.6	23.5	b.d.l.	b.d.l.	0.195	99.0		44.37	6.66	48.25	0.72	0.05
97	52.3	0.250	2.48	2.93	16.7	23.4	b.d.l.	0.953	0.234	99.3		47.21	4.28	47.64	0.86	0.03
98	51.4	0.438	3.16	4.09	16.0	23.6	b.d.l.	b.d.l.	0.186	99.2		45.31	5.95	48.05	0.69	0.04
99	52.0	0.333	2.85	3.38	16.6	23.3	b.d.l.	0.631	0.245	99.5		46.98	4.68	47.43	0.90	0.04
100	51.8	0.342	3.03	3.78	16.3	23.4	b.d.l.	0.554	0.200	99.5		46.26	5.36	47.64	0.74	0.04
101	51.0	0.483	3.69	4.75	15.6	23.5	b.d.l.	0.390	0.221	99.7		44.55	6.50	48.14	0.82	0.05
102	50.7	0.484	3.92	4.52	15.5	23.9	b.d.l.	0.277	0.211	99.6		44.31	5.96	48.95	0.78	0.05
103	51.9	0.345	2.91	3.45	16.5	23.3	b.d.l.	0.792	0.206	99.6		46.72	4.93	47.59	0.76	0.04
104	51.8	0.370	3.15	3.97	16.2	24.0	b.d.l.	0.391	0.138	100.0		45.57	5.38	48.53	0.51	0.04
105	46.9	1.054	6.77	7.83	13.0	23.2	b.d.l.	b.d.l.	0.431	99.3		38.61	10.19	49.54	1.67	0.08

Tab. A-4: continued

No	SiO_2	TiO_2	Al_2O_3	FeO	MgO	CaO	MnO	Cr_2O_3	Na_2O	Σ		en	fs	wo	ac	tsch
VUL 9701																
64	47.3	1.187	5.31	10.55	11.0	23.5	0.482	b.d.l.	0.628	99.9		32.70	14.97	49.92	2.42	0.04
65	48.8	0.890	4.42	9.86	11.8	23.1	0.486	b.d.l.	0.500	99.8		34.58	14.78	48.73	1.91	0.05
68	48.2	0.953	4.75	9.62	11.8	23.1	0.460	b.d.l.	0.512	99.3		34.74	14.28	49.01	1.97	0.05
69	47.8	0.955	5.21	9.34	11.8	23.3	0.397	b.d.l.	0.489	99.4		34.95	13.50	49.67	1.88	0.06
76	48.1	0.959	5.12	9.40	11.8	23.5	0.390	b.d.l.	0.450	99.7		34.89	13.60	49.78	1.73	0.05
78	45.9	1.414	6.49	11.02	10.3	23.3	0.456	b.d.l.	0.645	99.4		31.03	15.87	50.57	2.54	0.06
84	48.1	0.915	4.62	10.45	11.1	23.1	0.544	b.d.l.	0.567	99.3		32.86	15.78	49.18	2.19	0.05
86	47.9	1.103	5.13	10.07	11.3	23.3	0.447	b.d.l.	0.565	99.9		33.51	14.72	49.60	2.18	0.05
250	48.4	0.898	4.50	10.08	11.4	23.4	0.491	b.d.l.	0.542	99.7		33.61	14.88	49.43	2.08	0.05
251	48.4	0.986	4.45	10.03	11.4	23.4	0.517	b.d.l.	0.555	99.6		33.49	14.90	49.48	2.13	0.04
252	48.5	0.915	4.24	10.08	11.6	23.2	0.483	b.d.l.	0.552	99.5		34.17	14.80	48.91	2.11	0.04
253	45.6	1.466	6.41	11.02	10.2	23.2	0.473	b.d.l.	0.607	99.0		30.87	16.06	50.67	2.40	0.06
254	46.8	1.256	5.93	10.53	10.9	23.1	0.407	b.d.l.	0.580	99.5		32.67	15.37	49.70	2.26	0.06
255	45.2	1.535	7.08	10.83	10.3	23.0	0.476	b.d.l.	0.573	99.0		31.56	15.72	50.45	2.28	0.07
256	44.5	1.830	7.54	11.74	9.6	22.8	0.483	b.d.l.	0.654	99.1		29.67	17.25	50.46	2.62	0.07
257	44.2	1.880	7.76	12.13	9.3	22.8	0.507	b.d.l.	0.645	99.2		28.76	18.00	50.64	2.59	0.07
258	43.8	1.910	7.64	11.93	9.3	23.0	0.486	b.d.l.	0.681	98.7		28.81	17.29	51.15	2.74	0.06
259	45.4	1.644	6.92	11.26	10.1	22.9	0.514	b.d.l.	0.605	99.2		30.75	16.69	50.16	2.40	0.07
260	46.9	1.271	6.12	10.17	11.3	23.2	0.460	b.d.l.	0.527	99.9		33.66	14.63	49.66	2.05	0.06
261	45.7	1.605	7.08	10.68	10.7	23.1	0.413	b.d.l.	0.485	99.7		32.36	15.54	50.20	1.91	0.07
262	46.1	1.406	6.89	10.31	10.9	23.2	0.335	b.d.l.	0.539	99.6		32.80	14.77	50.32	2.12	0.07
263	46.1	1.316	6.71	10.17	11.2	23.2	0.378	b.d.l.	0.489	99.5		33.58	14.38	50.12	1.91	0.07
264	45.5	1.478	7.26	10.45	10.6	23.0	0.388	b.d.l.	0.567	99.2		32.17	15.12	50.47	2.25	0.08
265	45.1	1.505	7.27	10.47	10.7	23.3	0.304	b.d.l.	0.533	99.2		32.58	14.52	50.80	2.11	0.07
266	48.8	0.880	4.58	9.45	11.8	23.4	0.378	b.d.l.	0.497	99.8		34.72	13.98	49.41	1.90	0.05
267	49.2	0.822	4.42	9.67	12.1	23.2	0.449	b.d.l.	0.517	100.2		35.20	14.31	48.54	1.96	0.05
268	48.2	1.014	4.77	10.22	11.3	23.1	0.491	b.d.l.	0.555	99.7		33.39	15.32	49.16	2.13	0.05
269	48.4	1.006	4.80	9.91	11.5	23.2	0.505	b.d.l.	0.561	99.9		33.82	14.83	49.20	2.15	0.05
270	47.5	1.099	5.63	9.93	11.4	23.4	0.410	b.d.l.	0.514	99.8		33.82	14.35	49.85	1.99	0.06
271	46.3	1.254	6.32	10.70	10.7	23.3	0.439	b.d.l.	0.557	99.6		32.10	15.33	50.39	2.18	0.06
272	46.2	1.295	6.44	9.92	11.0	23.3	0.325	b.d.l.	0.523	98.9		33.17	14.20	50.57	2.06	0.07
273	46.3	1.396	6.16	10.64	10.6	23.2	0.505	b.d.l.	0.639	99.4		31.91	15.43	50.16	2.50	0.06
274	46.6	1.311	5.99	10.35	10.9	23.3	0.432	b.d.l.	0.504	99.4		32.78	15.07	50.19	1.97	0.06
275	46.8	1.263	6.01	9.76	11.2	23.2	0.326	b.d.l.	0.437	99.0		33.68	14.35	50.25	1.71	0.06
276	46.0	1.291	6.66	10.43	11.0	23.1	0.437	b.d.l.	0.474	99.4		33.00	15.01	50.13	1.86	0.07
277	46.8	1.263	6.30	9.77	11.3	23.5	0.332	b.d.l.	0.442	99.6		33.74	14.04	50.50	1.72	0.07
278	46.2	1.446	6.51	10.81	10.8	23.0	0.471	b.d.l.	0.623	99.8		32.42	15.46	49.68	2.43	0.06
279	46.4	1.413	6.37	10.84	10.5	22.8	0.491	b.d.l.	0.620	99.5		31.73	16.24	49.59	2.44	0.07
VUL 9702																
3	47.7	0.863	6.02	8.77	12.8	23.4	0.194	b.d.l.	0.193	100.0		36.70	14.40	48.18	0.72	0.00
6	46.3	1.579	8.44	7.11	12.7	23.0	b.d.l.	b.d.l.	0.197	99.3		37.80	11.93	49.50	0.77	0.00
7	47.3	0.849	6.07	8.69	12.7	23.4	0.186	b.d.l.	0.235	99.5		36.45	14.31	48.36	0.88	0.00
9	48.6	1.062	6.43	6.13	13.9	23.0	b.d.l.	0.365	0.157	99.6		40.79	10.11	48.50	0.60	0.00
11	47.5	1.094	6.53	8.12	13.1	22.5	0.178	b.d.l.	0.166	99.2		38.31	13.63	47.43	0.63	0.00
17	49.7	0.751	4.75	7.31	14.3	23.0	0.123	b.d.l.	0.208	100.1		40.55	11.82	46.86	0.77	0.00
19	44.5	1.790	8.77	8.74	11.8	22.8	0.139	b.d.l.	0.175	98.8		35.39	14.89	49.04	0.68	0.00
23	49.2	0.728	4.35	8.20	13.4	22.8	0.204	b.d.l.	0.132	99.1		38.70	13.58	47.22	0.49	0.00
25	46.8	0.942	6.27	10.01	11.4	23.3	0.254	b.d.l.	0.280	99.3		33.26	16.80	48.87	1.06	0.00
97	45.5	1.443	8.50	8.00	12.5	23.2	b.d.l.	b.d.l.	0.174	99.2		36.86	13.26	49.21	0.67	0.00

Tab. A-4: continued

No	SiO_2	TiO_2	Al_2O_3	FeO	MgO	CaO	MnO	Cr_2O_3	Na_2O	Σ		en	fs	wo	ac	tsch
VUL 9702																
98	45.6	1.449	8.72	8.01	12.2	22.9	0.175	b.d.l.	0.194	99.2		36.49	13.71	49.04	0.75	0.00
99	45.9	1.490	8.42	7.67	12.6	23.1	b.d.l.	b.d.l.	0.177	99.4		37.44	12.75	49.13	0.68	0.00
100	46.4	1.459	7.80	7.35	13.2	22.9	b.d.l.	b.d.l.	0.190	99.3		38.88	12.12	48.27	0.73	0.00
101	46.6	1.289	7.89	7.84	13.0	22.9	b.d.l.	b.d.l.	0.137	99.6		38.10	12.94	48.44	0.52	0.00
102	46.7	1.289	7.60	7.76	12.7	23.1	0.139	b.d.l.	0.199	99.4		37.37	13.05	48.82	0.76	0.00
103	44.9	1.605	8.99	9.06	11.6	23.0	b.d.l.	b.d.l.	0.193	99.3		34.66	15.18	49.41	0.75	0.00
104	45.0	1.541	8.92	8.89	11.8	23.0	0.168	b.d.l.	0.150	99.4		35.11	15.15	49.16	0.58	0.00
105	45.0	1.587	8.68	8.97	11.8	22.8	0.126	b.d.l.	0.185	99.1		35.23	15.23	48.82	0.72	0.00
106	46.9	0.919	6.05	9.73	11.4	23.4	0.280	b.d.l.	0.317	99.0		33.28	16.41	49.11	1.21	0.00
107	47.3	0.842	5.91	9.89	11.6	23.4	0.287	b.d.l.	0.324	99.6		33.44	16.55	48.79	1.22	0.00
108	48.1	0.905	5.80	8.04	12.8	23.3	0.174	b.d.l.	0.197	99.3		37.26	13.39	48.61	0.74	0.00
109	48.5	0.906	6.14	6.16	14.3	22.9	0.121	b.d.l.	0.154	99.2		41.47	10.22	47.73	0.58	0.00
110	48.9	0.820	6.19	6.27	14.3	22.8	0.114	b.d.l.	0.187	99.5		41.40	10.41	47.48	0.71	0.00
111	47.8	0.944	6.78	6.97	13.9	22.7	0.124	b.d.l.	0.213	99.5		40.34	11.53	47.32	0.80	0.00
112	48.5	0.901	6.02	6.35	14.1	23.1	0.135	b.d.l.	0.142	99.2		40.80	10.53	48.13	0.53	0.00
113	47.8	0.877	6.18	6.68	13.8	23.2	0.113	b.d.l.	0.175	98.9		39.92	11.05	48.37	0.66	0.00
114	46.4	0.982	7.29	8.20	12.8	22.9	0.153	b.d.l.	0.145	98.9		37.44	13.75	48.26	0.55	0.00
115	45.0	1.293	8.66	9.40	11.8	22.5	0.186	b.d.l.	0.228	99.0		35.03	16.00	48.09	0.88	0.00
116	50.8	0.605	3.90	5.80	15.6	22.8	0.111	b.d.l.	0.117	99.7		43.93	9.35	46.29	0.43	0.00
VUL 9703 B																
1	52.1	0.419	3.36	3.78	16.3	24.0	b.d.l.	b.d.l.	0.195	100.1		45.54	5.49	48.25	0.71	0.04
5	52.2	0.458	3.63	4.12	16.5	23.4	b.d.l.	b.d.l.	0.187	100.4		46.25	5.99	47.09	0.68	0.05
6	52.4	0.496	3.37	4.08	16.4	23.6	b.d.l.	b.d.l.	0.207	100.6		45.81	6.06	47.38	0.75	0.05
7	50.3	0.718	5.44	4.27	15.5	23.6	b.d.l.	b.d.l.	0.207	100.1		44.45	6.21	48.57	0.77	0.08
14	50.4	0.585	3.84	7.72	13.4	23.8	0.262	b.d.l.	0.462	100.4		38.51	10.83	48.94	1.72	0.05
11	52.2	0.301	1.39	9.65	12.6	23.4	0.859	b.d.l.	0.502	100.8		35.39	15.40	47.37	1.84	0.01
17	52.5	0.512	3.05	5.11	16.5	23.0	b.d.l.	b.d.l.	0.260	100.9		45.96	7.17	45.93	0.94	0.04
18	51.9	0.329	4.05	3.19	16.9	22.8	b.d.l.	0.995	0.304	100.4		47.88	4.37	46.63	1.12	0.06
20	50.7	0.660	5.18	4.37	15.5	23.5	b.d.l.	b.d.l.	0.212	100.0		44.27	6.67	48.27	0.79	0.08
21	50.9	0.636	5.21	4.31	15.4	23.7	b.d.l.	b.d.l.	0.134	100.2		44.18	6.64	48.68	0.50	0.08
27	52.1	0.577	2.49	6.38	16.6	21.4	0.183	b.d.l.	0.242	100.0		46.58	9.39	43.16	0.88	0.03
28	51.8	0.640	3.64	5.95	16.3	21.5	b.d.l.	b.d.l.	0.226	100.1		46.22	9.17	43.78	0.83	0.05
29	49.9	1.052	5.14	7.47	14.7	21.9	0.186	b.d.l.	0.278	100.6		42.43	11.12	45.41	1.04	0.07
30	51.7	0.571	2.21	9.01	13.1	23.1	0.461	b.d.l.	0.498	100.7		37.24	13.83	47.08	1.84	0.03
110	50.5	0.612	3.47	8.15	13.2	23.9	0.404	b.d.l.	0.454	100.6		37.64	11.64	49.03	1.69	0.04
111	50.4	0.560	3.56	8.14	13.3	23.4	0.371	b.d.l.	0.457	100.1		38.13	11.79	48.37	1.71	0.04
112	50.3	0.465	3.50	8.15	13.2	23.5	0.319	b.d.l.	0.446	99.9		37.98	11.78	48.58	1.67	0.04
113	50.7	0.599	3.51	7.94	13.5	23.6	0.331	b.d.l.	0.442	100.6		38.62	11.34	48.39	1.64	0.04
114	50.9	0.600	3.46	8.02	13.6	23.7	0.359	b.d.l.	0.431	101.0		38.67	11.49	48.25	1.59	0.04
115	50.4	0.577	3.56	8.12	13.3	23.4	0.368	b.d.l.	0.467	100.2		38.07	11.89	48.29	1.74	0.04
116	50.4	0.589	3.64	8.30	13.3	23.5	0.394	b.d.l.	0.484	100.6		38.08	11.87	48.25	1.80	0.04
117	51.1	0.451	4.41	3.48	16.0	23.5	b.d.l.	1.250	0.203	100.3		45.87	4.84	48.52	0.76	0.06
118	51.4	0.450	4.21	3.62	16.1	23.5	b.d.l.	1.150	0.204	100.6		45.90	5.11	48.23	0.76	0.05
119	51.2	0.516	4.60	3.60	16.0	23.5	b.d.l.	1.283	0.224	101.0		45.84	4.94	48.38	0.83	0.06
120	50.1	0.744	5.20	5.34	15.1	23.0	b.d.l.	b.d.l.	0.256	99.8		43.58	7.67	47.78	0.96	0.08
121	51.1	0.626	4.47	5.05	15.6	23.2	b.d.l.	b.d.l.	0.182	100.2		44.42	7.47	47.44	0.67	0.06
122	51.3	0.589	4.28	4.90	15.8	23.3	b.d.l.	b.d.l.	0.214	100.3		44.69	7.14	47.38	0.79	0.06
123	51.0	0.559	4.18	4.83	15.9	23.3	b.d.l.	b.d.l.	0.166	99.9		44.94	6.89	47.56	0.61	0.05
124	51.3	0.598	3.96	4.93	15.9	22.8	b.d.l.	b.d.l.	0.213	99.7		45.20	7.52	46.49	0.79	0.06

Tab. A-4: continued

No	SiO_2	TiO_2	Al_2O_3	FeO	MgO	CaO	MnO	Cr_2O_3	Na_2O	Σ		en	fs	wo	ac	tsch
VUL 9703 B																
125	51.1	0.596	4.02	5.03	15.9	22.9	b.d.l.	b.d.l.	0.230	99.8		45.09	7.20	46.86	0.85	0.06
126	50.9	0.614	4.41	5.13	15.6	23.0	b.d.l.	b.d.l.	0.243	100.0		44.54	7.40	47.16	0.90	0.06
127	50.4	0.653	4.77	5.19	15.6	23.0	b.d.l.	b.d.l.	0.199	99.7		44.52	7.56	47.19	0.74	0.06
128	50.9	0.616	4.40	5.09	15.8	23.0	b.d.l.	b.d.l.	0.179	99.9		44.83	7.56	46.95	0.66	0.06
129	48.4	0.981	6.54	6.57	14.3	22.2	b.d.l.	b.d.l.	0.280	99.3		42.38	9.43	47.11	1.08	0.09
130	51.0	0.670	4.02	4.97	15.8	23.2	b.d.l.	b.d.l.	0.234	99.8		44.76	7.10	47.28	0.86	0.05
131	50.7	0.642	4.53	5.05	15.6	23.1	b.d.l.	b.d.l.	0.205	99.8		44.55	7.21	47.48	0.76	0.06
132	50.9	0.598	4.22	5.08	15.8	23.3	b.d.l.	b.d.l.	0.269	100.1		44.83	6.79	47.39	0.99	0.05
133	51.2	0.608	4.14	5.00	15.8	23.2	b.d.l.	b.d.l.	0.217	100.1		44.75	7.22	47.23	0.80	0.06
134	50.4	0.694	4.46	5.07	15.5	23.2	b.d.l.	b.d.l.	0.238	99.6		44.32	7.13	47.66	0.89	0.06
135	50.7	0.686	4.28	5.02	15.7	23.0	b.d.l.	b.d.l.	0.213	99.6		44.76	7.27	47.18	0.79	0.05
136	52.8	0.340	2.86	3.53	17.0	23.6	b.d.l.	b.d.l.	0.182	100.3		47.29	4.99	47.06	0.66	0.04
137	51.1	0.641	3.70	6.62	14.5	23.5	0.222	b.d.l.	0.232	100.6		41.22	9.98	47.94	0.86	0.04
138	47.0	0.853	6.02	8.98	12.8	23.0	0.343	b.d.l.	0.383	99.4		37.74	12.03	48.76	1.47	0.05
139	50.5	0.637	3.52	8.42	13.2	23.5	0.399	b.d.l.	0.473	100.6		37.65	12.28	48.31	1.76	0.04
140	52.6	0.379	3.07	3.69	17.0	23.3	b.d.l.	b.d.l.	0.226	100.3		47.10	5.53	46.55	0.81	0.04
141	51.2	0.604	3.84	6.15	14.9	23.3	b.d.l.	b.d.l.	0.201	100.2		42.39	9.12	47.75	0.74	0.05
VUL 9705																
2	53.3	0.271	1.97	3.13	16.7	24.8	b.d.l.	b.d.l.	0.137	100.3		45.92	4.53	49.06	0.49	0.02
6	52.1	0.348	2.77	4.02	16.2	24.4	b.d.l.	b.d.l.	0.123	99.9		45.19	5.38	48.98	0.45	0.03
7	51.9	0.324	2.48	3.75	16.4	24.6	b.d.l.	b.d.l.	0.109	99.5		45.61	4.67	49.33	0.39	0.02
9	51.9	0.447	2.68	3.77	16.1	24.9	b.d.l.	b.d.l.	0.118	100.0		44.94	4.69	49.93	0.43	0.02
15	52.6	0.296	2.11	2.79	16.6	24.8	b.d.l.	0.778	0.106	100.0		46.35	3.66	49.60	0.38	0.01
16	52.4	0.395	2.64	3.78	16.1	24.8	b.d.l.	b.d.l.	0.130	100.2		44.87	5.16	49.50	0.47	0.03
18	53.6	0.338	1.56	3.09	17.0	24.6	b.d.l.	b.d.l.	0.081	100.2		46.63	4.58	48.50	0.29	0.02
19	50.2	0.507	4.36	4.83	14.8	24.4	0.115	b.d.l.	0.191	99.4		42.44	6.47	50.37	0.71	0.06
21	52.8	0.290	2.06	2.96	16.9	24.2	b.d.l.	0.515	0.116	99.8		47.10	4.06	48.43	0.42	0.02
25	51.5	0.530	3.45	3.30	16.0	24.0	b.d.l.	0.772	0.103	99.6		45.71	4.81	49.10	0.38	0.04
27	49.4	0.671	4.87	6.68	13.7	24.2	b.d.l.	b.d.l.	0.228	99.7		39.65	9.12	50.37	0.86	0.06
106	49.6	0.627	4.37	6.08	14.5	24.4	0.132	b.d.l.	0.140	99.8		41.35	7.88	50.25	0.52	0.04
107	45.3	1.306	8.19	9.40	10.7	23.3	0.189	b.d.l.	0.328	98.9		33.06	13.94	51.69	1.32	0.11
108	50.6	0.629	4.29	5.38	15.0	23.8	0.112	b.d.l.	0.156	99.9		42.94	7.63	48.85	0.58	0.06
109	52.5	0.359	2.40	3.68	16.3	24.4	0.124	b.d.l.	0.080	99.9		45.34	5.50	48.87	0.29	0.03
110	52.5	0.294	2.08	3.41	16.5	24.6	b.d.l.	b.d.l.	0.067	99.4		45.71	4.96	49.08	0.24	0.02
111	52.8	0.339	2.14	3.44	16.5	24.3	0.136	b.d.l.	0.085	99.7		45.93	5.29	48.48	0.31	0.03
112	52.5	0.361	2.19	3.76	16.4	24.4	b.d.l.	b.d.l.	0.066	99.7		45.55	5.43	48.78	0.24	0.02
113	52.4	0.354	2.48	3.67	16.1	24.4	b.d.l.	0.241	0.151	99.8		45.22	5.16	49.07	0.55	0.03
114	52.7	0.306	2.11	3.47	16.4	24.2	b.d.l.	0.296	0.105	99.5		45.85	5.03	48.74	0.38	0.03
115	52.9	0.326	2.18	3.45	16.4	24.4	b.d.l.	0.408	0.105	100.3		45.78	4.97	48.87	0.38	0.03
116	52.8	0.218	1.78	3.14	16.8	24.2	b.d.l.	0.625	0.122	99.6		46.79	4.31	48.45	0.44	0.01
117	53.4	0.212	1.90	2.86	16.8	24.3	b.d.l.	0.705	0.123	100.3		46.60	4.35	48.61	0.44	0.02
118	53.2	0.229	1.87	2.92	16.8	24.2	b.d.l.	0.665	0.120	99.9		46.72	4.41	48.44	0.43	0.02
119	52.7	0.303	2.30	3.52	16.3	24.3	0.117	0.302	0.106	100.0		45.64	5.13	48.85	0.39	0.03
120	52.2	0.386	2.50	3.65	16.3	24.4	b.d.l.	0.261	0.097	99.8		45.66	4.98	49.01	0.35	0.03
121	52.5	0.360	2.53	3.81	16.1	24.4	b.d.l.	b.d.l.	0.104	99.9		44.93	5.73	48.96	0.38	0.03
122	52.3	0.366	2.69	3.82	16.0	24.5	b.d.l.	b.d.l.	0.127	99.7		44.74	5.64	49.15	0.46	0.03
123	52.4	0.331	2.49	3.80	16.1	24.5	b.d.l.	b.d.l.	0.133	99.8		44.88	5.50	49.14	0.48	0.03
124	52.6	0.372	2.27	3.71	16.4	24.2	0.124	0.253	0.079	100.0		45.79	5.41	48.52	0.29	0.03
125	52.2	0.358	2.44	3.62	16.2	24.4	b.d.l.	0.265	0.111	99.7		45.49	4.98	49.12	0.41	0.03

Tab. A-4: continued

No	SiO_2	TiO_2	Al_2O_3	FeO	MgO	CaO	MnO	Cr_2O_3	Na_2O	Σ		en	fs	wo	ac	tsch
VUL 9705																
126	52.7	0.335	2.20	3.44	16.6	24.3	b.d.l.	b.d.l.	0.101	99.6		46.22	4.90	48.51	0.37	0.03
127	53.2	0.261	1.55	2.73	16.9	24.4	b.d.l.	0.419	0.081	99.4		46.92	4.03	48.76	0.29	0.02
128	53.2	0.305	1.94	2.60	16.8	24.3	b.d.l.	0.748	0.111	100.0		46.95	3.96	48.68	0.40	0.02
129	53.7	0.248	1.53	2.82	16.8	24.7	b.d.l.	0.261	0.104	100.2		46.47	4.19	48.97	0.37	0.02
130	53.7	0.259	1.40	2.61	17.2	24.5	b.d.l.	0.389	0.078	100.2		47.31	3.83	48.58	0.28	0.01
131	53.7	0.225	1.69	2.88	17.0	24.6	b.d.l.	b.d.l.	0.104	100.2		46.69	4.32	48.61	0.37	0.02
132	53.8	0.286	1.59	2.88	17.1	24.5	b.d.l.	b.d.l.	0.103	100.3		46.93	4.30	48.40	0.37	0.02
133	53.7	0.238	1.50	2.75	17.2	24.6	b.d.l.	b.d.l.	0.075	100.1		47.19	4.00	48.54	0.27	0.02
134	53.9	0.226	1.41	2.80	17.1	24.6	b.d.l.	b.d.l.	0.100	100.1		46.95	4.16	48.53	0.36	0.02
135	53.7	0.230	1.41	2.76	17.1	24.4	b.d.l.	b.d.l.	0.103	99.8		47.20	4.07	48.36	0.37	0.02
136	53.9	0.230	1.33	2.59	17.5	24.3	b.d.l.	b.d.l.	0.086	100.0		48.02	3.77	47.91	0.31	0.01
137	53.9	0.163	1.32	2.61	17.3	24.3	b.d.l.	b.d.l.	0.107	99.7		47.68	3.94	48.00	0.38	0.02
138	53.6	0.198	1.32	2.54	17.2	24.3	b.d.l.	0.213	0.083	99.4		47.67	3.78	48.25	0.30	0.02
139	53.8	0.244	1.42	2.52	17.3	24.4	b.d.l.	b.d.l.	0.086	99.8		47.40	4.05	48.25	0.31	0.02
140	53.5	0.217	1.28	2.52	17.3	24.3	b.d.l.	b.d.l.	0.074	99.2		47.81	3.78	48.14	0.27	0.01
141	54.0	0.191	1.28	2.51	17.5	24.3	b.d.l.	b.d.l.	0.101	99.9		47.85	3.84	47.95	0.36	0.02
142	54.0	0.269	1.31	2.66	17.4	24.2	b.d.l.	b.d.l.	0.107	99.9		47.77	4.16	47.68	0.38	0.02
143	54.0	0.223	1.32	2.60	17.4	24.5	b.d.l.	b.d.l.	0.084	100.1		47.71	3.85	48.14	0.30	0.02
144	53.0	0.295	2.36	3.26	16.5	24.5	b.d.l.	b.d.l.	0.074	100.0		45.82	4.91	49.00	0.27	0.03
145	51.9	0.379	2.82	3.69	15.9	24.9	b.d.l.	b.d.l.	0.089	99.6		44.52	5.01	50.15	0.32	0.03
146	53.1	0.312	1.92	3.36	16.5	24.7	b.d.l.	b.d.l.	0.095	100.0		45.72	4.78	49.15	0.34	0.02
147	53.8	0.235	1.33	2.65	17.3	24.8	b.d.l.	b.d.l.	0.106	100.1		47.25	3.68	48.70	0.38	0.01
148	54.2	0.242	1.28	2.58	17.2	24.7	b.d.l.	b.d.l.	0.064	100.2		47.11	4.01	48.66	0.23	0.02
149	54.0	0.257	1.27	2.71	17.1	24.6	b.d.l.	b.d.l.	b.d.l.	100.0		46.99	4.40	48.62	0.00	0.02
150	53.8	0.218	1.28	2.47	17.1	24.8	b.d.l.	b.d.l.	0.069	99.6		46.99	3.80	48.96	0.25	0.02
151	53.9	0.237	1.29	2.56	17.0	24.5	b.d.l.	b.d.l.	0.063	99.6		46.95	4.17	48.66	0.23	0.02
152	52.1	0.465	2.68	3.76	15.9	24.7	b.d.l.	b.d.l.	0.112	99.8		44.62	5.27	49.70	0.41	0.03
153	52.4	0.384	2.65	3.66	16.2	24.8	b.d.l.	b.d.l.	0.091	100.2		45.06	5.00	49.61	0.33	0.03
154	52.4	0.403	2.66	4.08	15.9	24.4	b.d.l.	b.d.l.	0.108	99.9		44.54	5.93	49.14	0.39	0.04
155	51.9	0.492	2.97	4.37	15.7	24.6	b.d.l.	b.d.l.	0.114	100.1		43.98	6.03	49.57	0.42	0.03
156	52.3	0.375	2.67	3.91	15.9	24.8	b.d.l.	b.d.l.	0.080	100.0		44.36	5.51	49.84	0.29	0.03
157	52.6	0.416	2.32	3.82	16.0	24.5	b.d.l.	b.d.l.	0.105	99.7		44.70	5.72	49.20	0.38	0.03
158	52.3	0.404	2.41	3.77	16.1	24.6	b.d.l.	b.d.l.	0.085	99.6		44.92	5.35	49.41	0.31	0.03
159	52.7	0.392	2.38	3.67	16.2	24.7	b.d.l.	b.d.l.	0.103	100.2		44.95	5.23	49.45	0.37	0.03
160	52.5	0.389	2.34	3.60	16.3	24.7	b.d.l.	b.d.l.	0.072	99.9		45.30	5.14	49.31	0.26	0.03
161	52.9	0.418	2.38	3.77	16.4	24.9	b.d.l.	b.d.l.	0.113	100.8		45.09	5.21	49.29	0.41	0.02
162	51.7	0.519	3.23	4.01	15.6	24.8	b.d.l.	b.d.l.	0.105	99.9		43.74	5.72	50.15	0.38	0.04
163	51.5	0.541	3.37	4.23	15.8	24.8	b.d.l.	b.d.l.	0.123	100.3		44.12	5.58	49.86	0.45	0.03
164	48.3	0.946	5.85	6.55	13.5	24.1	b.d.l.	b.d.l.	0.199	99.4		39.64	8.87	50.73	0.76	0.07
165	50.9	0.541	3.78	5.05	15.1	24.3	b.d.l.	b.d.l.	0.189	99.8		42.79	6.98	49.54	0.70	0.04
166	51.4	0.518	3.43	4.78	15.1	24.5	b.d.l.	b.d.l.	0.186	100.0		42.83	6.66	49.83	0.69	0.04
167	51.1	0.582	3.75	4.95	14.9	24.5	b.d.l.	b.d.l.	0.182	100.0		42.33	6.97	50.02	0.67	0.05
168	50.6	0.542	3.78	5.15	14.9	24.5	b.d.l.	b.d.l.	0.204	99.7		42.39	6.72	50.14	0.76	0.04
169	50.3	0.614	4.04	5.27	14.8	24.6	b.d.l.	b.d.l.	0.182	99.8		42.08	6.83	50.42	0.67	0.04
170	50.1	0.652	4.05	5.45	14.7	24.3	b.d.l.	b.d.l.	0.176	99.5		42.14	7.12	50.09	0.65	0.04
171	50.3	0.682	4.27	5.48	14.5	24.5	0.112	b.d.l.	0.196	99.9		41.45	7.46	50.36	0.73	0.05
172	49.4	0.674	4.30	5.60	14.4	24.3	b.d.l.	b.d.l.	0.148	98.8		41.73	7.34	50.37	0.56	0.04
173	49.9	0.687	4.50	5.79	14.5	24.2	0.125	b.d.l.	0.208	99.9		41.57	7.71	49.94	0.77	0.05
174	50.1	0.678	4.47	5.95	14.2	24.3	b.d.l.	b.d.l.	0.200	99.9		40.89	8.21	50.15	0.75	0.06
175	49.7	0.713	4.66	5.84	14.0	24.4	0.128	b.d.l.	0.185	99.6		40.52	8.09	50.69	0.70	0.06

Tab A-4: continued

No	SiO_2	TiO_2	Al_2O_3	FeO	MgO	CaO	MnO	Cr_2O_3	Na_2O	Σ		en	fs	wo	ac	tsch
VUL 9705																
176	49.4	0.700	4.68	6.14	14.0	24.0	0.142	b.d.l.	0.212	99.3		40.66	8.43	50.11	0.80	0.06
177	50.3	0.678	4.12	5.60	14.4	24.3	b.d.l.	b.d.l.	0.239	99.6		41.43	7.64	50.04	0.89	0.05
178	50.3	0.665	4.17	5.75	14.5	24.3	b.d.l.	b.d.l.	0.186	99.9		41.54	7.85	49.91	0.69	0.05
179	50.4	0.609	4.24	5.68	14.6	24.5	0.130	b.d.l.	0.201	100.3		41.63	7.51	50.11	0.74	0.05
180	48.7	0.885	5.56	6.57	13.6	24.0	b.d.l.	b.d.l.	0.202	99.5		39.76	9.07	50.40	0.77	0.07
181	50.3	0.682	4.13	5.54	14.7	24.3	b.d.l.	b.d.l.	0.182	99.8		42.07	7.48	49.78	0.68	0.05
182	52.3	0.329	2.79	3.69	16.4	24.6	b.d.l.	0.552	0.149	100.8		45.60	4.71	49.15	0.54	0.02
183	52.0	0.326	2.70	3.53	16.1	24.5	b.d.l.	0.603	0.117	99.8		45.38	4.73	49.46	0.43	0.03
VUL 9707																
74	45.1	1.316	7.46	11.09	10.1	23.2	0.287	b.d.l.	0.412	98.9		29.89	18.97	49.55	1.59	0.00
75	43.7	1.402	8.04	12.30	9.1	23.0	0.402	b.d.l.	0.439	98.4		27.34	21.39	49.56	1.71	0.00
78	46.9	1.061	6.30	9.79	11.2	23.5	0.206	b.d.l.	0.364	99.3		32.72	16.43	49.46	1.39	0.00
79	45.3	1.336	7.28	11.32	10.0	23.1	0.374	b.d.l.	0.477	99.2		29.59	19.40	49.18	1.83	0.00
81	44.7	1.514	8.42	10.64	10.2	23.2	0.250	b.d.l.	0.395	99.3		30.34	18.25	49.87	1.53	0.00
85	46.6	1.016	6.46	10.44	10.9	23.4	0.251	b.d.l.	0.330	99.4		31.97	17.54	49.23	1.25	0.00
91	42.5	1.450	10.40	12.10	8.7	23.3	0.163	b.d.l.	0.342	99.0		26.48	21.01	51.15	1.36	0.00
194	42.8	1.810	9.85	11.91	8.9	23.2	0.264	b.d.l.	0.374	99.1		27.02	20.78	50.71	1.48	0.00
195	42.6	1.800	9.90	11.82	9.0	23.1	0.245	b.d.l.	0.380	98.9		27.38	20.57	50.54	1.50	0.00
196	42.4	1.930	10.01	11.98	8.9	23.4	0.223	b.d.l.	0.356	99.2		26.96	20.72	50.91	1.40	0.00
197	45.5	1.227	7.50	10.30	10.8	23.8	0.252	b.d.l.	0.360	99.7		31.47	17.29	49.88	1.37	0.00
198	45.7	1.181	7.35	10.30	10.7	23.8	0.269	b.d.l.	0.344	99.7		31.41	17.34	49.95	1.31	0.00
199	46.9	1.033	6.27	10.33	11.2	23.5	0.246	b.d.l.	0.405	99.8		32.28	17.19	49.00	1.52	0.00
200	45.3	1.214	7.56	10.81	10.2	23.7	0.261	b.d.l.	0.372	99.4		30.08	18.29	50.21	1.42	0.00
201	46.5	1.081	6.42	10.29	11.1	23.6	0.367	b.d.l.	0.398	99.7		32.06	17.34	49.10	1.50	0.00
202	46.8	0.984	6.02	9.62	11.6	23.6	0.284	b.d.l.	0.277	99.2		33.67	16.10	49.19	1.04	0.00
203	47.7	0.944	5.51	9.55	11.6	23.5	0.263	b.d.l.	0.329	99.4		33.78	15.99	49.00	1.24	0.00
204	47.4	0.860	5.77	9.32	11.6	23.8	0.287	b.d.l.	0.350	99.3		33.59	15.62	49.46	1.32	0.00
205	47.7	0.900	5.71	9.45	11.7	23.9	0.252	b.d.l.	0.342	99.8		33.63	15.69	49.40	1.28	0.00
206	47.4	0.985	5.96	9.50	11.4	23.9	0.282	b.d.l.	0.384	99.8		32.96	15.88	49.72	1.44	0.00
207	47.1	0.956	6.07	9.75	11.4	23.8	0.276	b.d.l.	0.359	99.6		32.86	16.29	49.49	1.35	0.00
208	47.2	1.058	6.16	10.71	10.7	23.5	0.350	b.d.l.	0.471	100.1		31.12	18.05	49.05	1.78	0.00
209	47.2	0.941	6.85	9.63	10.8	23.0	0.289	b.d.l.	0.322	98.9		32.34	16.73	49.67	1.26	0.00
210	45.6	1.278	7.07	11.26	10.1	23.2	0.418	b.d.l.	0.475	99.3		29.68	19.33	49.17	1.82	0.00
212	46.9	1.112	6.35	10.32	11.0	23.5	0.329	b.d.l.	0.467	100.0		31.82	17.36	49.06	1.76	0.00
239	45.0	1.418	7.37	10.96	10.4	23.3	0.303	b.d.l.	0.463	99.3		30.59	18.51	49.14	1.76	0.00
240	44.6	1.352	7.99	10.88	10.2	23.6	0.299	b.d.l.	0.449	99.3		29.92	18.48	49.88	1.72	0.00
241	44.4	1.507	8.27	11.04	10.1	23.4	0.327	b.d.l.	0.381	99.4		29.87	18.90	49.76	1.47	0.00
242	45.7	1.303	7.06	11.25	10.5	23.3	0.321	b.d.l.	0.515	99.8		30.44	18.92	48.70	1.95	0.00
243	45.5	1.336	7.22	11.26	10.0	23.5	0.371	b.d.l.	0.483	99.6		29.41	19.18	49.55	1.85	0.00
244	45.0	1.367	7.56	11.59	9.8	23.3	0.362	b.d.l.	0.528	99.5		28.93	19.77	49.28	2.02	0.00
245	44.7	1.457	8.19	10.91	10.1	23.4	0.237	b.d.l.	0.408	99.4		29.88	18.60	49.95	1.58	0.00
246	45.1	1.431	8.06	10.47	10.2	23.6	0.322	b.d.l.	0.446	99.6		30.28	17.91	50.09	1.72	0.00
247	44.7	1.609	7.89	11.23	10.0	23.1	0.340	b.d.l.	0.435	99.3		29.64	19.29	49.38	1.68	0.00
248	43.1	1.900	9.42	12.57	8.9	23.0	0.363	b.d.l.	0.535	99.7		26.54	21.78	49.59	2.09	0.00
249	42.7	1.810	9.45	12.90	8.5	22.9	0.431	b.d.l.	0.502	99.3		25.79	22.57	49.66	1.97	0.00
250	45.0	1.377	7.75	10.55	10.6	23.2	0.324	b.d.l.	0.370	99.2		31.33	18.00	49.25	1.42	0.00
251	43.6	1.564	9.17	11.59	9.4	23.2	0.295	b.d.l.	0.429	99.2		28.25	20.03	50.04	1.68	0.00
252	44.3	1.710	8.43	11.50	9.6	23.2	0.295	b.d.l.	0.499	99.5		28.63	19.73	49.70	1.94	0.00
253	44.2	1.635	8.19	12.15	9.1	23.0	0.424	b.d.l.	0.534	99.3		27.33	21.12	49.48	2.08	0.00

Tab. A-4: continued

No	SiO_2	TiO_2	Al_2O_3	FeO	MgO	CaO	MnO	Cr_2O_3	Na_2O	Σ		en	fs	wo	ac	tsch
ORC 9701																
5	53.7	0.809	0.71	4.84	17.7	22.2	0.221	0.197	0.242	100.6		48.64	6.62	43.87	0.86	0.00
14	53.7	1.018	0.71	5.70	17.2	21.3	0.185	b.d.l.	0.304	100.2		47.58	8.95	42.38	1.09	0.00
17	54.0	0.586	0.60	4.33	17.7	22.5	b.d.l.	0.516	0.178	100.4		48.83	6.01	44.53	0.64	0.00
20	53.4	0.791	0.73	6.13	17.0	21.1	0.185	0.167	0.229	99.8		47.38	9.54	42.25	0.83	0.00
35	53.0	0.933	0.67	6.19	17.1	21.4	0.242	b.d.l.	0.205	99.8		47.62	8.88	42.77	0.74	0.00
99	53.0	0.824	0.73	5.12	17.7	21.9	b.d.l.	0.178	0.184	99.6		49.23	6.40	43.71	0.66	0.00
100	53.4	0.819	0.62	4.64	17.6	22.2	0.180	0.432	0.142	100.1		48.81	6.33	44.35	0.51	0.00
101	53.5	0.826	0.71	4.52	17.6	22.1	0.177	0.496	0.168	100.1		48.88	6.37	44.14	0.61	0.00
102	53.6	0.647	0.64	3.97	17.6	22.3	b.d.l.	0.766	0.215	99.8		49.05	5.49	44.68	0.78	0.00
103	53.7	0.645	0.68	4.07	18.2	21.6	b.d.l.	0.736	0.194	99.8		50.37	5.85	43.08	0.70	0.00
104	53.8	0.622	0.52	4.25	17.6	22.4	b.d.l.	0.560	0.170	99.9		48.88	5.87	44.64	0.61	0.00
105	54.1	0.660	0.63	4.01	18.2	21.8	0.171	0.632	0.173	100.4		50.16	5.93	43.30	0.62	0.00
106	54.1	0.590	0.57	4.18	17.8	22.0	b.d.l.	0.578	0.156	100.0		49.21	6.54	43.69	0.56	0.00
107	52.0	0.671	0.75	4.46	17.7	22.1	b.d.l.	0.560	0.202	98.4		49.39	5.35	44.52	0.74	0.00
108	53.3	0.831	0.72	4.28	17.6	22.2	b.d.l.	0.541	0.239	99.7		49.12	5.66	44.36	0.87	0.00
109	53.6	1.005	0.83	4.60	17.5	21.8	b.d.l.	0.593	0.245	100.1		48.69	6.92	43.51	0.89	0.00
110	53.8	0.557	0.51	3.40	18.0	22.7	b.d.l.	0.918	0.225	100.2		49.88	4.07	45.24	0.81	0.00
111	54.0	0.585	0.56	3.58	18.0	22.4	b.d.l.	0.776	0.162	100.0		49.69	5.19	44.53	0.58	0.00
112	53.6	0.573	0.55	3.55	18.2	22.2	b.d.l.	0.783	0.235	99.7		50.44	4.29	44.41	0.85	0.00
113	53.9	0.569	0.52	3.97	18.0	22.6	b.d.l.	0.461	0.137	100.1		49.54	5.26	44.71	0.49	0.00
114	54.3	0.517	0.51	3.49	18.4	22.5	b.d.l.	0.747	0.182	100.6		50.41	4.61	44.34	0.65	0.00
115	54.1	0.398	0.46	3.39	18.1	22.5	b.d.l.	0.762	0.211	99.9		50.00	4.61	44.63	0.76	0.00
116	54.4	0.471	0.53	3.60	17.9	22.6	b.d.l.	0.630	0.203	100.3		49.20	5.59	44.49	0.72	0.00
117	54.0	0.562	0.53	3.63	17.9	22.8	b.d.l.	0.517	0.154	100.1		49.44	4.83	45.18	0.55	0.00
AMT 9703 II																
32	52.0	0.420	3.02	4.07	16.8	22.7	b.d.l.	0.250	0.086	99.3		47.51	5.99	46.18	0.32	0.04
33	52.2	0.475	3.00	4.18	17.1	22.8	b.d.l.	b.d.l.	0.133	99.9		47.78	6.05	45.69	0.48	0.04
37	52.8	0.326	2.42	3.63	16.9	23.0	b.d.l.	b.d.l.	0.113	99.1		47.46	5.70	46.43	0.41	0.04
40	52.2	0.472	3.11	3.90	16.6	22.8	b.d.l.	b.d.l.	0.153	99.3		46.94	6.18	46.31	0.56	0.05
51	52.7	0.382	2.78	3.84	17.0	22.9	b.d.l.	0.320	0.148	100.1		47.54	5.71	46.20	0.54	0.04
60	51.3	0.501	3.58	5.36	15.8	23.4	b.d.l.	b.d.l.	0.119	100.0		44.58	7.51	47.47	0.44	0.04
222	52.1	0.528	3.15	4.33	16.8	22.8	b.d.l.	0.208	0.095	100.0		47.30	6.22	46.14	0.35	0.04
223	52.4	0.389	3.00	4.15	17.0	22.8	b.d.l.	b.d.l.	0.132	100.0		47.54	6.16	45.82	0.48	0.04
224	51.7	0.518	3.09	4.40	16.5	22.9	0.149	b.d.l.	0.119	99.4		46.68	6.43	46.45	0.44	0.04
225	52.4	0.360	2.80	4.12	16.8	23.4	b.d.l.	b.d.l.	0.121	99.9		46.79	5.76	47.01	0.44	0.04
226	51.6	0.488	3.29	4.33	16.3	23.3	0.173	b.d.l.	0.157	99.6		45.90	6.19	47.33	0.58	0.04
227	51.3	0.618	4.05	5.09	16.0	23.1	0.116	b.d.l.	0.119	100.4		45.30	7.23	47.03	0.44	0.05
228	50.2	0.750	4.56	5.75	15.3	23.0	0.124	b.d.l.	0.150	99.8		43.88	8.11	47.45	0.56	0.06
229	50.6	0.595	4.21	5.55	15.7	22.9	b.d.l.	b.d.l.	0.123	99.7		44.73	7.81	47.01	0.46	0.05
230	49.6	0.793	5.02	6.35	14.8	22.7	0.174	b.d.l.	0.207	99.7		42.91	8.99	47.31	0.78	0.06
231	48.5	1.030	6.09	7.48	14.0	22.4	0.185	b.d.l.	0.169	99.8		41.10	10.89	47.37	0.64	0.08
232	47.7	0.749	4.78	13.09	9.4	23.2	0.332	b.d.l.	0.438	99.7		28.22	20.16	49.91	1.71	0.06
233	45.2	0.945	7.25	14.54	8.0	23.0	0.548	b.d.l.	0.494	100.0		24.71	22.47	50.85	1.98	0.09
234	44.6	0.937	7.26	14.36	7.9	22.8	0.475	b.d.l.	0.476	98.9		24.56	22.37	51.14	1.93	0.09

Tab. A-4: continued

No	SiO_2	TiO_2	Al_2O_3	FeO	MgO	CaO	MnO	Cr_2O_3	Na_2O	Σ		en	fs	wo	ac	tsch
AMT 9704 A																
38	53.3	0.179	1.67	3.01	17.5	23.2	b.d.l.	0.754	0.136	99.8		48.64	4.68	46.19	0.49	0.00
39	53.5	0.213	1.74	2.94	17.5	23.4	b.d.l.	0.710	0.141	100.2		48.39	4.55	46.55	0.51	0.00
40	53.7	0.264	1.63	3.05	17.3	23.2	b.d.l.	0.650	0.096	99.9		48.26	4.78	46.60	0.35	0.00
41	52.3	0.278	2.67	3.23	16.8	23.1	b.d.l.	0.984	0.210	99.5		47.31	5.12	46.80	0.77	0.00
42	53.7	0.206	1.47	2.87	17.4	23.4	b.d.l.	0.601	0.132	99.8		48.39	4.47	46.66	0.48	0.00
43	52.2	0.289	2.53	3.11	16.7	23.4	b.d.l.	1.012	0.155	99.4		47.11	4.91	47.42	0.57	0.00
44	53.3	0.194	1.64	2.94	17.3	23.1	b.d.l.	0.708	0.110	99.3		48.39	4.62	46.59	0.40	0.00
45	53.5	0.194	1.69	3.01	17.5	23.4	b.d.l.	0.702	0.120	100.2		48.42	4.67	46.48	0.43	0.00
139	53.6	0.276	1.74	2.94	17.7	23.6	b.d.l.	0.763	0.154	100.7		48.56	4.52	46.37	0.55	0.00
140	53.5	0.247	1.74	2.89	17.6	23.4	b.d.l.	0.735	0.111	100.2		48.59	4.48	46.53	0.40	0.00
141	53.7	0.236	1.78	2.87	17.6	23.3	b.d.l.	0.714	0.122	100.4		48.72	4.45	46.39	0.44	0.00
142	53.5	0.250	1.67	2.90	17.5	23.4	b.d.l.	0.713	0.133	100.1		48.52	4.50	46.50	0.48	0.00
143	53.5	0.201	1.67	3.04	17.5	23.1	b.d.l.	0.674	0.155	99.8		48.51	4.74	46.19	0.56	0.00
144	53.4	0.227	1.74	2.95	17.4	23.3	b.d.l.	0.676	0.154	99.8		48.42	4.60	46.43	0.56	0.00
145	53.6	0.254	1.79	2.96	17.5	23.2	b.d.l.	0.650	0.113	100.1		48.66	4.60	46.34	0.41	0.00
146	53.8	0.224	1.70	2.95	17.6	23.1	b.d.l.	0.726	0.117	100.1		48.80	4.60	46.17	0.43	0.00
147	52.3	0.290	2.89	3.02	16.7	23.0	b.d.l.	1.101	0.171	99.5		47.43	4.82	47.11	0.63	0.00
148	52.7	0.319	2.63	3.12	16.8	23.5	b.d.l.	1.038	0.196	100.3		47.12	4.91	47.25	0.71	0.00
149	52.6	0.302	2.69	3.10	16.8	23.3	0.115	1.059	0.177	100.1		47.13	5.07	47.15	0.65	0.00
150	52.4	0.292	2.69	3.09	16.7	23.4	b.d.l.	1.084	0.183	99.8		47.04	4.88	47.41	0.67	0.00
151	52.3	0.354	2.82	3.20	16.7	23.5	b.d.l.	1.023	0.157	100.1		46.92	5.04	47.47	0.57	0.00
152	52.9	0.336	2.61	3.32	16.5	23.5	b.d.l.	0.880	0.131	100.1		46.62	5.26	47.64	0.48	0.00
153	51.7	0.459	4.25	4.28	16.0	22.9	b.d.l.	b.d.l.	0.144	99.7		45.68	6.87	46.91	0.53	0.00
154	52.3	0.456	2.76	4.43	16.5	22.9	b.d.l.	b.d.l.	0.181	99.5		46.28	6.97	46.10	0.66	0.00
155	49.1	0.631	3.97	14.00	10.3	20.7	0.479	b.d.l.	0.239	99.4		30.52	24.20	44.35	0.93	0.00
RAD 9701																
86	54.0	0.373	0.29	20.04	23.2	2.3	0.530	b.d.l.	b.d.l.	100.8		63.84	31.67	4.49	0.00	0.00
88	51.9	0.893	2.49	6.91	17.0	20.3	0.187	0.357	0.207	100.1		47.36	11.16	40.73	0.75	0.00
91	53.2	0.491	1.74	5.63	17.5	20.9	b.d.l.	0.317	0.109	100.0		47.22	11.96	40.44	0.38	0.00
92	51.1	0.669	3.53	4.69	16.5	21.4	b.d.l.	0.966	0.201	99.1		44.87	12.55	41.86	0.71	0.00
93	51.9	0.760	2.97	5.24	16.7	21.7	b.d.l.	0.521	0.135	99.9		45.16	12.02	42.35	0.48	0.00
227	51.1	0.744	3.68	4.89	16.2	21.5	b.d.l.	0.760	0.174	99.0		43.44	14.43	41.52	0.61	0.00
228	51.4	0.627	3.27	4.74	17.0	21.4	b.d.l.	1.014	0.177	99.6		46.47	10.85	42.05	0.63	0.00
229	51.2	0.711	3.85	4.79	16.5	21.1	b.d.l.	1.022	0.162	99.4		44.07	14.83	40.54	0.56	0.00
230	51.1	0.759	3.77	4.66	16.7	21.5	0.162	1.042	0.161	99.7		45.48	11.91	42.04	0.57	0.00
231	50.9	0.663	3.93	4.56	16.5	21.4	b.d.l.	1.123	0.190	99.3		44.64	13.12	41.58	0.67	0.00
232	52.7	0.511	2.41	5.02	17.9	20.5	b.d.l.	0.706	0.126	99.8		48.27	11.66	39.63	0.44	0.00
233	51.9	0.651	3.39	4.86	16.6	21.5	0.163	0.953	0.207	100.3		44.65	13.20	41.43	0.72	0.00
234	51.9	0.658	2.68	5.95	16.8	20.6	b.d.l.	0.857	0.227	99.6		45.98	12.51	40.70	0.81	0.00
235	51.7	0.692	2.52	6.64	16.9	20.3	0.187	0.793	0.212	99.9		47.24	11.21	40.78	0.77	0.00
236	51.3	0.800	2.83	6.42	16.6	20.7	0.167	0.946	0.217	99.9		46.82	10.45	41.93	0.80	0.00
237	50.9	0.964	2.90	7.09	16.0	19.8	0.178	0.951	0.234	99.1		44.88	14.43	39.84	0.85	0.00
238	51.6	0.586	3.54	4.71	16.6	21.6	b.d.l.	0.994	0.190	99.8		44.52	13.27	41.55	0.66	0.00
239	50.9	0.845	4.59	4.98	16.2	21.4	b.d.l.	0.727	0.200	99.8		42.55	16.34	40.43	0.68	0.00
240	51.6	0.604	3.05	6.05	16.2	20.9	b.d.l.	0.827	0.218	99.4		43.97	14.41	40.85	0.77	0.00
241	51.9	0.787	3.45	5.28	16.4	21.5	0.174	0.630	0.151	100.2		43.78	14.60	41.09	0.52	0.00
242	52.1	0.802	3.03	5.51	16.7	21.5	b.d.l.	0.349	0.194	100.1		44.93	12.87	41.53	0.68	0.00
243	52.2	0.672	2.91	5.31	16.8	21.6	b.d.l.	0.456	0.185	100.1		45.11	12.65	41.60	0.65	0.00
244	51.4	0.547	3.73	4.34	17.3	21.2	b.d.l.	0.992	0.190	99.7		46.62	11.50	41.21	0.67	0.00
245	51.5	0.602	4.66	4.33	16.9	20.8	b.d.l.	1.228	0.209	100.1		43.61	17.06	38.62	0.70	0.00
246	52.0	0.652	2.92	5.29	17.1	21.2	b.d.l.	0.657	0.188	100.0		46.64	11.35	41.35	0.66	0.00

Tab. A-4: continued

No	SiO_2	TiO_2	Al_2O_3	FeO	MgO	CaO	MnO	Cr_2O_3	Na_2O	Σ		en	fs	wo	ac	tsch
RAD 9702 A																
61	50.5	0.852	4.08	4.43	16.5	21.4	b.d.l.	1.242	0.210	99.2		47.54	7.18	44.49	0.79	0.00
66	51.0	0.590	4.05	4.12	16.7	21.0	b.d.l.	1.436	0.221	99.0		48.56	6.74	43.86	0.84	0.00
67	50.5	0.649	4.77	4.53	16.8	20.2	b.d.l.	1.255	0.190	98.9		49.19	7.45	42.63	0.72	0.00
68	52.5	0.461	1.95	5.34	17.8	20.2	b.d.l.	0.525	0.111	98.9		50.25	8.45	40.89	0.41	0.00
73	50.9	0.722	3.92	4.84	16.5	21.1	b.d.l.	0.896	0.203	99.0		47.63	7.84	43.77	0.76	0.00
91	51.6	0.608	3.32	4.51	16.5	21.7	b.d.l.	0.977	0.172	99.4		47.41	7.26	44.69	0.64	0.00
247	52.8	b.d.l.	2.01	4.70	19.0	19.5	b.d.l.	0.814	0.191	99.0		52.91	7.34	39.06	0.69	0.00
248	53.0	b.d.l.	2.02	4.49	18.8	19.9	b.d.l.	0.834	0.148	99.2		52.51	7.04	39.91	0.54	0.00
249	51.8	0.494	3.29	4.26	17.6	20.5	b.d.l.	1.236	0.199	99.3		50.30	6.84	42.12	0.74	0.00
250	50.6	0.659	4.46	4.11	16.5	21.2	b.d.l.	1.470	0.246	99.2		48.08	6.70	44.29	0.93	0.00
251	50.6	0.625	4.78	4.19	16.8	21.2	b.d.l.	1.357	0.209	99.6		48.48	6.79	43.94	0.78	0.00
252	51.4	0.483	3.23	3.98	17.4	21.1	b.d.l.	1.258	0.240	99.0		49.55	6.36	43.21	0.89	0.00
253	50.1	0.704	4.71	4.34	16.7	20.8	b.d.l.	1.352	0.208	98.9		48.68	7.10	43.44	0.79	0.00
254	51.6	0.569	3.49	4.17	17.3	20.8	b.d.l.	1.256	0.199	99.3		49.67	6.71	42.87	0.74	0.00
255	51.9	0.470	3.63	4.02	17.3	20.9	b.d.l.	1.286	0.200	99.6		49.67	6.49	43.10	0.75	0.00
256	50.8	0.598	4.10	4.23	16.7	21.1	b.d.l.	1.242	0.193	99.0		48.48	6.88	43.91	0.73	0.00
257	51.4	0.522	3.97	4.27	17.0	21.1	b.d.l.	1.155	0.247	99.6		48.68	6.88	43.52	0.92	0.00
258	51.5	0.683	2.79	6.01	17.0	20.6	b.d.l.	0.577	0.204	99.3		47.95	9.51	41.79	0.75	0.00
259	52.2	0.887	1.91	6.88	16.8	20.3	b.d.l.	b.d.l.	0.182	99.0		47.34	10.89	41.10	0.67	0.00
TA 9701 whole rock																
27	54.0	0.550	1.23	4.65	18.0	20.8	b.d.l.	0.465	0.126	99.8		50.38	7.30	41.86	0.46	0.00
29	53.5	0.625	1.18	3.94	17.3	22.0	b.d.l.	0.660	0.164	99.4		48.70	6.22	44.48	0.60	0.00
30	54.2	0.527	1.18	3.78	17.8	21.7	b.d.l.	0.832	0.163	100.2		49.72	5.94	43.75	0.59	0.00
37	54.2	0.407	0.95	3.25	18.1	22.2	b.d.l.	0.887	0.155	100.1		50.16	5.06	44.23	0.56	0.00
215	54.8	0.398	0.57	4.30	18.2	21.6	b.d.l.	b.d.l.	0.096	99.9		50.15	6.66	42.85	0.34	0.00
216	54.5	0.405	0.73	4.23	18.5	20.7	b.d.l.	0.476	0.094	99.7		51.55	6.61	41.50	0.34	0.00
217	54.2	0.409	0.63	3.67	18.2	21.8	b.d.l.	0.565	0.113	99.6		50.47	5.71	43.41	0.41	0.00
218	54.3	0.455	0.75	4.58	18.2	20.9	b.d.l.	0.458	0.081	99.7		50.80	7.15	41.76	0.29	0.00
219	54.1	0.472	0.97	5.92	18.0	20.0	b.d.l.	b.d.l.	0.099	99.5		50.18	9.28	40.18	0.36	0.00
220	53.6	0.457	1.01	6.59	16.9	21.0	b.d.l.	b.d.l.	0.080	99.7		47.16	10.33	42.22	0.29	0.00
221	53.8	0.515	0.80	5.35	17.6	21.1	b.d.l.	b.d.l.	0.103	99.2		48.91	8.36	42.35	0.37	0.00
TA 9701 peridotitic xenolith																
187	53.8	0.552	0.96	4.33	18.3	21.3	b.d.l.	0.598	0.134	99.9		50.43	6.71	42.38	0.48	0.00
188	53.6	0.422	0.96	3.74	17.9	21.8	b.d.l.	0.799	0.134	99.4		49.86	5.85	43.80	0.48	0.00
189	53.7	0.547	1.17	4.13	17.5	22.0	b.d.l.	0.608	0.131	99.7		48.84	6.47	44.22	0.47	0.00
190	53.3	0.657	1.22	4.19	16.9	22.5	b.d.l.	0.473	0.106	99.3		47.50	6.60	45.51	0.39	0.00
191	54.2	0.451	1.02	4.10	18.2	21.4	b.d.l.	0.575	0.160	100.1		50.39	6.38	42.66	0.58	0.00

Tab. A-5: Chemical composition of orthopyroxenes by EMPA.

No	SiO_2	TiO_2	Al_2O_3	FeO	MgO	CaO	MnO	Cr_2O_3	Σ		en	fs	wo	tsch
AMT 9702														
68	51.4	0.201	0.403	32.05	15.4	1.232	0.705	b.d.l.	101.4		44.38	53.06	2.56	0.00
72	51.2	b.d.l.	0.377	32.08	15.3	1.410	0.665	b.d.l.	101.1		44.16	52.92	2.92	0.00
73	51.1	0.197	0.590	32.88	14.8	1.283	0.769	b.d.l.	101.6		42.74	54.59	2.67	0.00
74	51.7	0.217	0.672	31.52	16.1	1.162	0.712	b.d.l.	102.1		46.00	51.62	2.38	0.00
75	51.2	0.209	0.568	31.87	15.4	1.520	0.740	b.d.l.	101.5		44.23	52.63	3.14	0.00
78	51.5	b.d.l.	0.295	32.52	15.0	1.302	0.737	b.d.l.	101.4		43.36	53.93	2.70	0.00
97	51.3	b.d.l.	0.434	31.74	15.5	1.080	0.913	b.d.l.	100.9		44.77	52.99	2.24	0.00
101	51.2	b.d.l.	0.405	32.70	14.6	1.393	0.801	b.d.l.	101.0		42.43	54.66	2.91	0.00
103	50.9	0.324	1.056	32.42	14.7	1.071	0.783	b.d.l.	101.2		43.11	54.63	2.26	0.02
108	51.4	b.d.l.	0.388	31.79	15.3	1.356	0.753	b.d.l.	100.9		44.24	52.93	2.82	0.00
221	51.2	b.d.l.	0.369	31.77	15.0	1.347	0.701	b.d.l.	100.4		43.84	53.33	2.83	0.01
222	51.5	b.d.l.	0.434	32.20	14.9	1.388	0.780	b.d.l.	101.2		43.36	53.74	2.90	0.01
223	50.8	b.d.l.	0.504	32.92	14.8	1.357	0.785	b.d.l.	101.2		42.68	54.51	2.81	0.00
224	51.2	b.d.l.	0.388	32.12	15.3	1.470	0.792	b.d.l.	101.2		43.85	53.10	3.04	0.00
225	51.4	0.201	0.424	32.21	15.1	1.313	0.802	b.d.l.	101.4		43.73	53.54	2.73	0.00
226	51.1	b.d.l.	0.470	32.55	14.9	1.286	0.759	b.d.l.	101.0		43.08	54.24	2.68	0.00
227	51.1	b.d.l.	0.450	32.57	14.9	1.326	0.734	b.d.l.	101.1		43.18	54.06	2.76	0.00
228	50.8	b.d.l.	0.629	32.80	14.6	1.315	0.826	b.d.l.	101.0		42.42	54.83	2.75	0.00
229	50.9	b.d.l.	0.677	32.82	14.5	1.343	0.835	b.d.l.	101.1		42.23	54.96	2.81	0.01
230	51.6	b.d.l.	0.576	32.12	15.1	1.276	0.827	b.d.l.	101.5		43.84	53.51	2.65	0.01
231	51.3	b.d.l.	0.762	32.42	14.5	1.347	0.780	b.d.l.	101.1		42.48	54.68	2.84	0.02
232	51.4	b.d.l.	0.632	32.81	14.6	1.264	0.782	b.d.l.	101.5		42.53	54.82	2.64	0.01
233	51.4	0.208	0.543	30.98	15.9	1.370	0.750	b.d.l.	101.1		45.85	51.32	2.84	0.00
234	51.5	0.222	0.502	31.11	16.0	1.293	0.672	b.d.l.	101.4		46.09	51.24	2.67	0.00
235	51.5	0.218	0.460	30.97	15.8	1.375	0.746	b.d.l.	101.1		45.70	51.45	2.86	0.00
236	51.5	0.212	0.640	31.26	16.0	1.371	0.708	b.d.l.	101.6		45.74	51.43	2.83	0.00
237	51.3	0.205	0.534	30.88	15.8	1.321	0.679	b.d.l.	100.7		45.77	51.47	2.76	0.01
238	51.6	b.d.l.	0.535	31.15	16.0	1.371	0.705	b.d.l.	101.3		45.83	51.34	2.83	0.00
239	51.4	0.243	0.647	31.13	15.9	1.367	0.694	b.d.l.	101.3		45.71	51.46	2.83	0.01
240	51.7	b.d.l.	0.564	31.05	15.8	1.377	0.646	b.d.l.	101.1		45.68	51.45	2.86	0.01
241	51.6	b.d.l.	0.562	31.20	15.9	1.340	0.701	b.d.l.	101.3		45.78	51.45	2.77	0.01
242	51.8	b.d.l.	0.558	31.42	16.0	1.400	0.721	b.d.l.	101.9		45.67	51.45	2.88	0.00
243	51.1	0.220	0.486	32.02	15.1	1.420	0.679	b.d.l.	101.0		43.85	53.19	2.96	0.00
244	51.3	b.d.l.	0.347	32.39	15.0	1.286	0.714	b.d.l.	101.1		43.52	53.80	2.68	0.00

Tab. A-5: continued

No	SiO_2	TiO_2	Al_2O_3	FeO	MgO	CaO	MnO	Cr_2O_3	Σ		en	fs	wo	tsch
TA 9701 peridotitic xenolith														
2	55.6	b.d.l.	3.710	6.24	33.2	0.909	b.d.l.	0.523	100.1		88.43	9.83	1.74	0.06
3	55.8	b.d.l.	3.610	6.04	33.1	0.862	b.d.l.	0.419	99.8		88.54	9.80	1.66	0.07
153	55.5	b.d.l.	3.690	5.91	32.9	0.882	b.d.l.	0.535	99.4		88.56	9.73	1.71	0.07
154	55.3	b.d.l.	3.630	6.18	33.0	0.922	b.d.l.	0.523	99.6		88.52	9.71	1.77	0.06
155	55.6	b.d.l.	3.560	6.15	33.2	0.925	b.d.l.	0.528	99.9		88.61	9.62	1.78	0.06
156	55.7	b.d.l.	3.730	6.06	33.1	0.878	b.d.l.	0.531	99.9		88.49	9.83	1.69	0.07
157	55.4	b.d.l.	3.730	6.02	32.8	0.851	b.d.l.	0.569	99.4		88.47	9.88	1.65	0.07
158	56.1	b.d.l.	3.720	6.05	33.2	0.871	b.d.l.	0.573	100.6		88.60	9.74	1.67	0.07
159	55.7	b.d.l.	3.650	6.15	33.0	0.914	b.d.l.	0.520	99.9		88.35	9.89	1.76	0.07
160	55.5	b.d.l.	3.710	6.20	33.1	0.931	b.d.l.	0.535	100.0		88.63	9.58	1.79	0.06
161	55.4	b.d.l.	3.700	6.09	33.0	0.859	b.d.l.	0.529	99.5		88.60	9.74	1.66	0.07
162	55.8	b.d.l.	3.650	6.04	32.9	0.909	b.d.l.	0.531	99.8		88.36	9.89	1.75	0.07
163	55.3	b.d.l.	3.670	5.92	33.2	0.906	b.d.l.	0.579	99.5		89.04	9.22	1.75	0.06
164	55.8	b.d.l.	3.710	6.21	33.0	0.939	b.d.l.	0.547	100.2		88.23	9.97	1.80	0.07
165	55.6	b.d.l.	3.660	5.95	32.8	0.829	b.d.l.	0.504	99.4		88.55	9.84	1.61	0.07
166	55.6	b.d.l.	3.590	6.11	32.9	0.863	b.d.l.	0.541	99.6		88.38	9.95	1.67	0.07
167	55.6	b.d.l.	3.600	6.03	33.1	0.860	b.d.l.	0.513	99.7		88.68	9.67	1.66	0.07
168	55.6	b.d.l.	3.590	6.08	32.8	0.864	b.d.l.	0.549	99.4		88.28	10.05	1.67	0.07
169	55.3	b.d.l.	3.740	6.07	32.8	0.884	b.d.l.	0.508	99.3		88.44	9.84	1.72	0.07
170	55.7	b.d.l.	3.700	6.01	33.1	0.880	b.d.l.	0.541	99.9		88.56	9.74	1.70	0.07
171	55.6	b.d.l.	3.640	6.20	33.2	0.872	b.d.l.	0.539	100.0		88.59	9.74	1.67	0.06
172	56.3	b.d.l.	3.740	6.03	32.9	0.873	b.d.l.	0.510	100.3		88.06	10.26	1.68	0.07
173	55.8	b.d.l.	3.740	6.13	33.2	0.873	b.d.l.	0.531	100.3		88.55	9.78	1.67	0.07
174	55.7	b.d.l.	3.610	6.16	32.9	0.881	b.d.l.	0.469	99.7		88.32	9.97	1.70	0.07
175	55.8	b.d.l.	3.720	6.04	32.8	0.885	b.d.l.	0.449	99.8		88.27	10.02	1.71	0.08
176	55.8	b.d.l.	3.770	5.95	32.8	0.868	b.d.l.	0.482	99.7		88.40	9.92	1.68	0.08
177	55.8	b.d.l.	3.690	5.93	32.8	0.832	b.d.l.	0.494	99.6		88.38	10.01	1.61	0.07

Tab. A-6: Chemical composition of K-feldspars by EMPA.

No	SiO_2	TiO_2	Al_2O_3	FeO	CaO	BaO	Na_2O	K_2O	Σ		or	ab	an	cel
ROC 9701														
170	65.9	b.d.l.	18.7	b.d.l.	0.174	b.d.l.	3.22	11.61	99.6		69.76	29.36	0.88	0.00
171	65.6	b.d.l.	18.7	b.d.l.	0.167	b.d.l.	3.23	11.50	99.1		69.50	29.66	0.85	0.00
172	65.9	b.d.l.	18.8	b.d.l.	0.190	b.d.l.	3.29	11.62	99.8		69.23	29.83	0.95	0.00
173	66.0	b.d.l.	18.6	b.d.l.	0.179	b.d.l.	3.16	11.68	99.6		70.26	28.84	0.90	0.00
174	65.9	b.d.l.	18.7	b.d.l.	0.155	b.d.l.	3.57	11.08	99.4		66.59	32.62	0.78	0.00
247	65.6	b.d.l.	18.5	b.d.l.	0.215	b.d.l.	3.17	11.20	98.6		69.15	29.74	1.11	0.00
248	65.5	b.d.l.	18.6	b.d.l.	0.154	b.d.l.	3.11	11.18	98.5		69.75	29.45	0.81	0.00
249	65.8	b.d.l.	18.4	b.d.l.	0.165	b.d.l.	3.36	11.31	99.0		68.36	30.80	0.84	0.00
250	65.7	b.d.l.	18.6	b.d.l.	0.199	b.d.l.	3.21	11.23	99.0		69.00	29.97	1.02	0.00
251	65.9	b.d.l.	18.6	b.d.l.	0.215	b.d.l.	3.36	11.03	99.1		67.61	31.28	1.10	0.00
252	65.9	b.d.l.	18.6	b.d.l.	0.196	b.d.l.	3.38	11.17	99.3		67.83	31.17	1.00	0.00
253	65.8	b.d.l.	18.6	b.d.l.	0.178	b.d.l.	3.12	11.25	98.9		69.70	29.38	0.92	0.00
254	66.2	b.d.l.	18.7	b.d.l.	0.197	b.d.l.	3.24	11.14	99.5		68.61	30.37	1.02	0.00
255	65.8	b.d.l.	18.6	b.d.l.	0.202	b.d.l.	3.13	11.44	99.1		69.92	29.04	1.04	0.00
256	65.7	b.d.l.	18.7	b.d.l.	0.181	b.d.l.	3.21	11.32	99.2		69.23	29.84	0.93	0.00
257	65.9	b.d.l.	18.6	b.d.l.	0.199	b.d.l.	3.15	11.41	99.3		69.72	29.26	1.02	0.00
258	65.9	b.d.l.	18.7	b.d.l.	0.159	b.d.l.	3.16	11.43	99.3		69.82	29.37	0.81	0.00
259	66.2	b.d.l.	18.6	b.d.l.	0.135	b.d.l.	3.14	11.43	99.5		70.03	29.28	0.69	0.00
260	66.0	b.d.l.	18.6	b.d.l.	0.106	b.d.l.	3.14	11.52	99.3		70.30	29.16	0.54	0.00
261	65.7	b.d.l.	18.7	b.d.l.	0.140	b.d.l.	3.24	11.59	99.4		69.70	29.60	0.71	0.00
262	65.6	b.d.l.	18.5	b.d.l.	0.136	b.d.l.	3.16	11.37	98.8		69.79	29.51	0.70	0.00
263	66.0	b.d.l.	18.6	b.d.l.	0.155	b.d.l.	3.16	11.26	99.2		69.55	29.64	0.81	0.00
264	66.0	b.d.l.	18.7	b.d.l.	0.175	b.d.l.	3.15	11.40	99.4		69.81	29.29	0.90	0.00
265	65.9	b.d.l.	18.6	b.d.l.	0.190	b.d.l.	3.14	11.31	99.2		69.63	29.39	0.98	0.00
266	66.5	b.d.l.	18.8	b.d.l.	0.164	b.d.l.	3.12	11.38	99.9		70.00	29.16	0.85	0.00
267	65.9	b.d.l.	18.3	b.d.l.	0.174	b.d.l.	3.17	11.31	98.9		69.47	29.63	0.90	0.00
SVC 9702														
98	64.2	b.d.l.	18.6	b.d.l.	0.189	0.35	2.88	12.44	98.7		72.82	25.61	0.93	0.63
104	64.7	b.d.l.	18.4	b.d.l.	0.164	0.40	2.59	12.82	99.0		75.37	23.11	0.81	0.72
113	64.8	b.d.l.	18.5	b.d.l.	0.156	0.32	2.66	12.68	99.0		74.78	23.87	0.77	0.58
121	64.6	b.d.l.	18.7	b.d.l.	0.192	b.d.l.	2.88	12.34	98.7		73.12	25.93	0.96	0.00
126	65.1	b.d.l.	18.5	b.d.l.	0.148	0.37	2.64	12.60	99.4		74.80	23.79	0.73	0.68
131	65.1	b.d.l.	18.6	b.d.l.	0.146	b.d.l.	2.57	12.76	99.1		75.98	23.29	0.73	0.00
267	65.1	b.d.l.	18.6	b.d.l.	0.151	b.d.l.	2.47	13.03	99.4		77.03	22.22	0.75	0.00
268	65.1	b.d.l.	18.6	b.d.l.	0.155	b.d.l.	2.57	12.79	99.2		76.04	23.19	0.77	0.00
269	64.8	b.d.l.	18.7	b.d.l.	0.134	0.32	2.69	12.72	99.3		74.75	24.01	0.66	0.58
270	65.0	b.d.l.	18.8	b.d.l.	0.190	0.43	2.77	12.43	99.6		73.39	24.89	0.94	0.78
271	65.1	b.d.l.	18.7	b.d.l.	0.216	0.35	3.03	12.04	99.5		71.12	27.18	1.07	0.63
SVC 9703														
44	74.0	b.d.l.	16.2	1.023	0.521	b.d.l.	2.27	5.46	99.4		58.36	36.95	4.68	0.00
47	74.1	b.d.l.	15.9	0.964	0.483	b.d.l.	2.35	5.40	99.2		57.56	38.11	4.33	0.00
54	73.8	b.d.l.	13.1	0.972	0.479	b.d.l.	2.53	5.17	96.1		54.84	40.88	4.27	0.00
57	74.3	b.d.l.	16.1	1.123	0.466	b.d.l.	2.18	5.61	99.8		60.28	35.52	4.20	0.00
59	73.9	b.d.l.	16.1	0.969	0.484	b.d.l.	1.96	5.19	98.6		60.54	34.71	4.75	0.00
61	74.1	b.d.l.	15.3	0.989	0.479	b.d.l.	2.50	5.07	98.4		54.73	40.92	4.34	0.00
63	73.9	b.d.l.	16.3	0.999	0.496	b.d.l.	2.46	5.62	99.7		57.53	38.21	4.26	0.00

No	SiO_2	TiO_2	Al_2O_3	FeO	CaO	BaO	Na_2O	K_2O	Σ		or	ab	an	cel
VUL 9701														
67	60.9	0.155	20.6	0.234	0.631	4.60	3.20	9.58	99.9		58.47	29.66	3.23	8.63
92	62.3	b.d.l.	20.2	0.244	0.709	2.66	3.75	9.39	99.3		56.94	34.52	3.61	4.94
280	60.1	0.155	21.3	0.305	1.014	4.57	3.31	8.77	99.5		54.63	31.32	5.30	8.75
281	60.1	0.148	21.0	0.244	0.992	4.53	3.42	8.95	99.5		54.67	31.74	5.09	8.50
282	60.1	0.187	20.9	0.301	0.887	4.56	3.06	9.18	99.1		57.45	29.14	4.66	8.75
283	60.3	0.159	20.7	0.277	0.803	4.66	3.14	9.24	99.2		57.30	29.64	4.18	8.88
284	60.4	0.165	20.7	0.287	0.796	4.86	3.00	9.32	99.5		58.12	28.40	4.17	9.32
285	60.5	0.189	20.9	0.292	0.787	4.57	3.05	9.69	100.1		59.14	28.26	4.04	8.56
286	60.8	0.148	20.6	0.286	0.706	4.52	3.17	9.48	99.8		58.24	29.61	3.64	8.50
287	61.8	0.154	20.3	0.276	0.666	3.33	3.30	9.75	99.5		59.59	30.72	3.42	6.26
288	61.3	b.d.l.	20.5	0.275	0.879	2.97	3.36	9.44	98.7		58.26	31.55	4.56	5.64
289	61.3	0.152	20.1	0.252	0.700	3.24	3.50	9.47	98.7		57.83	32.51	3.59	6.07
290	61.6	b.d.l.	20.3	0.191	0.672	3.28	3.72	9.21	98.9		56.04	34.42	3.43	6.11
291	62.2	b.d.l.	20.4	0.227	0.930	2.80	4.47	8.07	99.1		48.88	41.17	4.73	5.22
292	62.2	0.154	20.3	0.244	0.930	2.86	4.44	8.15	99.3		49.19	40.79	4.71	5.30
VUL 9703 B														
13	64.0	0.270	19.5	0.681	1.560	b.d.l.	3.70	10.25	100.0		59.67	32.73	7.60	0.00
VUL 9705														
4	57.3	b.d.l.	22.4	0.351	b.d.l.	b.d.l.	3.34	15.99	99.4		75.91	24.09	0.00	0.00
ORC 9701														
2	65.3	0.238	17.9	0.583	b.d.l.	0.20	2.18	13.03	99.4		79.43	20.19	0.00	0.38
3	64.6	0.336	18.1	0.572	b.d.l.	0.75	2.10	13.02	99.4		79.19	19.42	0.00	1.39
16	64.8	0.347	18.1	0.487	b.d.l.	b.d.l.	2.54	12.66	98.9		76.59	23.41	0.00	0.00
19	64.8	0.373	17.3	0.828	b.d.l.	0.19	2.12	12.83	98.4		79.61	20.02	0.00	0.37
29	66.2	0.159	17.0	0.949	b.d.l.	b.d.l.	2.23	12.45	99.0		78.62	21.38	0.00	0.00
30	64.8	0.356	17.9	0.554	b.d.l.	b.d.l.	2.47	12.69	98.8		77.20	22.80	0.00	0.00
34	64.7	0.383	18.0	0.511	b.d.l.	0.77	2.33	12.64	99.3		77.03	21.54	0.00	1.44
37	65.0	0.326	18.0	0.537	b.d.l.	b.d.l.	2.48	12.57	98.8		76.95	23.05	0.00	0.00
38	65.5	0.267	17.9	0.483	b.d.l.	b.d.l.	2.38	12.94	99.5		78.16	21.84	0.00	0.00
45	65.9	0.311	17.5	0.535	b.d.l.	b.d.l.	2.45	12.40	99.1		76.90	23.10	0.00	0.00
ROC 9701														
48	65.9	b.d.l.	18.6	b.d.l.	0.160	b.d.l.	3.13	11.64	99.4		70.42	28.76	0.81	0.00
49	65.8	b.d.l.	18.3	b.d.l.	0.143	b.d.l.	3.16	11.37	98.7		69.77	29.49	0.74	0.00
58	65.2	b.d.l.	18.6	b.d.l.	0.150	b.d.l.	3.22	11.56	98.7		69.70	29.54	0.76	0.00
60	65.5	b.d.l.	18.4	b.d.l.	0.156	b.d.l.	3.16	11.50	98.7		69.97	29.24	0.80	0.00
66	65.6	b.d.l.	18.5	b.d.l.	0.169	b.d.l.	3.25	11.54	99.0		69.44	29.71	0.85	0.00
67	65.3	b.d.l.	18.5	b.d.l.	0.179	b.d.l.	3.25	11.66	98.9		69.59	29.51	0.90	0.00
68	65.6	b.d.l.	18.5	b.d.l.	0.187	b.d.l.	3.23	11.58	99.1		69.57	29.49	0.94	0.00
71	65.1	b.d.l.	18.4	b.d.l.	0.159	b.d.l.	3.26	11.50	98.4		69.33	29.87	0.81	0.00
72	65.3	b.d.l.	18.7	b.d.l.	0.187	0.35	3.16	11.40	99.1		69.26	29.13	0.95	0.65
73	65.5	b.d.l.	18.8	b.d.l.	0.164	b.d.l.	3.14	11.65	99.2		70.38	28.79	0.84	0.00
165	67.1	b.d.l.	18.3	b.d.l.	0.162	b.d.l.	4.56	9.13	99.3		56.39	42.77	0.84	0.00
166	66.1	b.d.l.	18.7	b.d.l.	0.138	b.d.l.	3.11	11.48	99.5		70.35	28.94	0.71	0.00
167	65.7	b.d.l.	18.7	b.d.l.	0.191	b.d.l.	3.22	11.34	99.2		69.16	29.87	0.98	0.00
168	65.3	b.d.l.	18.6	b.d.l.	0.208	b.d.l.	3.26	11.51	98.9		69.16	29.79	1.05	0.00
169	65.6	b.d.l.	18.6	b.d.l.	0.171	b.d.l.	3.11	11.41	98.8		70.06	29.06	0.89	0.00

A-6: continued

No	SiO_2	TiO_2	Al_2O_3	FeO	CaO	BaO	Na_2O	K_2O	Σ		or	ab	an	cel
AMT 9702														
64	65.0	b.d.l.	18.5	b.d.l.	0.318	b.d.l.	2.11	13.38	99.4		79.37	19.05	1.58	0.00
69	63.9	b.d.l.	20.0	0.479	2.090	0.32	2.82	10.39	100.0		62.91	25.89	10.61	0.59
82	65.7	b.d.l.	18.5	b.d.l.	0.268	b.d.l.	2.08	13.36	100.0		79.76	18.90	1.34	0.00
92	66.3	b.d.l.	18.4	b.d.l.	0.204	b.d.l.	2.02	13.45	100.3		80.57	18.41	1.03	0.00
200	65.6	b.d.l.	18.7	b.d.l.	0.253	0.32	1.96	13.31	100.0		80.20	17.94	1.28	0.58
201	65.1	b.d.l.	18.7	b.d.l.	0.288	0.38	2.01	13.23	99.7		79.51	18.34	1.45	0.70
202	65.5	b.d.l.	18.6	b.d.l.	0.348	0.31	2.04	13.37	100.1		79.34	18.36	1.73	0.57
203	65.5	b.d.l.	18.6	b.d.l.	0.320	0.30	2.11	13.35	100.1		78.89	18.98	1.59	0.54
204	65.5	b.d.l.	18.8	b.d.l.	0.316	b.d.l.	2.04	13.29	99.9		79.79	18.62	1.59	0.00
205	65.1	b.d.l.	18.7	b.d.l.	0.324	0.35	1.99	13.44	99.9		79.78	17.97	1.61	0.64
206	64.9	b.d.l.	18.5	b.d.l.	0.295	b.d.l.	2.03	13.34	99.1		79.99	18.53	1.49	0.00
207	65.7	b.d.l.	18.5	b.d.l.	0.301	b.d.l.	2.08	13.37	100.0		79.68	18.82	1.50	0.00
208	65.2	b.d.l.	18.5	b.d.l.	0.309	0.33	2.07	13.45	99.8		79.34	18.54	1.53	0.59
209	65.7	b.d.l.	18.9	b.d.l.	0.234	b.d.l.	2.00	13.35	100.1		80.49	18.32	1.19	0.00
210	65.1	b.d.l.	18.4	b.d.l.	0.308	b.d.l.	1.94	13.54	99.2		80.84	17.62	1.54	0.00
211	65.5	b.d.l.	18.5	b.d.l.	0.278	0.30	2.04	13.49	100.1		79.75	18.33	1.38	0.54
212	65.6	b.d.l.	18.4	b.d.l.	0.289	b.d.l.	1.89	13.44	99.6		81.21	17.33	1.46	0.00
213	65.5	b.d.l.	18.5	b.d.l.	0.239	b.d.l.	1.99	13.32	99.5		80.47	18.32	1.22	0.00
214	65.6	b.d.l.	18.4	b.d.l.	0.211	b.d.l.	1.91	13.38	99.5		81.25	17.67	1.08	0.00
215	65.4	b.d.l.	18.5	b.d.l.	0.260	b.d.l.	1.96	13.55	99.6		80.92	17.78	1.30	0.00
216	65.7	b.d.l.	18.5	b.d.l.	0.258	b.d.l.	2.02	13.50	100.0		80.39	18.32	1.29	0.00
217	66.0	b.d.l.	18.5	b.d.l.	0.218	b.d.l.	1.99	13.55	100.2		80.83	18.08	1.10	0.00
218	65.7	b.d.l.	18.5	b.d.l.	0.273	b.d.l.	2.09	13.45	100.0		79.78	18.86	1.36	0.00
219	65.6	b.d.l.	18.4	b.d.l.	0.277	b.d.l.	2.00	13.39	99.7		80.34	18.27	1.39	0.00
220	65.5	b.d.l.	18.5	b.d.l.	0.222	b.d.l.	1.99	13.45	99.7		80.74	18.15	1.12	0.00
AMT 9703 II														
34	64.0	b.d.l.	19.4	0.219	0.875	b.d.l.	1.86	13.33	99.6		78.92	16.72	4.35	0.00
42	64.6	b.d.l.	19.0	0.432	0.512	b.d.l.	1.84	13.88	100.2		81.17	16.31	2.51	0.00
47	64.7	b.d.l.	19.2	b.d.l.	0.429	b.d.l.	1.73	13.76	99.8		82.17	15.68	2.15	0.00
58	64.2	b.d.l.	18.8	0.196	0.364	0.20	1.62	14.03	99.4		83.19	14.63	1.81	0.37
AMT 9704 A														
36	64.4	b.d.l.	19.0	b.d.l.	0.412	0.83	1.87	13.29	99.8		79.39	17.03	2.07	1.52
186	63.8	b.d.l.	19.6	0.183	1.081	0.51	2.66	11.88	99.7		69.93	23.80	5.35	0.92
187	64.8	b.d.l.	18.8	0.196	0.556	b.d.l.	2.47	12.36	99.2		74.57	22.62	2.81	0.00
188	65.5	b.d.l.	18.5	b.d.l.	0.364	b.d.l.	2.40	13.12	99.9		76.86	21.35	1.79	0.00
189	65.4	b.d.l.	18.8	0.174	0.445	b.d.l.	2.39	13.05	100.2		76.55	21.26	2.19	0.00
190	65.7	b.d.l.	19.0	b.d.l.	0.426	b.d.l.	2.33	12.88	100.3		76.76	21.11	2.13	0.00
191	64.5	b.d.l.	18.9	b.d.l.	0.348	0.72	1.97	13.13	99.6		78.90	18.02	1.76	1.33
RAD 9701														
89	64.5	0.224	18.0	1.151	0.533	0.26	2.77	10.75	98.2		69.44	27.15	2.89	0.51
TA 9701 whole rock														
51	63.7	b.d.l.	19.4	0.319	1.387	b.d.l.	1.44	13.61	99.9		80.21	12.92	6.87	0.00
52	64.3	0.329	19.1	0.323	0.850	b.d.l.	1.42	13.74	100.1		82.71	13.00	4.30	0.00

Tab. A-7: Chemical composition of plagioclases by EMPA.

No	SiO_2	Al_2O_3	FeO	CaO	BaO	Na_2O	K_2O	Σ		or	ab	an	cel
Montefiascone													
29	47.0	31.6	0.462	1.24	b.d.l.	15.76	3.730	99.8		12.98	83.39	3.63	0.00
34	55.5	26.8	0.670	9.30	0.483	5.86	0.629	99.3		3.60	50.94	44.62	0.85
36	48.1	31.4	0.793	15.13	b.d.l.	2.65	0.176	98.3		1.04	23.80	75.16	0.00
37	52.9	28.5	0.566	10.94	b.d.l.	4.48	0.444	98.2		2.70	41.38	55.91	0.00
38	48.2	31.7	0.856	15.49	b.d.l.	2.46	0.086	98.9		0.51	22.22	77.27	0.00
42	47.6	32.6	1.198	16.17	b.d.l.	1.98	0.102	99.7		0.61	18.05	81.33	0.00
50	48.5	31.7	0.890	15.17	b.d.l.	2.47	0.156	99.0		0.93	22.56	76.51	0.00
51	55.1	27.3	0.657	9.24	0.419	5.68	0.617	99.0		3.60	50.36	45.29	0.75
52	48.9	31.0	0.840	14.78	b.d.l.	2.86	0.210	98.8		1.24	25.64	73.12	0.00
VUL 9701													
83	47.9	31.9	1.450	15.12	b.d.l.	2.52	0.164	99.0		0.98	22.92	76.09	0.00
101	48.3	31.6	0.680	14.84	b.d.l.	2.77	0.198	98.4		1.17	24.96	73.87	0.00
105	47.3	32.5	0.724	15.82	b.d.l.	2.11	0.094	98.5		0.56	19.36	80.08	0.00
VUL 9702													
8	44.6	34.0	0.718	18.22	b.d.l.	0.78	0.176	98.6		1.06	7.14	91.81	0.00
13	47.0	32.5	0.925	16.59	b.d.l.	1.96	0.149	99.2		0.87	17.43	81.69	0.00
16	44.4	34.5	0.654	18.70	b.d.l.	0.68	0.173	99.1		1.02	6.14	92.84	0.00
34	47.6	32.1	0.856	15.70	b.d.l.	1.99	0.355	98.6		2.14	18.28	79.58	0.00
124	44.3	34.6	0.617	18.89	b.d.l.	0.54	0.148	99.1		0.88	4.90	94.22	0.00
125	43.9	35.1	0.600	18.84	b.d.l.	0.51	0.155	99.0		0.92	4.60	94.48	0.00
126	44.0	34.6	0.616	18.89	b.d.l.	0.42	0.126	98.6		0.76	3.84	95.40	0.00
127	43.9	34.8	0.660	19.03	b.d.l.	0.50	0.135	99.1		0.80	4.51	94.69	0.00
128	44.0	35.2	0.630	19.08	b.d.l.	0.45	0.129	99.5		0.77	4.09	95.14	0.00
129	43.8	34.9	0.574	19.06	b.d.l.	0.47	0.089	98.9		0.53	4.27	95.21	0.00
130	44.0	35.1	0.594	19.12	b.d.l.	0.48	0.115	99.3		0.68	4.30	95.02	0.00
131	44.1	34.9	0.603	19.01	b.d.l.	0.47	0.271	99.7		1.60	4.18	94.22	0.00
132	44.0	35.2	0.603	19.06	b.d.l.	0.45	0.134	99.5		0.80	4.08	95.13	0.00
133	44.1	35.0	0.628	18.92	b.d.l.	0.43	0.111	99.2		0.67	3.92	95.42	0.00
134	44.2	34.7	0.591	19.06	b.d.l.	0.47	0.123	99.2		0.73	4.22	95.05	0.00
135	44.0	34.9	0.628	18.94	b.d.l.	0.45	0.137	99.1		0.81	4.12	95.07	0.00
136	43.7	34.9	0.653	19.05	b.d.l.	0.46	0.119	99.0		0.71	4.17	95.13	0.00
137	44.0	34.9	0.647	19.09	b.d.l.	0.47	0.092	99.1		0.55	4.26	95.19	0.00
138	46.7	33.0	0.905	16.83	b.d.l.	1.51	0.213	99.3		1.28	13.80	84.92	0.00
VUL 9703 B													
3	55.6	27.5	0.495	10.33	b.d.l.	5.22	0.736	99.8		4.24	45.75	50.01	0.00
25	46.8	32.5	0.609	16.97	b.d.l.	1.62	0.308	99.0		1.81	14.50	83.70	0.00
150	55.4	27.3	0.502	10.57	b.d.l.	5.25	0.596	99.6		3.41	45.72	50.87	0.00
151	54.7	27.8	0.539	11.17	b.d.l.	4.82	0.545	99.5		3.16	42.44	54.40	0.00
152	55.6	27.3	0.528	10.70	b.d.l.	5.28	0.644	100.0		3.65	45.43	50.92	0.00
153	55.5	27.4	0.494	10.80	b.d.l.	5.18	0.622	100.0		3.54	44.82	51.64	0.00
154	56.0	27.1	0.519	10.27	b.d.l.	5.44	0.806	100.2		4.55	46.72	48.72	0.00
155	56.6	26.3	0.517	9.32	b.d.l.	4.92	2.030	99.7		11.69	43.16	45.15	0.00

Tab. A-7: continued

No	SiO_2	Al_2O_3	FeO	CaO	BaO	Na_2O	K_2O	Σ		or	ab	an	cel
VUL 9707													
92	48.3	31.5	0.719	14.46	b.d.l.	2.51	0.385	97.9		2.35	23.33	74.31	0.00
232	47.4	32.4	0.667	15.80	b.d.l.	2.01	0.216	98.5		1.31	18.46	80.23	0.00
233	48.1	31.9	0.731	15.01	b.d.l.	2.42	0.243	98.4		1.47	22.22	76.31	0.00
234	48.0	32.1	0.644	14.87	b.d.l.	2.47	0.148	98.3		0.90	22.93	76.17	0.00
235	46.6	32.6	0.802	16.00	b.d.l.	1.86	0.141	98.0		0.86	17.20	81.93	0.00
236	47.2	32.5	0.775	15.41	b.d.l.	2.09	0.123	98.0		0.76	19.57	79.68	0.00
237	47.2	32.4	0.709	15.37	b.d.l.	2.22	0.116	98.0		0.71	20.55	78.74	0.00
238	46.9	32.5	0.740	15.87	b.d.l.	1.98	0.129	98.1		0.78	18.30	80.92	0.00
ROC 9701													
52	61.7	23.5	b.d.l.	5.32	b.d.l.	7.71	1.084	99.3		6.27	67.86	25.87	0.00
55	60.1	24.3	b.d.l.	6.37	b.d.l.	7.55	0.753	99.0		4.28	65.28	30.44	0.00
62	60.0	24.4	b.d.l.	6.57	b.d.l.	7.34	0.812	99.1		4.64	63.78	31.58	0.00
74	57.8	26.2	b.d.l.	8.17	b.d.l.	6.57	0.540	99.3		3.11	57.43	39.46	0.00
268	60.7	24.6	b.d.l.	6.22	b.d.l.	7.43	0.728	99.7		4.22	65.52	30.26	0.00
269	59.8	24.9	b.d.l.	6.87	b.d.l.	7.17	0.632	99.3		3.65	63.00	33.35	0.00
270	59.9	25.0	b.d.l.	6.72	b.d.l.	7.27	0.609	99.5		3.52	63.87	32.61	0.00
271	60.9	24.6	b.d.l.	6.22	b.d.l.	7.38	0.669	99.7		3.91	65.54	30.54	0.00
272	60.0	24.6	b.d.l.	6.55	b.d.l.	7.31	0.675	99.2		3.90	64.25	31.84	0.00
273	59.6	24.8	b.d.l.	6.95	b.d.l.	7.21	0.630	99.2		3.62	62.87	33.52	0.00
274	60.2	24.9	b.d.l.	6.47	b.d.l.	7.30	0.716	99.7		4.15	64.31	31.54	0.00
275	60.7	24.3	b.d.l.	6.34	b.d.l.	7.49	0.688	99.6		3.96	65.42	30.62	0.00
276	61.8	23.7	b.d.l.	5.34	b.d.l.	7.77	0.904	99.5		5.26	68.67	26.07	0.00
277	61.0	24.5	b.d.l.	6.10	b.d.l.	7.50	0.751	99.8		4.35	66.01	29.64	0.00
278	60.7	24.3	b.d.l.	6.23	b.d.l.	7.45	0.702	99.4		4.06	65.58	30.35	0.00
279	60.5	24.2	b.d.l.	6.11	b.d.l.	7.49	0.724	99.1		4.20	66.03	29.77	0.00
280	60.7	24.4	b.d.l.	6.28	b.d.l.	7.72	0.754	99.8		4.25	66.09	29.66	0.00
281	60.6	24.6	b.d.l.	6.20	b.d.l.	7.65	0.732	99.7		4.17	66.16	29.67	0.00
282	60.7	24.4	b.d.l.	6.11	b.d.l.	7.46	0.710	99.3		4.13	66.00	29.87	0.00
283	60.9	24.4	b.d.l.	6.02	b.d.l.	7.52	0.689	99.4		4.01	66.56	29.43	0.00
284	61.3	24.1	b.d.l.	5.96	b.d.l.	7.74	0.727	99.7		4.16	67.23	28.62	0.00
285	60.8	24.1	b.d.l.	5.83	b.d.l.	7.57	0.702	99.0		4.10	67.27	28.63	0.00
286	63.2	22.9	b.d.l.	4.42	b.d.l.	8.18	0.937	99.7		5.48	72.80	21.72	0.00
294	61.2	24.2	b.d.l.	6.02	b.d.l.	6.94	0.707	99.1		4.34	64.66	31.00	0.00
295	62.8	22.9	b.d.l.	4.57	b.d.l.	8.15	0.998	99.4		5.79	71.94	22.27	0.00
SVC 9702													
110	57.0	26.7	b.d.l.	8.70	b.d.l.	6.15	0.444	99.0		2.60	54.65	42.75	0.00
112	59.6	24.7	b.d.l.	6.69	b.d.l.	7.24	0.825	99.0		4.73	63.08	32.19	0.00
116	58.4	25.4	b.d.l.	7.59	b.d.l.	6.47	0.899	98.7		5.26	57.49	37.25	0.00
124	59.3	25.2	b.d.l.	7.35	b.d.l.	6.59	0.937	99.3		5.47	58.51	36.03	0.00
133	57.8	25.8	b.d.l.	8.06	b.d.l.	6.53	0.648	98.8		3.74	57.22	39.04	0.00
137	60.2	24.4	b.d.l.	6.30	b.d.l.	7.49	0.851	99.3		4.86	64.97	30.17	0.00
141	58.8	25.2	b.d.l.	7.22	b.d.l.	7.08	0.730	99.1		4.16	61.31	34.53	0.00
272	52.8	29.5	b.d.l.	12.15	b.d.l.	4.47	0.297	99.2		1.72	39.25	59.03	0.00
273	53.0	28.9	b.d.l.	11.55	b.d.l.	4.64	0.313	98.4		1.84	41.32	56.84	0.00
274	53.5	29.0	b.d.l.	11.42	b.d.l.	4.56	0.279	98.8		1.66	41.26	57.08	0.00
275	53.1	29.3	b.d.l.	11.82	b.d.l.	4.67	0.274	99.2		1.58	41.02	57.40	0.00
276	53.9	28.5	b.d.l.	10.89	b.d.l.	5.02	0.312	98.6		1.82	44.63	53.54	0.00
277	55.3	27.5	b.d.l.	9.78	b.d.l.	5.79	0.454	98.8		2.60	50.41	46.99	0.00

Tab. A-7: continued

No	SiO_2	Al_2O_3	FeO	CaO	BaO	Na_2O	K_2O	Σ		or	ab	an	cel
SVC 9702													
278	54.9	27.7	b.d.l.	9.99	b.d.l.	5.63	0.432	98.7		2.49	49.25	48.26	0.00
279	55.4	27.4	b.d.l.	9.60	b.d.l.	5.86	0.465	98.7		2.67	51.07	46.27	0.00
280	56.2	26.9	b.d.l.	9.24	b.d.l.	5.89	0.455	98.6		2.65	52.17	45.18	0.00
281	56.5	26.7	b.d.l.	9.02	b.d.l.	6.31	0.497	99.1		2.81	54.29	42.90	0.00
282	57.0	26.9	b.d.l.	9.03	b.d.l.	6.11	0.503	99.6		2.90	53.46	43.64	0.00
283	57.5	26.2	b.d.l.	8.20	b.d.l.	6.36	0.636	98.9		3.70	56.23	40.06	0.00
284	56.2	26.8	b.d.l.	9.21	b.d.l.	5.81	0.465	98.5		2.73	51.84	45.43	0.00
285	58.5	25.4	b.d.l.	7.56	b.d.l.	6.86	0.678	99.0		3.89	59.73	36.38	0.00
286	58.9	25.3	b.d.l.	7.41	b.d.l.	6.94	0.768	99.4		4.38	60.15	35.47	0.00
287	57.8	25.9	b.d.l.	7.90	b.d.l.	6.55	0.663	98.8		3.84	57.69	38.47	0.00
288	58.3	25.5	b.d.l.	7.61	b.d.l.	6.72	0.702	98.9		4.06	58.97	36.97	0.00
289	58.0	25.8	b.d.l.	7.97	b.d.l.	6.65	0.605	99.0		3.47	58.06	38.46	0.00
290	58.3	25.5	b.d.l.	7.59	b.d.l.	6.74	0.663	98.7		3.84	59.31	36.85	0.00
291	58.0	25.4	b.d.l.	7.65	b.d.l.	6.55	0.722	98.3		4.22	58.22	37.56	0.00
292	58.4	25.5	b.d.l.	7.76	b.d.l.	6.69	0.671	99.0		3.87	58.56	37.57	0.00
293	57.1	26.4	b.d.l.	8.53	b.d.l.	6.23	0.560	98.9		3.26	55.10	41.65	0.00
294	58.0	25.6	b.d.l.	7.85	b.d.l.	6.65	0.637	98.7		3.67	58.30	38.03	0.00
295	57.4	26.4	b.d.l.	8.50	b.d.l.	6.16	0.574	99.0		3.36	54.84	41.80	0.00
296	58.4	25.7	b.d.l.	7.81	b.d.l.	6.68	0.665	99.2		3.83	58.41	37.76	0.00
297	58.6	25.8	b.d.l.	7.82	b.d.l.	6.51	0.681	99.4		3.97	57.71	38.32	0.00
298	59.0	25.3	b.d.l.	7.23	b.d.l.	6.87	0.759	99.2		4.40	60.43	35.18	0.00
299	57.6	26.2	b.d.l.	8.44	b.d.l.	6.38	0.659	99.3		3.78	55.55	40.67	0.00
300	58.0	25.7	b.d.l.	7.96	b.d.l.	6.47	0.724	98.9		4.20	57.01	38.79	0.00
301	59.2	25.1	b.d.l.	7.10	b.d.l.	7.02	0.921	99.3		5.25	60.78	33.98	0.00
SVC 9703													
35	57.8	26.7	b.d.l.	8.79	b.d.l.	6.51	0.451	100.3		2.54	55.81	41.65	0.00
z1	55.8	28.2	b.d.l.	10.15	b.d.l.	5.72	0.439	100.2		2.49	49.25	48.26	0.00
z2	56.2	27.7	b.d.l.	9.74	b.d.l.	5.94	0.472	100.1		2.67	51.07	46.27	0.00
z3	57.2	27.0	b.d.l.	9.06	b.d.l.	6.13	0.504	99.9		2.90	53.46	43.64	0.00
z4	57.0	27.2	b.d.l.	9.36	b.d.l.	5.97	0.461	100.0		2.65	52.17	45.18	0.00
z5	56.9	26.9	b.d.l.	9.08	b.d.l.	6.35	0.500	99.7		2.81	54.29	42.90	0.00
z6	58.0	26.4	b.d.l.	8.27	b.d.l.	6.42	0.642	99.8		3.70	56.23	40.06	0.00
z7	58.4	26.1	b.d.l.	7.98	b.d.l.	6.62	0.670	99.9		3.84	57.69	38.47	0.00
z8	58.9	25.8	b.d.l.	7.68	b.d.l.	6.78	0.709	99.8		4.06	58.97	36.97	0.00
z9	59.0	26.2	b.d.l.	8.10	b.d.l.	6.76	0.615	100.6		3.47	58.06	38.46	0.00
z10	59.3	25.7	b.d.l.	7.65	b.d.l.	6.94	0.686	100.2		3.89	59.73	36.38	0.00
z11	59.1	25.4	b.d.l.	7.43	b.d.l.	6.96	0.771	99.7		4.38	60.15	35.47	0.00
z12	57.3	27.3	b.d.l.	9.38	b.d.l.	5.92	0.474	100.3		2.73	51.84	45.43	0.00
z13	59.0	25.9	b.d.l.	7.79	b.d.l.	6.67	0.735	100.1		4.22	58.22	37.56	0.00
z14	59.1	25.8	b.d.l.	7.70	b.d.l.	6.84	0.672	100.1		3.84	59.31	36.85	0.00
z15	57.8	26.7	b.d.l.	8.63	b.d.l.	6.30	0.567	100.0		3.26	55.10	41.65	0.00
z16	59.0	25.8	b.d.l.	7.84	b.d.l.	6.76	0.678	100.0		3.87	58.56	37.57	0.00
z17	58.7	25.9	b.d.l.	7.95	b.d.l.	6.73	0.645	99.9		3.67	58.30	38.03	0.00
z18	57.9	26.6	b.d.l.	8.57	b.d.l.	6.21	0.579	99.9		3.36	54.84	41.80	0.00
z19	58.9	25.9	b.d.l.	7.88	b.d.l.	6.74	0.671	100.0		3.83	58.41	37.76	0.00

Tab. A-7: continued

No	SiO_2	Al_2O_3	FeO	CaO	BaO	Na_2O	K_2O	Σ		or	ab	an	cel
AMT 9702													
84	50.8	31.0	b.d.l.	14.31	b.d.l.	3.35	0.321	99.8		1.84	29.22	68.93	0.00
102	55.8	27.8	b.d.l.	10.58	b.d.l.	5.08	0.696	99.9		4.02	44.64	51.34	0.00
106	55.0	28.2	0.189	11.43	b.d.l.	4.71	0.628	100.1		3.61	41.20	55.18	0.00
AMT 9704 A													
56	55.4	27.5	b.d.l.	10.30	b.d.l.	4.98	0.686	98.8		4.06	44.78	51.16	0.00
57	55.7	27.1	b.d.l.	9.99	b.d.l.	5.01	0.769	98.5		4.59	45.37	50.05	0.00
58	56.0	27.3	b.d.l.	10.12	b.d.l.	5.06	0.731	99.2		4.32	45.47	50.21	0.00
59	54.9	28.1	b.d.l.	10.69	b.d.l.	4.92	0.587	99.2		3.44	43.91	52.65	0.00
60	55.6	27.6	b.d.l.	10.30	b.d.l.	4.98	0.673	99.1		3.98	44.82	51.19	0.00
65	49.0	32.4	b.d.l.	15.40	b.d.l.	2.51	0.212	99.5		1.25	22.48	76.27	0.00
156	47.3	33.3	b.d.l.	16.73	b.d.l.	1.94	0.121	99.3		0.70	17.21	82.09	0.00
157	49.2	32.3	b.d.l.	15.46	b.d.l.	2.46	0.189	99.5		1.12	22.07	76.81	0.00
158	49.2	32.6	b.d.l.	15.59	b.d.l.	2.46	0.187	100.0		1.10	21.97	76.93	0.00
159	49.9	31.5	b.d.l.	14.78	b.d.l.	2.84	0.249	99.3		1.47	25.44	73.09	0.00
160	52.5	29.9	b.d.l.	12.64	b.d.l.	3.87	0.415	99.3		2.45	34.76	62.78	0.00
161	54.2	28.9	b.d.l.	11.71	b.d.l.	4.36	0.468	99.6		2.76	39.14	58.10	0.00
162	55.1	27.9	b.d.l.	10.66	b.d.l.	4.89	0.593	99.1		3.49	43.76	52.75	0.00
163	55.1	28.2	b.d.l.	10.76	b.d.l.	4.69	0.597	99.2		3.56	42.52	53.91	0.00
164	55.3	28.1	b.d.l.	10.76	b.d.l.	4.94	0.619	99.7		3.61	43.73	52.66	0.00
165	55.3	28.1	b.d.l.	10.76	b.d.l.	4.90	0.642	99.7		3.75	43.48	52.77	0.00
166	55.2	28.3	b.d.l.	10.73	b.d.l.	4.75	0.611	99.6		3.63	42.85	53.52	0.00
167	55.4	28.1	b.d.l.	10.61	b.d.l.	5.01	0.626	99.7		3.65	44.40	51.95	0.00
168	56.0	27.8	b.d.l.	10.35	b.d.l.	5.03	0.669	99.9		3.93	44.93	51.14	0.00
169	56.5	27.4	b.d.l.	10.10	b.d.l.	5.09	0.755	99.9		4.45	45.57	49.98	0.00
170	56.3	27.4	b.d.l.	9.89	b.d.l.	5.14	0.696	99.4		4.14	46.48	49.38	0.00
171	56.4	27.5	b.d.l.	9.86	b.d.l.	5.42	0.746	99.9		4.32	47.72	47.96	0.00
172	56.9	27.0	b.d.l.	9.66	b.d.l.	5.31	0.772	99.6		4.56	47.58	47.86	0.00
173	55.6	27.7	b.d.l.	10.37	b.d.l.	5.01	0.664	99.4		3.91	44.83	51.26	0.00
174	55.7	27.6	b.d.l.	10.32	b.d.l.	5.02	0.698	99.3		4.11	44.90	50.99	0.00
175	55.9	27.7	b.d.l.	10.36	b.d.l.	5.09	0.698	99.7		4.07	45.18	50.75	0.00
176	55.9	27.8	b.d.l.	10.27	b.d.l.	4.96	0.678	99.6		4.03	44.72	51.25	0.00
177	55.6	28.2	b.d.l.	10.64	b.d.l.	4.95	0.669	100.1		3.90	43.91	52.19	0.00
178	57.1	27.1	b.d.l.	9.59	b.d.l.	5.28	0.794	99.9		4.70	47.58	47.72	0.00
179	56.2	27.1	b.d.l.	9.74	b.d.l.	5.29	0.798	99.2		4.69	47.22	48.10	0.00
180	56.5	27.5	b.d.l.	9.93	b.d.l.	5.19	0.756	99.8		4.45	46.42	49.12	0.00
181	56.3	27.7	b.d.l.	10.07	b.d.l.	5.15	0.728	99.9		4.28	46.03	49.69	0.00
182	57.0	27.1	b.d.l.	9.58	b.d.l.	5.33	0.814	99.8		4.80	47.79	47.41	0.00
183	55.4	28.0	b.d.l.	10.56	b.d.l.	4.90	0.685	99.5		4.03	43.79	52.18	0.00
184	55.8	27.8	0.169	10.26	b.d.l.	4.82	0.733	99.6		4.40	43.95	51.65	0.00
185	54.0	28.8	0.266	11.73	b.d.l.	4.43	0.492	99.7		2.88	39.46	57.67	0.00
RAD 9701													
85	48.5	32.0	0.494	15.89	b.d.l.	2.46	0.277	99.6		1.60	21.51	76.89	0.00
175	54.7	27.8	0.519	10.83	b.d.l.	5.37	0.386	99.7		2.19	46.28	51.53	0.00
176	50.4	30.3	0.546	14.11	b.d.l.	3.24	0.330	99.0		1.93	28.78	69.29	0.00
177	48.1	32.1	0.544	15.74	b.d.l.	2.34	0.221	99.0		1.30	20.90	77.80	0.00
178	49.4	31.4	0.486	15.10	b.d.l.	2.73	0.269	99.4		1.57	24.25	74.18	0.00
179	48.2	31.7	0.438	15.84	b.d.l.	2.29	0.223	98.7		1.31	20.49	78.20	0.00
180	48.6	31.2	0.803	15.23	b.d.l.	2.69	0.267	99.2		1.55	23.89	74.56	0.00
181	50.8	30.4	0.522	14.19	b.d.l.	3.33	0.330	99.6		1.90	29.26	68.83	0.00
182	50.6	30.5	0.504	13.86	b.d.l.	3.23	0.240	98.9		1.43	29.24	69.33	0.00

No	SiO_2	Al_2O_3	FeO	CaO	BaO	Na_2O	K_2O	Σ		or	ab	an	cel
RAD 9701													
183	46.4	33.4	0.291	17.63	b.d.l.	1.45	0.147	99.3		0.86	12.82	86.33	0.00
184	47.2	32.5	0.292	17.10	b.d.l.	1.82	0.190	99.2		1.10	15.96	82.94	0.00
185	49.0	31.7	0.345	15.70	b.d.l.	2.52	0.339	99.5		1.95	22.06	75.98	0.00
186	46.2	33.6	0.222	17.64	b.d.l.	1.44	0.141	99.2		0.82	12.73	86.45	0.00
187	46.6	33.0	0.230	17.20	b.d.l.	1.50	0.199	98.7		1.18	13.50	85.33	0.00
188	46.4	33.2	0.213	17.40	b.d.l.	1.61	0.200	99.0		1.16	14.17	84.67	0.00
189	47.7	32.4	0.276	16.35	b.d.l.	1.97	0.295	99.0		1.74	17.60	80.67	0.00
190	48.0	32.3	0.269	16.27	b.d.l.	2.18	0.305	99.4		1.76	19.16	79.08	0.00
191	47.0	33.0	0.219	16.88	b.d.l.	1.74	0.231	99.1		1.35	15.54	83.11	0.00
192	47.9	32.5	0.243	16.14	b.d.l.	2.07	0.319	99.2		1.88	18.46	79.66	0.00
193	46.4	33.2	0.303	17.42	b.d.l.	1.52	0.159	98.9		0.93	13.50	85.57	0.00
194	46.2	33.2	0.347	17.44	b.d.l.	1.45	0.149	98.8		0.87	13.00	86.12	0.00
195	46.0	33.5	0.323	17.68	b.d.l.	1.37	0.110	99.0		0.65	12.20	87.16	0.00
196	46.3	33.0	0.245	17.27	b.d.l.	1.63	0.157	98.6		0.92	14.47	84.61	0.00
197	46.9	32.3	0.579	16.85	b.d.l.	1.54	0.197	98.9		1.18	14.06	84.77	0.00
198	46.3	33.5	0.265	17.67	b.d.l.	1.45	0.160	99.3		0.93	12.84	86.23	0.00
199	46.6	33.1	0.263	17.32	b.d.l.	1.57	0.192	99.0		1.12	13.93	84.95	0.00
200	47.4	32.6	0.267	16.51	b.d.l.	1.81	0.236	98.8		1.40	16.34	82.25	0.00
201	46.8	32.6	0.294	16.92	b.d.l.	1.53	0.212	98.4		1.26	13.89	84.85	0.00
202	46.7	32.9	0.293	17.17	b.d.l.	1.57	0.163	98.7		0.96	14.04	85.00	0.00
203	47.3	32.7	0.271	16.85	b.d.l.	1.78	0.228	99.1		1.33	15.83	82.84	0.00
204	47.0	33.0	0.275	16.75	b.d.l.	1.55	0.200	98.8		1.20	14.13	84.66	0.00
205	47.9	32.2	0.318	16.14	b.d.l.	2.10	0.282	98.9		1.66	18.72	79.62	0.00
206	46.8	32.8	0.267	17.00	b.d.l.	1.76	0.235	98.9		1.36	15.61	83.03	0.00
207	47.0	32.9	0.332	16.92	b.d.l.	1.78	0.210	99.1		1.22	15.82	82.96	0.00
208	46.9	33.1	0.260	17.35	b.d.l.	1.61	0.187	99.4		1.09	14.25	84.67	0.00
209	48.6	31.5	0.282	15.62	b.d.l.	2.41	0.351	98.8		2.05	21.39	76.57	0.00
210	46.6	32.9	0.320	17.20	b.d.l.	1.72	0.163	98.9		0.95	15.17	83.88	0.00
211	48.3	31.6	0.380	15.69	b.d.l.	2.31	0.267	98.6		1.57	20.68	77.75	0.00
RAD 9702 A													
58	47.5	32.3	0.296	16.32	b.d.l.	2.04	0.307	98.8		1.79	18.12	80.09	0.00
59	48.7	31.7	0.350	15.40	b.d.l.	2.34	0.394	98.9		2.33	21.10	76.57	0.00
63	48.0	32.0	0.446	15.81	b.d.l.	2.38	0.217	98.9		1.26	21.17	77.57	0.00
64	46.8	32.8	0.365	16.58	b.d.l.	1.96	0.167	98.6		0.98	17.47	81.55	0.00
70	49.4	31.1	0.467	14.60	b.d.l.	2.96	0.383	98.8		2.23	26.22	71.54	0.00
72	47.2	32.6	0.334	16.28	b.d.l.	2.00	0.255	98.6		1.50	17.92	80.58	0.00
77	47.3	32.3	0.549	16.05	b.d.l.	2.05	0.153	98.4		0.91	18.58	80.51	0.00
222	46.0	33.6	0.277	17.49	b.d.l.	1.38	0.177	99.0		1.04	12.36	86.59	0.00
223	47.3	32.5	0.268	16.27	b.d.l.	1.91	0.273	98.4		1.62	17.24	81.14	0.00
224	46.3	33.1	0.280	16.85	b.d.l.	1.77	0.206	98.5		1.21	15.75	83.04	0.00
225	46.1	33.2	0.270	17.12	b.d.l.	1.54	0.201	98.5		1.19	13.86	84.96	0.00
226	46.4	33.5	0.243	17.24	b.d.l.	1.62	0.246	99.2		1.43	14.30	84.27	0.00
227	47.4	32.3	0.298	16.22	b.d.l.	2.01	0.295	98.5		1.74	18.01	80.25	0.00
228	47.8	32.0	b.d.l.	16.14	b.d.l.	2.16	0.330	98.4		1.92	19.13	78.95	0.00
229	48.3	32.0	0.332	15.86	b.d.l.	2.23	0.382	99.1		2.23	19.83	77.93	0.00
230	46.9	32.9	0.261	16.81	b.d.l.	1.83	0.246	98.9		1.43	16.24	82.33	0.00
231	47.4	32.1	0.315	16.14	b.d.l.	2.13	0.249	98.4		1.46	19.04	79.50	0.00
232	50.5	30.0	0.453	13.74	b.d.l.	3.22	0.629	98.5		3.69	28.67	67.64	0.00
233	46.9	32.9	0.435	16.42	b.d.l.	2.05	0.123	98.8		0.72	18.27	81.01	0.00
TA 9701 whole rock													
43	58.6	24.3	0.655	8.43	b.d.l.	2.63	4.930	99.9		30.79	25.01	44.20	0.00

Tab. A-8: Chemical composition of leucites by EMPA.

No	SiO_2	Al_2O_3	FeO	Na_2O	K_2O	Σ
VUL 9701						
63	55.7	22.6	0.341	0.146	20.9	99.7
72	55.6	22.6	0.278	0.111	20.7	99.2
73	55.5	22.3	0.316	0.256	20.8	99.2
74	55.8	22.2	0.329	0.222	20.6	99.1
75	55.2	22.4	0.344	0.170	20.7	98.8
81	55.5	22.4	0.298	0.250	20.8	99.2
85	55.6	22.5	0.345	0.164	20.8	99.4
99	55.9	22.4	0.310	0.273	20.8	99.6
235	55.8	22.6	0.334	0.094	20.9	99.7
236	55.8	22.4	0.356	0.202	20.7	99.5
237	55.8	22.1	0.304	0.266	20.6	99.1
238	55.7	22.3	0.332	0.275	20.8	99.4
239	55.9	22.4	0.331	0.093	20.9	99.6
240	55.7	22.4	0.318	0.138	20.7	99.3
241	55.8	22.3	0.326	0.098	20.7	99.3
242	55.7	22.4	0.342	0.093	21.0	99.4
243	55.7	22.3	0.407	0.178	20.9	99.4
244	56.0	22.6	0.295	0.162	20.8	99.7
245	55.6	22.3	0.289	0.286	20.6	99.0
246	56.0	22.3	0.315	0.226	20.7	99.5
247	55.9	22.3	0.342	0.236	20.7	99.5
248	55.3	22.6	0.339	0.111	20.6	98.9
249	56.3	22.5	0.296	0.208	20.8	100.1
VUL 9705						
10	55.2	22.6	0.538	0.305	20.9	99.5
12	55.1	22.9	0.334	0.328	20.8	99.5
13	54.8	22.8	0.350	0.386	20.7	99.1
22	55.0	22.6	0.354	0.373	20.9	99.2
23	54.8	22.8	0.351	0.323	20.8	99.1
29	55.0	22.7	0.651	0.253	21.2	99.8
194	55.2	22.8	0.320	0.367	20.8	99.5
195	55.2	22.8	0.305	0.361	20.8	99.5
196	55.2	22.9	0.311	0.326	20.7	99.4
197	54.6	22.9	0.351	0.321	20.7	99.0
198	55.2	22.8	0.314	0.356	20.6	99.2
199	54.9	22.7	0.280	0.371	20.8	99.1
200	55.0	22.8	0.314	0.368	20.8	99.3
201	55.2	23.0	0.303	0.306	20.8	99.6
202	55.1	22.6	0.286	0.310	20.7	99.0
203	55.0	22.8	0.352	0.309	20.5	98.9
204	55.1	22.9	0.299	0.362	20.8	99.5
205	55.3	22.8	0.334	0.385	20.8	99.6
206	55.2	22.8	0.343	0.324	20.7	99.4
207	55.3	22.8	0.383	0.378	20.9	99.8
208	55.1	22.9	0.462	0.328	20.8	99.6
209	57.0	23.7	0.496	0.326	18.4	99.9

Tab. A-8: continued

No	SiO_2	Al_2O_3	FeO	Na_2O	K_2O	Σ
VUL 9707						
69	56.1	22.5	0.310	0.321	20.5	99.7
70	55.8	22.8	0.376	0.454	20.4	99.8
72	55.5	22.6	0.265	0.258	20.3	99.0
73	55.5	22.4	0.279	0.346	20.4	98.9
83	55.5	22.6	0.287	0.369	20.7	99.4
84	55.7	22.6	0.346	0.276	20.5	99.4
86	55.7	22.3	0.396	0.261	20.6	99.3
213	55.7	22.5	0.329	0.316	20.5	99.3
214	56.1	22.5	0.342	0.371	20.3	99.6
215	56.0	22.4	0.332	0.328	20.4	99.5
216	55.6	22.6	0.394	0.455	20.5	99.5
217	55.8	22.6	0.315	0.370	20.4	99.5
218	55.6	22.6	0.313	0.277	20.7	99.4
219	55.5	22.6	0.367	0.319	20.6	99.3
220	55.3	22.3	0.340	0.310	20.6	98.8
221	55.8	22.7	0.348	0.398	20.3	99.6
222	56.0	22.4	0.359	0.288	20.6	99.6
223	55.9	22.5	0.382	0.341	20.4	99.5
224	55.8	22.5	0.342	0.290	20.6	99.6
225	55.9	22.5	0.338	0.335	20.4	99.5
226	56.0	22.7	0.331	0.446	20.1	99.5
227	56.1	22.5	0.360	0.295	20.5	99.8
228	55.4	22.5	0.303	0.316	20.5	99.0
229	55.4	22.6	0.340	0.398	20.4	99.1
230	55.6	22.6	0.328	0.251	20.7	99.5
231	56.1	22.7	0.332	0.185	20.8	100.0

Tab. A-9: Chemical composition of micas by EMPA.

No	SiO_2	TiO_2	Al_2O_3	FeO	MgO	CaO	MnO	BaO	Cr_2O_3	Na_2O	K_2O	Σ		mineral
VUL 9702														
2	36.2	3.98	16.02	12.35	16.59	b.d.l.	b.d.l.	0.504	b.d.l.	0.264	9.52	95.4		phl
14	35.7	3.87	15.82	13.29	16.01	0.185	0.135	0.420	b.d.l.	0.398	9.40	95.2		phl
15	36.2	4.00	16.00	11.06	17.30	b.d.l.	b.d.l.	0.632	b.d.l.	0.424	9.47	95.1		phl
22	36.3	4.00	15.81	10.48	17.63	b.d.l.	b.d.l.	0.520	b.d.l.	0.342	9.51	94.6		phl
28	36.4	4.08	16.41	9.45	18.45	b.d.l.	b.d.l.	0.569	b.d.l.	0.357	9.62	95.3		phl
117	36.3	4.19	16.14	11.24	17.34	b.d.l.	b.d.l.	0.510	b.d.l.	0.352	9.62	95.7		phl
118	36.4	4.10	16.17	11.40	17.12	b.d.l.	b.d.l.	0.658	b.d.l.	0.335	9.60	95.7		phl
119	36.4	4.14	15.82	11.16	17.24	b.d.l.	b.d.l.	0.450	b.d.l.	0.309	9.51	95.1		phl
120	36.4	4.26	16.24	11.19	17.22	b.d.l.	b.d.l.	0.506	b.d.l.	0.357	9.63	95.8		phl
121	36.0	4.28	15.97	11.03	17.16	b.d.l.	b.d.l.	0.594	b.d.l.	0.318	9.47	94.9		phl
122	36.8	4.44	16.12	11.44	17.52	b.d.l.	b.d.l.	0.539	b.d.l.	0.366	9.45	96.7		phl
123	36.6	4.24	16.07	11.70	17.15	b.d.l.	b.d.l.	0.451	b.d.l.	0.398	9.48	96.1		phl
ORC 9701														
21	39.2	7.73	11.58	7.26	19.42	b.d.l.	b.d.l.	1.570	0.236	0.456	8.22	95.7		phl
31	38.7	8.16	11.48	9.59	17.56	b.d.l.	b.d.l.	1.470	b.d.l.	0.424	8.67	96.1		phl
32	38.6	8.66	11.77	9.90	16.68	b.d.l.	b.d.l.	1.660	b.d.l.	0.374	8.66	96.3		phl
33	38.7	7.72	11.44	8.00	18.81	b.d.l.	b.d.l.	1.590	b.d.l.	0.449	8.58	95.3		phl
36	39.0	8.53	11.67	8.76	17.60	b.d.l.	b.d.l.	1.520	b.d.l.	0.456	8.71	96.2		phl
43	38.6	8.51	11.91	9.06	17.70	b.d.l.	b.d.l.	1.710	b.d.l.	0.435	8.75	96.7		phl
44	38.0	9.34	12.04	9.18	16.41	b.d.l.	b.d.l.	1.670	b.d.l.	0.374	8.87	95.8		phl
46	38.5	7.31	11.14	8.05	19.50	b.d.l.	b.d.l.	1.490	b.d.l.	0.441	8.18	94.6		phl
47	38.4	7.38	11.54	7.86	19.11	b.d.l.	b.d.l.	1.540	b.d.l.	0.421	8.70	95.0		phl
159	39.7	7.60	11.35	9.60	17.63	b.d.l.	b.d.l.	b.d.l.	b.d.l.	0.432	9.05	95.3		phl
160	38.2	8.09	11.60	9.73	16.75	0.827	b.d.l.	1.480	b.d.l.	0.412	8.46	95.5		phl
161	38.5	7.94	11.42	10.01	17.60	b.d.l.	b.d.l.	1.510	b.d.l.	0.403	8.49	95.8		phl
162	39.2	7.73	11.06	10.17	17.75	b.d.l.	b.d.l.	1.440	b.d.l.	0.465	8.09	95.9		phl
163	38.6	8.19	11.67	9.39	17.38	b.d.l.	b.d.l.	1.520	b.d.l.	0.379	8.81	96.0		phl
164	38.7	8.44	11.42	9.63	17.47	b.d.l.	b.d.l.	0.755	b.d.l.	0.441	9.03	95.9		phl
291	39.3	7.88	11.12	9.62	18.00	b.d.l.	b.d.l.	0.436	b.d.l.	0.445	8.58	95.4		phl
ROC 9701														
50	34.9	4.42	16.32	24.58	6.54	b.d.l.	0.191	b.d.l.	b.d.l.	0.504	8.45	95.9		bio
51	34.8	4.39	16.05	24.86	6.74	b.d.l.	0.221	b.d.l.	b.d.l.	0.574	8.57	96.2		bio
53	35.7	4.40	15.78	24.53	6.75	b.d.l.	0.225	b.d.l.	b.d.l.	0.529	8.64	96.5		bio
56	33.9	4.30	15.99	26.31	6.44	b.d.l.	0.217	b.d.l.	b.d.l.	0.656	8.23	96.0		bio
61	34.8	3.76	17.09	24.78	5.61	b.d.l.	0.188	b.d.l.	b.d.l.	0.631	8.38	95.3		bio
64	35.1	4.47	16.44	24.68	6.53	b.d.l.	0.225	b.d.l.	b.d.l.	0.581	8.67	96.7		bio
65	34.6	4.34	16.35	25.46	6.36	b.d.l.	0.203	b.d.l.	b.d.l.	0.596	8.38	96.2		bio
70	34.3	4.18	17.20	25.15	6.33	b.d.l.	0.206	b.d.l.	b.d.l.	0.515	8.74	96.7		bio
SVC 9702														
96	35.1	4.45	16.57	20.71	9.19	b.d.l.	b.d.l.	b.d.l.	b.d.l.	0.511	9.20	95.7		bio
97	35.4	3.82	16.81	18.37	11.22	b.d.l.	b.d.l.	b.d.l.	b.d.l.	0.594	9.19	95.4		bio
101	35.9	4.04	16.17	19.73	11.15	b.d.l.	b.d.l.	b.d.l.	b.d.l.	0.576	8.96	96.5		bio
117	34.9	5.09	16.57	22.06	8.62	b.d.l.	b.d.l.	b.d.l.	b.d.l.	0.539	9.21	96.9		bio
120	35.4	4.43	16.54	20.06	9.79	b.d.l.	b.d.l.	b.d.l.	b.d.l.	0.564	9.13	95.9		bio
139	35.9	4.70	15.59	19.88	10.45	b.d.l.	b.d.l.	b.d.l.	b.d.l.	0.494	8.88	95.9		bio
260	35.0	3.88	16.81	18.76	11.26	b.d.l.	b.d.l.	b.d.l.	b.d.l.	0.503	9.19	95.4		bio
261	35.6	3.71	16.62	18.44	11.38	b.d.l.	b.d.l.	b.d.l.	b.d.l.	0.519	9.19	95.4		bio

Tab. A-9: continued

No	SiO_2	TiO_2	Al_2O_3	FeO	MgO	CaO	MnO	BaO	Cr_2O_3	Na_2O	K_2O	Σ		mineral
SVC 9702														
262	35.4	3.90	16.49	18.39	11.26	b.d.l.	b.d.l.	b.d.l.	b.d.l.	0.547	9.19	95.2		bio
263	35.3	4.00	16.51	18.48	11.38	b.d.l.	b.d.l.	b.d.l.	b.d.l.	0.555	9.39	95.6		bio
264	35.5	4.06	16.34	19.42	11.48	b.d.l.	b.d.l.	b.d.l.	b.d.l.	0.535	9.13	96.4		bio
265	35.3	4.24	16.04	18.98	10.84	b.d.l.	b.d.l.	b.d.l.	b.d.l.	0.624	9.06	95.1		bio
266	36.1	4.24	16.70	15.98	11.89	b.d.l.	b.d.l.	b.d.l.	b.d.l.	0.556	8.79	94.3		bio
SVC 9703														
32	36.8	4.63	15.30	22.45	8.85	b.d.l.	b.d.l.	b.d.l.	b.d.l.	0.516	8.67	97.2		bio
38	35.3	4.76	17.01	23.63	7.11	b.d.l.	b.d.l.	b.d.l.	b.d.l.	0.593	8.96	97.3		bio
41	36.3	4.36	15.66	23.58	8.18	b.d.l.	b.d.l.	b.d.l.	b.d.l.	0.628	8.81	97.5		bio
48	37.1	4.17	17.07	21.50	8.20	b.d.l.	b.d.l.	b.d.l.	b.d.l.	0.535	8.47	97.1		bio
53	35.5	4.89	16.60	23.22	7.36	b.d.l.	b.d.l.	0.295	b.d.l.	0.458	8.93	97.2		bio
58	35.2	4.83	16.65	23.30	7.15	b.d.l.	b.d.l.	b.d.l.	b.d.l.	0.571	8.99	96.7		bio
AMT 9702														
76	37.8	5.74	13.47	17.54	12.70	b.d.l.	b.d.l.	b.d.l.	b.d.l.	0.346	9.50	97.1		bio
83	37.3	5.82	13.30	17.72	12.42	b.d.l.	b.d.l.	b.d.l.	b.d.l.	0.408	9.18	96.2		bio
85	36.9	6.29	14.18	18.30	11.63	b.d.l.	b.d.l.	0.852	b.d.l.	0.439	9.14	97.7		bio
86	37.8	5.82	13.06	19.04	11.77	b.d.l.	b.d.l.	b.d.l.	b.d.l.	0.506	9.37	97.3		bio
89	37.2	6.48	13.84	18.17	11.84	b.d.l.	b.d.l.	0.522	b.d.l.	0.424	9.12	97.6		bio
95	37.2	5.98	13.61	18.07	12.07	b.d.l.	b.d.l.	0.491	b.d.l.	0.439	9.15	97.0		bio
AMT 9703 II														
31	38.0	2.52	15.52	8.00	20.47	b.d.l.	b.d.l.	0.385	b.d.l.	0.292	9.89	95.0		phl
38	35.7	2.88	15.98	20.33	11.78	b.d.l.	0.227	0.269	b.d.l.	0.348	9.50	97.0		bio
41	37.8	2.81	15.57	8.70	19.65	b.d.l.	b.d.l.	0.523	b.d.l.	0.207	10.11	95.4		phl
48	36.3	3.24	16.19	12.49	16.65	b.d.l.	b.d.l.	0.614	b.d.l.	0.234	9.79	95.5		phl
210	37.6	2.90	15.66	9.01	19.45	b.d.l.	b.d.l.	0.503	b.d.l.	0.251	10.01	95.4		phl
211	37.1	2.99	15.68	9.85	18.52	b.d.l.	b.d.l.	0.539	b.d.l.	0.250	9.92	94.8		phl
212	35.9	3.22	15.91	15.15	14.89	b.d.l.	0.191	0.510	b.d.l.	0.270	9.57	95.6		bio
213	34.8	3.11	16.04	19.26	12.24	b.d.l.	0.276	0.624	b.d.l.	0.327	9.34	96.0		bio
214	36.2	3.04	15.51	13.23	16.45	b.d.l.	0.143	0.533	b.d.l.	0.259	9.73	95.1		phl
215	36.0	3.09	15.69	12.87	16.84	b.d.l.	b.d.l.	0.497	b.d.l.	0.228	9.83	95.0		phl
216	36.5	3.34	16.09	11.96	16.98	b.d.l.	0.109	0.596	b.d.l.	0.270	9.69	95.6		phl
217	35.7	3.39	16.14	14.54	15.16	b.d.l.	0.111	0.660	b.d.l.	0.237	9.57	95.5		bio
218	34.4	3.63	16.29	19.53	11.23	b.d.l.	0.233	0.791	b.d.l.	0.293	9.35	95.7		bio
219	33.9	3.40	16.79	20.70	10.44	b.d.l.	0.295	0.782	b.d.l.	0.291	9.20	95.8		bio
220	34.7	3.09	14.55	20.05	11.94	b.d.l.	0.300	b.d.l.	b.d.l.	0.339	9.37	94.4		bio
221	34.7	3.13	14.48	19.77	11.90	b.d.l.	0.242	b.d.l.	b.d.l.	0.314	9.44	93.9		bio
AMT 9704 A														
37	36.1	6.07	14.22	17.65	11.75	0.062	0.116	0.640	b.d.l.	0.485	8.90	96.0		bio
192	36.7	5.25	13.96	20.53	10.58	b.d.l.	0.140	0.371	b.d.l.	0.423	9.06	97.0		bio
193	36.7	5.88	13.54	18.68	11.84	b.d.l.	b.d.l.	0.606	b.d.l.	0.530	8.88	96.6		bio

Tab. A-9: continued

No	SiO_2	TiO_2	Al_2O_3	FeO	MgO	CaO	MnO	BaO	Cr_2O_3	Na_2O	K_2O	Σ		mineral
TA 9701 whole rock														
25	40.2	3.43	13.14	4.87	22.51	b.d.l.	b.d.l.	b.d.l.	b.d.l.	0.107	10.24	94.5		phl
31	39.8	3.36	13.51	4.55	21.96	0.112	b.d.l.	b.d.l.	1.324	0.175	10.17	95.0		phl
35	40.5	3.27	13.15	4.56	22.44	b.d.l.	b.d.l.	b.d.l.	b.d.l.	0.145	10.44	94.5		phl
45	36.2	7.00	16.40	16.68	10.94	b.d.l.	b.d.l.	b.d.l.	b.d.l.	0.419	9.43	97.1		bio
46	38.2	7.15	13.61	5.40	19.24	b.d.l.	b.d.l.	0.398	1.001	0.182	9.90	95.1		phl
47	37.9	8.26	13.53	6.08	19.03	b.d.l.	b.d.l.	0.425	0.586	0.138	9.99	95.9		phl
53	36.0	7.11	16.42	15.78	11.56	b.d.l.	b.d.l.	b.d.l.	b.d.l.	0.357	9.57	96.8		bio
203	36.0	6.71	16.52	17.18	10.65	b.d.l.	b.d.l.	b.d.l.	b.d.l.	0.436	9.58	97.1		bio
204	35.9	6.78	16.57	17.29	10.45	b.d.l.	b.d.l.	b.d.l.	b.d.l.	0.357	9.34	96.7		bio
205	35.9	6.60	16.86	17.35	10.49	b.d.l.	b.d.l.	b.d.l.	b.d.l.	0.374	9.48	97.1		bio
206	36.2	6.41	16.61	17.42	10.60	b.d.l.	b.d.l.	b.d.l.	b.d.l.	0.414	9.34	97.0		bio
207	36.0	6.60	16.78	17.02	10.57	b.d.l.	b.d.l.	b.d.l.	b.d.l.	0.330	9.31	96.6		bio
208	36.1	6.56	16.50	17.13	10.83	b.d.l.	b.d.l.	b.d.l.	b.d.l.	0.419	9.63	97.2		bio
209	36.2	6.61	16.42	17.40	10.52	b.d.l.	b.d.l.	b.d.l.	b.d.l.	0.421	9.45	97.0		bio
210	35.7	6.62	16.58	17.08	10.49	b.d.l.	b.d.l.	b.d.l.	b.d.l.	0.342	9.61	96.4		bio
211	35.9	6.58	16.51	17.38	10.70	b.d.l.	b.d.l.	b.d.l.	b.d.l.	0.406	9.46	97.0		bio
212	36.0	6.67	16.65	17.22	10.70	b.d.l.	b.d.l.	b.d.l.	b.d.l.	0.417	9.40	97.1		bio
213	32.8	6.08	13.90	19.61	9.49	0.241	b.d.l.	b.d.l.	b.d.l.	0.278	6.88	89.3		bio
214	36.0	6.91	15.86	12.69	13.60	b.d.l.	b.d.l.	b.d.l.	b.d.l.	0.261	9.40	94.8		bio
TA 9701 peridotitic xenolith														
9	39.4	3.34	13.52	4.37	21.98	b.d.l.	b.d.l.	b.d.l.	1.570	0.110	10.07	94.4		phl
10	39.9	3.53	13.75	4.18	21.69	b.d.l.	b.d.l.	b.d.l.	1.660	0.154	10.22	95.0		phl
178	40.4	3.73	13.22	4.54	22.19	b.d.l.	b.d.l.	0.296	0.545	0.179	10.14	95.2		phl
179	39.8	3.42	13.67	4.29	21.63	b.d.l.	b.d.l.	b.d.l.	1.389	0.153	10.13	94.5		phl
180	40.1	3.13	13.70	4.54	22.28	b.d.l.	b.d.l.	b.d.l.	0.886	0.126	10.14	94.9		phl
181	40.8	3.45	13.43	4.42	21.47	b.d.l.	b.d.l.	b.d.l.	0.835	0.159	10.10	94.6		phl
182	39.7	3.34	14.04	4.16	21.36	b.d.l.	b.d.l.	0.304	2.040	0.196	9.96	95.1		phl
183	40.2	3.48	13.70	4.73	21.49	b.d.l.	b.d.l.	0.290	0.879	0.169	10.12	95.0		phl
184	40.5	3.24	13.52	4.58	21.50	b.d.l.	b.d.l.	b.d.l.	0.753	0.156	10.13	94.4		phl
185	40.2	3.21	13.65	4.76	21.98	b.d.l.	b.d.l.	b.d.l.	0.748	0.148	9.97	94.7		phl
186	40.0	3.33	13.76	4.64	21.83	b.d.l.	b.d.l.	b.d.l.	0.796	0.169	10.02	94.5		phl

Tab. A-10: Chemical composition of cordierites by EMPA.

No	SiO_2	Al_2O_3	FeO	MgO	CaO	MnO	Na_2O	K_2O	Σ
SVC 9703									
31	49.0	33.0	10.96	6.84	b.d.l.	0.238	0.147	0.257	100.5
36	49.2	32.7	9.88	7.48	b.d.l.	0.304	0.177	0.262	100.0
39	49.2	32.6	10.15	7.47	b.d.l.	0.208	b.d.l.	0.182	99.9
46	49.6	33.6	7.45	9.27	b.d.l.	b.d.l.	0.105	0.173	100.2
49	49.4	33.1	10.52	7.30	b.d.l.	0.232	b.d.l.	0.191	100.7
60	49.7	33.8	6.30	9.97	b.d.l.	b.d.l.	0.237	0.102	100.0
156	48.2	33.4	10.93	6.76	0.108	0.265	0.224	0.185	100.1
157	48.3	32.6	12.49	5.66	b.d.l.	0.337	b.d.l.	0.199	99.7
158	48.2	32.4	12.77	5.59	b.d.l.	0.356	b.d.l.	0.216	99.5
159	48.5	32.3	12.97	5.53	b.d.l.	0.263	b.d.l.	0.183	99.7
160	49.1	33.2	9.42	8.00	b.d.l.	b.d.l.	b.d.l.	0.152	99.9
161	49.3	33.1	9.17	8.22	b.d.l.	b.d.l.	b.d.l.	0.171	100.0
162	49.1	33.3	9.04	8.20	b.d.l.	0.183	b.d.l.	0.174	100.0
163	49.2	33.1	8.94	8.21	b.d.l.	0.186	b.d.l.	0.172	99.8
164	49.4	33.5	8.01	8.92	b.d.l.	b.d.l.	0.094	0.179	100.0
165	49.3	33.4	7.63	9.29	b.d.l.	b.d.l.	b.d.l.	0.215	99.9
166	49.4	33.6	7.63	9.38	b.d.l.	b.d.l.	b.d.l.	0.176	100.2
167	49.7	33.6	7.47	9.36	b.d.l.	b.d.l.	b.d.l.	0.178	100.3
168	49.6	33.6	7.44	9.26	b.d.l.	b.d.l.	b.d.l.	0.159	100.0
169	49.7	33.3	7.61	9.25	b.d.l.	b.d.l.	b.d.l.	0.159	100.0
170	49.4	33.8	7.38	9.28	b.d.l.	b.d.l.	b.d.l.	0.300	100.2
171	49.4	33.2	7.22	9.19	b.d.l.	b.d.l.	b.d.l.	0.183	99.3
172	49.5	33.6	7.37	9.33	b.d.l.	b.d.l.	b.d.l.	0.199	100.0
173	49.6	33.5	7.28	9.18	b.d.l.	b.d.l.	b.d.l.	0.209	99.7
174	49.8	33.4	7.29	9.50	b.d.l.	b.d.l.	b.d.l.	0.205	100.2
175	49.3	33.4	7.50	9.32	b.d.l.	b.d.l.	b.d.l.	0.212	99.7
176	49.1	33.2	8.13	8.68	0.113	b.d.l.	0.252	0.247	99.8
177	48.4	33.0	10.62	7.15	b.d.l.	0.224	0.119	0.333	99.8
178	48.7	32.8	11.77	6.43	b.d.l.	0.235	b.d.l.	0.210	100.1
179	48.7	32.6	12.16	6.18	b.d.l.	0.267	b.d.l.	0.194	100.1
180	48.3	32.7	12.65	5.81	b.d.l.	0.259	b.d.l.	0.232	99.9
181	48.3	32.7	12.82	5.52	b.d.l.	0.280	b.d.l.	0.237	99.8
182	48.4	32.7	12.94	5.53	b.d.l.	0.383	b.d.l.	0.222	100.2
183	48.4	33.0	12.73	5.44	b.d.l.	0.266	b.d.l.	0.206	100.1
184	48.7	33.1	10.48	7.26	b.d.l.	0.204	b.d.l.	0.115	99.8
185	49.1	33.3	10.56	7.31	b.d.l.	0.225	b.d.l.	0.116	100.6
186	49.1	33.1	10.40	7.22	b.d.l.	0.186	b.d.l.	0.126	100.1
187	49.1	32.9	10.47	7.37	b.d.l.	b.d.l.	b.d.l.	0.113	99.9
188	49.4	33.5	9.90	7.50	b.d.l.	b.d.l.	b.d.l.	0.097	100.4
189	49.3	33.6	9.62	7.76	b.d.l.	b.d.l.	b.d.l.	0.106	100.4
190	49.3	33.5	7.85	9.13	b.d.l.	b.d.l.	0.121	0.162	100.1
191	49.1	33.6	7.98	8.92	b.d.l.	b.d.l.	0.189	0.147	99.9
192	49.4	33.4	8.74	8.46	b.d.l.	b.d.l.	0.108	0.124	100.2
193	49.3	33.3	9.25	8.17	b.d.l.	b.d.l.	0.160	0.119	100.2
194	48.7	33.5	9.55	7.79	b.d.l.	b.d.l.	0.191	0.151	99.9
195	48.5	33.2	10.82	7.04	b.d.l.	0.221	0.192	0.132	100.1
196	48.6	32.8	11.90	6.34	b.d.l.	0.271	0.113	0.169	100.2
197	48.2	33.2	12.10	6.00	b.d.l.	0.262	b.d.l.	0.245	100.0
198	49.1	33.0	11.46	6.37	b.d.l.	0.241	b.d.l.	0.118	100.3

Tab. A-11: Chemical composition of minerals of the spinel group by EMPA.

No	SiO_2	TiO_2	Al_2O_3	FeO	MgO	CaO	MnO	BaO	Cr_2O_3	K_2O	Σ
Montefiascone											
2	b.d.l.	0.33	37.18	19.5	18.01	b.d.l.	b.d.l.	b.d.l.	23.74	b.d.l.	98.8
3	b.d.l.	0.76	21.43	17.4	14.98	b.d.l.	b.d.l.	b.d.l.	43.93	b.d.l.	98.6
7	b.d.l.	0.47	10.92	24.9	11.82	b.d.l.	b.d.l.	b.d.l.	51.37	b.d.l.	99.6
20	b.d.l.	10.18	5.90	75.6	2.21	b.d.l.	0.805	b.d.l.	b.d.l.	b.d.l.	94.9
21	b.d.l.	10.63	4.86	75.3	1.76	b.d.l.	0.767	b.d.l.	b.d.l.	b.d.l.	93.5
24	b.d.l.	10.89	4.40	74.8	1.55	b.d.l.	1.009	b.d.l.	b.d.l.	0.049	92.9
27	b.d.l.	11.99	3.17	76.5	1.27	b.d.l.	0.785	b.d.l.	b.d.l.	b.d.l.	93.8
31	b.d.l.	10.25	3.61	76.5	1.41	b.d.l.	0.961	b.d.l.	b.d.l.	b.d.l.	92.9
35	0.520	12.51	2.84	75.2	1.22	b.d.l.	0.708	b.d.l.	b.d.l.	b.d.l.	93.1
40	b.d.l.	11.82	2.97	75.8	1.14	b.d.l.	0.816	b.d.l.	b.d.l.	b.d.l.	92.7
VUL 9701											
66	b.d.l.	6.74	3.58	81.0	1.72	0.064	1.257	b.d.l.	b.d.l.	b.d.l.	94.4
70	b.d.l.	5.74	3.90	80.6	2.94	0.109	0.856	b.d.l.	b.d.l.	b.d.l.	94.1
71	b.d.l.	6.34	3.70	81.2	2.51	b.d.l.	1.056	b.d.l.	b.d.l.	b.d.l.	94.8
77	b.d.l.	6.28	3.92	81.5	1.78	b.d.l.	1.225	b.d.l.	b.d.l.	b.d.l.	94.7
79	b.d.l.	6.70	3.63	81.8	1.63	b.d.l.	1.132	b.d.l.	b.d.l.	b.d.l.	94.9
80	b.d.l.	8.63	3.05	80.7	1.19	b.d.l.	1.570	b.d.l.	b.d.l.	b.d.l.	95.1
82	b.d.l.	6.68	3.78	81.6	1.23	b.d.l.	1.320	b.d.l.	b.d.l.	b.d.l.	94.6
87	b.d.l.	7.86	3.11	81.1	1.24	b.d.l.	1.610	b.d.l.	b.d.l.	b.d.l.	94.9
89	b.d.l.	0.30	b.d.l.	81.5	b.d.l.	b.d.l.	b.d.l.	b.d.l.	b.d.l.	b.d.l.	81.8
96	b.d.l.	0.30	b.d.l.	81.5	b.d.l.	b.d.l.	0.112	b.d.l.	b.d.l.	b.d.l.	81.9
VUL 9702											
4	b.d.l.	5.59	6.86	77.5	4.57	b.d.l.	0.358	b.d.l.	b.d.l.	b.d.l.	94.9
5	b.d.l.	6.19	7.27	75.8	5.11	b.d.l.	0.438	b.d.l.	b.d.l.	b.d.l.	94.8
12	b.d.l.	4.47	6.84	79.1	2.73	b.d.l.	0.518	b.d.l.	b.d.l.	b.d.l.	93.7
18	0.300	5.24	8.71	75.7	3.78	0.134	0.487	b.d.l.	b.d.l.	b.d.l.	94.4
20	0.318	4.84	9.50	75.1	3.80	0.181	0.427	b.d.l.	b.d.l.	b.d.l.	94.1
21	b.d.l.	5.51	10.69	72.6	4.57	0.224	0.419	b.d.l.	b.d.l.	b.d.l.	94.0
24	b.d.l.	5.34	7.06	77.9	3.15	0.172	0.327	b.d.l.	b.d.l.	b.d.l.	93.9
VUL 9703 B											
9	b.d.l.	0.53	31.90	19.6	17.00	b.d.l.	b.d.l.	b.d.l.	30.73	b.d.l.	99.8
10	b.d.l.	8.86	6.17	74.8	5.44	b.d.l.	0.392	b.d.l.	b.d.l.	b.d.l.	95.6
15	b.d.l.	3.51	10.07	73.0	7.82	0.298	1.045	b.d.l.	b.d.l.	b.d.l.	95.7
22	b.d.l.	0.53	22.23	26.1	12.91	b.d.l.	b.d.l.	b.d.l.	37.01	b.d.l.	98.8
VUL 9705											
3	0.612	2.96	1.97	83.0	0.46	0.181	0.324	b.d.l.	b.d.l.	0.112	89.6
5	b.d.l.	0.82	3.11	83.8	1.54	0.229	1.490	b.d.l.	b.d.l.	0.098	91.1
11	0.353	10.07	12.16	67.5	0.98	0.272	0.534	b.d.l.	b.d.l.	0.079	92.0
VUL 9707											
68	b.d.l.	8.13	4.22	78.1	1.19	b.d.l.	1.390	b.d.l.	b.d.l.	b.d.l.	93.1
71	b.d.l.	5.86	3.58	81.1	0.81	b.d.l.	1.430	b.d.l.	b.d.l.	b.d.l.	92.8
76	b.d.l.	5.96	3.90	81.3	1.53	b.d.l.	1.055	b.d.l.	b.d.l.	b.d.l.	93.7
77	b.d.l.	6.31	3.60	81.1	1.03	b.d.l.	1.340	b.d.l.	b.d.l.	b.d.l.	93.4
80	b.d.l.	10.73	2.55	77.2	0.58	b.d.l.	1.680	b.d.l.	b.d.l.	b.d.l.	92.7
82	b.d.l.	6.59	2.11	81.6	0.56	0.092	1.570	b.d.l.	b.d.l.	b.d.l.	92.5

Tab. A-11: continued

No	SiO_2	TiO_2	Al_2O_3	FeO	MgO	CaO	MnO	BaO	Cr_2O_3	K_2O	Σ
ORC 9701											
18	b.d.l.	8.57	1.10	62.0	3.47	b.d.l.	0.360	b.d.l.	19.82	0.045	95.3
23	b.d.l.	6.51	0.43	60.9	2.70	b.d.l.	0.326	b.d.l.	23.32	0.055	94.2
25	b.d.l.	8.68	0.82	60.4	2.99	b.d.l.	0.388	b.d.l.	21.70	b.d.l.	94.9
SVC 9702											
102	3.790	0.13	1.96	83.1	0.14	0.345	0.030	0.027	0.00	0.064	89.6
AMT 9703 II											
35	0.350	5.48	3.00	83.4	0.85	0.052	0.598	b.d.l.	b.d.l.	0.113	93.8
36	b.d.l.	17.05	6.78	64.3	2.02	0.123	0.595	b.d.l.	b.d.l.	0.086	90.9
39	b.d.l.	5.98	4.39	80.8	0.96	0.062	0.673	b.d.l.	b.d.l.	0.053	92.9
43	b.d.l.	5.90	3.37	82.3	0.38	b.d.l.	0.231	b.d.l.	b.d.l.	0.051	92.3
49	b.d.l.	11.07	6.28	72.8	1.36	b.d.l.	0.386	b.d.l.	b.d.l.	b.d.l.	91.9
52	b.d.l.	b.d.l.	b.d.l.	74.2	b.d.l.	0.380	b.d.l.	b.d.l.	b.d.l.	b.d.l.	74.6
RAD 9701											
77	b.d.l.	3.88	12.94	42.3	4.82	b.d.l.	0.218	b.d.l.	32.84	b.d.l.	97.0
293	b.d.l.	3.99	12.75	42.0	4.87	b.d.l.	0.196	b.d.l.	32.84	b.d.l.	96.7
RAD 9702 A											
80	b.d.l.	0.41	16.91	35.2	5.79	b.d.l.	b.d.l.	b.d.l.	38.34	b.d.l.	96.6
86	b.d.l.	b.d.l.	12.65	43.8	5.36	b.d.l.	0.462	b.d.l.	33.11	b.d.l.	95.3
TA 9701 whole rock											
38	b.d.l.	1.39	4.37	13.7	14.17	b.d.l.	b.d.l.	b.d.l.	63.79	b.d.l.	97.4
42	b.d.l.	0.54	3.37	18.6	10.12	b.d.l.	b.d.l.	b.d.l.	65.67	b.d.l.	98.3
TA 9701 peridotitic xenolith											
6	b.d.l.	0.98	6.86	22.0	8.22	b.d.l.	b.d.l.	b.d.l.	58.33	0.077	96.5
12	b.d.l.	0.86	11.98	19.5	11.75	b.d.l.	b.d.l.	b.d.l.	54.73	0.132	99.0
19	b.d.l.	0.61	11.46	17.6	12.80	b.d.l.	b.d.l.	b.d.l.	55.77	0.154	98.3

Tab. A-12: Chemical composition of ilmenites by EMPA.

No	TiO_2	Al_2O_3	FeO	MgO	CaO	MnO	Cr_2O_3	K_2O	Σ
ORC 9701									
4	48.9	b.d.l.	45.7	2.72	b.d.l.	0.725	b.d.l.	0.077	98.1
11	49.5	b.d.l.	44.0	3.91	0.059	0.545	0.221	0.088	98.3
12	47.0	b.d.l.	46.6	2.59	0.126	0.640	b.d.l.	0.085	97.0
15	47.4	b.d.l.	45.8	2.64	0.231	0.715	b.d.l.	0.161	96.9
SVC 9702									
107	52.4	b.d.l.	45.1	1.21	b.d.l.	0.721	b.d.l.	b.d.l.	99.4
118	48.1	b.d.l.	44.8	2.26	b.d.l.	2.270	b.d.l.	0.156	97.5
127	50.8	b.d.l.	45.2	1.52	b.d.l.	1.340	b.d.l.	b.d.l.	98.8
129	49.1	b.d.l.	45.7	2.09	b.d.l.	0.947	b.d.l.	0.086	98.0
135	52.3	b.d.l.	43.4	1.79	b.d.l.	0.663	b.d.l.	b.d.l.	98.1
SVC 9703									
34	53.9	b.d.l.	43.9	1.49	b.d.l.	0.586	b.d.l.	b.d.l.	99.9
42	53.6	b.d.l.	42.9	1.68	b.d.l.	0.579	b.d.l.	b.d.l.	98.8
43	54.4	b.d.l.	42.7	1.71	b.d.l.	0.599	b.d.l.	b.d.l.	99.4
45	53.2	0.189	43.8	1.33	b.d.l.	0.596	b.d.l.	b.d.l.	99.2
51	53.6	b.d.l.	44.1	1.44	b.d.l.	0.628	b.d.l.	b.d.l.	99.8
62	54.6	0.191	42.8	1.63	b.d.l.	0.558	b.d.l.	b.d.l.	99.7
199	53.7	b.d.l.	44.2	1.45	b.d.l.	0.573	b.d.l.	b.d.l.	99.9
AMT 9702									
67	52.5	b.d.l.	45.8	1.57	b.d.l.	0.631	b.d.l.	b.d.l.	100.4
71	52.7	b.d.l.	44.9	1.73	b.d.l.	0.596	b.d.l.	b.d.l.	100.0
79	53.1	b.d.l.	44.3	1.76	b.d.l.	0.588	b.d.l.	b.d.l.	99.7
87	53.1	0.192	44.3	1.94	b.d.l.	0.669	b.d.l.	b.d.l.	100.2
90	53.1	0.221	45.0	1.99	b.d.l.	0.681	b.d.l.	b.d.l.	100.9
91	52.1	b.d.l.	44.2	2.45	b.d.l.	0.646	b.d.l.	b.d.l.	99.5
93	53.2	0.190	44.2	1.82	b.d.l.	0.597	b.d.l.	b.d.l.	100.0
98	52.5	b.d.l.	44.3	2.01	b.d.l.	0.566	b.d.l.	b.d.l.	99.4
99	52.9	0.183	44.3	1.85	b.d.l.	0.639	b.d.l.	b.d.l.	99.9
100	52.3	0.194	45.2	1.74	b.d.l.	0.567	b.d.l.	b.d.l.	100.0
AMT 9704 A									
52	52.1	0.266	42.7	3.03	b.d.l.	0.724	b.d.l.	b.d.l.	98.8
61	51.2	b.d.l.	44.2	2.49	b.d.l.	0.618	b.d.l.	b.d.l.	98.5
64	51.5	b.d.l.	44.2	2.75	b.d.l.	0.642	b.d.l.	b.d.l.	99.0
RAD 9701									
78	48.8	b.d.l.	45.9	2.50	0.050	0.638	b.d.l.	0.045	97.9
84	45.9	b.d.l.	46.3	2.00	b.d.l.	0.617	b.d.l.	b.d.l.	94.8
87	50.5	b.d.l.	44.7	2.93	0.066	0.613	b.d.l.	0.103	99.1
RAD 9702 A									
71	41.9	0.376	45.0	4.71	0.149	b.d.l.	b.d.l.	0.116	92.3
78	50.3	1.624	38.6	3.32	b.d.l.	b.d.l.	b.d.l.	0.049	93.8
87	42.8	b.d.l.	45.3	4.15	0.077	0.623	b.d.l.	0.075	93.1

Tab. A-12: continued

No	TiO_2	Al_2O_3	FeO	MgO	CaO	MnO	Cr_2O_3	K_2O	Σ
TA 9701 whole rock									
24	54.6	0.313	35.4	9.10	b.d.l.	b.d.l.	b.d.l.	b.d.l.	99.5
32	49.4	0.322	43.6	3.47	b.d.l.	0.490	0.612	0.100	98.0
48	55.1	0.456	29.8	12.66	b.d.l.	b.d.l.	0.582	b.d.l.	98.6
49	55.9	0.288	29.5	12.69	b.d.l.	b.d.l.	0.478	b.d.l.	98.8
50	54.6	0.278	34.7	9.42	b.d.l.	0.470	b.d.l.	b.d.l.	99.5
54	53.4	0.403	35.5	8.69	b.d.l.	b.d.l.	b.d.l.	0.087	98.2

Tab. A-13: Chemical composition of apatites by EMPA.

No.	SiO_2	Al_2O_3	FeO	MgO	CaO	Na_2O	K_2O	P_2O5	La_2O_3	Ce_2O_3	Pr_2O_3	Nd_2O_3	S
Montefiascone													
46	b.d.l.	b.d.l.	0.194	0.176	54.8	b.d.l.	0.182	40.2	0.328	0.594	b.d.l.	0.227	97.5
47	1.082	0.128	0.209	0.102	53.0	b.d.l.	0.643	39.8	0.483	0.964	0.163	0.273	96.8
48	0.769	b.d.l.	0.207	0.150	53.7	b.d.l.	0.430	39.3	0.470	0.794	b.d.l.	0.290	96.2
VUL 9701													
48	2.710	0.294	0.435	0.075	52.4	0.223	0.023	36.8	0.578	1.240	0.186	0.589	95.5
49	2.610	0.190	0.356	0.118	52.2	0.270	0.028	36.9	0.508	1.112	0.124	0.482	94.9
50	2.170	0.307	0.171	0.068	53.1	0.261	0.030	38.1	0.526	1.027	b.d.l.	0.505	96.4
VUL 9707													
39	18.680	6.460	0.261	b.d.l.	38.2	1.430	2.270	29.6	0.440	0.923	b.d.l.	0.364	98.7
40	9.660	6.840	0.270	b.d.l.	45.5	0.443	0.064	32.0	0.449	0.924	b.d.l.	0.390	96.7
41	8.000	5.380	0.216	b.d.l.	47.9	0.424	0.062	33.0	0.475	0.951	b.d.l.	0.471	97.0
44	7.230	2.280	0.243	0.079	48.7	0.422	0.740	36.3	0.594	1.220	0.121	0.545	98.5
45	1.662	0.122	0.122	0.053	52.3	0.146	0.470	39.9	0.256	0.607	b.d.l.	0.260	95.9
ORC 9701													
41	2.610	0.110	1.018	2.200	49.2	0.191	0.198	39.2	0.513	1.280	0.164	0.767	97.5
44	3.240	b.d.l.	0.493	0.971	50.7	0.229	0.244	39.2	0.550	1.370	b.d.l.	0.823	98.0
46	b.d.l.	b.d.l.	0.264	0.135	52.7	0.225	0.168	41.5	0.557	1.270	0.172	0.768	98.4
57	0.799	0.099	0.289	0.168	52.1	0.256	0.119	41.0	0.579	1.320	0.181	0.824	97.7
SVC 9702													
11	b.d.l.	0.205	0.974	0.200	53.5	b.d.l.	b.d.l.	41.8	0.079	0.244	b.d.l.	0.230	97.9
12	b.d.l.	b.d.l.	1.910	0.413	52.9	b.d.l.	0.079	42.5	0.096	0.230	b.d.l.	0.185	98.7
60	b.d.l.	b.d.l.	2.460	0.442	51.9	b.d.l.	0.108	42.3	0.058	0.243	b.d.l.	0.238	98.2
SVC 9703													
19	b.d.l.	b.d.l.	0.747	0.210	53.4	b.d.l.	0.088	42.9	b.d.l.	0.157	b.d.l.	0.125	98.2
28	1.509	0.671	1.880	0.394	51.9	b.d.l.	0.061	40.7	0.066	0.176	b.d.l.	0.119	97.8
29	1.709	0.770	2.020	0.426	51.2	b.d.l.	0.085	40.9	b.d.l.	0.173	b.d.l.	0.178	97.8
AMT 9704 A													
51	b.d.l.	b.d.l.	0.251	0.078	55.2	b.d.l.	0.106	43.2	0.196	0.464	b.d.l.	0.347	100.5
52	b.d.l.	0.111	0.290	0.053	54.9	b.d.l.	0.065	42.1	0.173	0.398	b.d.l.	0.236	98.8
53	b.d.l.	0.104	0.247	0.069	54.3	b.d.l.	0.024	42.3	0.153	0.435	b.d.l.	0.273	98.4
54	b.d.l.	b.d.l.	0.273	0.060	55.3	b.d.l.	0.060	42.4	0.132	0.449	0.127	0.282	99.5

Tab. A-14: Chemical composition of olivines by LA-ICP-MS.

No	mineral	Cr	Ni	Rb	Sr	Ba	La	Ce	Pr	Nd	Sm	Eu	Gd	Dy	Yb
VUL 9703 B															
51	ol	< 60	799	< 7.9	< 0.56	< 2.9	< 0.094	< 0.075	< 0.086	< 0.21	0.19	< 0.19	< 0.11	< 0.12	< 0.13
ORC 9701															
222	ol	166	584	46	24	9.2	15	38	5	21	3	0.38	1.2	0.6	0.36
223	ol	207	1296	< 7.9	1.3	< 2.9	0.32	1.1	0.11	< 0.21	0.27	< 0.19	< 0.11	< 0.12	< 0.13
224	ol	89	725	< 7.9	4.2	4	3.2	6.2	0.86	4.2	0.55	< 0.19	0.12	< 0.12	< 0.13
225	ol	< 60	2288	< 7.9	0.75	< 2.9	0.23	0.77	< 0.086	0.39	< 0.16	< 0.19	< 0.11	< 0.12	< 0.13
RAD 9701															
113	ol	< 60	559	< 7.9	4.1	< 2.9	0.21	1.1	< 0.086	0.53	0.37	< 0.19	0.13	< 0.12	0.28
116	ol	< 60	818	< 7.9	< 0.56	< 2.9	< 0.094	< 0.075	< 0.086	< 0.21	< 0.16	< 0.19	< 0.11	< 0.12	0.22
117	ol	< 60	170	< 7.9	0.82	< 2.9	< 0.094	< 0.075	< 0.086	< 0.21	< 0.16	< 0.19	< 0.11	< 0.12	0.38
120	ol	< 60	1669	< 7.9	12	< 2.9	0.18	0.35	< 0.086	< 0.21	< 0.16	< 0.19	< 0.11	< 0.12	0.34
RAD 9702 A															
126	ol	< 60	373	15	62	168	6	13	1.5	5.7	0.88	0.3	0.69	0.56	0.49
128	ol	114	488	< 7.9	1.3	7.5	0.17	0.19	< 0.086	< 0.21	0.37	< 0.19	< 0.11	0.17	< 0.13
132	ol	85	331	< 7.9	< 0.56	< 2.9	< 0.094	< 0.075	< 0.086	< 0.21	< 0.16	< 0.19	< 0.11	0.21	< 0.13
136	ol	316	768	< 7.9	31	290	3.7	5.3	0.97	3.4	0.75	< 0.19	0.83	1	1.2
TA 9701 whole rock															
102	ol	< 60	4740	< 7.9	7.5	17	1.5	3.2	0.45	1.7	0.16	< 0.19	0.2	< 0.12	< 0.13
106	ol	< 60	898	< 7.9	< 0.56	< 2.9	< 0.094	0.23	< 0.086	< 0.21	< 0.16	< 0.19	< 0.11	< 0.12	< 0.13
110	ol	< 60	< 14	< 7.9	3.1	< 2.9	0.71	2.9	0.17	0.67	0.25	< 0.19	0.12	< 0.12	< 0.13
TA 9701 peridotitic xenolith															
82	ol	< 60	< 14	< 7.9	2.1	< 2.9	< 0.094	< 0.075	< 0.086	< 0.21	< 0.16	< 0.19	< 0.11	< 0.12	0.14
83	ol	224	< 14	< 7.9	< 0.56	< 2.9	< 0.094	< 0.075	< 0.086	0.28	< 0.16	< 0.19	< 0.11	< 0.12	< 0.13
84	ol	217	< 14	< 7.9	< 0.56	< 2.9	0.12	0.24	< 0.086	< 0.21	< 0.16	< 0.19	0.15	< 0.12	0.17
85	ol	170	< 14	< 7.9	< 0.56	< 2.9	< 0.094	< 0.075	< 0.086	< 0.21	0.23	< 0.19	< 0.11	< 0.12	< 0.13

Tab. A-15: Chemical composition of clinopyroxenes by LA-ICP-MS.

No	mineral	Cr	Ni	Rb	Sr	Ba	La	Ce	Pr	Nd	Sm	Eu	Gd	Dy	Yb
VUL 9701															
28	cpx	< 60	< 14	< 7.9	458	< 2.9	88	266	43	212	45	8.1	33	24	10
29	cpx	< 60	< 14	11	576	13	199	503	73	319	63	9.8	48	32	13
30	cpx	< 60	< 14	< 7.9	859	5.1	189	541	86	418	92	16	67	49	19
31	cpx	< 60	< 14	< 7.9	426	< 2.9	86	281	43	207	43	8.2	33	22	8.1
32	cpx	< 60	< 14	< 7.9	509	< 2.9	84	257	41	200	43	7.7	30	21	8.9
33	cpx	< 60	< 14	< 7.9	491	7.2	87	271	44	212	46	8.3	35	24	8.1
VUL 9702															
42	cpx	< 60	16	< 7.9	139	< 2.9	11	39	7.3	43	10	2.3	9.1	6.6	1.9
43	cpx	< 60	24	25	304	133	20	56	9.1	48	11	2.4	9.2	6.3	1.9
44	cpx	149	34	8.6	169	86	13	29	4.5	24	5.3	1.2	4.4	3.2	0.92
45	cpx	< 60	< 14	< 7.9	100	10	8.1	29	5.4	30	7.5	1.7	6.3	5.5	1.4
46	cpx	< 60	< 14	< 7.9	50	< 2.9	2.8	12	2.2	12	3.9	0.67	2.6	2	0.63
VUL 9703 B															
52	cpx	6111	192	< 7.9	59	< 2.9	2.8	9.5	1.9	10	3	0.83	3	3.2	0.88
53	cpx	2461	176	< 7.9	75	4.6	5.2	16	3.2	17	4.8	1.1	4.6	4.2	1.8
54	cpx	2360	194	< 7.9	63	< 2.9	3.7	14	2.3	15	3.2	0.92	3.3	2.9	1.1
55	cpx	1544	180	< 7.9	62	3.3	4.1	17	2.5	14	3.8	1	3.8	2.8	1.2
56	cpx	1830	214	< 7.9	90	19	8.1	27	4.5	25	7.9	1.4	7.1	5.7	2.2
57	cpx	256	101	< 7.9	126	39	6.9	36	6.7	28	5	1.1	3.8	3	0.96
58	cpx	11689	224	< 7.9	92	< 2.9	4.1	13	2.3	13	3.5	0.8	3.6	2.9	1
VUL 9705															
61	cpx	< 60	147	< 7.9	352	< 2.9	6.1	22	3.4	16	5.2	1.1	2.2	1.1	0.29
62	cpx	< 60	229	< 7.9	262	< 2.9	5.6	19	3.3	15	3.3	0.51	2.3	1.4	0.23
63	cpx	< 60	680	< 7.9	199	< 2.9	4.4	15	2.6	13	2.7	0.56	2.4	1	0.32
64	cpx	< 60	222	< 7.9	217	< 2.9	5.1	18	3.1	16	2.7	0.79	2.4	1.3	0.33
65	cpx	< 60	< 14	< 7.9	133	< 2.9	3.3	10	1.6	9	2.3	0.44	1.7	0.87	0.19
66	cpx	< 60	21	< 7.9	103	< 2.9	2.4	7.6	1.7	8.6	2.3	0.44	1.4	0.78	0.23
67	cpx	< 60	224	< 7.9	122	< 2.9	5.2	17	3.2	16	4.1	0.78	3.2	1.7	0.46
VUL 9707															
72	cpx	< 60	16	< 7.9	571	< 2.9	93	227	37	183	38	7.1	24	16	5.8
73	cpx	< 60	< 14	< 7.9	459	39	69	190	34	162	36	6.7	24	16	5.8
74	cpx	< 60	< 14	< 7.9	359	53	50	155	26	129	30	5.6	20	13	4.4
76	cpx	< 60	< 14	< 7.9	422	5	82	212	34	152	33	5.7	24	16	5.8
ORC 9701															
219	cpx	2797	84	< 7.9	95	8.5	17	42	8.9	51	12	1.5	7	2.6	1.1
220	cpx	2291	57	< 7.9	119	< 2.9	20	60	11	63	13	1.6	6	2.4	0.63
221	cpx	1774	43	< 7.9	76	< 2.9	21	43	7.7	39	8.6	1.1	4.8	2.3	0.57
227	cpx	3628	131	< 7.9	285	3.2	65	186	32	165	32	4.2	15	6.9	1.8
229	cpx	3104	126	23	342	24	93	232	38	207	36	4.8	20	6.9	0.9
231	cpx	4758	150	< 7.9	334	< 2.9	82	214	36	183	34	4.2	15	6.3	1.8
AMT 9703 II															
146	cpx	731	113	< 7.9	96	< 2.9	5.9	18	3.2	18	4.8	0.88	4.3	3	0.85
147	cpx	1016	108	< 7.9	114	3.3	8.6	24	4.2	22	6.1	1.1	5.1	3.1	0.99
148	cpx	977	133	< 7.9	135	9.2	9.3	28	6.1	26	7.2	1.7	5.7	5.5	2.1
150	cpx	600	89	< 7.9	115	< 2.9	6.5	20	4	23	6	1.2	5.8	3.5	1.1

Tab. A-15: continued

No	mineral	Cr	Ni	Rb	Sr	Ba	La	Ce	Pr	Nd	Sm	Eu	Gd	Dy	Yb
AMT 9704 A															
137	cpx	4822	125	< 7.9	75	< 2.9	2.2	7.5	1.4	7.8	2.2	0.48	2.2	1.5	0.52
138	cpx	4231	113	< 7.9	75	< 2.9	2.4	7.8	1.5	7.7	2.1	0.49	2.1	1.5	0.36
139	cpx	5568	108	< 7.9	83	< 2.9	3.2	10	1.9	10	3	0.55	2.6	1.7	0.5
140	cpx	6880	99	< 7.9	78	< 2.9	3.1	9.9	1.8	10	2.5	0.59	2.3	1.4	0.47
141	cpx	839	65	17	125	85	14	26	5.5	28	6.9	1.2	5.4	3.8	1.5
RAD 9701															
112	cpx	< 60	71	< 7.9	20	13	4.3	15	3.2	18	7.8	0.84	7.7	6.9	2.4
114	cpx	< 60	19	< 7.9	32	4.2	3.6	14	3	18	5.7	0.64	5.9	4.5	1.8
121	cpx	522	< 14	8	48	20	4.5	14	3.1	17	6.1	0.98	6.3	6.1	2.2
122	cpx	< 60	< 14	< 7.9	34	6.8	4.8	18	3.9	24	5.9	0.7	5.4	4.8	2
123	cpx	< 60	< 14	< 7.9	26	< 2.9	4.3	17	3.7	20	5.8	0.75	6	4.6	2
RAD 9702 A															
124	cpx	5322	44	< 7.9	21	< 2.9	3.8	14	3	18	6.3	0.66	5.4	4.1	1.7
127	cpx	2857	33	< 7.9	21	4.7	2.4	9.2	1.9	11	3	0.39	2.7	2.2	0.9
135	cpx	8066	50	< 7.9	36	3.5	4.5	17	3.5	23	5.9	0.7	5.4	4.7	1.9
TA 9701 peridotitic xenolith															
86	cpx	< 60	< 14	< 7.9	25	< 2.9	24	57	7.9	37	9.6	1	10	9.9	3.2
87	cpx	< 60	< 14	< 7.9	24	< 2.9	25	60	8	38	10	0.95	11	9.8	3.1
88	cpx	< 60	< 14	< 7.9	18	< 2.9	25	68	8.9	39	9.5	1.1	9.9	9.1	3.4
89	cpx	< 60	< 14	< 7.9	18	< 2.9	22	64	7.8	36	8.2	0.95	8.4	7.9	2.7

Tab. A-16: Chemical composition of orthopyroxenes by LA-ICP-MS.

No	SiO_2	TiO_2	Al_2O_3	FeO	MgO	CaO	MnO	Cr_2O_3	Σ		en	fs	wo	tsch
AMT 9702														
68	51.4	0.201	0.403	32.05	15.4	1.232	0.705	b.d.l.	101.4		44.38	53.06	2.56	0.00
72	51.2	b.d.l.	0.377	32.08	15.3	1.410	0.665	b.d.l.	101.1		44.16	52.92	2.92	0.00
73	51.1	0.197	0.590	32.88	14.8	1.283	0.769	b.d.l.	101.6		42.74	54.59	2.67	0.00
74	51.7	0.217	0.672	31.52	16.1	1.162	0.712	b.d.l.	102.1		46.00	51.62	2.38	0.00
75	51.2	0.209	0.568	31.87	15.4	1.520	0.740	b.d.l.	101.5		44.23	52.63	3.14	0.00
78	51.5	b.d.l.	0.295	32.52	15.0	1.302	0.737	b.d.l.	101.4		43.36	53.93	2.70	0.00
97	51.3	b.d.l.	0.434	31.74	15.5	1.080	0.913	b.d.l.	100.9		44.77	52.99	2.24	0.00
101	51.2	b.d.l.	0.405	32.70	14.6	1.393	0.801	b.d.l.	101.0		42.43	54.66	2.91	0.00
103	50.9	0.324	1.056	32.42	14.7	1.071	0.783	b.d.l.	101.2		43.11	54.63	2.26	0.02
108	51.4	b.d.l.	0.388	31.79	15.3	1.356	0.753	b.d.l.	100.9		44.24	52.93	2.82	0.00
221	51.2	b.d.l.	0.369	31.77	15.0	1.347	0.701	b.d.l.	100.4		43.84	53.33	2.83	0.01
222	51.5	b.d.l.	0.434	32.20	14.9	1.388	0.780	b.d.l.	101.2		43.36	53.74	2.90	0.01
223	50.8	b.d.l.	0.504	32.92	14.8	1.357	0.785	b.d.l.	101.2		42.68	54.51	2.81	0.00
224	51.2	b.d.l.	0.388	32.12	15.3	1.470	0.792	b.d.l.	101.2		43.85	53.10	3.04	0.00
225	51.4	0.201	0.424	32.21	15.1	1.313	0.802	b.d.l.	101.4		43.73	53.54	2.73	0.00
226	51.1	b.d.l.	0.470	32.55	14.9	1.286	0.759	b.d.l.	101.0		43.08	54.24	2.68	0.00
227	51.1	b.d.l.	0.450	32.57	14.9	1.326	0.734	b.d.l.	101.1		43.18	54.06	2.76	0.00
228	50.8	b.d.l.	0.629	32.80	14.6	1.315	0.826	b.d.l.	101.0		42.42	54.83	2.75	0.00
229	50.9	b.d.l.	0.677	32.82	14.5	1.343	0.835	b.d.l.	101.1		42.23	54.96	2.81	0.01
230	51.6	b.d.l.	0.576	32.12	15.1	1.276	0.827	b.d.l.	101.5		43.84	53.51	2.65	0.01
231	51.3	b.d.l.	0.762	32.42	14.5	1.347	0.780	b.d.l.	101.1		42.48	54.68	2.84	0.02
232	51.4	b.d.l.	0.632	32.81	14.6	1.264	0.782	b.d.l.	101.5		42.53	54.82	2.64	0.01
233	51.4	0.208	0.543	30.98	15.9	1.370	0.750	b.d.l.	101.1		45.85	51.32	2.84	0.00
234	51.5	0.222	0.502	31.11	16.0	1.293	0.672	b.d.l.	101.4		46.09	51.24	2.67	0.00
235	51.5	0.218	0.460	30.97	15.8	1.375	0.746	b.d.l.	101.1		45.70	51.45	2.86	0.00
236	51.5	0.212	0.640	31.26	16.0	1.371	0.708	b.d.l.	101.6		45.74	51.43	2.83	0.00
237	51.3	0.205	0.534	30.88	15.8	1.321	0.679	b.d.l.	100.7		45.77	51.47	2.76	0.01
238	51.6	b.d.l.	0.535	31.15	16.0	1.371	0.705	b.d.l.	101.3		45.83	51.34	2.83	0.00
239	51.4	0.243	0.647	31.13	15.9	1.367	0.694	b.d.l.	101.3		45.71	51.46	2.83	0.01
240	51.7	b.d.l.	0.564	31.05	15.8	1.377	0.646	b.d.l.	101.1		45.68	51.45	2.86	0.01
241	51.6	b.d.l.	0.562	31.20	15.9	1.340	0.701	b.d.l.	101.3		45.78	51.45	2.77	0.01
242	51.8	b.d.l.	0.558	31.42	16.0	1.400	0.721	b.d.l.	101.9		45.67	51.45	2.88	0.00
243	51.1	0.220	0.486	32.02	15.1	1.420	0.679	b.d.l.	101.0		43.85	53.19	2.96	0.00
244	51.3	b.d.l.	0.347	32.39	15.0	1.286	0.714	b.d.l.	101.1		43.52	53.80	2.68	0.00

Tab. A-16: continued

No	SiO_2	TiO_2	Al_2O_3	FeO	MgO	CaO	MnO	Cr_2O_3	Σ		en	fs	wo	tsch
TA 9701 peridotitic xenolith														
2	55.6	b.d.l.	3.710	6.24	33.2	0.909	b.d.l.	0.523	100.1		88.43	9.83	1.74	0.06
3	55.8	b.d.l.	3.610	6.04	33.1	0.862	b.d.l.	0.419	99.8		88.54	9.80	1.66	0.07
153	55.5	b.d.l.	3.690	5.91	32.9	0.882	b.d.l.	0.535	99.4		88.56	9.73	1.71	0.07
154	55.3	b.d.l.	3.630	6.18	33.0	0.922	b.d.l.	0.523	99.6		88.52	9.71	1.77	0.06
155	55.6	b.d.l.	3.560	6.15	33.2	0.925	b.d.l.	0.528	99.9		88.61	9.62	1.78	0.06
156	55.7	b.d.l.	3.730	6.06	33.1	0.878	b.d.l.	0.531	99.9		88.49	9.83	1.69	0.07
157	55.4	b.d.l.	3.730	6.02	32.8	0.851	b.d.l.	0.569	99.4		88.47	9.88	1.65	0.07
158	56.1	b.d.l.	3.720	6.05	33.2	0.871	b.d.l.	0.573	100.6		88.60	9.74	1.67	0.07
159	55.7	b.d.l.	3.650	6.15	33.0	0.914	b.d.l.	0.520	99.9		88.35	9.89	1.76	0.07
160	55.5	b.d.l.	3.710	6.20	33.1	0.931	b.d.l.	0.535	100.0		88.63	9.58	1.79	0.06
161	55.4	b.d.l.	3.700	6.09	33.0	0.859	b.d.l.	0.529	99.5		88.60	9.74	1.66	0.07
162	55.8	b.d.l.	3.650	6.04	32.9	0.909	b.d.l.	0.531	99.8		88.36	9.89	1.75	0.07
163	55.3	b.d.l.	3.670	5.92	33.2	0.906	b.d.l.	0.579	99.5		89.04	9.22	1.75	0.06
164	55.8	b.d.l.	3.710	6.21	33.0	0.939	b.d.l.	0.547	100.2		88.23	9.97	1.80	0.07
165	55.6	b.d.l.	3.660	5.95	32.8	0.829	b.d.l.	0.504	99.4		88.55	9.84	1.61	0.07
166	55.6	b.d.l.	3.590	6.11	32.9	0.863	b.d.l.	0.541	99.6		88.38	9.95	1.67	0.07
167	55.6	b.d.l.	3.600	6.03	33.1	0.860	b.d.l.	0.513	99.7		88.68	9.67	1.66	0.07
168	55.6	b.d.l.	3.590	6.08	32.8	0.864	b.d.l.	0.549	99.4		88.28	10.05	1.67	0.07
169	55.3	b.d.l.	3.740	6.07	32.8	0.884	b.d.l.	0.508	99.3		88.44	9.84	1.72	0.07
170	55.7	b.d.l.	3.700	6.01	33.1	0.880	b.d.l.	0.541	99.9		88.56	9.74	1.70	0.07
171	55.6	b.d.l.	3.640	6.20	33.2	0.872	b.d.l.	0.539	100.0		88.59	9.74	1.67	0.06
172	56.3	b.d.l.	3.740	6.03	32.9	0.873	b.d.l.	0.510	100.3		88.06	10.26	1.68	0.07
173	55.8	b.d.l.	3.740	6.13	33.2	0.873	b.d.l.	0.531	100.3		88.55	9.78	1.67	0.07
174	55.7	b.d.l.	3.610	6.16	32.9	0.881	b.d.l.	0.469	99.7		88.32	9.97	1.70	0.07
175	55.8	b.d.l.	3.720	6.04	32.8	0.885	b.d.l.	0.449	99.8		88.27	10.02	1.71	0.08
176	55.8	b.d.l.	3.770	5.95	32.8	0.868	b.d.l.	0.482	99.7		88.40	9.92	1.68	0.08
177	55.8	b.d.l.	3.690	5.93	32.8	0.832	b.d.l.	0.494	99.6		88.38	10.01	1.61	0.07

Tab. A-17: Chemical composition of sanidines by LA-ICP-MS.

No	mineral	Cr	Ni	Rb	Sr	Ba	La	Ce	Pr	Nd	Sm	Eu	Gd	Dy	Yb
ORC 9701															
226	san	< 60	15	704	888	1367	53	134	18	73	10	2.8	4.6	2.5	1.1
228	san	< 60	22	707	1563	992	30	55	6.9	29	3.6	2	1.8	0.55	0.54
230	san	< 60	76	596	1137	437	260	575	88	380	53	6.9	22	10	3.6
232	san	< 60	72	640	677	398	116	289	38	151	20	2.8	9	4.4	2.3
233	san	< 60	183	464	314	172	206	483	62	248	34	3.7	15	8	4.2
ROC 9701															
201	san	< 60	< 14	199	278	1599	1.4	1.1	< 0.086	< 0.21	0.27	1.7	< 0.11	< 0.12	< 0.13
202	san	< 60	< 14	223	316	2080	1.8	1.4	0.095	< 0.21	< 0.16	1.9	< 0.11	< 0.12	< 0.13
203	san	< 60	< 14	177	294	1876	1.4	1.5	< 0.086	< 0.21	< 0.16	1.8	< 0.11	< 0.12	< 0.13
204	san	< 60	< 14	276	126	390	1.9	1.5	0.19	0.32	< 0.16	0.75	0.12	< 0.12	< 0.13
SVC 9702															
174	san	< 60	< 14	261	145	327	67	113	16	62	10	1	7.5	6.4	3.5
175	san	< 60	< 14	235	86	183	26	38	6.2	26	5	0.57	4.2	2.5	1.2
176	san	< 60	< 14	303	238	625	119	204	28	114	18	1.4	11	10	17
179	san	< 60	< 14	223	878	277	39	54	7.1	28	4.6	1.6	3.6	2.8	1.2
189	san	< 60	< 14	235	220	280	43	57	9.1	37	7.4	1.3	4.9	3.7	1.2
191	san	< 60	32	325	158	482	22	29	4.4	18	3.8	0.78	1.9	1.6	1
192	san	< 60	< 14	223	67	240	19	36	4.8	19	3.4	0.45	2.6	2.1	0.83
SVC 9703															
8	san	< 60	< 14	161	129	155	8.7	17	1.9	6.9	1.7	1	1.9	1.3	0.52
9	san	< 60	< 14	165	132	162	9	17	2	7.2	1.7	1.1	1.9	1.3	0.53
10	san	< 60	< 14	407	65	340	17	37	4.3	18	4	0.68	4.5	4	1.5
11	san	< 60	< 14	420	42	317	15	35	4.1	15	3.7	0.41	3.3	3.7	1.4
12	san	< 60	< 14	470	42	328	15	36	4	15	4	0.41	3.9	3.6	1.6
25	san	< 60	< 14	232	35	131	6.1	13	1.4	4.8	1.3	0.24	1.2	1	0.46
26	san	< 60	< 14	293	28	169	7.6	18	2	6	1.7	0.2	2.2	1.5	0.95
AMT 9702															
156	san	< 60	< 14	201	661	1368	4.9	4.1	0.2	0.44	< 0.16	2.3	< 0.11	< 0.12	< 0.13
157	san	< 60	< 14	155	560	1244	3.1	2	0.11	< 0.21	< 0.16	1.8	< 0.11	< 0.12	< 0.13
158	san	< 60	< 14	154	436	793	3.5	2	0.12	0.23	< 0.16	1.4	< 0.11	< 0.12	< 0.13
159	san	< 60	< 14	160	370	749	3	1.8	0.1	< 0.21	< 0.16	1.2	< 0.11	< 0.12	< 0.13
AMT 9703 II															
151	san	< 60	< 14	452	2095	1783	108	153	19	71	10	3.1	6.8	3.9	1.3
152	san	< 60	< 14	442	2224	1686	187	294	36	129	20	3.3	13	8.2	3.1
153	san	< 60	< 14	365	1578	785	135	236	26	90	13	2.1	8.1	4.6	1.5
154	san	< 60	66	413	1996	1114	157	248	31	112	17	3	13	7.2	3.4
155	san	< 60	< 14	359	2127	1710	106	159	19	67	10	2.6	6.1	3.5	1.1
TA 9701 whole rock															
103	san	< 60	462	309	582	1194	103	205	28	114	19	2.7	10	5.9	2.1
104	san	< 60	656	338	498	837	82	168	22	96	15	2.3	9.2	5	1.7
105	san	< 60	689	158	69	116	21	47	5.8	22	3.7	0.43	1.6	1.1	0.55
111	san	< 60	< 14	463	918	1097	134	262	35	146	23	4.3	13	9.2	4.5

Tab. A-18: Chemical composition of plagioclases by LA-ICP-MS.

No	mineral	Cr	Ni	Rb	Sr	Ba	La	Ce	Pr	Nd	Sm	Eu	Gd	Dy	Yb
VUL 9701															
34	plg	< 60	< 14	10	6396	1141	106	151	15	53	7.8	2.4	4.4	3.5	1.6
35	plg	< 60	< 14	32	1367	4141	96	173	19	73	12	2.6	8.1	5.3	2.6
36	plg	< 60	< 14	39	4250	3355	74	110	11	35	4.5	2.6	3.3	2.7	1.3
37	plg	< 60	< 14	< 7.9	7608	757	182	326	36	138	20	4.5	13	7	1.9
38	plg	< 60	< 14	< 7.9	3967	431	58	82	7.4	21	2	1.8	1.8	0.68	0.42
39	plg	< 60	< 14	10	10633	1032	315	583	66	249	36	7.9	24	12	3.4
VUL 9702															
47	plg	< 60	< 14	< 7.9	5726	320	17	22	2.3	6.7	< 0.16	1.1	< 0.11	< 0.12	< 0.13
48	plg	< 60	< 14	29	5054	304	20	31	3.4	13	1.6	1.1	1.1	0.5	< 0.13
49	plg	< 60	< 14	20	7027	215	48	63	5.1	14	1.2	1.8	1.1	0.23	< 0.13
50	plg	91	68	50	11048	685	38	66	7.5	28	4.1	2.5	2.3	1.4	0.67
VUL 9703 B															
59	plg	< 60	16	< 7.9	1802	164	6.1	10	1.1	4.1	1.4	0.55	< 0.11	< 0.12	< 0.13
60	plg	< 60	< 14	17	2549	239	31	29	4.3	14	1.9	0.96	1.9	2.3	< 0.13
VUL 9707															
75	plg	< 60	< 14	< 7.9	5010	744	29	31	3.5	11	1.3	0.97	1.1	0.82	< 0.13
77	plg	< 60	< 14	12	7366	2058	100	134	16	50	7.5	2.3	4.9	3.2	1.7
78	plg	< 60	23	12	2926	1417	69	94	11	35	5.6	1.6	3.4	2.5	1.4
ROC 9701															
208	plg	< 60	< 14	< 7.9	244	14	20	31	3.2	10	1.7	1.3	1.1	0.89	< 0.13
209	plg	< 60	< 14	< 7.9	442	119	29	47	4.7	15	2.6	2.6	1.1	0.58	0.2
210	plg	< 60	< 14	< 7.9	548	121	45	65	6.3	20	2.8	3	1.5	0.55	0.19
211	plg	< 60	< 14	< 7.9	284	46	24	36	3.5	11	2	1.5	1.3	0.56	< 0.13
212	plg	< 60	< 14	< 7.9	298	61	24	37	3.6	12	1.6	1.9	0.9	0.49	0.16
SVC 9702															
177	plg	< 60	< 14	< 7.9	694	95	25	33	3.3	11	1.4	3.1	0.9	0.4	< 0.13
178	plg	< 60	< 14	< 7.9	567	39	21	30	3.3	12	2	2.5	1.2	0.77	0.14
180	plg	< 60	< 14	< 7.9	958	177	36	49	4.8	17	2.3	4.7	1.2	0.39	< 0.13
181	plg	< 60	< 14	< 7.9	965	153	36	50	4.9	16	2.2	4.1	1.2	0.56	< 0.13
182	plg	< 60	< 14	10	727	63	14	25	2.1	7.1	1.3	2.4	0.63	0.36	< 0.13
190	plg	< 60	< 14	< 7.9	544	132	52	65	7.5	25	4.8	3.5	3.3	1.3	0.28
194	plg	< 60	< 14	< 7.9	325	48	12	16	1.6	5.5	0.68	1.7	0.5	0.14	< 0.13
SVC 9703															
1	plg	< 60	< 14	58	618	165	37	60	5.5	17	2.7	3.3	1.6	0.87	0.26
2	plg	< 60	< 14	52	965	289	45	78	7.1	21	2.4	5.1	1.7	0.99	0.38
3	plg	< 60	< 14	< 7.9	1031	321	47	80	7.1	20	2.5	5.1	1.4	0.56	< 0.13
4	plg	< 60	< 14	< 7.9	1241	389	54	88	7.1	22	2.5	6.5	1.5	0.56	0.22
5	plg	< 60	< 14	< 7.9	1059	317	50	93	7.4	22	2.3	6.5	1.8	0.68	0.19
6	plg	< 60	< 14	< 7.9	944	269	46	75	6.3	20	2.2	5.2	1.4	0.34	< 0.13
7	plg	< 60	< 14	< 7.9	177	12	13	23	1.9	5.8	1	0.77	0.69	0.34	< 0.13

Tab. A-18: continued

No	mineral	Cr	Ni	Rb	Sr	Ba	La	Ce	Pr	Nd	Sm	Eu	Gd	Dy	Yb
AMT 9702															
164	plg	< 60	< 14	< 7.9	837	43	36	47	4.5	13	1.5	2.6	0.66	0.3	< 0.13
165	plg	< 60	21	8	702	34	35	47	4.7	15	1.6	2.4	0.94	0.4	0.17
166	plg	< 60	< 14	< 7.9	870	36	37	49	4.7	13	1.3	2.7	0.41	0.2	< 0.13
167	plg	< 60	< 14	< 7.9	939	52	38	51	5.1	17	2	2.8	0.86	0.61	0.17
AMT 9703 II															
149	plg	206	57	277	890	745	84	118	14	52	8.6	1.7	5.7	3.4	1.3
AMT 9704 A															
142	plg	< 60	15	12	794	261	39	38	5.9	21	2.8	2.2	1.8	1.3	0.71
143	plg	< 60	< 14	< 7.9	834	134	40	47	5.5	18	2.3	2.5	1.7	0.88	0.29
144	plg	93	36	59	1243	482	40	43	9.1	36	6.6	2.3	5.9	4.4	2.5
145	plg	186	24	74	401	224	49	83	16	73	17	1.3	14	11	5.6
RAD 9701															
115	plg	< 60	26	13	935	179	10	18	2.3	9.2	1.8	2.8	0.94	0.8	0.43
118	plg	< 60	< 14	< 7.9	889	189	7.4	12	1.4	5.3	0.61	2.1	0.42	0.27	< 0.13
119	plg	< 60	< 14	< 7.9	1003	184	7.6	12	1.4	4.3	0.54	2.4	0.28	0.27	< 0.13
RAD 9702 A															
130	plg	< 60	< 14	< 7.9	448	77	3.3	6.5	0.7	2.5	0.48	1.1	0.17	< 0.12	< 0.13
131	plg	< 60	< 14	< 7.9	464	94	3	5	0.56	2.1	0.38	0.96	0.15	< 0.12	< 0.13
133	plg	< 60	< 14	< 7.9	855	122	4.5	6.9	0.73	3	0.57	2.1	0.14	< 0.12	< 0.13
134	plg	< 60	< 14	< 7.9	794	106	3.7	5.8	0.65	2.5	0.22	1.6	0.16	< 0.12	< 0.13

Tab. A-19: Chemical composition leucites by LA-ICP-MS.

No	mineral	Cr	Ni	Rb	Sr	Ba	La	Ce	Pr	Nd	Sm	Eu	Gd	Dy	Yb
VUL 9701															
40	lc	< 60	< 14	1303	21	17	0.16	0.21	< 0.086	< 0.21	0.29	< 0.19	< 0.11	< 0.12	< 0.13
41	lc	< 60	< 14	1797	< 0.56	< 2.9	< 0.094	< 0.075	< 0.086	< 0.21	0.61	< 0.19	0.12	< 0.12	< 0.13
VUL 9705															
68	lc	< 60	17	1289	3.5	1172	0.12	0.42	< 0.086	0.61	< 0.16	< 0.19	< 0.11	< 0.12	< 0.13
69	lc	< 60	< 14	1605	53	663	1.5	2.9	0.3	0.97	0.19	< 0.19	< 0.11	< 0.12	< 0.13
70	lc	< 60	< 14	1907	374	953	26	42	4.4	14	1.9	0.32	1.2	0.56	0.23
71	lc	< 60	< 14	1823	24	524	1.2	2.5	0.26	0.75	< 0.16	< 0.19	0.12	< 0.12	< 0.13
VUL 9707															
79	lc	< 60	34	765	17	20	26	41	4.3	15	2.1	0.54	1.4	1.1	0.54
80	lc	< 60	< 14	750	51	18	1.2	2.2	0.23	0.86	0.18	< 0.19	0.12	< 0.12	< 0.13
81	lc	< 60	61	692	11	10	2.2	3.5	0.31	1.3	0.22	< 0.19	< 0.11	< 0.12	< 0.13

Tab. A-20: Chemical composition of micas by LA-ICP-MS.

No	mineral	Cr	Ni	Rb	Sr	Ba	La	Ce	Pr	Nd	Sm	Eu	Gd	Dy	Yb
ROC 9701															
205	bio	290	42	552	3.8	492	188	336	43	169	29	0.29	18	8.6	0.7
206	bio	107	20	369	2.8	265	0.29	0.81	< 0.086	0.37	< 0.16	< 0.19	< 0.11	< 0.12	< 0.13
207	bio	662	64	657	4.7	685	407	720	92	360	62	0.65	42	20	1.8
213	bio	109	38	476	1.9	241	< 0.094	< 0.075	< 0.086	< 0.21	< 0.16	< 0.19	< 0.11	< 0.12	< 0.13
214	bio	64	28	395	0.9	122	< 0.094	< 0.075	< 0.086	< 0.21	< 0.16	< 0.19	< 0.11	< 0.12	< 0.13
215	bio	237	51	585	6.8	373	0.18	0.16	< 0.086	< 0.21	< 0.16	< 0.19	< 0.11	< 0.12	< 0.13
216	bio	< 60	< 14	157	4.5	43	2.3	4.7	0.59	2.3	0.6	< 0.19	0.71	1	0.62
217	bio	< 60	< 14	91	3.1	7.9	1.2	2.6	0.33	1.2	0.35	< 0.19	0.44	0.78	0.32
218	bio	< 60	< 14	286	8.1	124	4.4	8.8	1.1	4.4	0.94	< 0.19	1.8	2.2	1.4
SVC 9702															
183	bio	381	134	1096	19	1182	1.7	1.7	0.47	2.6	0.45	< 0.19	0.56	0.35	0.29
184	bio	< 60	88	788	11	836	0.75	0.61	0.22	1.1	< 0.16	< 0.19	0.17	< 0.12	< 0.13
185	bio	726	193	1286	30	1405	3.4	3.6	0.94	4.8	0.97	0.21	1.2	0.75	0.64
186	bio	281	118	1390	25	759	4.5	7.5	1.2	5.5	0.98	< 0.19	0.82	1.1	0.49
187	bio	< 60	46	1058	13	556	0.49	0.8	0.16	0.5	0.16	< 0.19	0.11	< 0.12	< 0.13
188	bio	974	179	1624	83	1181	31	53	7.7	41	3.8	0.67	3.1	6.8	1.5
193	bio	138	44	296	5.2	314	0.73	1.5	0.26	1.1	0.32	< 0.19	0.64	0.49	< 0.13
195	bio	124	23	254	5.5	569	3.5	7.8	1.4	7.1	2.4	< 0.19	2.9	3.1	2.2
196	bio	< 60	< 14	223	3.2	411	0.43	0.81	0.16	0.67	0.17	< 0.19	0.15	< 0.12	< 0.13
197	bio	505	29	463	9.5	803	6.4	16	2.8	16	5	< 0.19	6.4	7.3	5
198	bio	< 60	< 14	118	14	39	4.3	7.6	1.1	3.9	0.89	< 0.19	0.8	1.1	0.73
199	bio	< 60	< 14	54	6.6	8.9	1.8	3.2	0.44	1.7	0.47	< 0.19	0.46	0.82	0.54
200	bio	124	15	268	33	138	13	17	2.5	9.2	2.1	0.21	2.5	1.9	1.3
SVC 9703															
13	bio	< 60	69	551	7	1255	0.11	0.25	< 0.086	0.33	< 0.16	< 0.19	0.48	< 0.12	< 0.13
14	bio	< 60	38	322	1.9	796	< 0.094	< 0.075	< 0.086	< 0.21	< 0.16	< 0.19	< 0.11	< 0.12	< 0.13
15	bio	< 60	133	875	21	1754	0.35	0.68	0.13	1.3	< 0.16	< 0.19	1.2	0.16	0.33
16	bio	< 60	76	494	3.6	765	2.2	7.1	1.3	6.2	2.4	< 0.19	2.9	2.8	0.91
17	bio	< 60	21	290	0.95	402	< 0.094	0.19	< 0.086	< 0.21	< 0.16	< 0.19	0.19	< 0.12	< 0.13
18	bio	< 60	158	761	9.3	1318	14	43	8.6	38	14	0.2	17	18	5.2
19	bio	< 60	91	617	4.4	1288	4.4	15	2.6	13	4.3	< 0.19	5.5	4.8	2.2
20	bio	< 60	44	415	3	888	1.1	3.7	0.66	2.1	0.68	< 0.19	1.1	1.2	0.33
21	bio	< 60	132	851	6.7	1746	15	49	9	45	14	0.21	19	18	8.3
22	bio	< 60	85	532	6.9	927	28	58	5.5	20	3	< 0.19	2.8	1.7	0.27
23	bio	< 60	41	275	2.1	377	0.18	1.3	0.17	0.61	< 0.16	< 0.19	0.27	0.12	< 0.13
24	bio	< 60	174	888	22	1533	161	324	31	109	14	0.65	11	10	2.7
AMT 9702															
160	bio	223	55	226	37	2130	3	1.4	0.52	2	0.28	< 0.19	0.27	0.19	< 0.13
161	bio	205	44	250	17	1415	0.88	4.1	0.14	0.62	< 0.16	< 0.19	< 0.11	< 0.12	< 0.13
162	bio	191	40	221	23	2410	0.77	27	0.12	0.42	< 0.16	< 0.19	< 0.11	< 0.12	< 0.13
163	bio	225	41	251	23	2910	1.5	1.7	0.18	0.62	< 0.16	< 0.19	< 0.11	< 0.12	< 0.13
168	bio	114	29	13	32	31	27	21	4.5	16	3.6	< 0.19	3.6	5.6	5.7
169	bio	< 60	< 14	< 7.9	5.8	9.6	3.3	3.6	0.79	3.2	0.38	< 0.19	1.3	3.2	4.4
170	bio	250	36	35	75	61	72	53	11	40	7.5	0.43	6.2	8.6	7.7
171	bio	< 60	29	55	69	112	158	351	50	224	49	0.66	37	25	9.1
172	bio	< 60	19	< 7.9	0.87	< 2.9	1.1	2.9	0.61	4.8	1.3	< 0.19	2.7	5.2	3.6
173	bio	< 60	37	127	161	322	435	977	145	633	143	1.4	107	68	18

Tab. A-20: continued

No	mineral	Cr	Ni	Rb	Sr	Ba	La	Ce	Pr	Nd	Sm	Eu	Gd	Dy	Yb
TA 9701 whole rock															
107	phl	< 60	< 14	337	569	979	96	192	27	115	19	2.8	10	5.9	2.1
108	phl	< 60	< 14	226	398	723	76	149	21	89	14	2.2	7.7	4.6	1.7
109	phl	1624	1938	540	852	1219	126	254	35	148	27	4	14	7.7	2.5
TA 9701 peridotitic xenolith															
90	phl	55071	718	211	163	351	16	38	4.1	16	2.9	0.82	1.8	1.4	0.9
91	phl	< 60	115	123	76	209	6.2	15	1.7	6.4	1	0.41	0.56	0.66	0.46
92	phl	539810	3365	353	259	518	37	96	8.7	30	5.7	1.1	3.2	2.3	1.4
93	phl	67234	680	235	249	467	22	45	6	25	4.1	1	2.6	1.7	0.76
94	phl	< 60	101	116	87	214	8.8	18	2.5	10	1.5	0.37	1.1	0.56	0.4
95	phl	716781	3710	378	373	642	31	70	9	42	6.8	1.8	4.2	2.8	1.2
96	phl	86201	473	255	222	451	20	45	5.4	21	3.4	0.84	1.9	1.3	0.57
97	phl	< 60	122	171	119	323	13	31	4.5	18	2.7	0.65	1.1	1	0.33
98	phl	798629	2040	398	299	535	24	54	6.5	26	4	1.1	2.6	1.6	0.81
99	phl	106270	477	218	290	427	62	118	16	63	11	1.3	5.6	3.5	1.5
100	phl	< 60	170	158	201	249	49	89	12	49	8.6	0.99	4.2	2.6	1
101	phl	938344	1861	343	386	583	77	138	19	75	13	1.7	6.5	4.7	1.9

Tab. A-21: Oxygen isotope ratios (‰, SMOW).

No	1	2	3	4	5	6	7	8	9	10	11	12	13	14	av.	s
VUL 9701																
plg	9.7	9.5													9.6	0.1
cpx	8.9	8.7	8.4	8.5	8.7	9.1	9.0	9.0	9.2	9.5					8.9	0.3
VUL 9702																
cpx	8.1	7.9	7.8	8.1	8.0	8.1	7.5	7.2							7.8	0.3
VUL 9703 A																
cpx	6.9	6.8	7.4	7.6	8.3	7.5									7.4	0.5
ol	6.9	6.9	7.4	7.1	7.3										7.1	0.2
VUL 9703 B																
cpx	7.1	7.3	7.9	7.5	6.7	8.3	7.5								7.5	0.5
ol	7.5	7.3	7.4	7.0	6.5	6.5									7.0	0.4
VUL 9704																
cpx	8.3	8.4	7.9	7.7	8.1										8.1	0.3
VUL 9705																
plg	11.8														11.8	
cpx	7.7	7.6	8.7	8.8	7.5	8.3	7.7	8.7	7.4	7.5	8.1				8.0	0.5
VUL 9706																
cpx	8.6	8.8	8.5	8.6	8.9	8.4									8.6	0.2
VUL 9707																
cpx	8.3	8.4	9.1	8.7	8.8										8.7	0.3
Montefiascone																
plg	12.1	11.3	12.0	11.4	11.5										11.7	0.4
cpx	7.6	7.4	7.8	7.1	7.3	7.6	7.9	8.0	8.3	7.2	7.3	7.1			7.6	0.4
ol	6.8	7.2	6.2	6.9	6.4	6.7	7.1	7.0	6.0	6.8	6.6	6.9	6.5		6.7	0.4
ORC 9701																
san	11.6	11.3	10.9	11.2	10.7	10.6	11.3								11.1	0.4
ol	7.0	7.4	7.3	7.1											7.2	0.2
ROC 9701																
qz	13.7	12.8	13.2	13.2	13.4										13.3	0.3
san	12.4	12.0	12.3	12.1	12.6	12.4	12.3	12.6							12.3	0.2
plg	11.5	11.7	11.6	11.3	11.3	11.4	11.3	11.4	11.3	11.3	11.2	11.4	11.4		11.4	0.1
matrix	12.2	11.6	11.4												11.7	0.4
ROC 9702																
qz	13.3	12.9	12.9	13.1	13.3										13.1	0.2
san	12.4	12.7	12.6	12.5	12.4	12.3	12.4								12.5	0.1
plg	11.4	11.8	11.5	11.3	11.6	11.5	11.5								11.5	0.2
SVC 9701																
qz	13.3	14.1	14.8	13.5	14.8	13.6	15.6	15.7							14.4	0.9
san	12.5	13.9	13.3	14.0	12.4	13.9									13.3	0.7
plg	14.6	10.8	11.5	12.1	13.9	14.2									12.9	1.6
opx	9.3	9.4	9.3	9.8											9.5	0.2
SVC 9702																
qz	14.4	14.4	13.4	14.1	13.6										14.0	0.5
san	12.5	12.8	12.6	13.1	12.0	12.3									12.6	0.4
plg	10.8	12.0	11.5	11.8	10.6										11.3	0.6
SVC 9703																
qz	15.0	15.3	15.4												15.2	0.2
san	14.2	14.4	14.0	14.5	14.4										14.3	0.2
plg	13.1	13.1	13.1	13.0	13.2	13.3									13.1	0.1
matrix	15.0														15.0	

Tab. A-21: continued

No	1	2	3	4	5	6	7	8	9	10	11	12	13	14	av.	s
AMT 9701																
qz	14.5	14.9													14.7	0.3
san	12.0	12.3	12.4	12.5	12.1	12.3	13.0	12.4	12.7	12.9	12.7	12.7	12.5	12.6	12.5	0.3
bio	11.0														11.0	
AMT 9702																
qz	15.5	15.1													15.3	0.3
san	12.6	12.5	12.8	12.5	12.9	12.9	13.1								12.8	0.2
opx	10.1	10.8	11.2	11.1											10.8	0.5
AMT 9703 I I																
san	11.9														11.9	
cpx	7.7	7.1	7.6	7.8	7.3	7.2	7.6	7.2	7.1	7.2					7.4	0.3
AMT 9704 A																
plg	12.0	12.6	12.7	12.2	12.5										12.4	0.3
cpx	8.7	8.5	9.5	8.2	9.0	8.6	8.7	8.7	8.7	9.4					8.8	0.4
AMT 9704 B																
plg	12.0	12.0	12.1	11.4	11.1	11.2	11.8	11.8							11.7	0.4
cpx	9.2	9.0	8.7	8.9	9.4	9.1	9.3	9.0	8.8	8.9	8.7				9.0	0.2
matrix	10.3	12.2													11.3	1.3
RAD 9701																
ol	7.5	7.6	7.5	7.1	7.4	7.7	7.3								7.4	0.2
RAD 9702 A																
cpx	7.0	7.5	7.4	7.6	7.2	7.5	7.3	7.5							7.4	0.2
ol	7.0	6.8	7.0	7.4	7.3	7.2	6.9	7.1							7.1	0.2
matrix	7.1	7.3	7.3	7.6											7.3	0.2
RAD 9702 B																
cpx	7.6	7.8	7.6	7.5	7.4	7.5	7.3								7.5	0.2
RAD 9703																
ol	6.9	7.2	7.4	7.3	7.0	7.4	7.4								7.2	0.2
RAD 9705																
ol	7.3	6.9	7.5	7.4	7.5	7.2	7.0								7.3	0.2
TA 9701 whole rock																
ol	6.7	6.4	7.3	7.4	8.4	9.1	6.6	5.3	7.2	6.1					7.1	1.1
matrix	13.4	13.1	13.0	13.3	12.6	13.2									13.1	0.3
TA 9701 peridotitic xenolith																
opx	8.8														8.8	
ol	7.0	6.9	7.9	10.9	6.6	7.8	8.0	5.9	8.2	10.8	6.3	7.4			7.8	1.6
TA 9701 crustal xenolith																
qz	14.6														14.6	
matrix	14.0	14.2	13.7	14.2	14.0										14.0	0.2
TA 9702																
ol	5.3	5.5													5.4	0.1

Tab. A-22: Radiogenic isotope ratio analyses: selected samples have kindly been analyzed by Prof. A. Peccerillo from the Univeristy of Perugia (personal information).

Sample	^{87}Sr / ^{86}Sr	^{143}Nd / ^{144}Nd	^{206}Pb / ^{204}Pb	^{207}Pb / ^{204}Pb	^{208}Pb / ^{204}Pb
VUL 9703 A	0.709972	0.51219	18.752	15.702	39.071
ORC 9702	0.715201	0.5121	18.729	15.715	39.192
MVC 9701	0.716909	0.512099	18.757	15.675	39.116
TA 9701	0.716246	0.512068	18.661	15.658	38.855
RAD 9702 B	0.713363	0.51218	18.686	15.674	39.984
RAD 9706	0.713847	0.512137	18.683	15.664	39.963

Acknowledgements

I gratefully acknowledge Prof. Dr. J. Hoefs for the allocation of the very interesting project and for supporting me in both advice and discussions.

I am especially grateful to Prof. Dr. A. Peccerillo from the University of Perugia for the introduction in the regional geology and petrology of central Italy and for supporting the sampling. Prof. Dr. A. Peccerillo is also gratefully appreciated for helpful discussions and comments.

I thank Prof. Dr. S. F. Foley from the University of Greifswald for beeing the co-advisor.

Furthermore I thank Dr. J. Fiebig (LA-SIRMS), Dr. G. Hartmann (XFA), Dr. A. Kronz (EMPA), R. Przybilla (LA-SIRMS), and Dr. K. Simon (ICP-MS, LA-ICP-MS) for helpful discussions and technical advice. I also thank A. Reitz and E. Schiffcyzk for supporting me by common problems of laboratory working.

I thank B. Hagen (University of Bonn) for carrying out CO_2 LA-SIRMS analyses of phenocrystals from selected samples.

I am especially indebted to S. Schlabach for helping me at any problems.

This project was financially granted by the Deutsche Forschungsgemeinschaft (project no. Ho 375 / 16-1 and Ho 375 / 16-2).

Curriculum Vitae

Date and place of birth: 4th of December 1969, Bremen (Germany)

1976-1990	Grundschule, Orientierungsstufe and Gymnasium in the municipality of Ganderkesee, school leaving exam: Allgemeine Hochschulreife
1990-1991	National service in Goslar and Delmenhorst
1991-1996	Study of mineralogy at the Georg-August Universität, Göttingen
1996	Diploma in Mineralogy Advisor: Prof. Dr. H. Heinrichs, Co-advisor: Prof. Dr. J. Hoefs Thesis for diploma: "Der Einfluß der Silikatverwitterung auf den Chemismus abgepreßter Porenlösungen von versauerten Böden (Harz, Solling)" (translated: "The Influence of Silicate Weathering on the Chemistry of Squeezed Pore Solutions from Acidic Soils (Harz mountains, Solling mountains)")
1997-1999	Doctorate studies, scientific assistant at the Geochemisches Institut, University of Göttingen, in the project "^{18}O-Zusammensetzung von Phenocrysten in Vulkaniten analysiert durch Laser-Evaporation"
2000	Thesis: "Volcanic Rocks from Central Italy: An Oxygen Isotopic Microanalytical and Geochemical Study" Advisor: Prof. Dr. J. Hoefs, Co-advisor: Prof. Dr. S.F. Foley (University of Greifswald)
since July 2000	R & D manager at Merck KGaA, Darmstadt, Germany, in the department of research on pigments